



# Spatial optimisation for resilient infrastructure services

**Fulvio Domenico Lopane**

School of Engineering

Newcastle University

Thesis submitted for the degree of Doctor of Philosophy

April 2022



## Abstract

Infrastructure networks provide crucial services to the functioning of human settlements. Extreme weather events, especially flooding, can lead to disruption or complete loss of these crucial infrastructure services, which can have significant impacts on people's health and wellbeing, as well as being costly to repair. Urban areas concentrate infrastructure and people, and are consequently particularly sensitive to disruptions due to natural (and human-made) disasters. Flooding alone constituted 47% of all weather-related disasters between 1995 and 2015, causing enormous loss of lives and economic damages. Climate change is projected to further exacerbate the impacts that natural disasters have on cities.

Choices about where to site infrastructure have a significant impact on the impacts of extreme weather events. For example, investments in flood risk management have typically focussed on prioritising interventions to protect people, houses and businesses. Protection of infrastructure services has either been a bonus benefit of flood defence protection of property, or been implemented by individual infrastructure operators. Spatial planning is a key process to influence the distribution of people and activities over broad spatial scales. However, decision-making processes to locate infrastructure services does not typically consider resilience issues at broad spatial scales which can lead to inefficient use of resources. Moreover, spatial planning typically requires consideration of multiple, sometimes competing, objectives with solutions that are not readily tractable.

Balancing multiple trade-offs in spatial planning with multiple variables at high spatial resolution is computationally demanding. This research has developed a new framework for multi-objective Pareto-optimal location-allocation problems solving. The RAO (Resource Allocation Optimisation) framework developed here is a heuristic approach that makes use of a Genetic Algorithm (GA) to produce Pareto-optimal spatial plans that balance a typical trade-off in spatial planning: the maximisation of accessibility of a given infrastructure service vs the minimisation of the costs of providing that service. The method is applied to two case studies: (i) Storage of temporary flood defences, and (ii) Location of healthcare facilities.

The RAO is first applied to a flood risk management case study in the Humber Estuary, UK, to optimise the strategic allocation of storing space for emergency resources (like temporary flood barriers, portable generators, pumps etc.) by maximising the accessibility of warehouses (i.e. minimising travel times from storing locations to deployment sites) and minimising costs.

The evaluation of costs involves both capital and operational costs such as the length of temporary defences needed, storage site locations, number of lorries and personnel to enable their deployment, and maintenance costs. A baseline is tested against a number of scenarios, including a flood disrupting road network and thereby deployment operations, as well as variable infrastructure and land use costs, different transportation and deployment strategies and changing the priority of protecting different critical infrastructures.

Key findings show investment in strategically located warehouses decreases deployment time across the whole region by several hours, while prioritising the protection of the infrastructure assets serving larger shares of population can cut costs by 30%. Moreover, the analysis of the ensemble of all scenarios provides crucial insights for spatial planners. For example, storage sites in Hull or Hedon, and in the areas of Withernsea and Drax are robust choices under all scenarios. Meanwhile, the Humber Bridge is shown to play a crucial role in enabling regional coverage of temporary barriers.

The second case study shows how emergency response strategies can be enhanced by optimal allocation of healthcare facilities at a regional scale. The RAO framework allocates healthcare facilities in Northland (New Zealand) balancing the trade-off between maximisation of accessibility (i.e. minimisation of travel times between households and GP clinics) and minimisation of costs (i.e. number of clinics and doctors). Results show how c.80% of Northland's population lives within a 20 minutes drive from the closest GP, but this can be increased to 90% with strategic investment and relocation of doctors and clinics. By accounting for flood and landslide risk, the RAO is used to identify strategies that improve accessibility to healthcare services by up to 5% even during extreme events (when compared to the current business as usual service accessibility).

Application to these two problems demonstrates that the RAO framework can identify optimal strategies to deploy finite resources to maximise the resilience of infrastructure services. Moreover, it provides an analytical appreciation of the sensitivity between planning tradeoffs and therefore the overall robustness of a strategy to uncertainty. The method is consequently of benefit to local authorities, infrastructure operators and agencies responsible for disaster management. Following successful application to regional scale case studies, it is recommended that future work scale the analysis to consider resource allocation to protect infrastructure at a national scale.

## Acknowledgements

I would like to thank my supervisors Richard Dawson, Stuart Barr and Philip James for their precious guidance and support during my PhD. Thanks also to Newcastle University and The University of Auckland for hosting me during the development of this work and to the Engineering and Physical Sciences Research Council for funding it. Special thanks to Andrea Raith and Melanie Reuter-Opper mann for supporting me in New Zealand and to Maria Pregolato and Grant Tregonning for being inspiring colleagues, precious advisors and invaluable friends during the years of my PhD. Thanks also to Thomas, for being there, always. Thanks to my family; without their loving support, I could not have achieved anything of this. And finally, thanks to Vale, who made a scientist believe in magic.



## Publications based on this research

Lopane, F. D.; Barr, S.; James, P.; Dawson, R. (2019). "Optimization of resource storage location for managing flood emergencies". Proceedings of the 2<sup>nd</sup> International Conference on Natural Hazards & Infrastructure, Chania (Greece), June 2019.

Lopane, F. D.; Dawson, R.; Barr, S.; James, P. (2017) "Resilient infrastructure networks - spatial optimisation applied to emergency management". Proceedings of ICFM7, Leeds (UK), September 5-7.





## Table of contents

Abstract .....	3
Acknowledgements .....	5
Publications based on this research .....	7
I. List of figures .....	13
II. List of tables .....	21
1. Introduction.....	23
1.1. Infrastructure and climate risks.....	23
1.2. Methods.....	24
1.3. Thesis outline .....	25
2. Infrastructure resilience and emergency planning .....	29
2.1. Introduction Chapter 2 .....	29
2.2. Climate risks in urban areas.....	29
2.2.1. Strategic infrastructure .....	29
2.2.2. Climate change-related problems in cities .....	31
2.2.3. Infrastructure resilience to natural hazards .....	32
2.3. Flood emergency planning .....	35
2.3.1. Flood risk management.....	35
2.3.2. Flood defences .....	40
2.3.2.1. Structural measures.....	40
2.3.2.2. Temporary measures.....	41
2.4. Summary.....	46
3. Review of optimisation techniques.....	47
3.1. Introduction to chapter 3 .....	47
3.2. Definition of optimisation problems .....	47
3.3. Multi-objective optimisation problems.....	52
3.4. Literature review of spatial optimisation techniques .....	55
3.4.1. Linear programming.....	55
3.4.2. Simulated annealing.....	57
3.4.3. Tabu search .....	58
3.4.4. Particle swarm.....	59
3.4.5. Genetic algorithms.....	60
3.5. Contribution of this research to the optimisation field.....	62

3.6.	Summary.....	63
4.	RAO (Resource Allocation Optimisation) framework.....	65
4.1.	Introduction Chapter 4.....	65
4.2.	Problem formulation: optimal resource allocation .....	65
4.2.1.	Optimisation methodology.....	65
4.2.2.	Framework structure and software implementation.....	66
4.2.2.1.	Initialisation phase .....	70
4.2.2.2.	Iterator .....	75
4.2.2.3.	Evolutionary operators .....	77
4.2.2.4.	Constraints and evaluate .....	79
4.2.2.5.	Multi-Objective Pareto-Optimal set maintenance .....	83
4.2.2.6.	Outputs .....	84
4.3.	Development environment.....	87
4.4.	Genetic Algorithm .....	88
4.5.	Summary.....	89
5.	Humber Estuary (UK) case study .....	91
5.1.	Introduction Chapter 5.....	91
5.2.	Introduction to case study .....	92
5.3.	Data .....	93
5.4.	RAO framework applied to Humber Estuary case study.....	95
5.4.1.	Input phase .....	95
5.4.2.	Problem formulation .....	95
5.4.3.	Initialisation .....	96
5.4.4.	Evaluation .....	99
5.4.5.	Constraints.....	112
5.4.6.	GA calibration .....	114
5.4.7.	Output phase .....	116
5.5.	Results .....	117
5.5.1.	Scenario 1: Uniform rent price, discrete cost function .....	118
5.5.2.	Scenario 2: Uniform rent price, discrete cost function with road network disruption .....	127
5.5.3.	Scenario 3: Uniform rent price, linear continuous cost function .....	134
5.5.4.	Scenario 4: Variable rent price (R/U), linear cost function with fixed number of lorries	136

5.5.5.	Scenario 5: Variable rent price (R/S/U), linear cost function with fixed number of lorries	139
5.5.6.	Scenario 6: Variable rent price (R/S/U), non-linear cost function with variable number of lorries (1)	141
5.5.7.	Scenario 7: Variable rent price (R/S/U), non-linear cost function with variable number of lorries (2)	144
5.5.8.	Scenario 8: Variable rent price (R/S/U), non-linear cost function with variable number of lorries (3)	147
5.5.9.	Scenario 9: Variable rent price (R/S/U), non-linear cost function with variable number of lorries (0.5)	150
5.5.10.	Scenario 10: Variable rent price (R/S/U), non-linear cost function with variable number of lorries (1), SI priority (top 3)	153
5.5.11.	Scenario 11: Variable rent price (R/S/U), non-linear cost function with variable number of lorries (1), SI priority (top 5)	156
5.5.12.	Scenario 12: Variable rent price (R/S/U), non-linear cost function with variable number of lorries (1), SI priority (top 10)	159
5.5.13.	Scenario 13: Variable rent price (R/S/U), non-linear cost function with variable number of lorries (1), SI priority (top 10 – excluding police and fire stations)	162
5.6.	Discussion of Humber Estuary case study results	165
5.7.	Summary	171
6.	Northland (NZ) case study	173
6.1.	Introduction Chapter 6	173
6.2.	Introduction to case study	174
6.3.	Data	177
6.4.	RAO applied to Northland case study	179
6.4.1.	Input phase	179
6.4.2.	Problem formulation	179
6.4.3.	Initialisation	180
6.4.4.	Evaluation	181
6.4.5.	Constraints	183
6.4.6.	GA applied to the Northland case study	184
6.5.	Results	187
6.5.1.	Business as usual (BAU) scenario	188
6.5.1.1.	BAU scenario – Target ratio patients/GPs: 1500	189
6.5.1.2.	BAU scenario – Target ratio patients/GPs: 2500	197
6.5.2.	Disruption scenario	202

6.5.2.1.	Disruption scenario – Target ratio patients/GPs: 1500 .....	202
6.5.2.2.	Disruption scenario – Target ratio patients/GPs: 2500 .....	208
6.6.	Discussion of Northland case study results.....	214
6.7.	Summary.....	222
7.	Discussion .....	225
7.1.	Introduction.....	225
7.2.	Balancing conflicts and trade-offs in spatial planning .....	226
7.3.	Flood Incident Management .....	227
7.4.	Embedding infrastructure network vulnerability into strategic planning .....	231
7.5.	Model limitations and future development.....	233
7.6.	Software challenges for spatial optimisation.....	237
8.	Conclusions .....	241
8.1.	Review of Objective 1: flood risk management and infrastructure resilience .....	241
8.2.	Review of Objective 2: optimisation techniques .....	242
8.3.	Review of Objective 3: the RAO framework .....	243
8.4.	Review of Objective 4: case studies .....	244
8.5.	Review of Objective 5: cases studies’ results analysis .....	244
8.6.	Implications of the research.....	246
9.	References .....	249

## I. List of figures

Figure 1 - Developed from (Rinaldi et al., 2001), examples of infrastructure networks interdependencies.....	31
Figure 2 - Definition of resilience: the capacity of a system to recover after a disruption. ....	33
Figure 3 - UN Sustainable Development Goals. ....	34
Figure 4 - Indicative percentages of the population at risk of flooding from rivers and the sea. Developed from Cabinet Office and DEFRA (2016).....	37
Figure 5 - Examples of temporary flood defences. a) Frame barriers, b) free-standing barriers (rigid), c) free-standing barriers (flexible), d) tubes, e) water-filled container, f) aggregate-filled container.....	43
Figure 6 - Examples of solutions space and Pareto fronts for multi-objective minimisation and maximisation problems. ....	54
Figure 7 - General workflow of a genetic algorithm. Picture from Lopane et al. (2019). ....	61
Figure 8 - Resource Allocation Optimisation framework flowchart with indication of sections numbers where the different components are described.....	67
Figure 9 - Scheme of the python modules of the Resource Allocation Optimisation (RAO) framework with respective functions and dependencies.....	68
Figure 10 - Dimension reduction in Lookup table creation.....	72
Figure 11 - Relationship between spatial plans (i.e. potential solutions) and Lookup table. ..	74
Figure 12 - Evolution of Pareto fronts for minimisation and maximisation problems. G represents the number of Generations in the evolution process (the values are purely indicative). ....	76
Figure 13 - Creation of Proposed sites variable to reduce the dimension of the Spatial plan vector for a lighter and more computationally efficient data handling. ....	77
Figure 14 - Two-point crossover operator mechanism, adapted from Caparros-Midwood (2015).....	78
Figure 15 - Mutation operator mechanism, adapted from Caparros-Midwood (2015). ....	78
Figure 16 - Example of application of evolutionary operators that do not meet the constraint of the min/max allowed number of assets allocation.....	81
Figure 17 - Non dominated sorting, adapted from Deb et al. (2002). ....	84
Figure 18 - Format of Pareto sets. The Pareto sets are saved as text files in the output folder and also plotted in a a graph representing the optimisation objectives on each axis. ....	85
Figure 19 - Creation of raster output from the Pareto-optimal spatial plans contained in the Pareto sets (i.e. Pareto-optimal solutions produced by the Genetic Algorithm). Raster outputs are saved in the GeoTIFF format and can be imported in any GIS environment. ....	86
Figure 20 – Great Britain and Humber Estuary map. ....	93
Figure 21 - K-means clustering of strategic infrastructure assets. Assignment to closest cluster centroid is performed according to proximity evaluated as travel time on the road network. Figures a) to e) show different ways to cluster strategic infrastructure assets according to the increasing number of clusters considered (respectively from 1 to 5). ....	98
Figure 22 - Industrial rent prices per square metre in Yorkshire (2017). Green dots represent warehouses for rent outside urban areas, while grey dots represent warehouses within town borders. ....	103

Figure 23 - Relationship between warehouses' dimension and annual rent price with logarithmic regression. ....	104
Figure 24 - Rural, suburban and urban areas in the Humber Estuary according to the Degree of urbanization definition. ....	108
Figure 25 - Humber Estuary case study: available locations and strategic infrastructure assets.....	113
Figure 26 - Flowchart of the initialisation process for the Humber Estuary case study.....	114
Figure 27 - Pareto fronts evolution of the Humber Estuary case study: a) Business as usual scenario; b) Disruption scenario. ....	116
Figure 28 - Solution space and Pareto-front for Humber Estuary case study. Scenario 1. ...	119
Figure 29 - Normalised solution space and Pareto-front for Humber Estuary case study. Scenario 1.....	119
Figure 30 - Thresholds in the solution space for the Humber Estuary case study – Scenario 1. Orange threshold: result-driven. Green thresholds: objective-driven.....	120
Figure 31 - Highlight of the Pareto-front for the Humber Estuary – Scenario 1 - with the indication of the number of Pareto-optimal spatial plans. Figures A, B, C, D, E and F are visualised respectively in Figure 32, Figure 33, Figure 34, Figure 35, Figure 36 and Figure 37. ....	123
Figure 32 - Humber Estuary Scenario 1, Solution A. The green lines are for visualisation purposes: they connect each infrastructure asset to the closest warehouse. They do not represent distances, as distances are measured as travel times on the road network.....	124
Figure 33 - Humber Estuary Scenario 1, Solution B. The green lines are for visualisation purposes: they connect each infrastructure asset to the closest warehouse. They do not represent distances, as distances are measured as travel times on the road network. ....	124
Figure 34 - Humber Estuary Scenario 1, Solution C. The green lines are for visualisation purposes: they connect each infrastructure asset to the closest warehouse. They do not represent distances, as distances are measured as travel times on the road network.....	125
Figure 35 - Humber Estuary Scenario 1, Solution D. The green lines are for visualisation purposes: they connect each infrastructure asset to the closest warehouse. They do not represent distances, as distances are measured as travel times on the road network. ....	125
Figure 36 - Humber Estuary Scenario 1, Solution E. The green lines are for visualisation purposes: they connect each infrastructure asset to the closest warehouse. They do not represent distances, as distances are measured as travel times on the road network. ....	126
Figure 37 - Humber Estuary Scenario 1, Solution F. The green lines are for visualisation purposes: they connect each infrastructure asset to the closest warehouse. They do not represent distances, as distances are measured as travel times on the road network. ....	126
Figure 38 - Disconnected areas due to the flooded road network.....	127
Figure 39 - Solution space and Pareto-front for Humber Estuary case study. Scenario 2. ...	129
Figure 40 - Highlight of the Pareto-front for the Humber Estuary disruption scenario with the indication of the number of Pareto-optimal spatial plans. Solutions A, B, C, D, E and F are visualised respectively in Figure 41, Figure 42, Figure 43, Figure 44, Figure 45 and Figure 46. ....	130

Figure 41 - Humber Estuary Scenario 2, Solution A. The green lines are for visualisation purposes: they connect each infrastructure asset to the closest warehouse. They do not represent distances, as distances are measured as travel time on the road network. ....	130
Figure 42 - Humber Estuary Scenario 2, Solution B. The green lines are for visualisation purposes: they connect each infrastructure asset to the closest warehouse. They do not represent distances, as distances are measured as travel time on the road network. ....	131
Figure 43 - Humber Estuary Scenario 2, Solution C. The green lines are for visualisation purposes: they connect each infrastructure asset to the closest warehouse. They do not represent distances, as distances are measured as travel time on the road network. ....	131
Figure 44 - Humber Estuary Scenario 2, Solution D. The green lines are for visualisation purposes: they connect each infrastructure asset to the closest warehouse. They do not represent distances, as distances are measured as travel time on the road network. ....	132
Figure 45 - Humber Estuary Scenario 2, Solution E. The green lines are for visualisation purposes: they connect each infrastructure asset to the closest warehouse. They do not represent distances, as distances are measured as travel time on the road network. ....	132
Figure 46 - Humber Estuary Scenario 2, Solution F. The green lines are for visualisation purposes: they connect each infrastructure asset to the closest warehouse. They do not represent distances, as distances are measured as travel time on the road network. ....	133
Figure 47 - Solution space for Scenario 3. ....	135
Figure 48 - Humber Estuary Scenario 3 Solution. The green lines are for visualisation purposes: they connect each infrastructure asset to the closest warehouse. They do not represent distances, as distances are measured as travel times on the shortest path on the road network. ....	135
Figure 49 - Solution space and Pareto-front for Humber Estuary case study. Scenario 4. With the indication of Solutions A, B and C that are visualised respectively in Figure 50, Figure 51 and Figure 52. ....	137
Figure 50 - Humber Estuary Scenario 4 Solution A. The green lines are for visualisation purposes: they connect each infrastructure asset to the closest warehouse. They do not represent distances, as distances are measured as travel times on the shortest path on the road network. ....	137
Figure 51 - Humber Estuary Scenario 4 Solution B. The green lines are for visualisation purposes: they connect each infrastructure asset to the closest warehouse. They do not represent distances, as distances are measured as travel times on the shortest path on the road network. ....	138
Figure 52 - Humber Estuary Scenario 4 Solution C. The green lines are for visualisation purposes: they connect each infrastructure asset to the closest warehouse. They do not represent distances, as distances are measured as travel times on the shortest path on the road network. ....	138
Figure 53 - Solution space and Pareto-front for Humber Estuary case study. Scenario 5. With the indication of the SolutionA that is visualised in Figure 54. ....	140
Figure 54 - Humber Estuary Scenario 5 Solution A. The green lines are for visualisation purposes: they connect each infrastructure asset to the closest warehouse. They do not represent distances, as distances are measured as travel times on the shortest path on the road network. ....	140

Figure 55 - Solution space and Pareto-front for Humber Estuary case study. Scenario 6. With the indication of Solutions A, B and C that are visualised respectively in Figure 56, Figure 57 and Figure 58.....	141
Figure 56 - Humber Estuary Scenario 6 Solution A. The green lines are for visualisation purposes: they connect each infrastructure asset to the closest warehouse. They do not represent distances, as distances are measured as travel times on the shortest path on the road network.....	142
Figure 57 - Humber Estuary Scenario 6 Solution B. The green lines are for visualisation purposes: they connect each infrastructure asset to the closest warehouse. They do not represent distances, as distances are measured as travel times on the shortest path on the road network.....	142
Figure 58 - Humber Estuary Scenario 6 Solution C. The green lines are for visualisation purposes: they connect each infrastructure asset to the closest warehouse. They do not represent distances, as distances are measured as travel times on the shortest path on the road network.....	143
Figure 59 - Solution space and Pareto-front for Humber Estuary case study. Scenario 7. With the indication of Solutions A, B and C that are visualised respectively in Figure 60, Figure 61 and Figure 62.....	144
Figure 60 - Humber Estuary Scenario 7 Solution A. The green lines are for visualisation purposes: they connect each infrastructure asset to the closest warehouse. They do not represent distances, as distances are measured as travel times on the shortest path on the road network.....	145
Figure 61 - Humber Estuary Scenario 7 Solution B. The green lines are for visualisation purposes: they connect each infrastructure asset to the closest warehouse. They do not represent distances, as distances are measured as travel times on the shortest path on the road network.....	145
Figure 62 - Humber Estuary Scenario 7 Solution C. The green lines are for visualisation purposes: they connect each infrastructure asset to the closest warehouse. They do not represent distances, as distances are measured as travel times on the shortest path on the road network.....	146
Figure 63 - Solution space and Pareto-front for Humber Estuary case study. Scenario 8. With the indication of Solutions A, B and C that are visualised respectively in Figure 64, Figure 65 and Figure 66.....	147
Figure 64 - Humber Estuary Scenario 8 Solution A. The green lines are for visualisation purposes: they connect each infrastructure asset to the closest warehouse. They do not represent distances, as distances are measured as travel times on the shortest path on the road network.....	148
Figure 65 - Humber Estuary Scenario 8 Solution B. The green lines are for visualisation purposes: they connect each infrastructure asset to the closest warehouse. They do not represent distances, as distances are measured as travel times on the shortest path on the road network.....	148
Figure 66 - Humber Estuary Scenario 8 Solution C. The green lines are for visualisation purposes: they connect each infrastructure asset to the closest warehouse. They do not	



represent distances, as distances are measured as travel times on the shortest path on the road network. ....	149
Figure 67 - Solution space and Pareto-front for Humber Estuary case study. Scenario 9. With the indication of Solutions A, B and C that are visualised respectively in Figure 68, Figure 69 and Figure 70. ....	150
Figure 68 - Humber Estuary Scenario 9 Solution A. The green lines are for visualisation purposes: they connect each infrastructure asset to the closest warehouse. They do not represent distances, as distances are measured as travel times on the shortest path on the road network. ....	151
Figure 69 - Humber Estuary Scenario 9 Solution B. The green lines are for visualisation purposes: they connect each infrastructure asset to the closest warehouse. They do not represent distances, as distances are measured as travel times on the shortest path on the road network. ....	151
Figure 70 - Humber Estuary Scenario 8 Solution C. The green lines are for visualisation purposes: they connect each infrastructure asset to the closest warehouse. They do not represent distances, as distances are measured as travel times on the shortest path on the road network. ....	152
Figure 71 - Solution space and Pareto-front for Humber Estuary case study. Scenario 10. With the indication of Solutions A, B and C that are visualised respectively in Figure 72, Figure 73 and Figure 74. ....	154
Figure 72 - Humber Estuary Scenario 10 Solution A. The green lines are for visualisation purposes: they connect each infrastructure asset to the closest warehouse. They do not represent distances, as distances are measured as travel times on the shortest path on the road network. ....	154
Figure 73 - Humber Estuary Scenario 10 Solution B. The green lines are for visualisation purposes: they connect each infrastructure asset to the closest warehouse. They do not represent distances, as distances are measured as travel times on the shortest path on the road network. ....	155
Figure 74 - Humber Estuary Scenario 10 Solution C. The green lines are for visualisation purposes: they connect each infrastructure asset to the closest warehouse. They do not represent distances, as distances are measured as travel times on the shortest path on the road network. ....	155
Figure 75 - Solution space and Pareto-front for Humber Estuary case study. Scenario 11. With the indication of Solutions A, B and C that are visualised respectively in Figure 76, Figure 77 and Figure 78. ....	156
Figure 76 - Humber Estuary Scenario 11 Solution A. The green lines are for visualisation purposes: they connect each infrastructure asset to the closest warehouse. They do not represent distances, as distances are measured as travel times on the shortest path on the road network. ....	157
Figure 77 - Humber Estuary Scenario 11 Solution B. The green lines are for visualisation purposes: they connect each infrastructure asset to the closest warehouse. They do not represent distances, as distances are measured as travel times on the shortest path on the road network. ....	157

Figure 78 - Humber Estuary Scenario 11 Solution C. The green lines are for visualisation purposes: they connect each infrastructure asset to the closest warehouse. They do not represent distances, as distances are measured as travel times on the shortest path on the road network.....	158
Figure 79 - Solution space and Pareto-front for Humber Estuary case study. Scenario 12. With the indication of Solutions A, B and C that are visualised respectively in Figure 80, Figure 81 and Figure 82.....	159
Figure 80 - Humber Estuary Scenario 12 Solution A. The green lines are for visualisation purposes: they connect each infrastructure asset to the closest warehouse. They do not represent distances, as distances are measured as travel times on the shortest path on the road network.....	160
Figure 81 - Humber Estuary Scenario 12 Solution B. The green lines are for visualisation purposes: they connect each infrastructure asset to the closest warehouse. They do not represent distances, as distances are measured as travel times on the shortest path on the road network.....	160
Figure 82 - Humber Estuary Scenario 12 Solution C. The green lines are for visualisation purposes: they connect each infrastructure asset to the closest warehouse. They do not represent distances, as distances are measured as travel times on the shortest path on the road network.....	161
Figure 83 - Solution space and Pareto-front for Humber Estuary case study. Scenario 13. With the indication of Solutions A, B and C that are visualised respectively in Figure 84, Figure 85 and Figure 86.....	162
Figure 84 - Humber Estuary Scenario 13 Solution A. The green lines are for visualisation purposes: they connect each infrastructure asset to the closest warehouse. They do not represent distances, as distances are measured as travel times on the shortest path on the road network.....	163
Figure 85 - Humber Estuary Scenario 13 Solution B. The green lines are for visualisation purposes: they connect each infrastructure asset to the closest warehouse. They do not represent distances, as distances are measured as travel times on the shortest path on the road network.....	163
Figure 86 - Humber Estuary Scenario 13 Solution C. The green lines are for visualisation purposes: they connect each infrastructure asset to the closest warehouse. They do not represent distances, as distances are measured as travel times on the shortest path on the road network.....	164
Figure 87 - Pareto front heatmap representing the probability of allocation of a warehouse by the RAO framework. a) BAU scenario. b) Disruption scenario. ....	167
Figure 88 - Comparison of Pareto fronts from different scenarios. ....	169
Figure 89 - Pareto front heatmap representing the probability of allocation of a warehouse by the RAO framework in all scenarios with a fully functional road network.....	171
Figure 90 - New Zealand and Northland maps. ....	174
Figure 91 - Current distribution of clinics and general practitioners in Northland. ....	176
Figure 92 - Available locations for clinics and meshblock centroids in Northland. ....	178

Figure 93 - Pareto fronts evolution of the Northland case study: a) Business as usual scenario, target ratio patients/GPs 1500; b) Business as usual scenario, target ratio 2500; c) Disruption scenario, target ratio 1500; d) Disruption scenario, target ratio 2500. ....	186
Figure 94 - Major risk areas in Northland. Map developed from Northland Regional Council (2018).....	188
Figure 95 - Solution space and Pareto-front for Northland case study. BAU scenario, target ratio 1500. ....	190
Figure 96 - Thresholds in the solution space for Northland case study. BAU scenario, target ratio 1500. ....	191
Figure 97 - Highlight of the Pareto-front for the Northland BAU scenario (target ratio 1500) with the indication of the number of Pareto-optimal spatial plans. Solutions A and B are visualised in Figure 98, Figure 99, Table 15 and Table 16. ....	192
Figure 98 - Northland Case study, BAU scenario, Target ratio patients/GPs: 1500, Solution A (from Figure 97). The green lines are for visualisation purposes: they connect each meshblock centroid to the closest GP clinic. They do not represent distances, as distances are measured as travel times on the shortest path on the road network.....	193
Figure 99 - Northland Case study, BAU scenario, Target ratio patients/GPs: 1500, Solution B (from Figure 97). The green lines are for visualisation purposes: they connect each meshblock centroid to the closest GP clinic. They do not represent distances, as distances are measured as travel times on the shortest path on the road network.....	195
Figure 100 - Solution space and Pareto-front for Northland case study. BAU scenario, target ratio 2500. ....	197
Figure 101 - Highlight of the Pareto-front for the Northland BAU scenario (target ratio 2500) with the indication of the number of Pareto-optimal spatial plans. Solution A and B are visualised in Figure 102, Figure 103, Table 17 and Table 18. ....	198
Figure 102 - Northland Case study, BAU scenario, Target ratio patients/GPs: 2500, Solution A (from Figure 101). The green lines are for visualisation purposes: they connect each meshblock centroid to the closest GP clinic. They do not represent distances, as distances are measured as travel times on the shortest path on the road network.....	199
Figure 103 - Northland Case study, BAU scenario, Target ratio patients/GPs: 2500, Solution B (from Figure 101). The green lines are for visualisation purposes: they connect each meshblock centroid to the closest GP clinic. They do not represent distances, as distances are measured as travel times on the shortest path on the road network.....	201
Figure 104 - Thresholds in the solution space for Northland case study. Disruption scenario, target ratio 1500.....	203
Figure 105 - Highlight of the Pareto-front for the Northland disruption case study (target ratio 1500) with the indication of the number of Pareto-optimal spatial plans. Solutions A and B are visualised in Figure 106, Figure 107, Table 19 and Table 20.....	204
Figure 106 - Northland Case study, disruption scenario, Target ratio patients/GPs: 1500, Solution A (from Figure 105). The green lines are for visualisation purposes: they connect each meshblock centroid to the closest GP clinic. They do not represent distances, as distances are measured as travel times on the shortest path on the road network.....	205
Figure 107 - Northland Case study, disruption scenario, Target ratio patients/GPs: 1500, Solution B (from Figure 105). The green lines are for visualisation purposes: they connect	

each meshblock centroid to the closest GP clinic. They do not represent distances, as distances are measured as travel times on the shortest path on the road network. .... 207

Figure 108 - Solution space and Pareto-front for Northland case study. Disruption scenario, target ratio 2500. .... 209

Figure 109 - Highlight of the Pareto-front for the Northland disruption scenario (target ratio 2500) with the indication of the number of Pareto-optimal spatial plans. Solutions A and B are visualised in Figure 110 Figure 111, Table 21 and Table 22. .... 210

Figure 110 - Northland Case study, disruption scenario, Target ratio patients/GPs: 2500, Solution A (from Figure 109). The green lines are for visualisation purposes: they connect each meshblock centroid to the closest GP clinic. They do not represent distances, as distances are measured as travel times on the shortest path on the road network. .... 211

Figure 111 - Northland Case study, disruption scenario, Target ratio patients/GPs: 2500, Solution B (from Figure 109). The green lines are for visualisation purposes: they connect each meshblock centroid to the closest GP clinic. They do not represent distances, as distances are measured as travel times on the shortest path on the road network. .... 213

Figure 112 - Comparison of different levels of accessibility in different scenarios: a) BAU scenario, b) Disruption scenario. .... 216

Figure 113 - Comparison of infrastructure cost with respect to current Northland situation for different values of  $\gamma_c$  and TR for a fixed value of  $f_{time}$ . .... 221

## II. List of tables

Table 1 - Environment Agency's flood risk zones for England. ....	36
Table 2 - Table of evolutionary operators used in the RAO framework .....	88
Table 3 - UK case study problem definition summary table. ....	91
Table 4 - Input data for the Humber Estuary case study. ....	94
Table 5 - Average perimeter of strategic infrastructure assets in the Humber Estuary region. ....	102
Table 6 - Sizes of warehouses for the Humber Estuary case study.....	102
Table 7 - Regression options for annual rent prices and warehouses' dimensions.....	104
Table 8 - Scenario assumptions - Uniform rent price, discrete cost function.....	118
Table 9 - Solutions forming the Pareto-front of the Humber Estuary – scenario 1. ....	122
Table 10 - Scenario assumptions - Uniform rent price, discrete cost function - disrupted road network.....	127
Table 11 - Northland case study problem definition summary table. ....	173
Table 12 - Result of the preliminary analysis of primary healthcare accessibility in Northland. ....	175
Table 13 - Input data for the Northland case study. ....	179
Table 14 - Risks on critical road sections in Northland. ....	187
Table 15 - Northland case study, BAU scenario, target ratio patients/GPs: 1500, solution A (from Figure 97). Accessibility table. ....	194
Table 16 - Northland case study, BAU scenario, target ratio patients/GPs: 1500, solution B (from Figure 97). Accessibility table. ....	196
Table 17 - Northland case study, BAU scenario, target ratio patients/GPs: 2500, solution A (from Figure 101). Accessibility table. ....	200
Table 18 - Northland case study, BAU scenario, target ratio patients/GPs: 2500, solution B (from Figure 101). Accessibility table. ....	202
Table 19 - Northland case study, Disruption scenario, target ratio patients/GPs: 1500, solution A (from Figure 105). Accessibility table.....	206
Table 20 - Northland case study, Disruption scenario, target ratio patients/GPs: 1500, solution B (from Figure 105). Accessibility table.....	208
Table 21 - Northland case study, Disruption scenario, target ratio patients/GPs: 2500, solution A (from Figure 109). Accessibility table.....	212
Table 22 - Northland case study, Disruption scenario, target ratio patients/GPs: 2500, solution B (from Figure 109). Accessibility table.....	214
Table 23 - Northland scenarios accessibility comparison. The current distribution of clinics and GPs in Northland is considered as the baseline for the assessment of the improvements provided by the different Pareto-optimal solutions in terms of accessibility and costs. ....	217
Table 24 - Accessibility analysis of BAU scenario for different values $\gamma_c$ of and TR for a vixed value of $f_{time}$ . ....	220



# 1. Introduction

## 1.1. Infrastructure and climate risks

Six hundred million human lives claimed and four billion people impacted by extreme weather are the numbers of the last two decades of environmental crisis (CRED and UNISDR, 2015). In fact, floods, storms, heatwaves and other weather-related events have caused more than 90% of natural disasters in the last 20 years.

Future natural disasters are foreseen to become more frequent and more severe (Global Commission on Adaptation, 2019) and their impact will be higher on cities as the world urban population is arising – more than half of the world population already lives in urban environments and by 2050 the projections say that it will be around 68% (Batty, 2018; United Nations, 2019) .

Together with high concentrations of population, urban areas imply high concentrations of infrastructure. Infrastructure networks are the backbone of all human and economic activities undergoing in cities. Therefore, ensuring a high level of resilience to natural disasters to strategic infrastructure means making communities more resilient.

Strategic infrastructure is a particular class of infrastructure that comprises telecommunications, power systems, banking and finance, transportation, water supply, government and emergency services. Their disruption would imply potentially disastrous effects on human lives and economic activities of the country (US President's Commission on Critical Infrastructure Protection, 1997).

Among the other climate change-related hazards that endanger human settlements, flooding is particularly devastating both in terms of human lives and economic losses. Floods are a worldwide threat and different countries adopt different flood management approaches according to the different nature of their environments, their risks and their legislations.

Current approaches to flood risk management focus on protecting people, as it is not always possible to protect infrastructure (especially linear infrastructure networks). This would simply require too many resources and too high costs. Hence the need for a sensible approach to identifying where to strategically allocate limited resources, in order to optimise investments and achieve the best possible results at minimum cost.

The National Flood Resilience Review (Cabinet Office and DEFRA, 2016) provides an overview of the UK government’s strategy in addressing flood risk management in the country. It highlights the fundamental role of strategic infrastructure in underpinning business as usual economic activities and even more so during emergencies.

It also explores the potential role of temporary flood defences not only as a ‘backup’ solution, but also as a valid alternative to structural measures to take into consideration when designing flood mitigation strategies. The review also presents the funding allocation and plan to increase the Environment Agency’s temporary defences stock together with the Agency’s intention not only to increase the currently available stock of temporary flood defences, but also to identify “further strategic storage sites across the country, enabling temporary barrier deployment anywhere in England within 12 hours (3 hours driving and 9 hours loading and unloading)” (Cabinet Office and DEFRA, 2016).

Temporary flood defences are the focus of the main case study of the present work. Starting from a real-life allocation problem, this research proposes a spatial multi-objective location-allocation optimisation methodology.

## 1.2. Methods

A Resource Allocation Optimisation (RAO) methodology is developed to solve the spatial optimisation problem of temporary flood defences storage space allocation. Nevertheless, the optimisation framework is designed to be general enough to be applied to different allocation problems of the same nature.

This choice is justified by the fact that many resource allocation problems dealing with emergency response or infrastructure resilience to natural disasters share a common conceptual (and therefore mathematical) formulation. A common feature of such problems is the presence of conflicting objectives that make it impossible to find a global optimal solution of the problem, as improving the performance of solutions with respect to one objective necessarily implies the worsening of some other objective.

An example of this dynamics – relative to spatial optimisation problems – regards the conflict between the maximisation of accessibility and the minimisation of costs. When designing



emergency response strategies, resources' accessibility maximisation and costs minimisation are the main ingredients of efficient and cost-effective plans.

These objectives are contrasting by nature and their simultaneous optimisation is impossible by definition. Consequently, multi-objective optimisation aims at trade-off balancing; its outcome is a portfolio of different solutions that optimally balance the trade-off between conflicting objectives, rather than a single optimal global solution

A series of available optimisation techniques are currently available and extensive literature provides methodologies and applications to different problems. However, a spatial optimisation framework explicitly designed to solve resources allocation in an emergency response context is not present in the literature.

The digital revolution provides us today with unprecedented tools for complex analyses involving big data, together with a likewise unprecedented computational power availability. Nonetheless, some problems still involve too big data or too complex analyses to be solved with mathematical exact methods in a reasonable time. This is why this work contemplates the use of heuristic computational approaches that allow the exploration of broader and more complex formulations, considering the acceptance of a margin of error.

This work applies spatial optimisation to infrastructure resilience and sustainability in emergency planning problems. It addresses these problems by proposing a RAO framework meant as a potential support tool for urban planners and decision-makers when designing emergency management strategies. The final goal is to provide a methodology able to support planning decisions that efficiently make use of the available means, ultimately saving money and resources, which implicitly implies cost-efficiency and sustainability.

### 1.3. Thesis outline

This work aims to develop and demonstrate an optimisation-based decision support tool to help infrastructure operators and urban planners to identify strategies that improve the resilience of infrastructure services during disruptive natural hazards. In order to achieve this aim, the thesis has five objectives:

1. To review the field of flood risk management to identify the conflicts and barriers that can occur in the allocation of resources to enhance infrastructure resilience;
2. To review optimisation techniques, in particular their application to spatial resource allocation problems, to identify a suitable approach;
3. To develop a Resource Allocation Optimisation (RAO) framework that generates optimal spatial plans, to support infrastructure and urban planners to meet criteria identified in objective 2;
4. The application and demonstration of the RAO approach to different case studies to demonstrate its utility and transferability;
5. The analysis of the results from case studies and discussion of the utility of spatial optimisation to help improve infrastructure resilience.

Objective 1 aims at understanding the state of the art of current flood risk management approaches and identifying new strategies to enhance infrastructure resilience. Chapter 2 presents a review of different flood management strategies and introduces temporary flood defences as a potential viable alternative to structural measures for strategic infrastructure flood protection.

Objective 2 has the goal to set the methodological ground of the research and to understand the current availability of optimisation techniques in the scientific community, review them and find the most suitable to constitute the architecture of the framework to be built. This is the topic of Chapter 3, where the mathematical formulation of optimisation problems is initially presented, followed by a review of different techniques available for spatial problems.

Objective 3 aims at the formulation of a mathematically-based approach to solve urban planning problems meant to increase infrastructure resilience to natural hazards. This is addressed in Chapter 4, where the architecture of the RAO framework is explained together with the details and the algorithm's workflow.

Objective 4 consists in the application of the RAO developed by Objective 3 to two different case studies as proof of concept. Chapter 5 presents a UK case study on temporary flood defences storing space optimisation. Here the RAO provides solutions that balance the trade-off between accessibility maximisation to emergency resources and costs minimisation. Chapter 6 presents a second case study in New Zealand, where the RAO is applied to a

different problem with a similar mathematical formulation: the spatial optimisation of healthcare infrastructure assets allocation.

Finally, Objective 5, addressed in Chapters 5, 6 and 7, concerns the analysis of the results of the case study and explores the potential generalisation and application to other real-life urban planning resource management problems.



## 2. Infrastructure resilience and emergency planning

### 2.1. Introduction Chapter 2

Chapter 2 presents a literature review on emergency planning and climate risks in urban areas exploring the role of strategic infrastructure in emergency response operations. A definition and classification of strategic infrastructure are provided in section 2.2.1, followed by an analysis of the urban dimension of climate risks and a highlight of the close relation between infrastructure resilience to natural hazards and sustainable planning. The following section 2.3 presents an overview of different flood emergency planning approaches comparing flood protection strategies in the UK and overseas. Finally, temporary flood defences are introduced and their use compared to structural measures in section 2.3.2.2, this is particularly relevant for the case study described in Chapter 5.

### 2.2. Climate risks in urban areas

#### 2.2.1. Strategic infrastructure

Strategic infrastructure networks underpin the functioning of every human and economic activity in urban and rural areas. Understanding and protecting them is crucial to guarantee the normal functioning of cities, to prevent failures and to cope with catastrophic events.

The US President's Commission on Critical Infrastructure Protection (1997) identified different typologies of strategic infrastructure: telecommunications, power systems (electric, natural gas & oil), banking and finance, transportation, water supply systems, government services and emergency services. They are acknowledged as “strategic” because their failure or disruption would have severe and potentially catastrophic effects on citizens’ safety or the country’s defence and economic security. The same report highly stresses the absolute priority of guaranteeing the security, continuity, and availability of such infrastructure networks (Vamvakeridou-Lyroudia *et al.*, 2018; Gibson *et al.*, 2019; Vamvakeridou-Lyroudia *et al.*, 2020).

Strategic infrastructures are complex adaptive systems (Axelrod and Cohen, 2000): following complex systems’ logic, infrastructure networks cannot just be considered the mere sum of their different components, since they constantly interact with and influence each other

evolving through time, learning and improving from past experiences. An example of such additional complexity is the fact that the well-placed disposition of all the components of a water supply system does not guarantee an efficient water supply service; that depends from a precise number of other factors, frameworks and services that are external to the physical network (e.g. workforce organisation, power supply, telecommunication, etc.). This is typical of complex systems: they present an emergent behaviour that is beyond the simple sum of their components (Bonabeau *et al.*, 1999).

Rinaldi *et al.* (2001) provide a qualitative analysis of infrastructure interdependencies taking into account different factors like:

- 1) infrastructure characteristics (organisational, operational, temporal, spatial);
- 2) their state of operation (normal, repair/restoration, stressed/disrupted);
- 3) different types of failure (common cause, cascading, escalating);
- 4) different types of interdependencies (physical, cyber, logical, geographic);
- 5) coupling and response behaviour (adaptive, loose/tight, inflexible, linear/complex).

They also provide a clear example of connections and interdependencies between critical infrastructure networks, highlighting how failures or disruptions can have direct or indirect effects on the entire system. Figure 1 summarises such a series of dependencies and interdependencies among different components of the system and emphasises the importance of knowing and understanding them in the perspective of the system's defence and resilience.

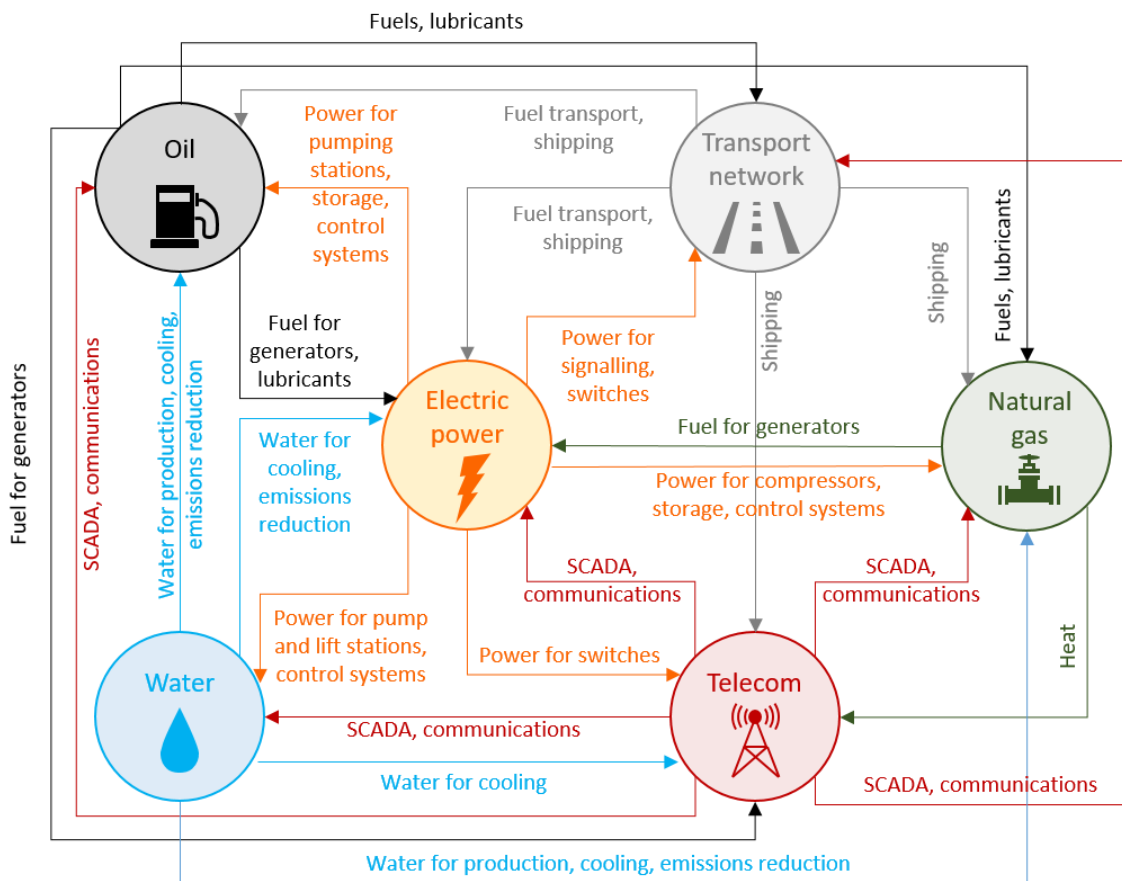


Figure 1 - Developed from (Rinaldi et al., 2001), examples of infrastructure networks interdependencies.

In a world of increasing complexity due to unprecedented technological progress, it will become more and more important to study, analyse, understand and manage complex systems of systems to ensure safety and resilience in light of future challenges due to a changing climate. This research models several infrastructure disruption scenarios to evaluate and improve their resilience to natural disasters, making use of artificial intelligence techniques like genetic algorithms and machine learning to cope with the high computational effort required by multi-objective optimisation.

### 2.2.2. Climate change-related problems in cities

The world faces an environmental crisis: more than 90% of disasters of the last two decades have been caused by floods, storms, heatwaves and other weather-related events, claiming six hundred millions human lives and leaving a total of four billion people in an emergency condition (CRED and UNISDR, 2015). Climate is changing and will continue to change; humans' only choice is to adapt (IPCC, 2014). Climate change's impacts are predicted to become more

severe in the near future in terms of global higher temperatures, rising oceans, more violent and unpredictable storms and rainfall (Global Commission on Adaptation, 2019).

Climate change will have higher repercussions in cities than everywhere else since urban environments are where the majority of people lives (55% of the world population in 2018) with an even higher predicted concentration in the future (68% by 2050). In western societies, the urban population is even higher (around 80%), with European peaks of 92% (Netherlands) and 98% (Belgium). Regarding the case studies analysed in this work, the urban population is still widely above the global average: 83% for the UK and 87% for New Zealand (United Nations, 2019).

Urban areas are also the places where a higher number of infrastructure networks are concentrated and deeply interconnected and where the majority of human and economic activities take place. Therefore, cities are necessarily more sensitive to natural hazards' effects, whose impacts are potentially catastrophic because of the high number of people, infrastructure and economic interests involved (Garschagen and Romero-Lankao, 2015; Lu *et al.*, 2018).

### 2.2.3. Infrastructure resilience to natural hazards

Resilience is commonly defined as the capacity of a system of recovering from a disruption (Holling, 1973; Holling, 1996; Folke *et al.*, 2010). Such a definition is very broad and somehow vague; in fact, numerous different definitions of resilience can be found according to what this concept is applied to. In this work, the main interest is the capacity of infrastructure systems to cope and recover after natural disasters, with a particular focus on flood events (see chapter 2.3).



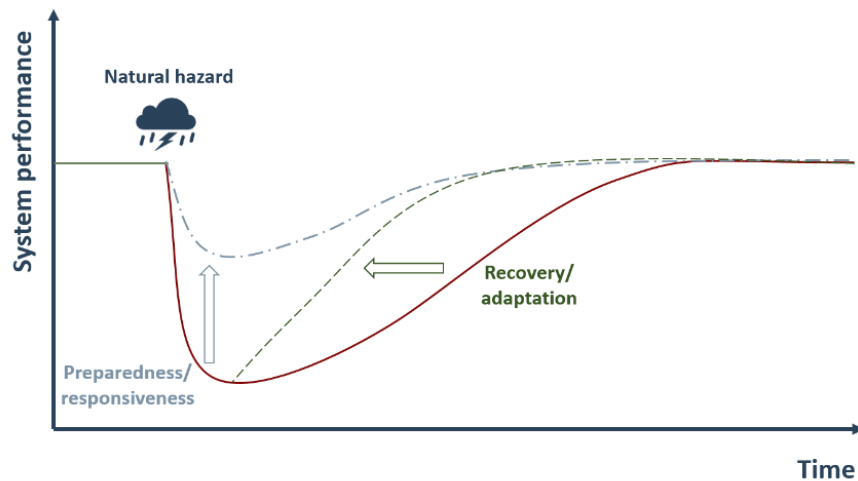


Figure 2 - Definition of resilience: the capacity of a system to recover after a disruption.

Figure 2 shows different ways to make a system resilient to a specific natural hazard. The red line represents the performance of the system after the disastrous event: after a certain amount of time and investment of resources, the system returns to its standard status of “normality”.

Making the system more resilient means reducing the amount of time necessary to bring it back to normality. To achieve this goal, one way is to invest in the recovery side (green line in Figure 2): this implies spending resources after the disaster occurred in order to accelerate recovery. On the other hand, it is possible to invest on the preparedness or responsiveness side (light blue line in Figure 2): this implies investing resources beforehand in order to reduce the impact of possible disasters, cutting down the recovery time.

The second approach is more cost-effective than acting on the restoration side, and more cost-effective investments imply lower wastefulness of resources, capitals, emissions and ultimately higher sustainability (Tainter and Taylor, 2014). Therefore, this study focuses on the preparedness/responsiveness approach with the aim of providing a scientifically-based methodology to: 1) solve the real-life problems presented in the case studies of Chapters 5 and 6 and 2) present a general methodological framework to optimise natural disasters preparedness of strategic infrastructure systems.

In light of this, the present research is framed within three UN Sustainable Goals (UN General Assembly, 2015): 9) Industry innovation and infrastructure, 11) Sustainable cities and communities and 13) Climate action (Figure 3) (Adshead *et al.*, 2019).



Figure 3 - UN Sustainable Development Goals.

Sustainable Development (SD), Climate Change Adaptation (CCA) and Disaster Risk Reduction (DRR) constitutes different communities, each one with its own framework of reference. The 2030 Agenda for sustainable development (UN General Assembly, 2015) is the primary reference framework for the Sustainable Development community. The Paris Agreement (UNFCCC, 2015) is an international legally binding document signed by governments to set a common agenda in terms of climate change actions. DRR community's main reference, instead, is the Sendai framework for disaster risk reduction (UNISDR, 2015).

Despite the similarity of their objectives, the three communities address these topics independently and often with a lack of coordination and cooperation. All the aforementioned reference documents have very similar main objectives, the same timeframe (2015-2030) and they have been published almost simultaneously. Nevertheless, they adopt different perspectives and rarely overlap nor cite each other's main topics. For example, the Paris agreement cites DRR just one time and no other reference is made in the whole document to this field and the Sendai framework actively sustains the artificial distinction between CCA, DRR and Sustainable Development (Kelman, 2017).

A shared focus, instead, is the attention to the urban dimension that all the Post-2015 frameworks have. They all identify cities and urban areas as critical contexts where policies, actions and measures should be concentrated to maximise their impact (Cabinet Office, 2011; Garschagen and Romero-Lankao, 2015; Gencer, 2017). It is in this perspective that the focus of this work - resilient urban systems - is not just framed within the DRR perspective, but is part of the broader picture also involving CCA and SD.

Given the current uncertainty regarding the future and the rapidly evolving climate situation, current measures, interventions and policies need to be continuously kept up to date, also with the awareness that actions taken today may worsen tomorrow's reality in case of design exceedance (Dawson, 2007; Aerts *et al.*, 2011; IPCC, 2012; Pregolato, 2017).

## 2.3. Flood emergency planning

### 2.3.1. Flood risk management

Flooding is a major problem both in the UK and overseas (Hu *et al.*, 2019). Many countries worldwide periodically face natural disasters like recent events in the USA, with Hurricane Harvey (Blake and Zelinsky, 2018), and the devastating floods of the Philippines (Cabrera and Lee, 2018) and Japan (Niroshinie *et al.*, 2016; Shakti *et al.*, 2018). In Europe, the most recent events happened in Spain (Lorenzo-Lacruz *et al.*, 2019), Italy (Arrighi and Castelli, 2020) and Germany (Meyer and Schwarze, 2019). The UK is facing catastrophic flood events with increasing recurrence, like Storm Desmond and its consequences on strategic infrastructure collapse in Lancaster (Ferranti *et al.*, 2017) and other flood-prone regions that have been hit by disastrous floods in the past years like Somerset, Cumbria and Yorkshire. Here 20,000 properties flooded in 2015/16 with estimate damages of ~£1.5 billion (Cabinet Office and DEFRA, 2016).

Besides, the situation is not expected to improve: the wettest February on record (2020) witnessed storms Ciara and Dennis, which had a severe impact on UK infrastructure, causing major floods throughout the country (The Parliamentary Office of Science and Technology, 2020).

Floods' heavy toll on economies and human lives make them one of the most significant threats of climate change. Hence the interest of the present work to focus on flooding and on strategic infrastructure resilience to flooding. In fact, the spatial optimisation analyses of the two case studies presented (the first in the UK and the second in New Zealand) consider flooding as the natural hazard of reference (with the addition of landslides in the NZ instance).

The 2016 UK National Flood Resilience Review (Cabinet Office and DEFRA, 2016) provides an interesting overview of several international approaches to flood resilience. Three EU

countries (UK, France and the Netherlands) and three extra-EU countries (USA, Japan and Australia) are compared.

A first analysis regards the number of people at risk; Figure 4 shows a chart with indicative percentages of the at-risk population for each country, with specifications (where available) of the annual chance of flooding people are exposed to.

16% of England’s mainland, comprising around 8% of the country’s population, has an annual flood risk greater than 0.1% (Environment Agency, 2015). The UK National Flood Risk Management and Coastal Erosion Strategy (Environment Agency and DEFRA, 2011) presents an extensive array of approaches to tackle flood risk elaborated after 2007 England flooding events and the following Pitt Review (Pitt, 2008). Flood risk is mapped at the national level by the Environment Agency, who divided the country into three zones with different associated risk levels, as summarised in Table 1.

*Table 1 - Environment Agency's flood risk zones for England.*

	<b>England’s land area %</b>	<b>Annual chance of flooding from rivers</b>	<b>Annual chance of flooding from the sea</b>
Zone 3	10%	≥ 1%	≥ 0.5%
Zone 2	2%	≤ 1% and ≥ 0.1%	≤ 0.5% and ≥ 0.1%
Zone 1	78%	< 0.1%	< 0.1%

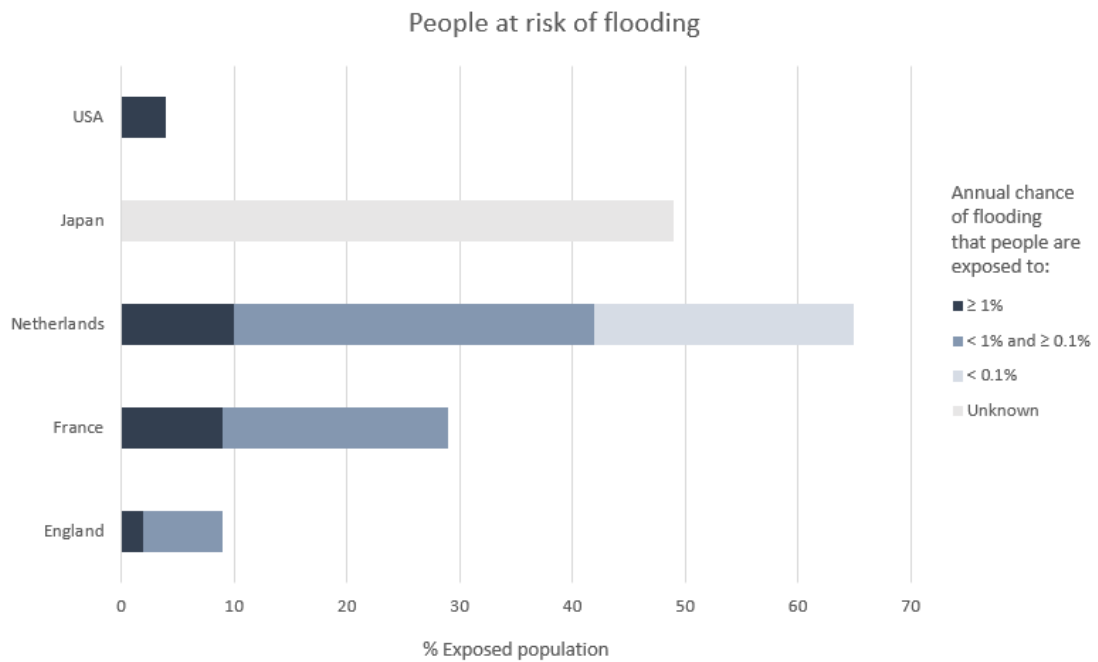


Figure 4 - Indicative percentages of the population at risk of flooding from rivers and the sea. Developed from Cabinet Office and DEFRA (2016).

According to the French National preliminary Flood Risk Assessment (Ministère de L'Écologie, 2011), in France, the percentage of the country's population with an annual flood risk of 0.1% rises to 28%. If we consider 100 years return period events, 8% of the population would be at risk. To address this problem, the French Government implemented different flood risk management strategies, like restricted-development areas (flood risk is mapped at the national level) and a governmental flood compensation fund. The two reference documents with respect to these different approaches are the Programmes d'Action de Prévention des Inondations – PAPI (Ministère de l'Écologie, 2017) and the Plan Submersions Rapide (Ministère de l'Écologie *et al.*, 2010). In 2014, the French government initiated a decentralisation process shifting flood risk management responsibilities to local authorities (Larrue *et al.*, 2016).

Relative numbers significantly grow when considering the Netherlands: 59% of the country's mainland is at risk of flood, and almost the totality (98%) of this land is protected by dykes (PBL Netherlands Environmental Assessment Agency, online). Despite these protection structures, 65% of the population live in areas that have an annual chance of flooding between 0.4% and 0.01%. This is due to the peculiar land conformation of the country: a combination of several major European river deltas (Rhine and Meuse) and vast portions of the country

that are below sea level. Taking that into consideration, flood response lead times are, regardless, relatively high (Thieken *et al.*, 2014).

Differently from England and France, the Dutch government set a legal standard of protection, which is the reference that all the flood risk management measures aim to meet. The government's programme 'Ruimte voor de Rivier' (in English: room for the river) has been active from 2006 to 2015 and involved major actions in reducing riverine flood risk in the country adopting a multi-layer safety definition. The interventions included dykes relocation, flood bypasses, groynes height reduction, floodplain level lowering, obstacles removal and side channels depth lowering (Kaufmann *et al.*, 2016; Vergouwe *et al.*, 2016). Also in the Netherlands, flood risk is mapped at the national level, but here flood risk management is less centralised: local authorities are in charge to manage their own spatial zoning plans.

From the fluvial flood perspective, the physical geography of Japan puts the country in a completely different position with respect to the Netherlands. While the Dutch mainland is predominantly flat and positioned at the mouth of big continental rivers, Japan is an archipelago of mountainous islands in the Pacific Ocean. Its rivers are short and steep, implying way shorter flood response lead times (Adachi, 2009).

49% of the Japanese population (127 million people) lives in areas at risk of flood from different sources: rivers, heavy rains, tsunamis and typhoons (Adachi, 2009; Suppasri *et al.*, 2013; Ministry of Land, online). To cope with recurrent disastrous flood events, the Japanese government adopts a mixed strategy including structural defences and warning and evacuation plans (Huang, 2014; Cabinet Office and DEFRA, 2016).

Around 40% of the landmass of the United States of America lies within the Mississippi River basin. In addition to the fluvial origin of flood risk in the country, the three coasts contribute to different kinds of hazard due to their different physical characteristics. The East coast facing the Atlantic Ocean is subject to hurricanes, the Gulf coast is subject to heavy rainfalls related to the tropical climate of the area and finally, tsunamis and cyclones endanger the West coast facing the Pacific Ocean.

In terms of population at risk of flooding, 2% of the population live in areas with 1% annual coastal flood risk, while 1% of the country's population has an annual chance to be flooded by rivers of 1% (Climate Central and ICF International, 2015; World Resources Institute, online).

The US government adopts a mixed approach of structural defences and policies to mitigate the risk of flooding on its territory (American Society of Civil Engineers, 2017). For example, the Federal Emergency Management Agency (FEMA) implemented the National Flood Insurance Program (NFIP). This programme is designed to produce Flood Insurance Rate Maps and offer affordable insurance to private citizens and businesses and to encourage local communities to implement and enforce flood management regulations (FEMA, online). With regards to federal buildings, instead, by law, they must be constructed 'above the hazard level' (NFIP requirement).

Australia's climate is one of the driest of the world at a continental level; nevertheless, here, it is possible to find extraordinary annual rainfall and runoff variability (Wenger *et al.*, 2013). The eastern coastal edge of the country is the most vulnerable from the flooding perspective because of the frequency of cyclones. The Australian central government manages flood warnings through the Bureau of Meteorology and defines flood risk management best practice, but the responsibility of their implementation is held by the single states (Australian Emergency Management Institute, 2013; Wenger *et al.*, 2013; Cabinet Office and DEFRA, 2016). Flood risk mapping, instead, is managed at the state level or even at the municipal level; the central government sets guidelines for development in flood-prone zones, but they are not binding and the single states develop their own regulations. The Flood and coastal risk management Long-term Investment Scenarios (LTIS) 2019 (Environment Agency, 2019) provides indications on how flood risk management investment decisions are made in the UK. This document assesses several scenarios involving different challenges like climate change, assets deterioration and growing population to describe future risks, opportunities and different possible long-term investments. It is based on the 2014 report (Environment Agency, 2014) and includes risk analyses regarding rivers, surface water the sea and coastal erosion. Section 11 of LTIS 2019 reports that the optimum level of investment is greater than LTIS's 2014 baseline, and it is estimated to have a long-term annual average above £1 billion. The document is meant to analyse the cost-effectiveness of different investment strategies to provide guidelines for future funding allocation.

This brief overview of international approaches to flood management shows how different countries face the same problem – flooding – with the same objective: more resilient communities and infrastructure. Nevertheless, different geographies are impacted by

different sources of flooding (e.g. fluvial, pluvial, tidal, etc.). Also, different regulations and administrations lead to different flood management solutions, approaches and frameworks. Flood resilience is a complex matter that involves different factors (hazards and geographies), different governance structures (governments, local administrations, asset owners and operators) and a range of physical infrastructure (flood defences, transportation networks etc.). Designing effective flood management strategies should consist in a holistic process taking into account all these factors and the peculiarities of each case study.

This study helps address such diversity in areas by developing a framework to balance conflicting objectives to identify optimal strategies for resilience. This allows what-if scenarios to be tested to identify a portfolio of optimal solutions tailored to minimise local flood risk to infrastructure.

### 2.3.2. Flood defences

As mentioned in the previous section, the UK's approach towards flood management comprises a mixture of policies and defences aimed at both flood protection and mitigation. This section focusses on flood defences that can be firstly categorised into two big families: structural and temporary measures.

#### 2.3.2.1. Structural measures

Structural flood defences consist of all those measures that have a permanent nature. They can be sub-categorised into 'grey' and 'green' structures or 'hard' and 'soft' measures (Sayers *et al.*, 2013). Grey – or hard – structures consist of dams and levees, while soft structures consist in wetlands storage or green infrastructure.

Hard structural defences have been the traditional way to defend land and people from floods, defending them merely creating an obstacle big enough for water not to overcome it. They consist of large, permanent and usually expensive engineering structures like dams and levees. Due to the high investment these measures require, the interest in the optimisation of their design and location strategies is high. Often structural defence strategies require the modification of topographic elevation (for instance through levees) or the modification of soil



roughness (for example through revegetation). Typically, the strategy definition is tailored to the specific needs and peculiarities of each case study. New high-performance computational tools allow better surface water models and the fast development of machine learning techniques and black-box optimisation open new possibilities for the definition more general flood management design principles (Tasseff *et al.*, 2019).

Several examples of optimisation strategies applied to structural flood defences can be found in the literature, like Woodward *et al.* (2014) who developed a framework for the assessment of potential interventions in flood systems and applied it to the Thames Estuary (London, UK). In addition, Tasseff *et al.* (2019) presented an optimisation methodology for structural mitigation strategies with constraints that may be either economic or physical (or both).

This kind of structures provides a solid and robust defence against even the most severe events; nevertheless, several shortcomings are peculiar to this category of defences: they are permanent structures, so their impact on the territory is very heavy, their construction cost is high and their maintenance expensive, and, finally, their adaptability is very limited as their upgrade is difficult, making their original design binding and not flexible enough to adjust to rapidly changing climates.

#### 2.3.2.2. Temporary measures

Temporary measures constitute an alternative to permanent structural defences. They cannot provide the same level of safety and security of structural measures, but they can offer a set of advantages that make them a valuable alternative worth to be considered. Above all, they are cheap, fast to implement and – as their name suggests – they have a temporary (and therefore lighter) impact on the territory.

Temporary flood defences are not fixed to the ground, so they can be deployed for the necessary amount of time and then removed, stored and reused when needed. There are four main categories of temporary barriers (Cabinet Office and DEFRA, 2016): 1) frame barriers, 2) free-standing barriers, 3) tubes and 4) filled containers. As Figure 5 shows, filled containers can be in turn classified basing on their filling (aggregate or water), and free-standing barriers can be either rigid or flexible.

A large variety of frame barriers are available on the market; Figure 5.a shows an example of a demountable metal framework deployed on a riverside. Frame barriers can adapt to different surfaces except for disconnected hard ground; they can also be cleaned and reused and given their rigidity, minor maintenance is usually necessary when deployed. On the downside, they can be subject to leakages, they require a large amount of storage space and, with low water levels, they are vulnerable to strong winds (Cabinet Office and DEFRA, 2016).

Figure 5.b and Figure 5.c present respectively a rigid and a flexible free-standing barriers. Free-standing barriers are easy and quick to deploy since they do not require any machinery for installation. When the barrier is flexible, its stability is guaranteed by the hydrostatic pressure of the water, besides flexible barriers are lighter and require less storage space in comparison to the other kinds of temporary defences. Like frame barriers, rigid free-standing barriers require a lot of storage space and are challenging to deploy in uneven rigid surfaces. Despite being an advantage in terms of storage and transportation, flexible free-standing barriers' lightweight can result in potential weaknesses as well. For example, they are vulnerable to strong winds or leakages when the water level is particularly low (Cabinet Office and DEFRA, 2016).

Tubes (Figure 5.d) are flexible barriers that can be filled with air or water and deployed to block or deflect groundwater. Their flexibility implies small storage areas and ease in their transportation and deployment. On the other hand, they require access to a source of water for filling and a way to dispose of it. Also, supervision is necessary when in place for multiple reasons (like danger of vandalism or risk of undesired displacements due to high water loads) (Cabinet Office and DEFRA, 2016).

Finally, filled containers (Figure 5.e and Figure 5.f) can be deployed where needed and filled with water or aggregate to create an impermeable obstacle for floodwater. Differently from tubes, they do not require much supervision when in place. Several advantages characterise filled containers: for example, local material can be used to fill them, they do not require specialised workforce for their installation, can easily be deployed on different terrains and their height can be increased at different stages. In contrast, their impact on the soil is substantial due to high pressures, their reuse is limited and finally, it is not always available or accessible a place for filling material disposal (Cabinet Office and DEFRA, 2016).

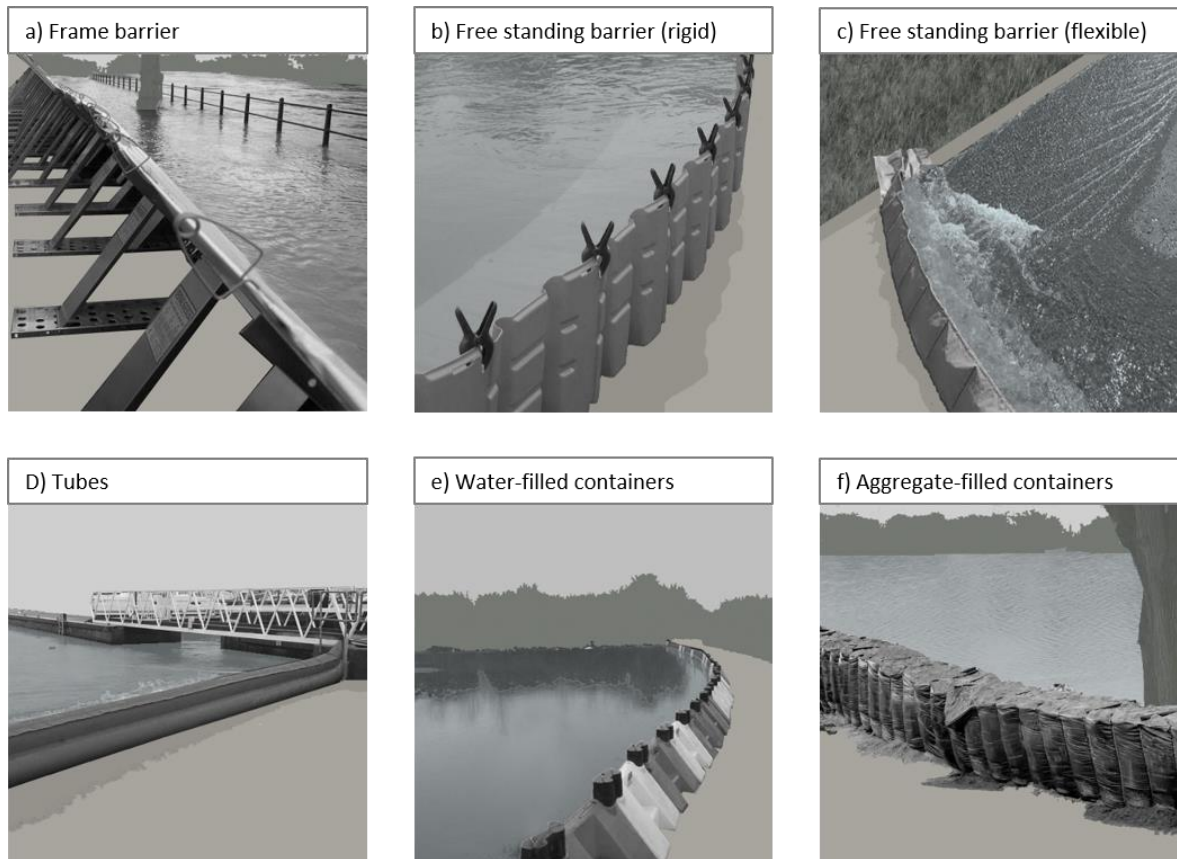


Figure 5 - Examples of temporary flood defences. a) Frame barriers, b) free-standing barriers (rigid), c) free-standing barriers (flexible), d) tubes, e) water-filled container, f) aggregate-filled container.

Temporary flood barriers are not an effective or unsuccessful flood protection measure per se. The applicability and cost-efficiency of this kind of approach vary from case to case depending on a series of factors. For instance, not all locations are suitable for all the typologies of temporary defences; moreover, this kind of procedure requires a certain amount of time for transportation and deployment, consequently good enough flood forecasts are a fundamental requisite for the efficacy of a temporary measure. Such forecasts are not always available, depending on the nature of the catchment taken into consideration (e.g. long rivers estuaries vs fast-responding mountain creeks).

Temporary defences' affordability and agility come with the price of lower protection levels with respect to permanent measures. According to Woolhouse (2017), the failure rate of temporary defences can vary between 20% and 30%, numbers that can be lowered with appropriate planning.

Another factor to take into consideration when assessing the advantages and disadvantages of temporary flood management measures is the necessity of staff to pick up, transport,

deploy, monitor, dismantle and store the flood defences. In addition to barriers, accessory items to carry, deploy and store can be pumps to use complementarily to barriers (or in substitution for small areas) and portable generators. The inclusion of the workforce makes the planning phase crucial for the efficacy of strategies.

The National Flood Resilience Review (Cabinet Office and DEFRA, 2016) dedicates an entire section (Chapter 3) to the analysis of temporary defences strategies to protect strategic infrastructure. A number of conclusions contained in this section constitute the base of some main assumptions at the base of the present research work:

1. 30% to 40% of local strategic infrastructure can be protected using temporary defences strategies according to the Environment Agency. Hence, the focus of this work on critical infrastructure protection optimisation.
2. The Environment Agency advises against the use of sandbags, despite their affordability, because of their low standard of protection and because of their very limited re-usability. For this reason, sandbags are not taken into account when evaluating volumes of required amounts of storing space in the optimisation framework presented in Chapter 5.
3. When assessing the suitability of temporary defences, the Environment Agency found that the category of strategic infrastructure protected is a "less of a determining factor than the size of the site". For this reason, different strategic infrastructure assets are generally differentiated only on the base of their site's dimension in the RAO framework presented in Chapter 5; however some scenarios also explore the prioritisation infrastructure assets's protection basing on their different categories.
4. Currently, temporary flood barriers cannot cope with water depths > 2 metres, and only a few have been tested above 1 metre. Hence, the choice to consider 1.5m as a reference height of flood defences when estimating maximum volumes required for storing space (Chapter 5).

This study contributes in assessing the efficacy and the cost-effectiveness of flood protection strategies involving different typologies temporary defences. In fact, the RAO framework presented in Chapter 4 and applied to a UK case study in Chapter 5 allows exploring different choices of temporary flood defences which entail different costs, volumes and deployment times.

Despite the National Flood Resilience Review (Cabinet Office and DEFRA, 2016) recognises the effectiveness of temporary flood defences, a systematic national strategy is currently missing. Every local authority autonomously decide how to include (or not to include) temporary flood barriers in their flood management strategies.

A clear example is represented by the case study presented in Chapter 5: the different flood protection strategies of the local governments of the Humber Estuary region (East Reading of Yorkshire, Kingston upon Hull and North Lincolnshire) do not take into account temporary flood defences in a systematic way.

Several investments and projects are currently under development to increase flood protection on the different banks of the Humber. For example, the Hull Frontage scheme (Environment Agency, 2019) is a £42 million investment flood alleviation scheme in the city of Hull on the north bank of the Humber. In the south bank, instead, a £12 million investment in flood defences started in 2019 in proximity South Ferriby (North Lincolnshire Council, 2019). Both these schemes have been completed in Spring 2021, and both of them only entail structural flood protection measures. The Local Flood Risk Management Strategy of The East Reading of Yorkshire (East Reading of Yorkshire Council, 2015) does not include the use of temporary flood barriers if not for extraordinary emergency situations, and it only contemplates the use of sandbags, which is deprecated by the National Flood Resilience Review (Cabinet Office and DEFRA, 2016). Also, the Flood risk management strategy of the city of Hull (Hull City Council, 2015) only mentions free-standing temporary flood barriers as an option for private citizens to protect their homes; considering it merely as a private voluntary optional initiative.

This research work provides a novel methodology and an optimisation platform to enrich and support the current practice by modelling, exploring and assessing resources' deployment strategies in a digital environment, with the ultimate goal to fill the gap between the national recommendations and the local implementation of flood protection strategies including temporary flood defences.

## 2.4. Summary

Chapter 2 focussed on climate risks in urban areas exploring the role of strategic infrastructure in emergency response operations. Section 2.2.3, in particular, highlighted the close relationship between infrastructure resilience to natural hazards and sustainable planning. Section 2.3, instead, presented an overview of different flood emergency planning approaches comparing the UK to other countries' strategies. Of particular interest for the following sections is section 2.3.2.2, where temporary flood defences are introduced and their use compared to structural measures, and where an analysis of the shortcomings of current emergency management involving temporary flood defences in the UK is presented, highlighting how the presented research outcomes could enrich and support current practice. As anticipated in Chapter 1, the present research aims to fill the gap in the literature concerning infrastructure resilience and emergency planning, optimal temporary emergency resources management and allocation strategies; therefore, the following Chapter 3 explores and reviews several optimisation techniques available in the literature to identify the most appropriate tools for the development of the RAO framework presented in Chapter 4.

### 3. Review of optimisation techniques

#### 3.1. Introduction to chapter 3

Chapter 3 presents a review of the optimisation techniques available in the literature to address spatial optimisation problems with the aim to identify the most suitable approach for the development of the optimisation framework. Section 3.2 presents an introduction to optimisation problems and section 3.3 focuses on the sub-category of interest: multi-objective optimisation problems. Section 3.4 reviews a series of popular optimisation techniques utilised in spatial problems and identifies genetic algorithms (section 3.4.5) as the most appropriate methodology to solve the problems of interest to this research. Finally, section 3.5 identifies the contributions of this research to the spatial optimisation discipline highlighting the theoretical advances and the technical improvements presented in this work.

#### 3.2. Definition of optimisation problems

Urban planning for disaster management requires the adoption of optimisation techniques due to the very nature of the problem: a limited amount of resources needs to be strategically allocated to maximise efficacy and efficiency of emergency response operations when natural disasters occur. Because of the complexity of the problems to solve and the high number of different variables involved, high computational costs are often required to perform such an optimisation. Modern technology allows the implementation of software frameworks handling huge amounts of data like never before. The unprecedented computational power available today allows finer models and reasonable run times of digital support tools available to engineers, urban planners and all the stakeholders involved in the decision-making process of disaster planning/management.

Current planning methodologies can, therefore, be integrated with data-driven support tools in allocation decisions. The literature is rich of examples of optimisation techniques applied to a range of different planning and design processes, like sewer networks (Liang *et al.*, 2004; Berardi *et al.*, 2009; Moeini and Afshar, 2017), transit networks (Kepaptsoglou and Karlaftis, 2009; Shimamoto *et al.*, 2010; Feng *et al.*, 2019), water distribution networks (Prasad and Park, 2004; Kapelan *et al.*, 2005; Vamvakieridou-Lyroudia *et al.*, 2005; Bieupoude *et al.*, 2012;

Monsef *et al.*, 2019) and land use allocation (Aerts *et al.*, 2005; Ligmann-Zielinska *et al.*, 2006; Li and Parrott, 2016; Wu *et al.*, 2018).

This work fits in the wide subject area of infrastructure development and management optimisation in relation to climate change-related challenges. This research grounds on a wide literature of past spatial optimisation applications; however, this research field is in continuous expansion and evolution. Many publications describing new software support tools for the decision-making processes for infrastructure management and development have been published in the last three years only (the same development time frame of the present work). This means that many research institutions are currently working to exploit the new possibilities provided by the digital revolution to develop new sustainable and resilient infrastructure systems.

For example, Poo (2020) points out the limited literature in terms of applications for the reduction of the uncertainties in the decision-making process when addressing natural disasters and climate change-related impacts on cities and human activities. Therefore, they present a multi-objective decision support framework for climate change adaptation for transport systems like airports and seaports. They make use of an ABC (Artificial Bee Colony) optimisation algorithm to enhance environmental sustainability in transport infrastructures. Finally, they also observe how climate change adaptation is still at an embryonic stage, advocating further research and support tools development for transport planners.

Together with the management and development of currently in-place infrastructure (like sea and air transport systems), recent optimisation frameworks are being developed for the design of future infrastructure, like the hydrogen fuelling infrastructure. Basing on the work of Agnolucci *et al.* (2013) on the development of SHIPMod (a mixed-integer linear programming model for hydrogen supply chains optimisation), Moreno-Benito *et al.* (2017) propose a SHIPMod extension called MILP (multi-period spatially-explicit mixed-integer linear programming) framework. They present an optimisation framework for hydrogen infrastructure development to support a low-carbon transport system transition in the UK.

In 2018, Triantafyllidis *et al.* (2018) presented resilience.io: an integrated optimisation platform for sustainable resource infrastructure planning. This platform makes use of mixed-integer linear programming to assess new infrastructure designs. The multi-objective



optimisation process aims at finding sustainable and cost-effective solutions to support and guide future infrastructure development.

In the following year, Alhamwi *et al.* (2019) developed FlexiGIS: a GIS-based framework for the optimal allocation of distributed battery storage in urban energy systems. In their case study of Oldenburg (Germany), FlexiGIS can evaluate different energy scenarios and provide optimal solutions for the urban energy infrastructure.

Multi-objective optimisation in the infrastructure field is not only applied to the improvement of infrastructures themselves but also their funding allocation decision-making process. In this regard, Samaniego and Treuner (2006) used simulated annealing for the optimisation of infrastructure investments in a region. More recently, instead, Saad *et al.* (2018) developed an optimisation framework able to handle conflicting objectives to support stakeholders in fund-allocation problems.

Oléron-Evans and Salhab (2021) applied multi-objective spatial optimisation to assess the feasibility and the progress of the Heathrow Airport expansion. They make use of linear programming for a multi-objective optimisation of land uses in the Heathrow Opportunity Area identified in the London Plan (Greater London Authority, 2021). The ultimate goal of this study is to identify how land uses can be best allocated to maximise home, job and gross value added in their study area meeting green belt constraints and the declared authorities' objectives.

In parallel, the literature is rich in examples of the development of digital tools for the risk assessments of infrastructure and urban systems. For instance, Chen *et al.* (2016) present a set of GIS-based tools for flood damage assessment in megacities, including the combination of multiple events to make predictions on annual damage expectations. Besides, Wang *et al.* (2018), developed an integrated holistic framework for high-resolution urban flood modelling. The framework makes use of a Cellular Automata model for flood inundation simulation, and it can take into account multiple information sources and urban features. These support tools are fundamental for optimisation applications as they allow to make realistic assumptions on hazards and risks at the base of infrastructure systems resilience evaluations.

These examples show how multi-objective optimisation research for better and more sustainable infrastructure systems and services is in rapid evolution and the RAO framework presented in this work adds up to the many applications developed in recent years in this field.

Computer methods allow considering a wide range of solutions with a vast number of variables. This, in turn, allows considering complex configurations with reasonably short solving times. The conceptual and mathematical formulation of optimisation problems, though, is independent of the computational technique adopted to get to the final solutions.

Human intuition or by hand solution can tackle the same kind of optimisation problems that machines solve, only with fewer variables, less formulation complexity and longer times. Concerning spatial optimisation, for simple problems, human intuition can also quite straightforwardly guess optimal solutions (with a considerably low margin of error) without even perform any calculation. Therefore, as a matter of example, if the problem is optimising the placement of a retail centre in a densely populated area, it is intuitive to place it somewhere near the geographical centroid. However, when, for instance, we want to take into consideration travel times instead of Euclidean distance, together with different transportation means (like cars, buses and trains) involving a cost variable to the problem and maybe not of just one asset, but numerous different retail centres, all with different typologies of target clientele, human intuition is not enough anymore. The complexity of the problem requires a precise mathematical formulation and a computer to solve it.

As explained by Papadimitriou and Steiglitz (1998), optimisation problems are mathematical approaches aimed at exploring, comparing and selecting potential solutions until an optimum is reached. The elements of any optimisation problem are: 1) the variables involved, 2) the objective functions to optimise and 3) the constraints defining the problem.

The nature of the variables involved in an optimisation problem defines the typology of the problem itself. The complete set of the variables form the variable space, whose dimension is defined by their number  $n$ :

$$X = (x_1, x_2, \dots, x_n) \quad (3.1)$$

Variables may consist of different kinds of data types: integer, discrete, binary or a combination of them. Integer programming makes exclusive use of integer or binary values;

when the objective function and the constraints are linear, the approach can be defined as “integer linear programming” (ILP) (Papadimitriou and Steiglitz, 1998). From the spatial optimisation point of view, several studies adopted integer programming, like Aerts *et al.* (2003) for multi-site land-use allocation and Álvarez-Miranda *et al.* (2020) for multi-criteria multi-action conservation plans.

Discrete variables can be used to define physical characteristics or different strategies in different optimisation problems like in Li *et al.* (2009) with truss structures or in Woodward *et al.* (2014) with flood management decisions.

Mixed-integer problems, instead, are those problems that make use of both discrete and non-discrete variables. Again, in the literature is possible to find different spatial problems that have been tackled with this kind of approach, like Schouwenaars *et al.* (2001) with their multi-vehicle path planning application or Molina Bacca *et al.* (2020) and their framework aimed at the determination of optimal microgrid configuration, capacity, and geographical location.

Optimisation problems aim to find optimal sets or combinations of those variables according to the very nature of the problem to solve. The problem formulation, therefore, translates into the definition of objective functions to either be minimised or maximised. Objective functions  $f$  are dependent from a set of variables  $X$ . The collection of all the  $m$  objective functions  $f(X)$  constitutes the set of objective functions  $F(X)$ .

$$F(X) = (f_1(X), f_2(X), \dots, f_m(X)) \quad (3.2)$$

Objective functions measure the performance of different sets of variables; the totality of such performances constitutes the objective space. The final goal of the optimisation process is to find the configuration  $X$  that generates an  $F(X)$  in the best possible region of the objective space (Caparros-Midwood, 2015).

Finally, setting constraints may be necessary to restrain the domain of the variables defining the problem. Very often, they aim to eliminate or not even consider unfeasible solutions or, in other words, to set the boundaries of the inspection field. For example, regarding spatial optimisation, defining physical boundaries is necessary to search for solutions only inside the case study area. Another kind of constraints in the spatial optimisation field can regard the quality of the solution instead of their location; for instance, in land use allocation problems,

only a limited set of potential land uses could be available for specified locations. A specific constraint is therefore needed to define the range of available choices as in Qian *et al.* (2010)'s land use application.

### 3.3. Multi-objective optimisation problems

Spatial optimisation, together with many other problem typologies, often require multiple objectives to optimise simultaneously, hence the need for a multi-objective optimisation approach. These multiple objectives are by nature conflicting (otherwise, they could be modelled or mathematically reduced as a single objective); this implies that a single optimal solution does not exist. Instead, a set of different optimal solutions that balance the trade-off between the conflicting objectives can be found with two different main techniques: weighted sum and Pareto-optimisation.

Weighted sum approach was the traditional methodology adopted for multi-objective optimisation problems (Jones *et al.*, 2002), as it is computationally less demanding. It consists in the reduction of the multi-objective optimisation problem to a single-objective optimisation problem by means of weights applied to the different functions to optimise. The result is the maximisation or minimisation of a single objective function  $F^w$  that is the sum of all the objective functions multiplied by their specific weight (preference vector).

$$F^w = (w^1 f_1 + w^2 f_2 + \dots + w^n f_n) \quad (3.3)$$

A single solution  $F^w$  is the result of the process of either maximisation or minimisation, and this solution is the optimal solution for the whole multi-objective optimisation problem. To avoid complications related to different orders of magnitude or scale of different optimisation functions, it is common practice to adopt weights that add up to 1 and/or to normalise the objective functions (Eastman *et al.*, 1995; Maliszewski *et al.*, 2012).

As well as for the weights, the values of the normalised functions  $f_n^{norm}$  would be in the range [0,1]:

$$f_n^{norm} = \frac{f_n - f_n^{max}}{f_n^{max} - f_n^{min}} \quad (3.4)$$

With  $f_n^{max}$  and  $f_n^{min}$  respectively the maximum and the minimum value of the function  $f_n$ .

Pareto-optimisation, instead, keeps the objective functions separate and independent from each other. In his book on genetic algorithms, Goldberg (1989) explains how the base of Pareto-optimisation is the concept of ‘domination’. In Pareto-optimisation, a solution is defined as optimal if it is ‘non-dominated’ by any other solution. Therefore, considering a minimisation problem, a solution  $s^1$  is defined as “non-dominated” by a solution  $s^2$  if  $s^1$  is not worse than  $s^2$  in all objectives and it is strictly better in at least one objective:

$$f_n(s^1) \leq f_n(s^2) \quad \forall n = 1, 2, \dots, N \quad (3.5)$$

$$f_n(s^1) < f_n(s^2) \text{ for at least one } n \in \{1, 2, \dots, N\} \quad (3.6)$$

Where  $f_n$  are the  $N$  objective functions. For a maximisation problem, instead, the definition becomes:

$$f_n(s^1) \geq f_n(s^2) \quad \forall n = 1, 2, \dots, N \quad (3.7)$$

$$f_n(s^1) > f_n(s^2) \text{ for at least one } n \in \{1, 2, \dots, N\} \quad (3.8)$$

After the application of a non-dominated sorting algorithm (Du *et al.* (2007), Mishra and Harit (2010)), the previous equations are applied to all the search results,  $S$ , to determine a set of non-dominated solutions (Caparros-Midwood, 2015). Such non-dominated solutions are selected and saved since they are equally Pareto-optimal, and no other solution could provide an improvement of one objective without worsening the others. The result is a Pareto-front like the ones shown in Figure 6, according to the nature of the multi-objective optimisation problem (minimisation or maximisation).

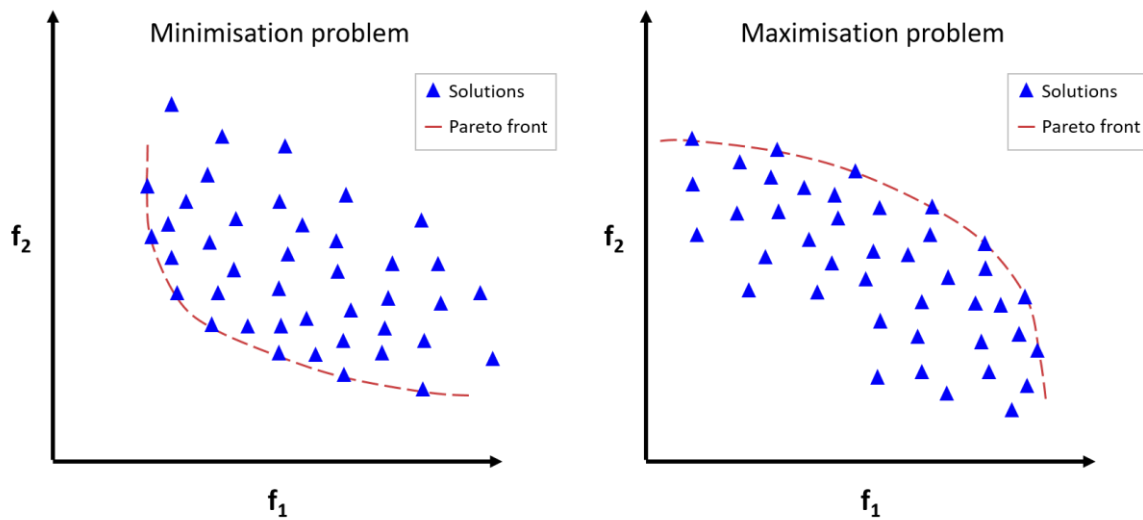


Figure 6 - Examples of solutions space and Pareto fronts for multi-objective minimisation and maximisation problems.

Comparing the two approaches, a disadvantage of weighted sum with respect to Pareto-optimisation is the high dependence of final results from initial assumptions. The weighting system of different objective functions is an a priori decision that heavily influences the entire optimisation process because it assigns different priorities to different objectives. Defining weights can be a rather arbitrary decision; also a priori knowledge for such a definition is not always available.

Pareto-optimisation allows avoiding the a priori determination of weighting vectors. On the other hand, Pareto-optimisation produces a set of equally optimal solutions, leaving the user to decide which solution may be more suitable for their problem. To make this choice, a high level of knowledge is required after the optimisation process, while in weighted sum a high level of knowledge is required a priori in the choice of weights (Caparros-Midwood, 2015).

Pareto-optimisation is more computationally demanding than weighted sum because of the exploration of a broader range of potential solutions. For this reason, weighted sum approaches are still used for applications that require quick results (Sayers *et al.*, 2014).

Goal Programming is a particular kind of weighted sum: weight vectors dynamically change during the optimisation process. An extensive literature is available concerning different applications of this technique like in Cao *et al.* (2012), Stewart and Janssen (2014), Romero *et al.* (1998) and Aerts *et al.* (2005).

The best advantage of Pareto-optimisation over weighted sum approaches is the display of the Pareto-front. It allows exploring multiple solutions that optimally balance the trade-off

between conflicting objectives, allowing cost-benefit analyses among different optimal solutions, ultimately providing a richer outcome.

For these reasons, Pareto-optimisation is the methodology chosen for the spatial multi-objective optimisation framework presented in Chapter 4. This methodology is largely used in spatial optimisation applications literature like Caparros-Midwood (2015), Khalili-Damghani *et al.* (2014), Jiang-Ping and Qun (2009), Masoomi *et al.* (2013) and Oléron-Evans and Salhab (2021). Moreover, the production of Pareto-fronts allows ideal final users of the Resource Allocation Optimisation framework (i.e. urban planners dealing with emergency response management) to perform the cost-benefit analysis at the base of their decision-making process.

### 3.4. Literature review of spatial optimisation techniques

Following on from Caparros-Midwood (2015)'s review of optimisation techniques, this section explores different approaches available in the literature to solve spatial optimisation problems with the aim of understanding which of them is the most appropriate to address the present research questions. This review will start investigating more straightforward approaches progressing to more sophisticated ones. The scope of the review is not to state which approach is the absolute best, as different techniques are more suitable to solve different problems. Moreover, in the choice of different approaches, it is always important to keep in mind the trade-off between the quality of the results and the computational effort necessary to achieve them; it is therefore up to the modeller to choose the most appropriate spatial optimisation technique that best suits their needs in terms of quality of results and affordability.

#### 3.4.1. Linear programming

Linear programming is an efficient optimisation technique for those problems that can be mathematically formulated as linear in terms of variables and constraints; it is simple, and the quality of the results is directly proportional to the fit of the problem with the linear model (Chuvienco, 1993; Tarp and Helles, 1997; Orsi *et al.*, 2011). A simple exemplary mathematical formulation is provided by Arthur and Nalle (1997):

$$\begin{cases} \text{optimise: } z = c \cdot x \\ \text{subject to: } A \cdot x \sim b \end{cases} \quad (3.9)$$

Where the optimisation is either a maximisation or a minimisation,  $z$  is a linear function of the variables vector  $x$ , and  $A$  and  $b$  represent any combination of matrix-vector able to define a linear constraint on the variables  $x$ .

The first land-use application in the literature is Schlager (1965), where a computer-based resolution via linear programming is advanced for the first time. Numerous other applications have been developed, among which the already cited Chuvieco (1993) with his rural unemployment minimisation case study, Cromley and Hanink (1999) with their raster GIS implementation, Aerts *et al.* (2003) and their multi-site land-use allocation (MLUA) problem and Oléron-Evans and Salhab (2021) with their land use allocation optimisation in the Heathrow Opportunity Area.

Linear integer programming (LIP) is a particular kind of linear programming where variables only have integer values; the MLUA problem mentioned above (Aerts *et al.*, 2003) is an example: each land parcel has an integer value assigned corresponding to its land-use. Also Ligmann-Zielinska *et al.* (2005) made use of linear integer programming in their land-use optimisation application on a hypothetical 400 cells raster case study. Tasseff *et al.* (2016), instead, make use of mixed-integer linear programming to design flood structural mitigation measures.

Baskent and Keles (2005) and Qian *et al.* (2010) are examples of applications that tried to overcome a classical limitation of linear programming: the ability to model only single-objective optimisation problems. In their studies, respectively on forest planning and land-use optimisation, they translated the multi-objective optimisation problem into a single objective one by turning the extra-objectives into constraints. Aerts *et al.* (2003), instead, transformed their multiple objectives into a single one by the attribution of weights (weighted sum) in order to be able to solve the problem with linear programming.

Notwithstanding this limitation, linear programming has been widely used in urban planning studies. In addition to the papers mentioned above, among many others, Maoh and Kanaroglou (2009) developed an operational integrated transportation and land-use model (ITLUM) for two Canadian cities and Loonen *et al.* (2007) compared the performance of linear



programming and genetic algorithms on different case studied characterised by different complexities. Their outcomes proved that for simpler problems, the performances are comparable, but when the complexity or the number of variables increases, more sophisticated methodologies are necessary to achieve good results.

### 3.4.2. Simulated annealing

Simulated annealing is a meta-heuristic approach. Meta-heuristic approaches differ from linear programming because they do not guarantee the finding of the global optimum of the problem as the search mechanism is not exhaustive. On the other hand, their great advantage is the possibility to widen the search keeping run times acceptable, consequently making feasible the solution of more complex problems (Loonen *et al.*, 2007). This additional complexity is translated as a higher number of variables taken into consideration, a richer formulation of objective functions (not linear) and more flexible constraints definitions (Papadimitriou and Steiglitz, 1998).

Kirkpatrick *et al.* (1983) was the first application of simulated annealing to optimisation problems, the approach is inspired by the physical process of cooling of metals, and it is designed to find the global minimum of an objective function avoiding to get stuck in local optima (Luke, 2015). A full mathematical formulation is provided by Aarts *et al.* (2005) and it is summarised by Dowsland (1993) as the following. The approach is very similar to the hill-climbing one (Weise, 2011), with the only exception that not only neighbouring solutions that improve the objective function are accepted, but also solutions that result in a worsening with a certain probability  $P(\delta)$ . This probability decreases with the progression of the algorithm and its primary function is to avoid local optima (Murray and Church, 1996). The mathematical formulation provided by Dowsland (1993) is:

$$P(\delta) = e^{-\frac{\delta}{t}} \quad (3.10)$$

Where  $\delta$  is the change in the objective function and the parameter  $t$  is called ‘temperature’ as the terminology follows the physical analogy with metal annealing. The temperature  $t$  has an initial high value in order to allow a high acceptance of ‘non-optimal’ solutions and then it

decreases progressively according to the cooling schedule (Dowsland, 1993; Caparros-Midwood, 2015).

Although simulated annealing cannot guarantee the finding of the global optimum (Rothlauf, 2011), it is, however, likely to provide good solutions in decent run times if the parameters governing the algorithm are appropriately set. The common issue among all heuristic approaches is the balancing of the trade-off between the quality of results and feasible run times. For simulated annealing, the main parameter governing the convergence is the temperature. High initial values and high variabilities allow wider searches and potentially better results as the solution space is more widely covered, but the cost of this is translated as higher computational efforts (Dowsland, 1996; Caparros-Midwood, 2015).

Simulated annealing has been proved an efficient tool to solve spatial optimisation problem as the wide literature available demonstrates. A significant example is provided by Aerts and Heuvelink (2002) who used simulated annealing to solve a non-linear optimisation problem for multi-site land-use allocation (MLUA) applied to a case study in Galicia (Spain). Another study that makes use of simulated annealing is Santé-Riveira *et al.* (2008), where the authors aim to allocate land units to a set of possible uses in the Terra Chá district (Galicia, Spain). In addition, Czyżżak and Jaszkiwicz (1998) developed a procedure to find good approximations of the solution set for a multi-objective combinatorial optimisation problem (Pareto simulated annealing). Finally, Nam and Park (2000) developed a multi-objective simulated annealing strategy able to compete and sometimes to perform even better than genetic algorithms in finding the Pareto front. That quality comes with a price though, as such good performances are only achievable for small problems.

### 3.4.3. Tabu search

Like simulated annealing, tabu search is a meta-heuristic approach. The philosophy of tabu search is similar to simulated annealing's one: finding the global optimum trying to avoiding local optima. Glover (1986) is the first formation of tabu search, which has been later formalised in Glover (1989) and Glover (1990). The principle of this methodology is to avoiding local sub-optima by: 1) allowing inferior solutions if no improvement is available and 2) prohibiting (hence the term 'tabu') considering previously inspected solutions.

Sung *et al.* (2007) used tabu search to solve a water distribution optimisation problem. They applied their methodology to three case studies: New York, Hanoi and Taichung, with good results in terms of quality and computational effort. Liang *et al.* (2004) applied tabu search to design gravity wastewater collection systems (GWCS) incorporating adaptive rule and a dynamic search strategy to find better solutions. Another network application is Costamagna *et al.* (1998), where tabu search is applied to broadband communication networks topological optimisation. These are examples where tabu search is a particularly efficient technique in terms of results quality and run times, but its limitation is its efficient applicability to discrete problems. When the variables are continuous or the complexity of the problem increases, the computational effort becomes too demanding and other heuristic approaches provide better balancing of the trade-off between quality of results and low run times (Zhang *et al.*, 2010).

#### 3.4.4. Particle swarm

Differently from simulated annealing and tabu search, Particle swarm is a population-based method. The main difference consists in the fact that it is not a single (the best) solution to be analysed and assessed at each step of the process, but instead an entire population of potential solutions in the spirit of Pareto optimisation.

This methodology has been first proposed by Kennedy and Eberhart (1995) in a paper where they explain the nature-based inspiration of the method: birds flocking. Solutions are regarded as particles that altogether form the ‘swarm’. These particles occupy the solution space and change their position during the iterations, exchanging information of their position in the process.

Pulido and Coello Coello (2004) provide a clear formulation: the best position of the particle at each iteration is stored in a variable  $g_{best}$  and the best solutions of the whole process are stored in  $p_{best}$ . A velocity vector for each  $id$  dimension for the particle  $V_{id}$  then determines where and how the swarm will move at the next iteration:

$$V_{id} = w \cdot V_{id} + c_1 \cdot r_1(p_{best,id} - x_{id}) + c_2 \cdot r_2(g_{best,id} - x_{id}) \quad (3.11)$$

Where  $c_1$  and  $c_2$  are randomly generated numbers in the empirically derived range [1.5, 2.5] and  $r_1$  and  $r_2$  are random values in the range [0.0, 1.0];  $w$  is called ‘inertia weight’ and  $x_{id}$  is the current position in the solution space.

Particle swarm’s nature makes it suitable for Pareto optimisation (Caparros-Midwood, 2015) and particularly good in local search for solution – where other evolutionary techniques are not always efficient – without the necessity to implement sophisticated evolutionary operators (Bai, 2010).

Particle swarm optimisation has been used for different applications, like in Masoomi *et al.* (2013) for land-use allocation or Reddy and Nagesh Kumar (2007) for reservoir operation optimisation. Nevertheless, it does not appear ideal for land use problems due to the requirement of continuous variables (Ma *et al.*, 2011).

#### 3.4.5. Genetic algorithms

Genetic Algorithms (GAs), like particle swarm, are a population-based methodology first developed in 1975 and later republished by Holland (1992). The most significant contribution for GAs formulation has been given by Goldberg (1989). GAs are inspired by natural evolution (hence their name) in the sense that they evolve a population of potential solutions to their Pareto-optimal state. This evolution process is based on the application of evolutionary operators meant to assess and select the best candidates of each generation to produce a new generation by mating and mutating them.

GAs are part of the larger family of Evolutionary Algorithms (EAs), which also include Evolutionary Programming (EP) (Fogel *et al.*, 1966) and Evolutionary Strategies (ESs) (Rechenberg, 1973). All these techniques are inspired by natural evolution and are variants basing on the same principle; in particular, genetic algorithms simulate the evolution process by the application of three evolutionary operators: selection, crossover and mutation.

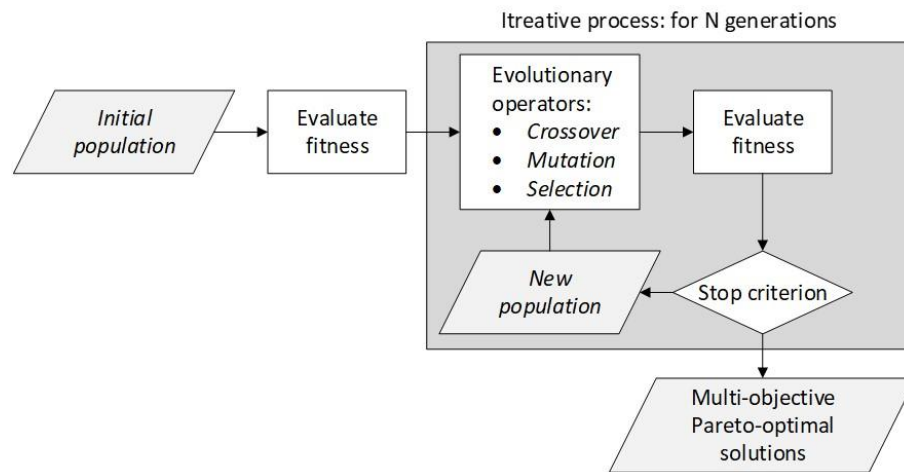


Figure 7 - General workflow of a genetic algorithm. Picture from Lopane et al. (2019).

Figure 7 represents a generic workflow of a genetic algorithm. An initial population of potential solutions is generated and evaluated; the best candidates are selected to produce the following generation, which is assessed again with the process continuing until a stop criterion is met (for more details see section 4.4). Crucial to this process is the definition of the selection process, as – like in natural evolution – it is the main factor in deciding which solutions survive and which are discarded Goldberg and Deb (1991).

An advantage of genetic algorithms, with respect to simulated annealing and tabu search, is their ability to explore broader areas of the solution space thanks to the crossover operator (for a formal definition see section 4.4). This allows finding global optima of different combinatorial problems with considerably shorter run times (Reeves, 1995; Mitchell, 1998; Caparros-Midwood, 2015).

GA's dynamicity also leads to a downside: the difficulty in setting constraints. Again, here the crossover operator is the main factor: swapping attributes between different solutions makes it difficult to meet different boundaries, both numerical and spatial. Various techniques can be adopted to overcome such difficulties; they are described in Chapter 4 in the constraints section.

GAs are the methodology adopted by a very high number of spatial studies, like Caparros-Midwood et al. (2019), Caparros-Midwood et al. (2017), Stewart and Janssen (2014), Sidiropoulos and Fotakis (2009), Comber et al. (2009), Aerts et al. (2005), and Feng and Lin (1999). GAs are widely used since they are particularly suitable for addressing problems considering large areas or a high number of variables (Loonen et al., 2007).

Several different approaches are available to handle evolution processes, the principal ones are: 1) the PAES (Pareto Archive Evolutionary Strategy) (Knowles and Corne, 2000), 2) the NSGA-II (Non-dominated Sorting Genetic Algorithm-II) (Deb, 2000) and 3) the SPEA2 (Strength Pareto Evolutionary Algorithm 2) (Zitzler *et al.*, 2001). Of these, the last two are the most used with GAs since the first (the PAES) is not a population-based method.

The Non-dominated Sorting Genetic Algorithm prevents Pareto-front regression during the iterative process by considering the best solution of both the current and the previous generation (Deb, 2001). The Strength Pareto Evolutionary Algorithm, instead, assigns different ranks to all the solutions basing on their level of dominance (Zitzler *et al.*, 2001). It is not possible to state which methodology is best in absolute terms, as one may be more appropriate than the other for some applications and the opposite can be true for other kinds of problems (Konak *et al.*, 2006). It is easier to claim, though, that SPEA2 requires on average longer running times than NSGA-II (Luke, 2015).

NSGA-II has been widely used in spatial applications, like by Khalili-Damghani *et al.* (2014) for land-use allocation, Shimamoto *et al.* (2010), for transit network optimisation (applied to Hiroshima's bus network) and Cao *et al.* (2012) for sustainable land-use optimisation.

### 3.5. Contribution of this research to the optimisation field

This research grounds on the wide literature of optimisation applications presented in section 3.4, and in particular contributes in expanding the knowledge of the sub-field of multi-objective spatial optimisation applied to resource allocation problems. As highlighted in section 3.4.5, Genetic Algorithms have a number of different advantages that make them particularly suitable to solve multi-objective optimisation problems. However, despite representing the best available choice for the development of the RAO framework (described in Chapter 4), when solving problems involving big data (e.g. due to wide geographical areas or high resolutions), long run times can constitute a limitation of this methodology.

This research contributes in improving the performance and the efficiency of evolutionary programming, by coupling it with Machine Learning (i.e. GAs and K-means clustering algorithms). To speed up the evolution process, initial populations are not randomly generated; instead, the GA is seeded with spatial plans resulting from a K-means clustering process (for

more details, see Chapter 4). This allows wider searches, bigger case studies, higher resolutions and a higher number of variables.

Two are the main contributions of this work to the spatial optimisation discipline: first a novel methodological framework that couples Genetic Algorithms evolutionary programming with an initialisation procedure that makes use of Machine Learning; second, a software optimisation application developed in Python and available on Github ([github.com/fdlopane/RAO\\_HumberEstuary](https://github.com/fdlopane/RAO_HumberEstuary)), to solve multi-objective spatial optimisation problems applied to infrastructure resilience to natural disasters. The software is open source and it is available to the scientific community to download and use.

### 3.6. Summary

Chapter 3 presented a literature review of available techniques to address spatial planning optimisation. First, the concepts of mathematical and spatial optimisation are introduced and then an overview of potential techniques is presented with the aim to understand which of these is more suitable to address the problem of interest of this research. Among the approaches introduced in section 3.4, genetic algorithms are identified as the most appropriate technique for the development of the RAO framework presented in Chapter 4. Finally, section 3.5 identifies the contributions of this research to the spatial optimisation discipline highlighting the theoretical advances and the technical improvements presented in this work.





## 4. RAO (Resource Allocation Optimisation) framework

### 4.1. Introduction Chapter 4

Chapter 4 introduces the Resource Allocation Optimisation (RAO) framework. The chapter describes the architecture and conceptual background of the methodology adopted by this research, together with the software implementation of the theoretical framework with an indication of the several phases and modules involved in the process (section 4.2). Details concerning the choice of the development environment can be found in section 4.3, while section 4.4 presents a description of the genetic algorithm adopted for the multi-objective spatial optimisation.

### 4.2. Problem formulation: optimal resource allocation

#### 4.2.1. Optimisation methodology

The aim of this research is the determination of Pareto-optimal locations for different facilities (warehouses, clinics etc.) with respect to multiple conflicting objectives (i.e. different formulations of accessibility and cost functions).

Among several spatial optimisation approaches (as discussed in Chapter 3), a Genetic Algorithm (GA) may be chosen to balance the trade-off between the conflicting objectives. Section 3.4.5 highlighted the efficacy of GAs for multi-objective optimisation and their application within urban science scholarship, given their improved convergence and quick run times (Xiao *et al.*, 2007; Sidiropoulos and Fotakis, 2009; Caparros-Midwood, 2015).

The presented RAO framework is composed of three phases: 1) Initialisation phase, 2) Solution phase and 3) Output phase. In the Initialisation phase, georeferenced vector and raster datasets are imported and elaborated. At this stage, if not directly imported from the input data, an “availability” dataset is created: here, all the possible locations that can be part of potential solutions are stored. The solution phase involves the GA, here a set of initial solutions (i.e. spatial plans) is generated and then evolved to its Pareto-optimal state by the application of three evolutionary operators: selection, crossover and mutation (see Chapter 4.2.2). Finally, the output phase presents the results in different forms: Pareto fronts, tables and Shapefiles for GIS map visualisation.

The optimisation criterion for the choice of solutions is Pareto efficiency, a methodology that has been widely utilised in engineering, urban planning and infrastructure optimisation (Vamvakeridou-Lyroudia *et al.*, 2005; Jiang-Ping and Qun, 2009; Cao *et al.*, 2011; Fu *et al.*, 2012). The main advantage of this approach is its independence from any a priori preference (in contrast with other traditional methods like weighted sums). In a multi-objective optimisation problem, a solution is defined “Pareto-optimal” based on the concept of domination (Goldberg, 1989): a solution is optimal if it is “non-dominated” by any other solution.

Considering the minimisation problem, a solution  $s^1$  is defined as “non-dominated” by a solution  $s^2$  if  $s^1$  is not worse than  $s^2$  in all objectives and it is strictly better in at least one objective:

$$f_n(s^1) \leq f_n(s^2) \forall n = 1, 2, \dots, N \quad (4.1)$$

$$f_n(s^1) < f_n(s^2) \text{ for at least one } n \in \{1, 2, \dots, N\} \quad (4.2)$$

Where  $f_n$  are the  $N$  objective functions. For a maximisation problem, instead, the definition becomes:

$$f_n(s^1) \geq f_n(s^2) \forall n = 1, 2, \dots, N \quad (4.3)$$

$$f_n(s^1) > f_n(s^2) \text{ for at least one } n \in \{1, 2, \dots, N\} \quad (4.4)$$

After the application of a non-dominated sorting algorithm (Du *et al.*, 2007; Mishra and Harit, 2010), the previous equations are applied to all search results,  $S$ , to determine a set of non-dominated solutions. Such non-dominated solutions are selected and saved since they are equally Pareto-optimal and no other solution could provide an improvement of one objective without worsening the others.

#### 4.2.2. Framework structure and software implementation

As introduced in Chapter 4.2.1, the RAO framework is structured in three phases: Input phase, Solution phase and Output phase. The Solution phase, in turn, can be subdivided in different processes, as highlighted in Figure 8.

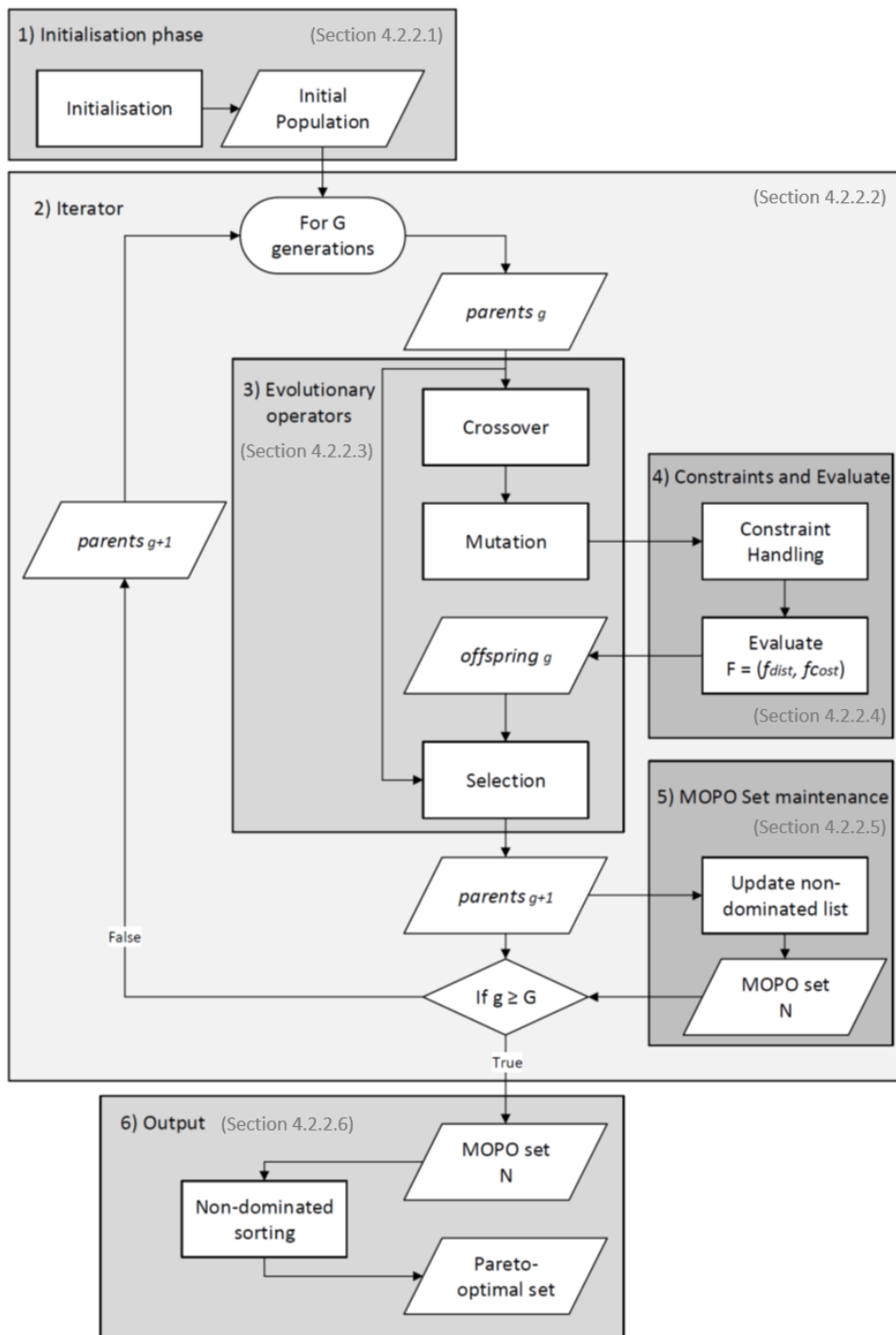


Figure 8 - Resource Allocation Optimisation framework flowchart with indication of sections numbers where the different components are described.

Figure 8 presents the phases and the components of the implemented RAO framework. Passing through six different phases and the iterative process, the framework generates and evolves a set of solutions to get to the final Multi-Objective Pareto-Optimal (MOPO) set N.

Referring to the framework structure described in Figure 8, a series of modules have been developed to handle the different operations belonging to the several phases of the optimisation framework.

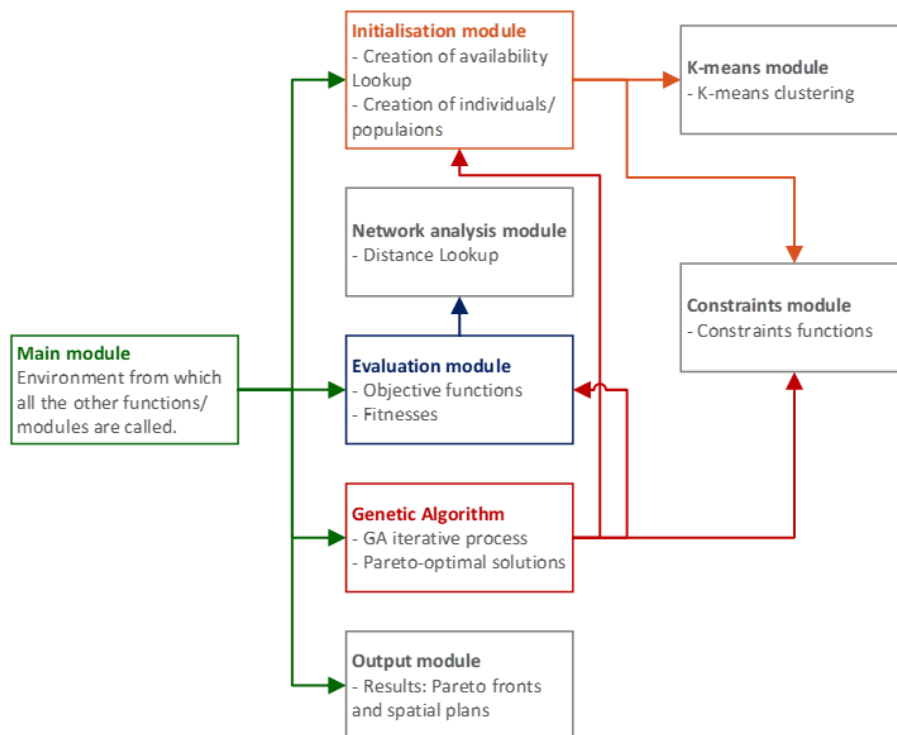


Figure 9 - Scheme of the python modules of the Resource Allocation Optimisation (RAO) framework with respective functions and dependencies.

Figure 9 presents an overview of the different python modules composing the RAO framework. The main module is where the principal parameters of the problem are defined by the user (see the case studies' chapters 5 and 6 for more details concerning the parameters governing the problem) and from which the Genetic algorithm is run (see section 4.4). From here, a series of dependent modules are called where needed.

The main module also allows the user to choose among a broad range of different scenarios to be run by the RAO framework: a significant step forward in terms of user interface and software structure has been made with respect to previous optimisation framework that made use of genetic algorithms (Caparros-Midwood (2015)). The introduction of "scenarios" in the main module allows the user to more easily define parameters within the problem formulation section of the code and ultimately create a more user friendly working environment.

The Initialisation module is where georeferenced input datasets are imported, and the 'available Lookup' is created (see section 4.2.2.1). Once the initialisation phase is completed, the iterative process of the genetic algorithm can start. The Initialisation module also relies on the results of the K-means module for the creation of the first generation. Spatial plans are then evaluated by the application of the functions of the Evaluation module (described in section 4.2.2.4), which, in turn, relies on the results produced by the network analysis module (presented in section 4.2.2.1).

The K-means module is independent to the other modules of the RAO, it is run beforehand and its results are used to create the first generation of solutions. K-means clustering (Ostrovsky *et al.*, 2013) is an unsupervised Machine Learning (ML) technique aimed at partitioning a series of  $n$  data into  $k$  clusters (hence the name). The SciKit-learn (Pedregosa *et al.*, 2011; Buitinck *et al.*, 2013) open source Python module utilises a K-means clustering of all the available locations and finding the centroids of these clusters. Different numbers of clusters are taken into consideration (e.g. in Chapter 5 case study: same range of minimum/maximum number of warehouses) and the coordinates of their centroids are saved and stored in the results folder.

The aim of the K-means module is to perform a K-means clustering of the target assets (destinations of the network analysis) and determine the centroids of the identified clusters. This information is useful for seeding the algorithm with not-randomly generated initial spatial plans. According to the case study, the user is able to decide whether to run the K-means clustering or not; this decision depends on the user's needs/intentions, as the K-means clustering speeds up the optimisation process, but also constrains the research space: not including the K-means clustering would lead to longer run times, but the inspected solution space would be wider. Balancing the trade-off between quality of results and run times is one of the main advantages of heuristic methods - for more details on this topic see Chapter 3.

The Network analysis module is run in parallel. Through NetworkX (Hagberg *et al.*, 2008), a network analysis is performed to calculate the shortest paths from each origin to each destination. The results (expressing distances in terms of travel times) are saved in a 'Distance Lookup' containing the travel times from each available location to every target asset present in the case study area (more details on this procedure in section 4.2.2.1).

The Constraints module described in section 4.2.2.4 contains all the functions that represent the constraints of the problem, functions that are needed when spatial plans are created both in the initialisation phase and after the application of the evolutionary operators.

Finally, after the last iteration of the evolutionary process, the Output module (section 4.2.2.6) is called directly from the Main environment to produce a log file with the details of each particular run and the results in the form of Pareto fronts plots and georeferenced datasets containing the spatial plans of Pareto-optimal solutions.

#### 4.2.2.1. Initialisation phase

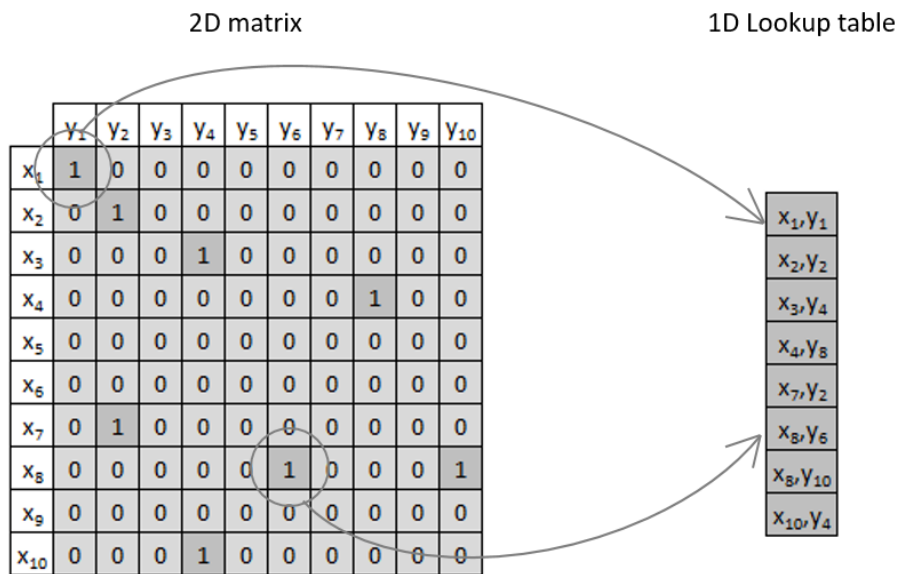
In this initial phase, a set of georeferenced datasets are imported into the Python environment. A first innovative feature of the RAO framework, with respect to previous optimisation platforms (e.g. Caparros-Midwood (2015)), consists in its flexibility in terms of input data. Both vector and raster datasets can be used as inputs to model the geographies and the constraints of the case study areas. This allows a wider transferability and scalability of the methodology to different areas and scales in response to different data formats.

These datasets are pre-processed in a GIS environment and they represent the spatial domain of the case study. Different case studies rely upon different datasets and typically consist of the road network, destinations (e.g. strategic infrastructure assets to be protected during flood events), constraints etc. The initialisation processes are handled by the Initialise.py module which contains several functions designed to import spatial data and generate lookup tables and spatial plans' population to evolve to their optimal state by the genetic algorithm.

At this stage, another significant innovation is introduced to enhance the flexibility and the transferability of the methodology: the option to choose whether to import an availability raster or to automatically generate it. This is particularly relevant for transferability because the knowledge of which are the suitable locations for the final optimal allocation of resources is not always available in advance. In response to the case study in question, the modeller may not know which locations are available for resource allocations or in other cases they might not want to constrain the search to a set of pre-determined locations.

The two case studies presented in Chapters 5 (UK) and 6 (New Zealand) showcase the adoption of these two assumptions: in the UK case study, the initialisation phase entails the generation of an availability raster, in the New Zealand case study, it is imported directly from the input data folder. The “Generate\_Availability” function takes into account a series of physical constraints to model natural barriers (like surface water) and logistic constraints (like distance from main roads) to generate an availability raster where cells are defined as “available” if they meet all the constraints (for an example of this application, see section 5.4.5). The outcome is a georeferenced raster image in a GeoTIFF format that can be imported into a GIS environment for visualisation purposes and that can be used in the RAO framework to generate a lookup table of available locations.

Lookup tables are also generated in the initialisation phase; they are useful tools to improve the efficiency (and consequently reduce run times) of the whole framework primarily by reducing the variables dimensions: since spatial data always have (at least) two dimensions, they are represented as 2D variables, i.e. matrices. The use of lookup table allows to collapse the bi-dimensionality into a 1D vector variable by creating a list of ordered tuples containing the coordinates of each cell (see Figure 10). In this way, it is possible to store bi-dimensional spatial data in monodimensional list of coordinates, ultimately making the entire framework more computationally efficient.



Spatial data are usually represented as matrices, where the cells contain a value (e.g. 1 = available, 0 = not available) and the rows and columns represent their coordinates.

A vector representation allows to store the coordinates of all those cells that have a particular value (e.g. all the available cells that have a value = 1)

Figure 10 - Dimension reduction in Lookup table creation.

One of the most significant theoretical innovations introduced in this thesis is the coupling of the genetic algorithm procedure with the K-means clustering methodology. Such a combination of different approaches contributes in improving the performance and the efficiency of evolutionary programming. To speed up the evolution process, initial populations are not randomly generated; instead, the GA is seeded with spatial plans resulting from a K-means clustering process. This allows wider searches, bigger case studies, higher resolutions and a higher number of variables.

Subsequently, a network analysis is performed to calculate travel times from each available location and the closest cluster centroid. The analysis is performed evaluating shortest paths where distances are measured as travel times. Then, the available locations are ranked according to their proximity to the centroid of their cluster.

The procedure described above is handled by the `KMeans_clustering.py` module, which produces a series of outputs: shapefiles containing the centroids of all the generated clusters, csv files containing the coordinates of the centroids of all the clusters and csv files with



available cells ranked according to their distance from their cluster's centroid. These files are useful for visualisation purposes (shapefiles) and are used in the spatial plans generation when creating populations of potential solutions (csv files).

As mentioned above, the `KMeans_clustering.py` module makes use of information regarding distances among different locations (e.g. centroids and available cells). The evaluation of distances is another stage of the initialisation phase, and it is carried out by the Network Analysis Module.

The Network analysis module is then run independently from all the other modules of the RAO framework (see Figure 9) and it produces a Distance Lookup containing all the distances between the potential origins and all the potential destinations of the study area. This information is necessary to perform the accessibility optimisation central to the RAO framework. The input of this module is a shapefile representing the network on which to perform the distance analysis: the case studies of Chapter 5 and 6 use the road network and distances are measured as travel times (expressed in minutes in the Distance Lookup).

The Network Analysis Module makes use of the Python package NetworkX (Hagberg et al., 2008), through which it is possible to calculate the shortest paths from each origin to each destination using Dijkstra's algorithm. The wider the study area (or the higher its spatial resolution), the higher the computational effort is; computing shortest paths with NetworkX can result in long run times, this is the reason why the evaluation of distances is not performed at each iteration of the genetic algorithm, but it is performed in advance, and only once.

Once the Distance Lookup is created and saved in the data folder, it is possible to run as many different possible scenarios as required by the user without having to perform a network analysis every time. This results in considerable time saving and ultimately a higher efficiency of the whole optimisation framework: when travel time information is required by the GA, it is directly loaded from the Distance Lookup table instead of being computed.

The last operation performed in the initialisation phase is the generation of spatial plans (in Chapter 5: warehouse spatial plans and in Chapter 6: GP clinics spatial plans). Spatial plans constitute the initial population of potential solutions that will be evolved to its Pareto-optimal state by the genetic algorithm further on. In this phase, spatial plans can be generated either considering the K-Means clustering algorithm seeding or neglecting it according to the

user's interests (seeding the algorithm reduces run times but also reduces the solutions' search range). Both these two different options are presented in the case studies of Chapter 5 and 6.

The primary purpose of the spatial plan creation is the allocation of assets (i.e. warehouses in Chapter 5 case study, or clinics and general practitioners in Chapter 6 case study) to the available cells. The number of allocated assets is variable and it is randomly chosen within an allowed range (defined by the user). The outcome is a vector (the spatial plan) with a length equal to the Lookup table (i.e. list of coordinates of available cells) and with values equal to 0 and 1 according to whether an asset (e.g. warehouse or clinic) is allocated to that particular available cell (see Figure 11). Representing spatial plans as vectors containing zeroes and ones rather than 2D matrices with values and coordinates allows lower run times due to a more efficient data handling. This operation is repeated a number of times equal to the dimension of the initial population of solutions (defined by the user) that constitutes Generation 0 of solutions, which will be evolved to its Pareto-optimal state in the Iterator described in Section 4.2.2.2.

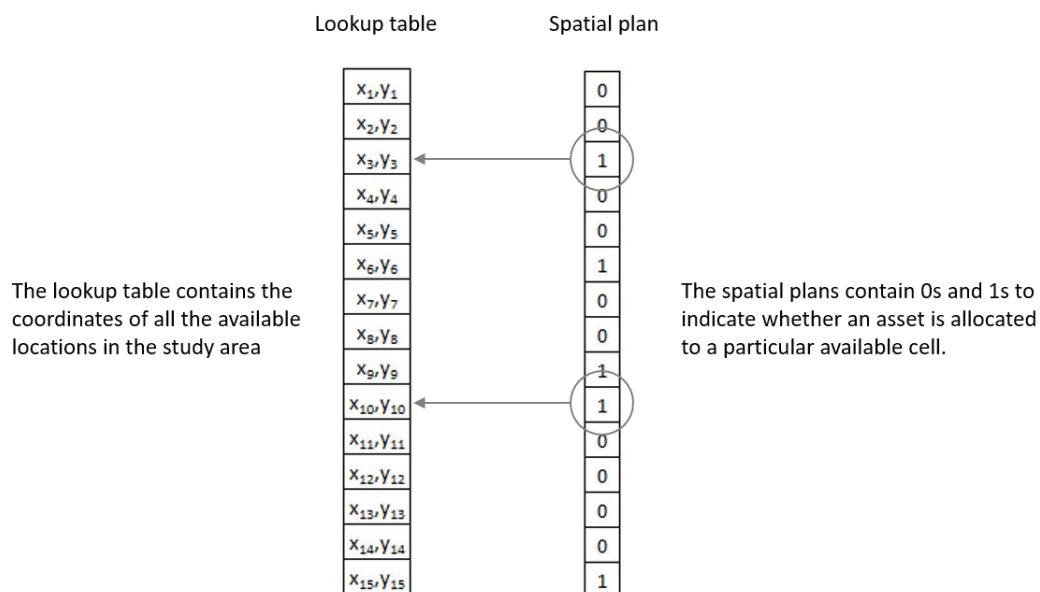


Figure 11 - Relationship between spatial plans (i.e. potential solutions) and Lookup table.

If the K-Means clustering module is used, 80% of available cells will be randomly selected among the top 50 ranking locations in term of proximity to their cluster's centroid, while the other 20% of the spatial plan's locations are randomly selected from all the available locations

of the Lookup table. This means that, if the spatial plan has 10 warehouses or clinics to be allocated, the K-Means Module will generate 10 clusters and 8 out of the 10 assets will be close to their cluster's centroid, while the other 2 assets will be randomly chosen from all the available cells in the area. These percentages can be changed by the user according to the scenario of interest. If the K-means clustering is not performed, all the assets are randomly selected from all the available locations.

The RAO framework also allows the user to choose whether to include a distance constraint in the initialisation phase: according to the study interests, the user can define a minimum distance between assets' allocations. For instance, Chapter 5 presents the case in which, in the spatial plans generation, the distance between two allocated warehouses cannot be lower than 10 kilometres. For transferability and scalability purposes, this value can be defined by the user according to the scale and resolution of the study area.

After the input data managing process, an initial population of solutions is generated (Generation 0). The population is made of individuals that represent singular spatial plans, and it represents the initial parent set from which the following generations are created (see following section for more details on evolution of the solutions' population).

#### 4.2.2.2. Iterator

The iterative process constitutes the central part of the RAO framework and it is the one that requires the highest share of computational power. As shown in Figure 8, the iterator is subdivided in a number of different phases analysed in more detail in the next sections. The subsections of the iterator are: the application of the evolutionary operators (section 4.2.2.3), the evaluation phase with the application of constraints (section 4.2.2.4) and the Multi-Objective Pareto-Optimal (MOPO) set maintenance (section 4.2.2.5). All these operations are repeated for a number  $G$  of iterations, which are called "generations" in the evolutionary programming terminology.

The number of generations  $G$  is an input parameter defined by the user (in the software implementation it is represented by the variable  $NGEN$ ). If the user does not have a prior knowledge of the case framework, it is possible to calibrate the model by varying the number  $G$  to determine which is the most appropriate value. Very low values of  $G$  allow quick runs,

but they do not guarantee exhaustive searches of the solution space, while high values of  $G$  allow the inspection of a wider share of the solutions space with higher computational costs and therefore higher run times.

The determination of an appropriate value for  $G$  consists in balancing the trade-off between quality of results and computational effort. An effective way to perform such a calibration is analysing the evolution of the Pareto front. Typically, after a certain number of generations, the evolution of Pareto fronts slows down the closer it gets to the mathematical solution of the problem. After an optimal number  $G$  of generations, there is no further significant improvement in the quality of solutions. Figure 12 shows an example for minimisation and maximisation problems, while Chapters 5 and 6 present applied examples of calibration of the different case studies.

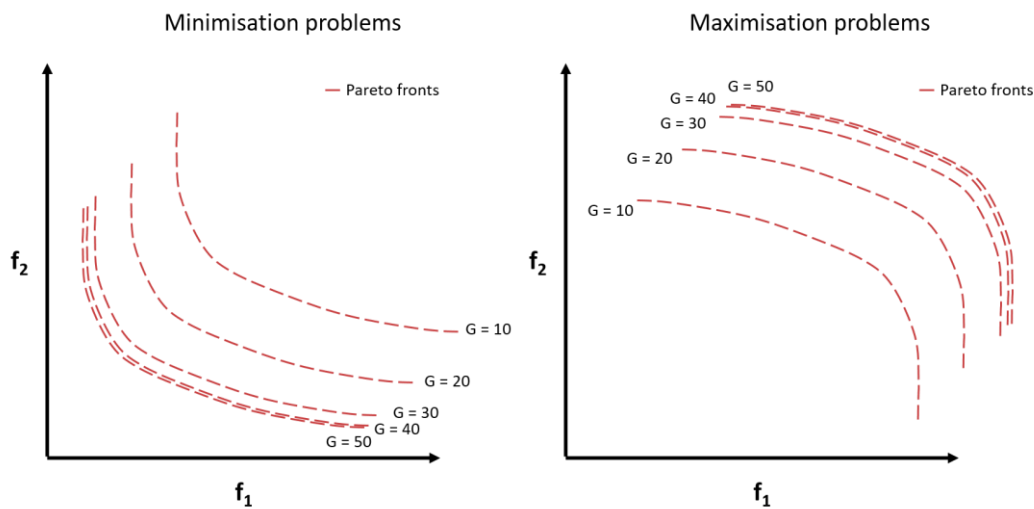


Figure 12 - Evolution of Pareto fronts for minimisation and maximisation problems.  $G$  represents the number of Generations in the evolution process (the values are purely indicative).

Each generation has a parent set ( $parents_g$ ) from which the child set ( $offspring_g$ ) is generated by the application of the three evolutionary operators: selection, crossover and mutation (see section 4.2.2.3 for more details on parents and offspring in the evolution process). In the following generation (i.e. iteration), a new set of parents is created after the application of the selection operator:  $parents_{g+1}$ . At this point, the process is repeated assigning  $parents_g = parents_{g+1}$  (see Figure 8).

The first generation of solutions (Generation 0) is created starting from the spatial plans generated in the initialisation phase (see section 4.2.2.1), and to improve the efficiency of data handling in the iterative process, a Python function named “*Generate\_Proposed\_Sites*”

further reduces the dimension of the spatial plan vectors decreasing the computational effort required to store the variables' length as shown in Figure 13.

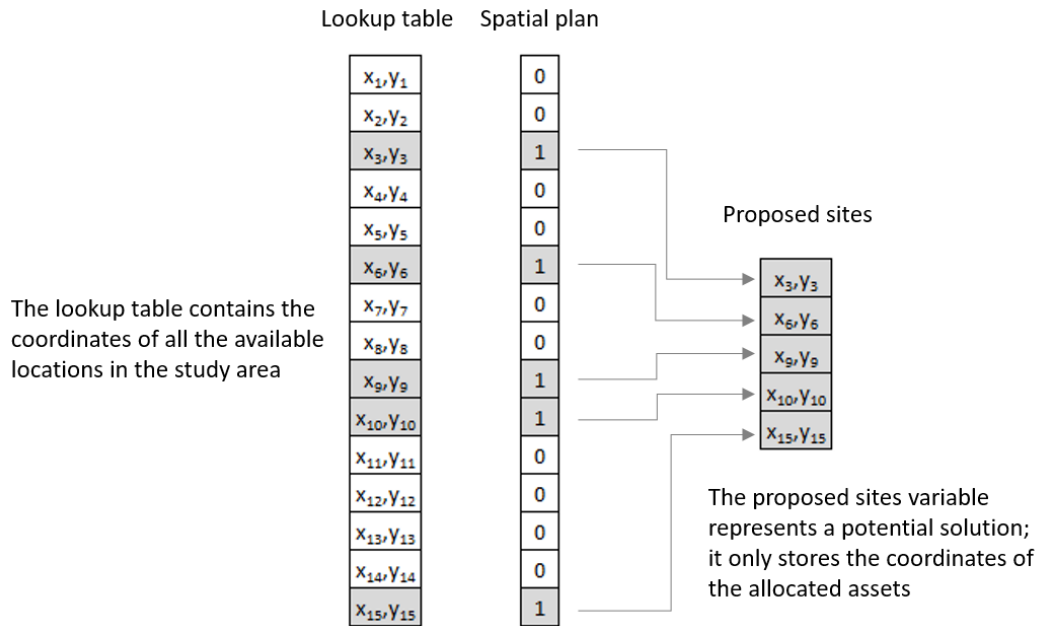


Figure 13 - Creation of Proposed sites variable to reduce the dimension of the Spatial plan vector for a lighter and more computationally efficient data handling.

#### 4.2.2.3. Evolutionary operators

The population of potential solutions generated in the initialisation phase (section 4.2.2.1) are evolved to their Pareto-optimal state in the iterative process presented in section 4.2.2.2. The spatial plans' evolution mimicks natural evolution by combining "parent" plans to generate "offspring" plans considering both "selection" (i.e. only the best solutions survive and mate) and random mutations taking place in the offspring generation. To translate the concept of natural evolution into computer programming, three evolutionary operators are introduced: 1) the crossover operator, 2) the mutation operator and finally 3) the selection operator.

The evolutionary operators are applied to the whole solutions' population at each generation (i.e. at each iteration) by the Genetic Algorithm. In order to generate new solutions avoiding local optima (Rothlauf, 2011), the evolutionary operators of crossover and mutation are applied to each spatial plan with a probability  $p_{crossover}$  and  $p_{mutation}$  in the Mu-plus-Lambda strategy (Mitchell, 1998).

A two-point crossover operator (Caparros-Midwood, 2015) is considered: it works by cutting two solutions,  $S^1$  and  $S^2$ , in two points,  $cx_1$  and  $cx_2$ , randomly chosen such that  $0 < cx_1 < cx_2 < L$  (with  $L$  = length of  $S^1$  and  $S^2$ ). Their attributes are swapped in the central part of the list (i.e. between  $cx_1$  and  $cx_2$ ) and two new solutions  $S^{1'}$  and  $S^{2'}$  are created with the following formulation:

$$\begin{cases} S^{1'}[cx_1:cx_2] = S^2[cx_1:cx_2] \\ S^{2'}[cx_1:cx_2] = S^1[cx_1:cx_2] \\ 0 < cx_1 < cx_2 < L \end{cases} \quad (4.5)$$

Figure 14 shows the details this process:

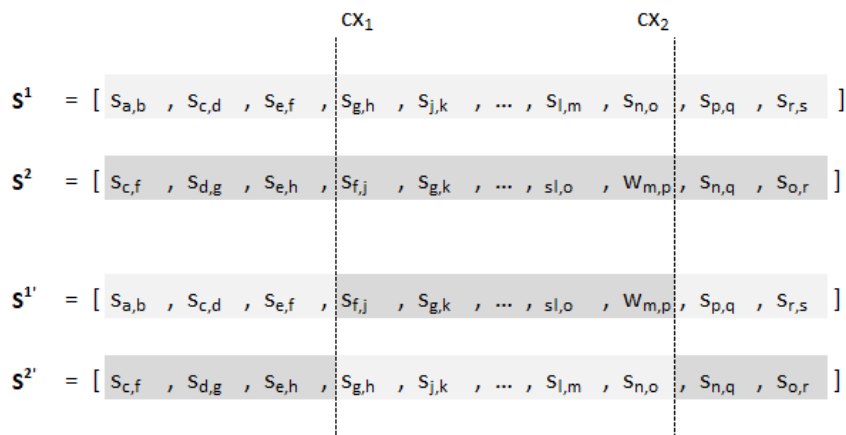


Figure 14 - Two-point crossover operator mechanism, adapted from Caparros-Midwood (2015).

Subsequently, with a probability  $p_{mutation}$ , the mutation operator is applied to those solutions on which the crossover has not been applied. In this process, a mutation of a randomly selected  $i, j$  location transforms the solution  $S$  into the new solution  $S'$  as described in Figure 15.

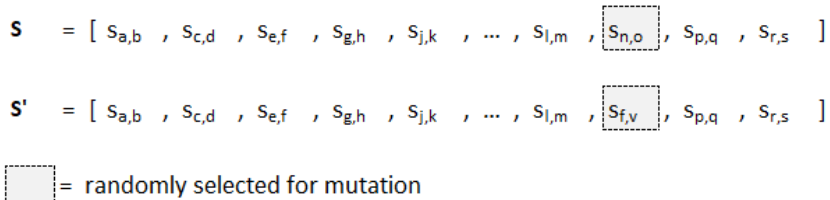


Figure 15 - Mutation operator mechanism, adapted from Caparros-Midwood (2015).

This operator has two advantages: the possibility to improve the performance of a solution in one or more objectives and the prevention of convergence on a small subset introducing new random locations and widening the search area in the solutions' space.

Following this, the selection operator is applied to generate a new set of solutions: *offspring<sub>g</sub>*. The chosen selection process is the Non-dominated Sorting Genetic Algorithm II (NSGA-II) (Deb *et al.*, 2002). NSGA-II is particularly appropriate for urban planning problems and has been extensively adopted (Jaeggi *et al.*, 2008; Zhang and Fujimura, 2010; Cao *et al.*, 2011; Caparros-Midwood *et al.*, 2017). Other conventional selection techniques, such as tournament and roulette selection, are inappropriate for Multi-Objective Pareto-Optimal (MOPO) sets. Zhang and Fujimura (2010) also show that NSGA-II is more efficient for multi-objective optimisation (compared to other widely utilised algorithms, like the Strength Pareto Evolutionary Algorithm) in the estimation of the Pareto front.

#### 4.2.2.4. Constraints and evaluate

The constraint-handling module (Constraints.py in the Python software framework) is designed to certify that the generated spatial plans do not exceed the boundaries of the case study area and meet other kinds of constraints like the minimum/maximum number of allocated resources. Following this, they are evaluated against the objective functions.

As exhibited by Konak *et al.* (2006), constraint handling in genetic algorithms can be performed with several expedients:

1. The removal of infeasible solutions.
2. The application of a penalty function to solutions that break constraints.
3. Production of only feasible solutions.
4. Adjusting unfeasible solutions during the process.

Despite being very popular (Coello Coello, 1999), applications of penalty functions have been criticised for the arbitrariness of the weights of the functions to be applied. Moreover, as Liu *et al.* (2015) observe, the application of a penalty function does not preclude the representation of infeasible solutions in the search.

Inspired by Cao *et al.* (2011)'s approach, the allocation of resources/assets is made based on a Lookup variable that contains the coordinates of available cells only (see section 4.2.2.1 for more details). Such coordinates derive from the available raster dataset created in the initialisation phase. In addition to the computational advantages derived from the variables'

dimensions reduction described in section 4.2.2.1, there are also advantages in using a Lookup table from a constraints handling perspective, such as the prevention of development outside the boundaries and the consequential avoidance of unfeasible solutions (Caparros-Midwood, 2015). Problems may occur in terms of spatial or numerical constraints when the evolutionary operators are applied, and that is why additional constraint checks are implemented according to the nature of the case study.

Due to the spatial nature of input data, some constraints are implicitly imported in the initialisation phase. These kinds of constraints can be defined in any dataset pre-processing or occur in the initialisation phase in the definition of “available” cells. For example, in the case study analysed in Chapter 5, among other requisites, cells are marked as “available” if they are within a distance of 500 metres from a major road. These kind of constraints are case-dependent, therefore – to guarantee the transferability and scalability of the methodology – no predefined formulation is present in the framework’s architecture and it is left up to the user to implement any kind formulation that may better represent the real-life problem.

Resolution represents another constraint of the framework; the architecture is flexible according to the dimension of the cells within the raster datasets. Besides, a series of other implicit constraints are inevitable when using GIS data. They consist of errors, imprecisions and inaccuracies that necessarily constrain any representation of the physical reality to be modelled (Pascual, 2011).

An additional constraint of the datasets is the definition of travel times. Often, road network datasets lack information regarding travel times or even allowed speeds on different edges of the network. In this case, such information must be evaluated basing on hypotheses that necessarily imply a certain degree of uncertainty. A standard procedure is to infer the allowed speed from the road typology and then calculate the free-flow speed. From this information, travel times can be evaluated in a ‘best case scenario’, i.e. without considering the traffic variable. This procedure has been adopted in the case studies analysed in the present work (see Chapters 5 and 6). This constitutes an implicit constraint due to the nature of the datasets; although it does not appear as an explicit constraint of the RAO, it is important to be aware of these kinds of limitations in problem definitions. However, to maximise its transferability, the optimisation framework is flexible to different kinds of input data and when complete/good-



quality input data contain all the needed information, no extra consideration regarding implicit constraints is needed.

The constraints module Constraints.py contains different functions that are designed to ensure that the mated, mutated and selected solutions meet the physical and numerical boundaries of the case study. These functions are of two types and are applied in two phases of the evolution process. Regarding the two typologies, the RAO framework has constraint functions that 1) check that potential solutions' assets allocations are distant enough from each other (e.g. allocated warehouses must be at least 10km apart in Chapter 5's case study) and that 2) check that the number of allocated resources meets the allowed boundaries. These two typologies of constraints are both applied at two stages of the optimisation process: 1) the initialisation phase and 2) the evolutionary operators application phase.

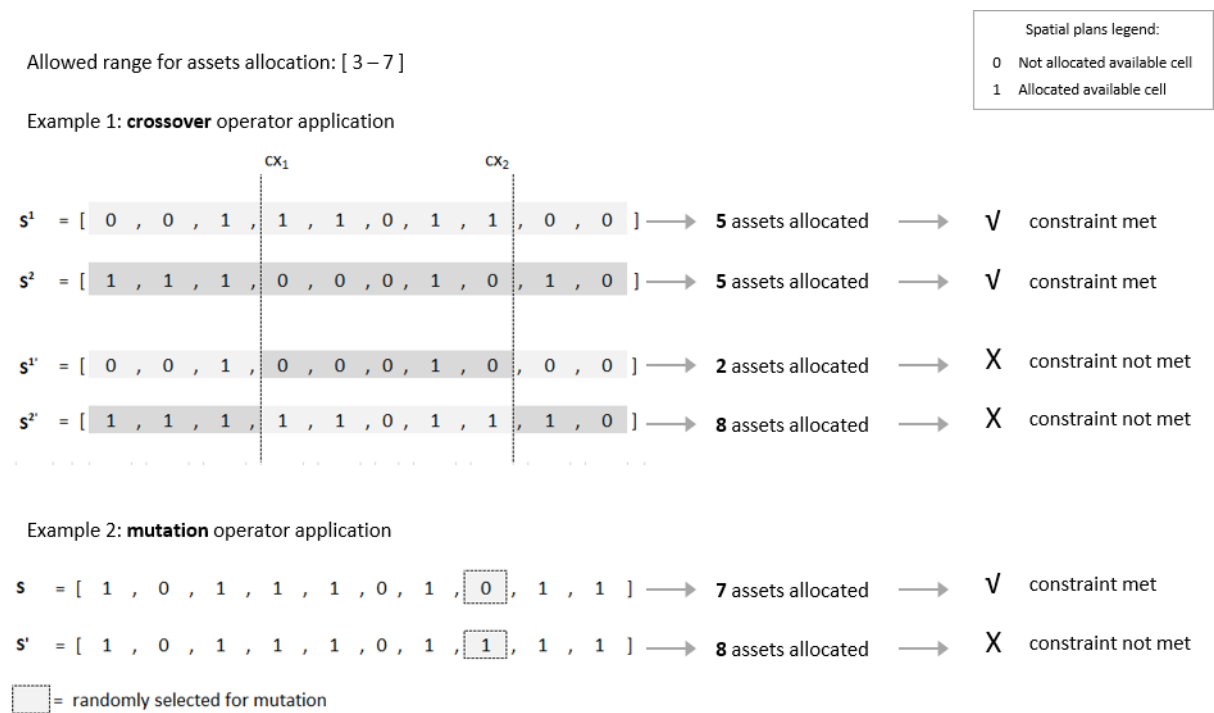


Figure 16 - Example of application of evolutionary operators that do not meet the constraint of the min/max allowed number of assets allocation

Figure 16 shows an application of evolutionary operators that does not meet the constraint of the allowed range of assets that can be allocated. As shown, all the initial solutions (i.e.  $S^1$  and  $S^2$  for the crossover application and  $S$  for the mutation application) have a number of allocations that are within the allowed range (i.e. 3-7), this means that in the initialisation phase the constraint on the number of asset is met. Nevertheless, combining or mutating acceptable solutions may not necessarily result in acceptable ones. This is why after the

application of the crossover and mutation operators – and before the selection process – the constraints functions of the Constraints.py module are applied a second time, as previously demonstrated within the initialisation process. This ‘double-check’ allows only feasible spatial plans to be part of the next generation of solutions.

Once all the spatial plans within the generation of solutions meet the constraints, they are evaluated against the objective functions, and the best-performing ones are selected to form the next generation of solutions and thereby undergo the next iteration of the optimisation process.

Although there is no formal restriction on the number of objectives that can be simultaneously considered in the optimisation process, the RAO applications presented in Chapters 5 and 6 both consider a particular trade-off between two conflicting objectives that are typical of spatial optimisation of resource allocation: the simultaneous maximisation of infrastructure accessibility and the minimisation of costs. This choice results in the definition of two objective functions used to evaluate the performance of each potential solution: 1) a distance function  $f_{dist}$  and 2) a cost function  $f_{cost}$ .

The distance function attributes a distance fitness ( $f_{dist}$ ) to each spatial plan. This fitness is minimised in the optimisation process. The fitness is a measure of the performance of the spatial plans with regards to a particular function. In both the applications presented in this study (UK and New Zealand case studies), distance is evaluated as travel time on the road network and travel times among all possible origins and destinations are directly read from the Distance Lookup variable created by the Network Analysis module presented in section 4.2.2.1.

Several metrics can be taken into consideration to measure the performance of different solutions; the RAO framework is extremely flexible in this regard to maximise transferability and scalability: since the formulation of optimisation functions is extremely case study dependent, Chapter 5 and 6 present a wide range of different formulations of objective functions to evaluate both distance and cost fitnesses. For example, regarding the distance function, among others, the average travel time between origins and destinations can be taken into account, a weighted average, the maximum travel time value, the average of the 90<sup>th</sup> quantile of the travel times or a Generalised Uniform Dose (see Chapter 5 for more

details) formulation can be adopted. Regarding the cost function formulation, the different scenarios presented in Chapters 5 and 6 present a broad range of different options, from linear to non-linear cost functions, from discrete to continuous formulations and from equations that take into account land values to the size of available vehicles' fleet to deploy strategic resources.

The choice of the metric has direct repercussions on the choice of Pareto-optimal solutions: same spatial plans may or may not result being Pareto-optimal according to different metrics. Since the objective functions definitions are strictly case-dependent, more details on the mathematical formulation adopted to evaluate spatial plans' fitness are provided in each scenario presentation in Chapters 5 and 6.

From the software architecture perspective, the evaluation of distance and cost fitnesses is handled by the Evaluate.py Python module. The main module, called RAO.py in the Python framework, has a function called "Evaluate" that takes a single spatial plan (i.e. a potential solution) as an input and, according to which scenario is selected by the user, returns its distance and cost fitness evaluated by calling the evaluation functions defined in Evaluate.py. The Evaluate function returns a tuple of values stored in the variables "Dist\_Fit" and "Cost\_Fit". This procedure is repeated for each Individual (i.e. spatial plan) that is part of the Generation of solutions.

#### 4.2.2.5. Multi-Objective Pareto-Optimal set maintenance

After the application of the constraint check and evaluation functions on *offspring<sub>g</sub>* (see section 4.2.2.4), the selection operator is applied to both *offspring<sub>g</sub>* and *parents<sub>g</sub>* to create *parents<sub>g+1</sub>*. Both *offspring<sub>g</sub>* and *parents<sub>g</sub>* have the same length; this length is:  $n_{parents}$ . *parents<sub>g+1</sub>* must have a length of  $n_{parents}$  as well. Figure 17 shows how to reduce the number  $2 \cdot n_{parents}$  of the combined sets *offspring<sub>g</sub>* and *parents<sub>g</sub>* to  $n_{parents}$  (which is the length of *parents<sub>g+1</sub>*).

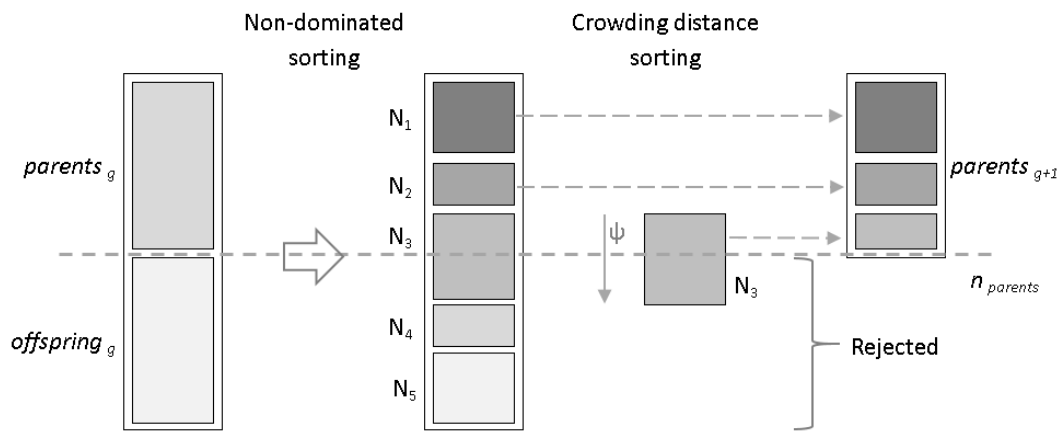


Figure 17 - Non dominated sorting, adapted from Deb et al. (2002).

First, a non-dominated sorting takes place among  $offspring_g$  and  $parents_g$ , the result is a series of  $N$  non-dominated sets. Once the first non-dominated set  $N_1$  is found, a new sorting takes place among the remaining solutions 'S' and the second set  $N_2$  is saved. Such a procedure does not stop until all S are allocated to a set  $N$ . The first  $N$  sets that can completely be part of  $offspring_{g+1}$  are stored into it, so referring to Figure 17:  $N_1$  and  $N_2$  are saved in  $offspring_{g+1}$ ,  $N_4$  and  $N_5$  are discarded, but part of  $N_3$  will be saved, and the other part rejected. They are sorted according to a crowding parameter  $\psi$  that is determined to decide which  $S \in N_3$  will be saved. The crowding distance determines the least represented parts of the Pareto front based upon the distance from the nearest solution in the objective space (Caparros-Midwood, 2015).

#### 4.2.2.6. Outputs

Once  $g = G$  (i.e. the maximum number of generations is reached), the genetic algorithm returns the final MOPO set  $N$  (see section 4.2.2.5). At this point, the last phase of the optimisation framework begins: the production of outputs. Outputs files are generated by the Output module (see Figure 8) which corresponds to the Outputs.py Python module in the RAO software application.

The outputs module constitutes another significant improvement with respect to previous optimisation frameworks due to its wide range of different output data types. This improvement broadens the horizon of possible visualisation techniques that can be adopted to present results due to the wider choice of output formats. Moreover, before saving the files

in the results folder, the Outputs module formats the information generated by the Genetic Algorithm in a suitable and intelligible way.

The first kind of generated output consists in the Pareto-optimal sets generated by the GA, these are the actual solutions of the multi-objective optimisation framework and they are saved in a text file stored in the outputs folder. They are formatted as shown in Figure 18.

	Solution ID	Spatial plan	$f_{dist}$	$f_{cost}$
Pareto set	[ 46745 ,	[ 0 , 0 , 1 , ... , 0 , 1 , 0 , 0 ] ,	[ 557.4 ,	2776672.0 ] ]
	[ 32788 ,	[ 0 , 0 , 0 , ... , 0 , 0 , 1 , 0 ] ,	[ 558.8 ,	2754827.0 ] ]
	.		.	
	.		.	
	[ 46743 ,	[ 1 , 0 , 0 , ... , 0 , 1 , 0 , 0 ] ,	[ 562.3 ,	2476334.0 ] ]
[ 10055 ,	[ 0 , 1 , 1 , ... , 0 , 0 , 0 , 1 ] ,	[ 553.1 ,	2788377.0 ] ]	
Normalised Pareto set	[ 46745 ,	[ 0 , 0 , 1 , ... , 0 , 1 , 0 , 0 ] ,	[ 0.0000 ,	0.401 ] ]
	[ 32788 ,	[ 0 , 0 , 0 , ... , 0 , 0 , 1 , 0 ] ,	[ 0.0082 ,	0.045 ] ]
	.		.	
	.		.	
	[ 46743 ,	[ 1 , 0 , 0 , ... , 0 , 1 , 0 , 0 ] ,	[ 0.0120 ,	0.005 ] ]
[ 10055 ,	[ 0 , 1 , 1 , ... , 0 , 0 , 0 , 1 ] ,	[ 0.3502 ,	0.000 ] ]	

Figure 18 - Format of Pareto sets. The Pareto sets are saved as text files in the output folder and also plotted in a graph representing the optimisation objectives on each axis.

The Pareto sets are then plotted on a graph representing the solution space, defined by the two optimisation objectives: solutions are plotted according to their  $f_{dist}$  and  $f_{cost}$  values. The plots are saved in JPEG format and are generated using the open source Python library Matplotlib (Hunter, 2007). Both the text files and the plots are produced for Pareto sets' absolute values and their normalised values. The "Normalise" function defined in the Outputs.py module normalises the pareto sets with respect the minimum and maximum values of their distance and cost fitnesses (respectively  $f_{dist}$  and  $f_{cost}$  ).

The second typology of output produced by the RAO framework consists in raster files representing Pareto-optimal spatial plans in TIFF format. The "Wrtie\_Rasters" function defined in the Outputs.py module makes use of the Python library rasterIO (Sean Gillies and others, 2013) to combine the spatial plans contained in the Pareto sets with their respective coordinates stored in the Lookup variable to produce a GeoTIFF file that can be imported in any GIS environment (see Figure 19).

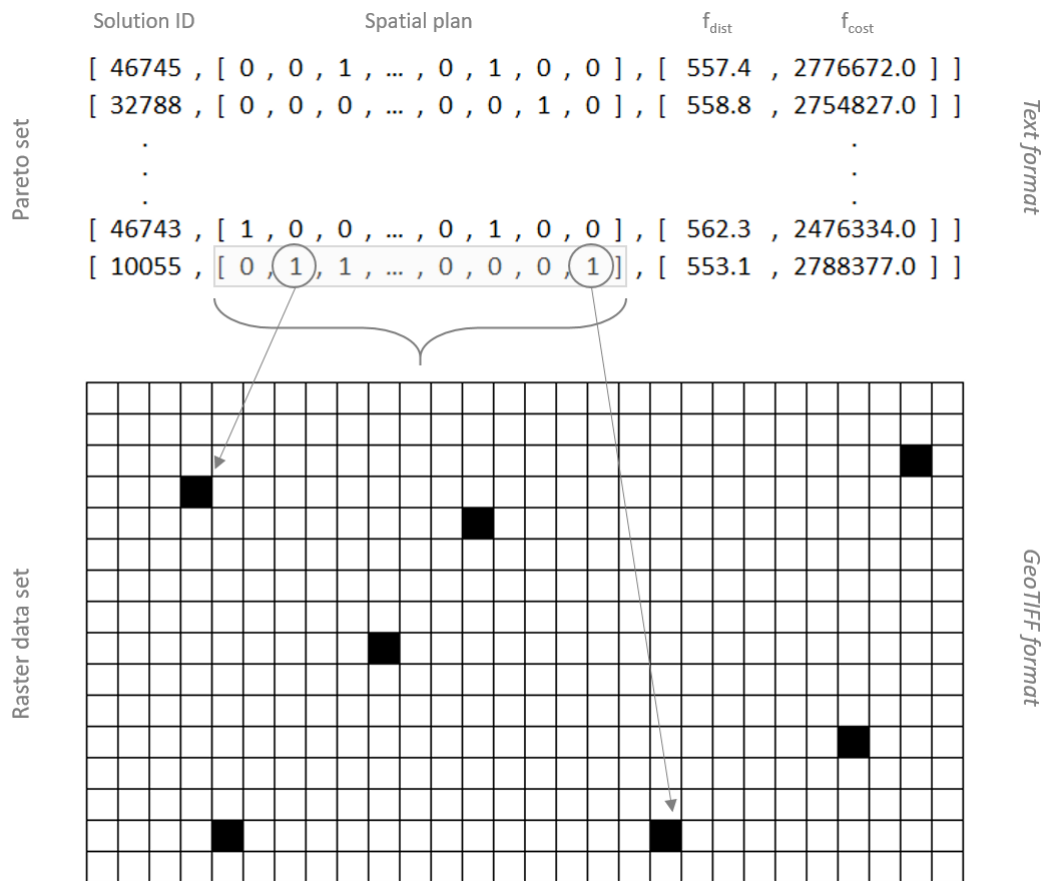


Figure 19 - Creation of raster output from the Pareto-optimal spatial plans contained in the Pareto sets (i.e. Pareto-optimal solutions produced by the Genetic Algorithm). Raster outputs are saved in the GeoTIFF format and can be imported in any GIS environment.

In addition to raster files, also vector files are created to allow the user to have a wide choice of formats for visualisation purposes. The procedure is the same as those demonstrated by the creation of raster data: the spatial plans contained in the Pareto sets are turned into shapefiles (.shp format) through the application of the “Generate\_sol\_shapefile” function defined in the Outputs.py Python module. This function makes use of the Python library GeoPandas (Jordahl *et al.*, 2020).

Finally, the last typology of output files produced by the RAO framework is comma-separated values (CSV) files containing information regarding the Pareto-fronts and the Pareto-optimal solutions. Pareto-fronts csv files have three columns: the first one indicates the solution number, the second one the distance fitness and the third one the cost fitness; they are created for both normalised and non-normalised Pareto-fronts. The spatial plans csv files also have three columns, but contain information regarding: 1) the solution ID, 2) the X coordinate and 3) the Y coordinate (for spatial representation in a GIS environment).

The RAO framework produces all the outputs described in the previous paragraphs for each generation (i.e. iteration) of the Genetic Algorithm, storing them in a subfolder called “Generations”. This allows the user to inspect the evolution of the Pareto-fronts for calibration purposes. To save memory, the user has the choice to only save the output files of the last iteration of the spatial optimisation iterative process.

#### 4.3. Development environment

The chosen programming environment is Python (Python Software Foundation, 2010). Python is a high-level open-source programming language with a wide range of mathematical and optimisation modules (Fortin *et al.*, 2012); Python is widely accessible, it easily interfaces with ArcGIS (ESRI, 2011) and it allows the use of the Geospatial Data Abstraction Library (GDAL/OGR contributors, 2019). Python is the programming reference language of a wide part of the literature regarding optimisation applications (Bröker *et al.*, 2005; Hebrard *et al.*, 2010; Matott *et al.*, 2011; Beham *et al.*, 2014) and spatial allocation optimisations (Ligmann-Zielinska *et al.*, 2005; Ligmann-Zielinska *et al.*, 2006; Ligmann-Zielinska and Jankowski, 2007; Ligmann-Zielinska *et al.*, 2008; Caparros-Midwood *et al.*, 2016).

RStudio (RStudio Team, 2015) is another open-source programming language that could have been chosen thanks to its ability to perform genetic algorithm optimisation (Scrucca, 2013) and its GDAL adaptation module: *rgdal* (Bivand *et al.*, 2019). Nevertheless, it is not broadly adopted in spatial optimisation literature and it is mainly used for visualisation purposes (Caparros-Midwood, 2015).

MATLAB (The MathWorks Inc., 2010) and AMPL (Fourer *et al.*, 2003) are both commercial software packages that could have been suitable choices as well. MATLAB (abbreviation for Matrix Laboratory) is a numerical computing environment in which it is possible to develop several optimisation applications (Sigmund, 2001; Lofberg, 2004). The main criticisms on the software are the non-user-friendly environment (Siauw and Bayen, 2014) and its inflexible language (Bröker *et al.*, 2005). AMPL (A Mathematical Programming Language) is another good alternative to perform complex mathematical processes; it is suitable for the development of optimisation applications (Fourer *et al.*, 2003), but, concerning spatial optimisation, its use is limited in the literature (Caparros-Midwood, 2015).

#### 4.4. Genetic Algorithm

Concerning the choice of the GA, Pyevolve (Perone, 2009) and Pygene (McNab, 2011) are two popular Python modules that can handle evolutionary operators. Nevertheless, Pyevolve lacks the necessary GAs necessary to perform multi-objective Pareto optimisation; Pygene has the operators, but its use in multi-objective optimisation is not well documented (Caparros-Midwood, 2015). Therefore, in this work, the very well documented DEAP (Distributed Evolutionary Algorithms in Python) module is used (Fortin *et al.*, 2012). Table 2 shows the DEAP modules used in the framework to handle the multi-objective Pareto-optimisation in the  $\mu + \lambda$  strategy (Fortin *et al.*, 2012).

Table 2 - Table of evolutionary operators used in the RAO framework

Operator	Module
Selection	<i>tools.selNSGA2</i>
Crossover	<i>tools.cxTwoPoint</i>
Mutation	<i>tools.mutUniformInt</i>

Referring to DEAP Documentation (DEAP Project, 2009), the *eaMuPlusLambda* function evolves a population of spatial plans and returns the optimised population together with a Logbook containing the statistics of the evolution process.

The main parameters of the *eaMuPlusLambda* function are the following:

- *population*: list of individuals (spatial plans).
- *toolbox*: used to “register” (i.e. define) individuals, population, the evolutionary operators and their decorator functions.
- *mu*: number of individuals selected to create the following generation.
- *lambda*: number of children to create at each generation.
- *cspb*: crossover probability.
- *mutpb*: mutation probability.
- *ngen*: total number of generations.

The evolution is performed by the application of the three evolutionary operators: selection (*tools.selNSGA2*), crossover (*tools.cxTwoPoint*) and mutation (*tools.mutUniformInt*). Their role is, respectively: evaluating and selecting the best performing solutions to create the



following generation, mating two “parents” spatial plans to create a new “child” spatial plan and, finally, randomly mutating a spatial attribute of a solution (for more details see section 4.2.2.3).

The choice of the values for the *lambda* and *ngen* parameters is the result of the calibration of the model, which consists in performing different runs varying those parameters and understanding a proper combination that can guarantee an acceptable quality of results and feasible running times.

The GA is run by the main Python module RAO.py in the function called “Genetic\_Algorithm”. This function first registers the population of solutions to consider as Generation 0 created in the initialisation phase (see section 4.2.2.1). Then, it runs DEAP’s function *eaMuPlusLambda*, and finally returns the variable “hof” (acronym of “hall of fame” as it registers the best performing solutions in the evolution process) that contains the Pareto-fronts.

As demonstrated in the previous paragraphs the “toolbox” is a special container in which to store a series of functions useful to the evolutionary process, such as initialisers, evolutionary operators and decorator functions. Decorator functions are key elements of the evolutionary process as they constitute the means through which the constraints functions defined in the Constraints.py module (see section 4.2.2.4) can be applied to the evolutionary operators.

#### 4.5. Summary

Chapter 4 introduced the methodology of the research conducted within this thesis. The details concerning the RAO framework are presented after an initial section presenting the problem formulation and describes the needs and drivers of this work. Basing on the information presented in chapter 3 concerning the several possible optimisation techniques, chapter 4 focuses on the justification of the choice of the genetic algorithm for producing Pareto-optimal solutions for the allocation problem.

The RAO framework presented in this chapter constitutes a unique collection of different components and techniques, combining established methods and innovative AI procedures incorporated in a novel software framework. It makes use of a GA in combination with a machine learning process (K-means clustering algorithm) and georeferenced data

management modules for input and output data. The development environment and the software implementation have been presented to describe the different phases and modules constituting the RAO framework, together with the input data and the output results. The application to real-life case studies of this methodology is presented in the following chapters.

## 5. Humber Estuary (UK) case study

### 5.1. Introduction Chapter 5

Chapter 5 presents the Humber Estuary case study. For this case study, the RAO framework is applied to an emergency planning optimisation problem. After an introduction to the context in which this study is applied (section 5.2), the gathered and produced datasets necessary to perform the study are presented (section 5.3). Section 5.4 covers the details of the application of the optimisation framework to this case study: from the problem formulation to the description of the different phases of the framework and from the definitions of the objective functions to the application of constraints. Finally, sections 5.5 and 5.6 present the results of the case study together with their discussion.

Table 3 presents a summary of the key information regarding the nature of the case study.

*Table 3 - UK case study problem definition summary table.*

Case study	Humber Estuary (UK)
Hazard	Flooding
Objectives	<ul style="list-style-type: none"> <li>- Minimisation of travel times between temporary flood defences storing facilities and deployment sites;</li> <li>- Minimisation of costs (i.e. number and size of warehouses).</li> </ul>
Scenarios	<ul style="list-style-type: none"> <li>- Scenario 1: Uniform rent price, discrete cost function</li> <li>- Scenario 2: Uniform rent price, discrete cost function with road network disruption</li> <li>- Scenario 3: Uniform rent price, linear continuous cost function</li> <li>- Scenario 4: Variable rent price (R/U), linear cost function with fixed number of lorries</li> <li>- Scenario 5: Variable rent price (R/S/U), linear cost function with fixed number of lorries</li> <li>- Scenario 6: Variable rent price (R/S/U), non-linear cost function with variable number of lorries (1)</li> <li>- Scenario 7: Variable rent price (R/S/U), non-linear cost function with variable number of lorries (2)</li> <li>- Scenario 8: Variable rent price (R/S/U), non-linear cost function with variable number of lorries (3)</li> <li>- Scenario 9: Variable rent price (R/S/U), non-linear cost function with variable number of lorries (0.5)</li> <li>- Scenario 10: Variable rent price (R/S/U), non-linear cost function with variable number of lorries (1), SI priority (top 3)</li> <li>- Scenario 11: Variable rent price (R/S/U), non-linear cost function with variable number of lorries (1), SI priority (top 5)</li> <li>- Scenario 12: Variable rent price (R/S/U), non-linear cost function with variable number of lorries (1), SI priority (top 10)</li> </ul>

	- Scenario 13: Variable rent price (R/S/U), non-linear cost function with variable number of lorries (1), SI priority (top 10 – excluding police and fire stations)
Main constraints	<ul style="list-style-type: none"> <li>- Minimum and maximum number of allowed warehouses</li> <li>- Minimum distance between allocated warehouses</li> <li>- Proximity of warehouses to major road</li> <li>- Maximum flood height: 1.5m</li> </ul>

## 5.2. Introduction to case study

Due to the extreme flood events occurred in recent years the UK (Somerset, Cumbria, Yorkshire, etc.), the UK government decided to take action to improve the resilience to flooding and ultimately increase the protection from disastrous events. Through the National Flood Resilience Review (Cabinet Office and DEFRA, 2016), the government committed £2.3 billion to be invested in a 6-year time frame to improve flood protection throughout the country. Part of this funding, namely £12.5 million, is explicitly allocated for temporary flood defences with the aim to improve the Environment Agency's stock.

Since the state of the art does not offer any efficient approach specifically designed for optimal investments in this kind of resources (Lopane *et al.*, 2019), this research presents a spatial optimisation framework – the RAO framework presented in Chapter 4 – originally applied for the allocation of temporary flood defences storing space, with the final goal to optimise the entire emergency response process.

The framework is designed to develop spatial plans that provide Pareto-optimal locations for warehouses to store temporary flood defences (refer to Chapter 2.3.2.2 for more details on temporary resources).

Strategic infrastructure networks are a priority in terms of protection during flood events, as their functioning guarantees the effective execution of emergency response operations. This is why, in this case study, strategic infrastructure assets are the main reference in the maximisation of the accessibility of emergency resources.

The multi-objective spatial optimisation framework balances the trade-off between two conflicting objectives. The first one consists is the minimisation of travel times from warehouses to strategic infrastructure assets (i.e. minimisation of transport and deployment

time of temporary flood defences). The second objective is the simultaneous minimisation of costs.

The Humber Estuary is a tidal estuary situated on the East coast of England, facing the North Sea; it sets the boundary between Yorkshire (North bank) and Lincolnshire (South bank) (Figure 20). It has been chosen as a case study area essentially for two reasons: 1) accessibility of data and 2) its nature of flood-prone area (e.g. 2007 and 2013 floods) (Coulthard and Frostick, 2010; Hull City Council, 2015; Environment Agency, 2016).



Figure 20 – Great Britain and Humber Estuary map.

### 5.3. Data

The source of the data used to model the case study area is the Ordnance Survey Collection available on the EDINA Digimap website ([digimap.edina.ac.uk](http://digimap.edina.ac.uk)). Georeferenced data representing geographical features of the studied area are collected in the form of raster and vector datasets and pre-processed in a GIS environment (ESRI, 2011).

They consist of physical constraints (like surface water and green areas) or critical infrastructure networks, like the road network (on which the network analysis to calculate travel times is based) and other strategic assets selected as priority targets to be protected during flood events (electricity production and distribution, gas distribution and storage, telecommunications, hospitals, fire stations and police stations).

The identification of priority strategic infrastructure assets is based on the fact that they are either functional to emergency response operations during disastrous events or particularly susceptible/dangerous in case of disruption (e.g. because of cascading effects with repercussions on other infrastructure).

This selection of high-priority strategic infrastructure assets can easily be modified in the input phase of the optimisation framework if the user is interested in considering additional or different types of infrastructure networks; the scenarios presented in section 5.5 present different options in the selection of different strategic infrastructure assets of which to prioritise protection.

Strategic infrastructure assets are considered as “destinations” in the accessibility optimisation process, while all the available locations for potential warehouses are assumed as “origins” of the journeys to transport and deploy temporary flood defences. The destinations’ locations are fixed parameters as they represent in-place infrastructure assets, while the origins’ locations are a variable of the the RAO framework, hence the necessity of a definition of “availability” for their allocation (for more details, see section 5.4.5).

*Table 4 - Input data for the Humber Estuary case study.*

<b>Input data</b>	<b>Format</b>	<b>Source</b>
Road network edges	Line shapefile	OS OpenData
Road network nodes	Point shapefile	OS OpenData
Green areas	Polygon shapefile	OS OpenData
Surface water	Polygon shapefile	OS OpenData
Power grid substations	Point shapefile	ITRC MISTRAL
Electricity production	Point shapefile	OS Digimap
Fire stations	Point shapefile	OS Digimap
Gas distribution/storage	Point shapefile	OS Digimap
Hospitals	Point shapefile	OS Digimap
Police stations	Point shapefile	OS DigiMap
Flood zones	Polygon shapefile	Environment Agency
Historic floods	Polygon shapefile	DEFRA

## 5.4. RAO framework applied to Humber Estuary case study

The RAO framework described in Chapter 4 is applied to the Humber Estuary case study introduced in chapter 5.2 to produce Pareto-optimal spatial plans of warehouses for storing emergency response resources. The following sections provide details regarding input parameters, variables, definitions and the different phases of the RAO framework applied to the Humber Estuary case study.

### 5.4.1. Input phase

Referring to the different phases of the optimisation framework described in Figure 9, the RAO framework initially takes a series of datasets as input and produces an availability raster indicating available locations for warehouses (see chapter 5.4.5 for the definition of “available” cells). On the base of this information, the variable “Lookup” is created, containing the coordinates of all available locations. Saving the coordinates in a lookup list rather than keeping a raster format is a standard procedure meant to reduce run time (refer to section 4.2.2.1 for more details on Lookup creation and data storing methodology of the RAO software framework).

### 5.4.2. Problem formulation

In the problem formulation phase, the user can set lower and upper bounds to the number of warehouses that can be taken into consideration in the solutions. For example, this study assumed a range between 2 and 10 warehouses, as for lower numbers and limited ranges (low variability), the RAO can produce Pareto-optimal solutions, but the potential of the approach is simply not exploited. For narrow ranges (e.g. exploring solutions with 3, 4 and 5 warehouses as well as considering solutions with 20, 21 or 22 warehouses) other approaches (e.g. exact methods) can be more efficient. The choice of a heuristic approach (thus the GA) is justified when considering a high variability of the number of warehouses taken into consideration: the higher this number, the higher the efficiency of this method (i.e. lower run times) with respect to exact optimisation methodologies.

The comparison between the heuristic approach here adopted and exact methods to solve multi-objective optimisation problems is framed in the broader topic of the balancing of the trade-off between the quality of results (i.e. how close to the mathematical optimum the solutions are) and feasibility (i.e. run times). This is the reason why the choice of the range of minimum and maximum number of warehouses to be considered in the solutions is fundamental to justify the appropriateness of the adopted optimisation methodology.

#### 5.4.3. Initialisation

The initialisation module is used at the beginning of the iterative process to generate the first generation of solutions. To speed up the evolution process, the initial population is not entirely randomly generated; the algorithm is seeded with some spatial plans resulting from a K-means clustering process aimed at providing potentially good locations for warehouses (refer to section 4.2.2.1 for a methodological definition of all the stages of the initialisation phase of the RAO framework).

K-means clustering (Ostrovsky *et al.*, 2013) is a machine learning technique aimed at partitioning a series of  $n$  data into  $k$  clusters. The SciKit-learn (Pedregosa *et al.*, 2011; Buitinck *et al.*, 2013) open source Python module allows performing a K-means clustering of all the available locations and finding the centroids of these clusters. The numbers of clusters taken into consideration is equal to the number of warehouses of each solution; this parameter does not have a fixed value as it constantly changes within the allowed range of minimum/maximum number of warehouses defined by the user. The coordinates of the clusters' centroids are the main outputs of the K-means module and are saved and stored in the results folder.

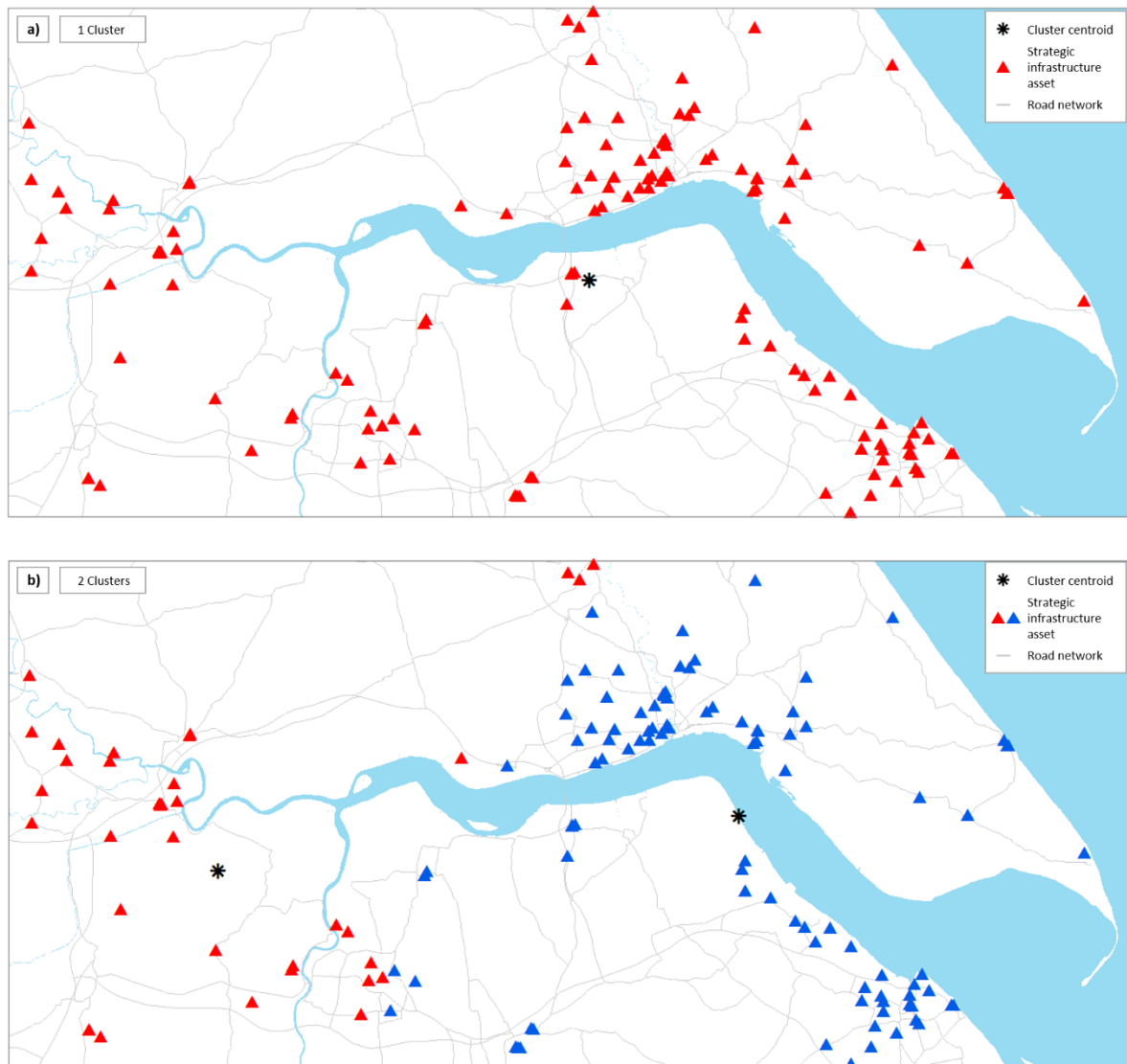
Subsequently, a network analysis is performed to calculate travel times from each available location and the closest cluster centroid (Figure 21). The analysis is performed evaluating shortest paths where distances are measured as travel times. Then, the available locations are ranked according to their proximity to the centroid of their cluster.

When the initial population of solutions is created, available cells close to their cluster centroid will be selected with a certain probability (definable and modifiable by the user – set at 80% in the following use cases), while the other locations are randomly selected from the Lookup



variable (see section 4.2.2.1 for more details on the software implementation of the K-means module and how its outputs are used in the generation of the initial population of spatial plans).

Figure 21 presents a visual example of the functioning of the K-means clustering: figures a) to e) show different ways to cluster strategic infrastructure assets according to the increasing number of clusters considered (respectively from 1 to 5).



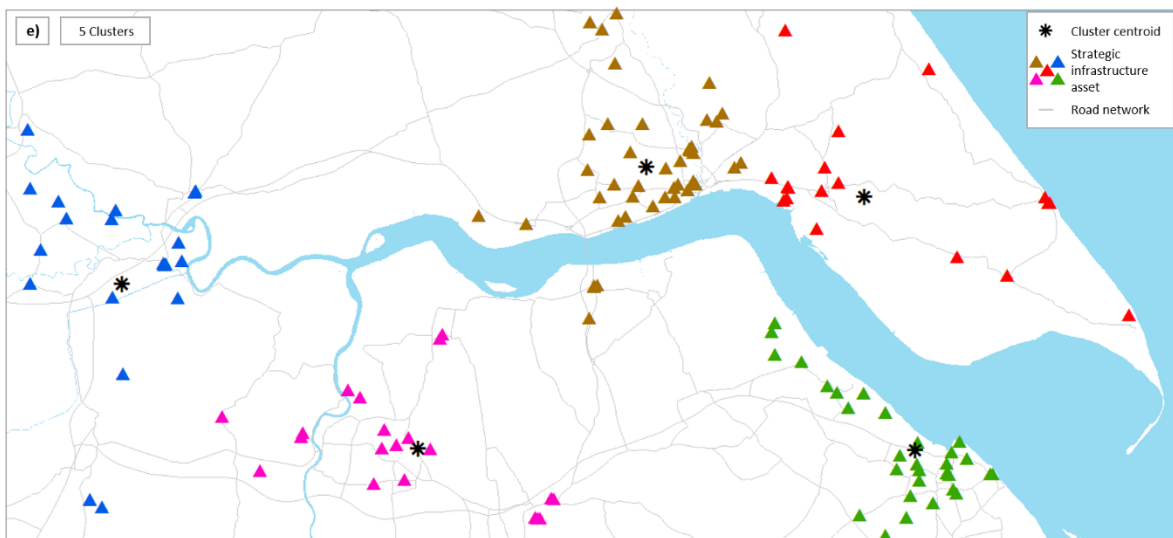
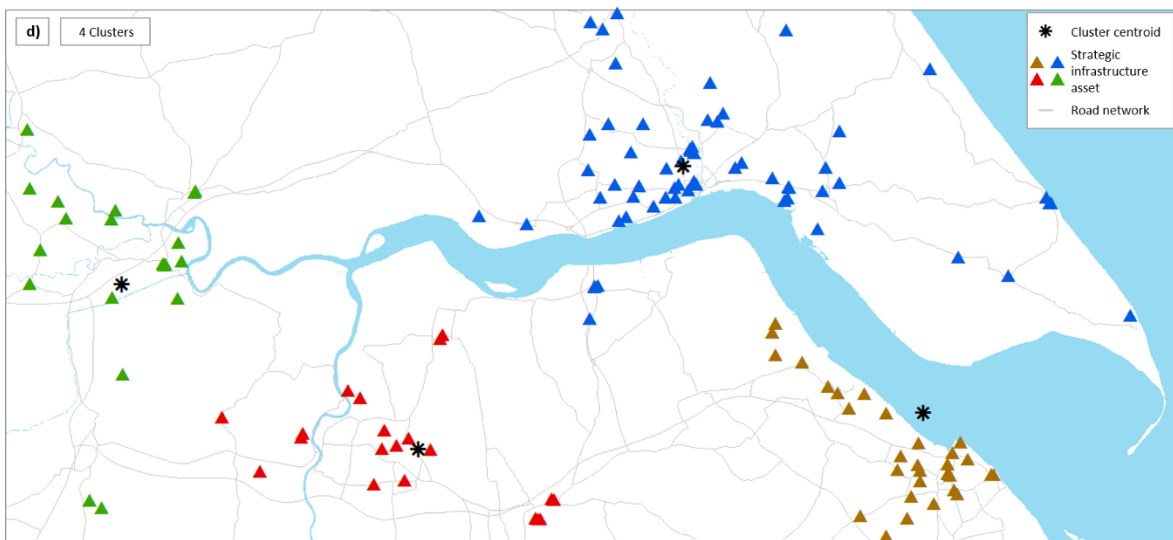
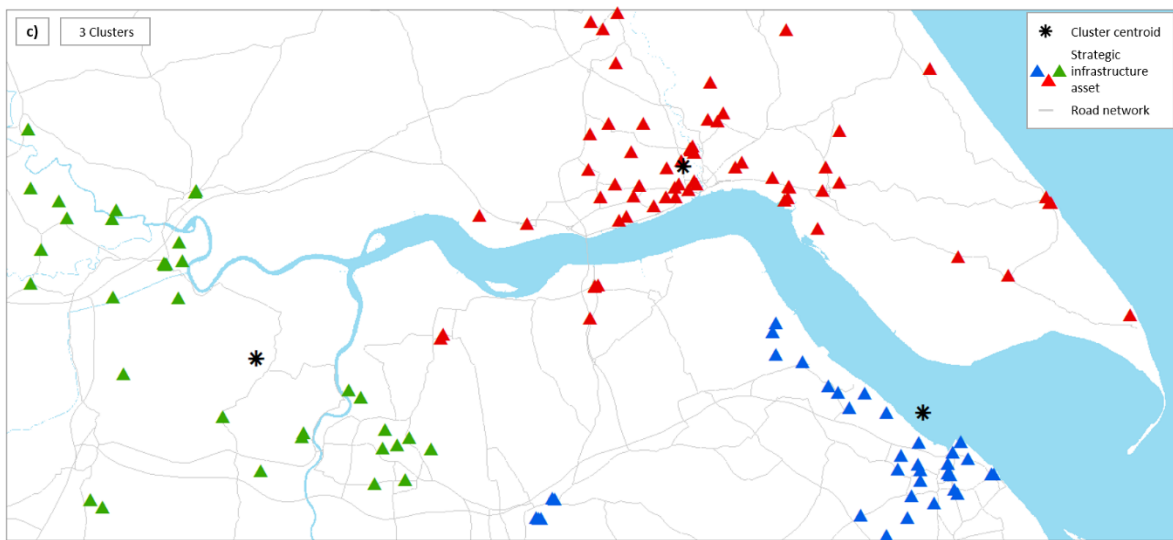


Figure 21 - K-means clustering of strategic infrastructure assets. Assignment to closest cluster centroid is performed according to proximity evaluated as travel time on the road network. Figures a) to e) show different ways to cluster strategic infrastructure assets according to the increasing number of clusters considered (respectively from 1 to 5).

#### 5.4.4. Evaluation

After the creation of the initial population, individuals (spatial plans) are evaluated against the objective functions, then the evolutionary operators are applied and the following generation is created. The procedure is repeated again in the iterative process: at every stage, the individuals of each generation are evaluated and assigned fitness values for each objective function.

##### *Distance function definition*

As presented in the methodology chapter (section 4.2.2.4), the objective functions are two: 1) a distance function  $f_{dist}$  and 2) a cost function  $f_{cost}$ . The distance function attributes a distance fitness ( $f_{dist}$ ) to each spatial plan. This fitness is minimised in the optimisation process. The fitness is a measure of the performance of the spatial plans with regards to a particular function. In this study, distance is evaluated as travel time on the road network. Several metrics can be taken into consideration to measure the performance of different solutions; for example, the average travel time from warehouses to strategic infrastructure assets, or the maximum travel time, or the average of the 90<sup>th</sup> quantile of the travel times. The choice of the metric has direct repercussions on the choice of Pareto-optimal solutions: same solutions may or may not be Pareto-optimal according to different metrics.

Two different distance function formulations are implemented in the RAO framework's Humber Estuary application: one is designed to maximise accessibility considering warehouses' service area as the main parameter, and the other is able to take into account the vehicles' fleet dimension to focus on the deployment time of temporary flood defences. The choice to maintain two options in the mathematical formulation of accessibility is aimed at maximising the flexibility, transferability and scalability of the methodology: according to the available input data (i.e. knowledge of details regarding available fleet) the user can choose among different optimisation functions the one that is most suitable for the specific scenario to evaluate.

The first definition of distance function consists in a weighted average of travel times from storing locations to strategic infrastructure assets that follows the rule:

$$f_{dist} = \sqrt[n]{\sum_{i=1}^A TT_i^n} \quad (5.1)$$

Where:

- $A$  = total number of strategic infrastructure assets,
- $TT_i$  = Travel times from each strategic infrastructure asset to the closest warehouse,
- $n = 2$ .

With this formulation, every journey time (from warehouses to strategic infrastructure asset) is weighted directly proportionally to its own value: i.e. the higher the travel time, the greater the weight. The reason for choosing this formulation is to penalise spatial plans with higher travel times without losing information about lower ones (i.e. to avoid bottleneck problems when considering wide ranges of possible travel times).

Equation (5.1) represents the formulation of the generalised Equivalent Uniform Dose (gEUD) (Niemierko, 1997), which is used in medical science to measure optimal radiation dosage to treat tumours, as cancer treatment is a spatial problem as well: clonogens (i.e. tumour cells) must be killed by irradiating the area with a specific amount of radiation (dose). The Equivalent Uniform Dose is the amount of uniformly distributed dose that keeps alive the same average number of clonogens than an equivalent non-homogeneous distribution. Therefore, the EUD is a parameter meant to easily compare different treatment plans when irradiations are not homogeneous (Henríquez and Castrillón, 2011).

In the same fashion, RAO's gEUD formulation provides a fitness measure that is ideal for comparing different non-homogeneous spatial plans like the ones inspected by the RAO. It helps to avoid problems especially with outliers and bottleneck effects. The  $n$  parameter of equation (5.1) has a value of 2 since the analysed spatial problems of this work are two-dimensional. Even though the distance function measures a mono-dimensional quantity (i.e. travel time), the nature of the problem is bi-dimensional because what this fitness actually wants to measure is the efficiency of the area of influence of each warehouse.

The alternative distance function formulation takes into account the number of lorries necessary to transport emergency resources to deployment sites and the necessary number of trips. The formulation is:

$$f_{dist} = \frac{\sum_{i=1}^{SI} 2 \cdot TT_i}{n_{EF}} \quad (5.2)$$

Where:

- $f_{dist}$  = total amount of time necessary to deploy all the strategic resources,
- $SI$  = number of Sritical Infrastructure assets,
- $TT_i$  = average Travel Time from i-th warehouse to SI sites (in minutes),
- $n_{EF}$  = Existing Fleet (i.e. number of available lorries).

### *Cost function definition*

The cost function attributes a cost fitness ( $f_{cost}$ ) to each spatial plan. Similarly to the distance function, the cost fitness is minimised in the optimisation process, and similarly to the distance function, several formulations of the cost function are implemented in the RAO framework to allow the user to choose the most appropriate to their goal and to their available information. The different scenarios presented in section 5.5 present several combinations of different distance and cost functions to demonstrate the flexibility and transferability of the methodology not only in terms of spatial domain, but also in terms of diversity of available data, a priori knowledge, assumptions and solutions' range of inspection.

The cost functions presented below have different characteristics in terms of function continuity (i.e. discrete functions vs continuous functions), linearity (linear vs non-linear) and in terms of external factors taken into account (e.g. land value, urban vs rural locations, decreasing market unitary process etc.).

The first distinction among cost function formulations is between discrete and continuous functions. The discrete formulation first calculates the total amount of flood defences that must be stored in each warehouse according to the served assets, then, basing on this information, it attributes a size to the warehouse. Finally, the cost of each warehouse is calculated basing on the annual average cost per square metre for warehouses in the studied area. The final value of  $f_{cost}$  is the sum of the costs of all the warehouses considered in each spatial plan.

Considering typical commercial temporary demountable flood barriers and considering flood heights up to 1.5 metres, 100m of barriers can be stored in a standard 20 ft shipping container

(dimensions: 6m x 2.44m x 2.6m). Maximum flood heights are considered because currently temporary flood barriers cannot cope with water depths greater than 2 m and only a few have been tested above 1 m (Cabinet Office and DEFRA, 2016).

The perimeter of strategic infrastructure assets of the case study area has been evaluated and an average perimeter has been considered for each typology of infrastructure (Table 5).

*Table 5 - Average perimeter of strategic infrastructure assets in the Humber Estuary region.*

Strategic infrastructure	Perimeter [m]
Power grid substations	400
Electricity production	2400
Fire stations	200
Gas distribution/storage	1200
Hospitals	900
Police stations	200

According to the amount of emergency response resources needed by the assets served by a particular warehouse, the cost function assigns a dimension to it. Five different typologies for warehouses are considered in this study according to their size; more details can be found in Table 6.

*Table 6 - Sizes of warehouses for the Humber Estuary case study.*

Warehouse dimension [m <sup>2</sup> ]	Warehouse typology (according to dimension)	Number of 20 ft shipping containers that is possible to store (on 2 levels)	Length of flood barriers that is possible to store
70	A	4	0.4 km
320	B	40	4 km
640	C	80	8 km
960	D	120	12 km
1280	E	160	16 km

A market analysis has been performed on industrial rents in the region of Yorkshire for the year 2017 (see Figure 22). According to its results, the first (and simplest) assumption is to consider the average cost of £55.00 per m<sup>2</sup> per annum as a strong correlation between rent prices and rural/urban areas does not appear evident.

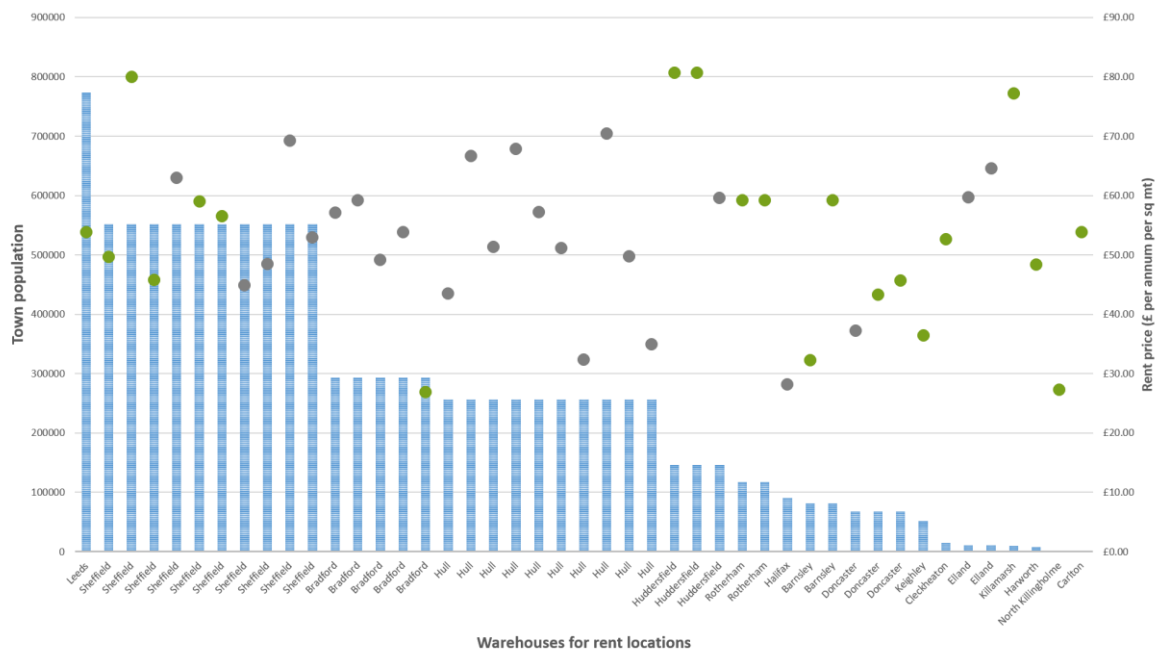


Figure 22 - Industrial rent prices per square metre in Yorkshire (2017). Green dots represent warehouses for rent outside urban areas, while grey dots represent warehouses within town borders.

However, the RAO framework allows the user to choose among different options in terms of linearity of warehouses' rent price. While the first scenarios presented in section 5.5 make use of the average rent price, also more advanced formulations are presented in the following scenarios with increasing level of complexity in their formulation.

When considering a non-linear function representing warehouses rent prices, a logarithmic regression provides the best fitting non-linear interpolation of the market research presented in Figure 22. Among the different available choices, the logarithmic regression presents the highest  $R^2$  value compared to the other regression techniques; Figure 23 and Table 7 present further details regarding the logarithmic regression and the comparison with different regression options.

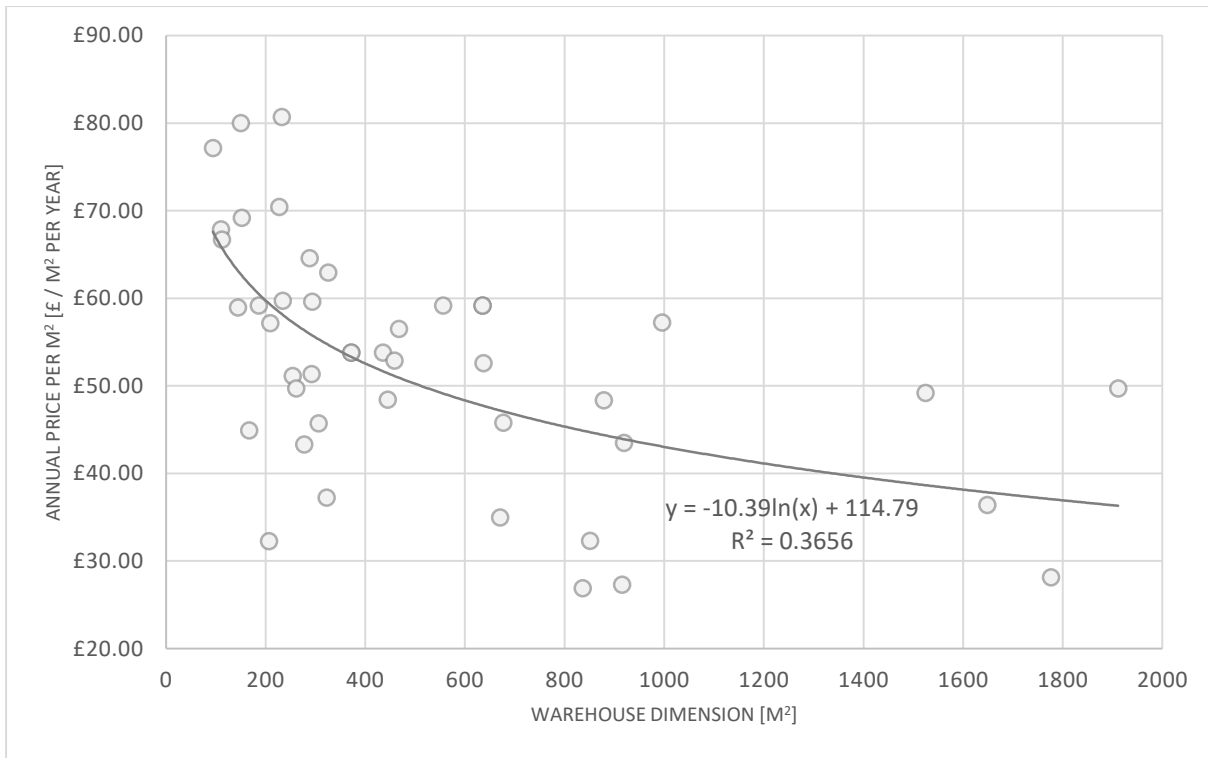


Figure 23 - Relationship between warehouses' dimension and annual rent price with logarithmic regression.

Table 7 - Regression options for annual rent prices and warehouses' dimensions.

Trendline	Equation	R <sup>2</sup> value
Logarithmic	$y = -10.39 \cdot \ln(x) + 114.79$	0.3656
Polinomial	$y = 0.00002 \cdot x^2 - 0.045 \cdot x + 68.612$	0.3566
Power	$y = 174.19 \cdot x^{-0.206}$	0.3393
Linear	$y = -0.0153 \cdot x + 60.856$	0.2686
Exponential	$y = -60.163 \cdot e^{0.0003 \cdot x}$	0.2671

For both discrete and continuous, and linear and non-linear formulations, the cost function includes capital and operational costs for both warehouses (W) and emergency resources (R) (Hendrickson, 1989; Ramos, 2017; Mishra, 2021); the most general formulation is:

$$f_{cost} = W + R \quad (5.3)$$

W and R can be further divided into capital (capex) and operational (opex) costs, to get to the following formulation:



$$f_{cost} = W_{capex} + W_{opex} + R_{capex} + R_{opex} \quad (5.4)$$

In the RAO application to the Humber Estuary case study, warehouses' and resources' capital and operational costs take into account a number of different parameters, and their formulation can be defined as:

$$W_{capex} = \begin{cases} \sum_{i=1}^W f_i \cdot p_i, & \text{linear formulation} \\ \sum_{i=1}^W (\alpha \cdot \ln(f_i) + \beta) \cdot p_i, & \text{non-linear formulation} \end{cases} \quad (5.5)$$

$$W_{opex} = m_w \quad (5.6)$$

$$R_{capex} = p_b \cdot l_b \quad (5.7)$$

$$R_{opex} = hp \cdot n_p \cdot n_h + p_l \cdot n_l + m_r \quad (5.8)$$

To get to the final equations, respectively for linear and non-linear formulations:

$$f_{cost} = \begin{cases} \sum_{i=1}^W f_i \cdot p_i + m_w + p_b \cdot l_{ab} + hp \cdot n_p \cdot n_h + p_t \cdot n_t + m_r & \text{linear} \\ \sum_{i=1}^W (\alpha \cdot \ln(f_i) + \beta) \cdot p_i + m_w + p_b \cdot l_{ab} + hp \cdot n_p \cdot n_h + p_l \cdot n_l + m_r & \text{non-linear} \end{cases} \quad (5.9)$$

Where:

- $f_{cost}$  = total cost of warehouses and emergency resources,
- $W$  = total number of warehouses,
- $f_i$  = floor space of the  $i$ -th warehouse (in  $m^2$ ) – floor space can take into account multi-storey even if this is unlikely.,
- $p_i$  = annual rental price per square metre of  $i$ -th warehouse – either average or function of the area (urban/rural),
- $\alpha, \beta$  = parameters of logarithmic equation (regression from Yorkshire rent prices – see Figure 23),
- $hp$  = hourly pay for personnel,
- $n_p$  = number of workers for strategic resources' deployment,
- $n_h$  = number of working hours for deployment and removal of temporary defences,

- $p_l$  = rent price of a lorry,
- $n_l$  = number of additional lorries to existing fleet,
- $m_w$  = warehouses maintenance costs,
- $m_r$  = emergency resources maintenance costs,
- $p_b$  = unitary price of demountable barriers (£/m),
- $l_{ab}$  = total length of additional demountable barriers needed.

### *Cost function – capital cost of warehouses*

Given the numerous factors that compose the cost function formulation, several assumptions have been made in the application of the RAO framework to the Humber Estuary case study. The first assumption regards the choice of considering warehouses' floor space to measure the capital cost of warehouses: doing so (instead of considering buildings' footprints) allows to take into account multi-storey warehouses, even if this is not a likely scenario as building in vertical is always more costly than building one-storey warehouses, especially in non densely populated areas. However, choosing floor space as reference measures guarantees a high transferability of the methodology even to highly urbanised case studies.

As anticipated, the parameter  $p_i$  represents warehouses' annual rental price per square metre, and its value is chosen by the user among different options. The scenarios of section 5.5 present several examples of different choices, which, however, can be summarised as:

1. Considering the average value of rent prices in the area;
2. Distinguish between urban and rural areas, considering urban locations as more expensive;
3. Subdivide the case study area in three different categories: urban, suburban and rural.

Consequently  $p_i$  assumes different values according to which scenario the user considers:

$$p_i = \begin{cases} p_{av} & \text{average rent price} \\ p_{av} \cdot \gamma_u + p_{av} \cdot \gamma_r & \text{urban + rural} \\ p_{av} \cdot \gamma_u + p_{av} \cdot \gamma_s + p_{av} \cdot \gamma_r & \text{urban + suburban + rural} \end{cases} \quad (5.10)$$

Where:

- $p_i$  = annual rental price per square metre of i-th warehouse (see equation (5.9))
- $p_{av}$  = average rent price of the case study;

- $\gamma_u$  = multiplier for urban areas;
- $\gamma_r$  = multiplier for rural areas;
- $\gamma_s$  = multiplier for suburban areas.

Regarding the assumptions made for the Humber Estuary application, the value of  $p_{av}$  has been calculated from the industrial rent prices per square metre in Yorkshire in 2017 (see Figure 22) as £55.00 per square metre per annum. Instead, due to lack of data, the multipliers  $\gamma_u$ ,  $\gamma_r$  and  $\gamma_s$  have been assumed respectively as 2.0, 1.0 and 1.5; implying that urban locations cost twice as much as rural ones, with suburban values in the middle.

#### *Cost function – urban, suburban and rural areas*

The definition of urban, suburban and rural areas required some research and ultimately some assumptions as well, as there is no consistent agreement among scholars concerning the definition of what is “urban” and what is not. For instance, D'Acci (2019) presents a case study on real estate values depending on several factors like the quality of urban area, the distance from city centre, and housing value for the area of Turin (Italy) and shows an incredibly high number of different examples from the literature (more than one hundred) that try to relate land value to positional factors like distance from CBDs, green areas, social contexts etc.

An option for the categorisation of urban, suburban and rural areas was the Coordination of Information on the Environment Land Cover (Corine Land Cover - CLC) (Heymann *et al.*, 1994). CLC is a computerised land cover inventory of EU countries, however, in most cases the dataset is outdated and data are only available for European countries, so a more generally applicable definition has been applied to maximise the transferability of the presented methodology.

The UK government introduced the Rural-Urban Definition (The Countryside Agency *et al.*, 2004) in 2004, determining that settlements with population of 10,000 are defined as urban and the rest of the land is defined as rural. Regarding boundaries, reference is made to Office for National Statistics' (ONS) data set based upon land use. Several rural-urban data sets are available on ONS's website for England and Wales at different levels of aggregation, like Output Areas (OAs), Lower layer Super Output Areas (LSOAs) and Middle layer Super Output Areas (MSOAs).

Dijkstra and Poelman (2014) introduce the “degree of urbanisation” (DEGURBA) classification, which identifies three categories: 1) densely populated areas (>50% living in high-density clusters), 2) intermediate (<50% of population living in rural grid cells and <50% living in high-density clusters) and 3) thinly populated areas (>50% living in rural grid cells). While Dijkstra *et al.* (2020) present the advantages of the “Degree of Urbanization” (European Commission *et al.*, 2020) (also endorsed by the UN Statistical Commission), which identifies three categories of settlements: 1) Cities (with population >50,000 and densities >1500 inhabitants/km<sup>2</sup>); 2) Towns (with population >5,000 and densities >300 inhabitants/km<sup>2</sup>) and 3) Rural areas.

To maximise the transferability of the methodology, European Commission *et al.* (2020)’s “Degree of Urbanization” is the definition adopted by the RAO application as it has been specifically designed to facilitate international comparisons. Available cells for warehouses allocation of the Humber Estuary area have been attributed to “urban”, “suburban” and “rural” areas according to the population densities of their corresponding Middle layers Super Output Areas (MSOAs) (see Figure 24).

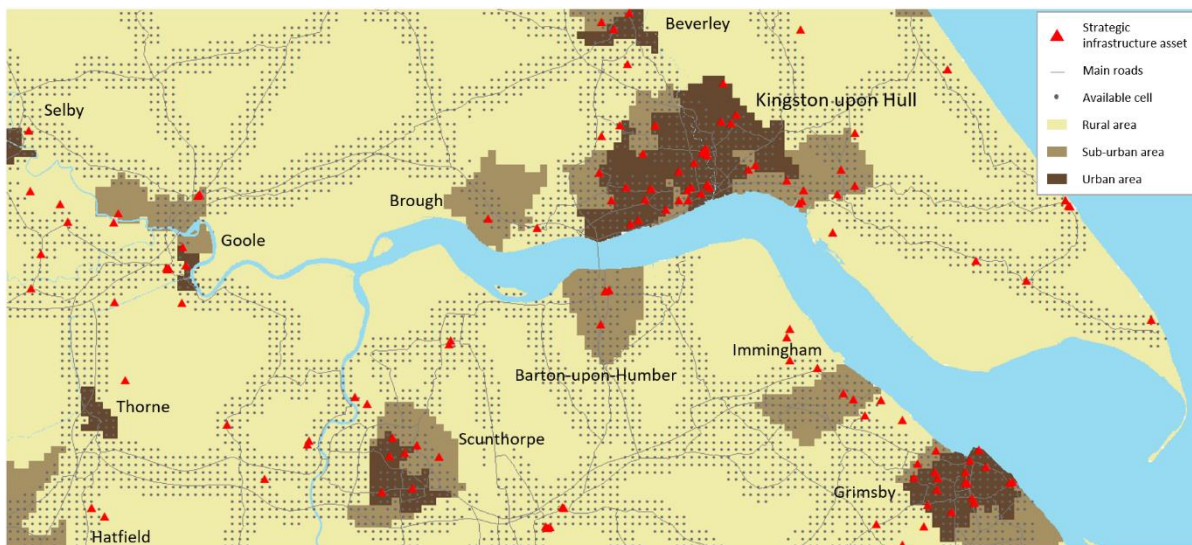


Figure 24 - Rural, suburban and urban areas in the Humber Estuary according to the Degree of urbanization definition.

#### Cost function – operational cost of warehouses

Regarding storing spaces’ operational costs, warehouses’ maintenance has been assumed proportional to the floor space. The  $m_w$  parameter of equation (5.9) constitutes an input parameter and the user can choose its value. To enrich the spectrum of analysis of the Humber

Estuary case study, the scenarios presented in section 5.5 explore different values of  $m_w$ : respectively 0.0 and  $0.2 \cdot W_{capex}$  (i.e. 20% of warehouses' capital cost). These two values are different because, for industrial rents, depending on different contracts' typologies, sometimes the maintenance costs are included in the lease and sometimes they have to be paid on top of it as NNNs. NNN is an acronym for "Net, Net, Net" and these fees include property taxes, property insurance and CAM (Common Area Maintenance).

#### *Cost function – personnel costs*

Environment Agency's Temporary and Demountable Flood Protection Guide (Ogunyoye *et al.*, 2011) provides useful information concerning the assumptions on personnel costs adopted in the Humber Estuary RAO framework application. This report highlights how frequently flood emergencies occur at nighttime and outside working hours; this has repercussions on the safety of personnel, since they are often called to address the emergency after a whole day of work, being tired and operating in often "dark, wet, cold and slippery conditions".

To minimise the risk of accidents, Ogunyoye *et al.* (2011) provide a series of recommendations for emergency procedures, suggesting that they should pay particular attention to staff management and shifts allocations for portable barriers deployment when transportation and installation require more than six hours.

Based on this evidence, the assumption adopted in the RAO software application is that the parameter  $n_p$  in equation (5.9) is initialised to 0. This implies that no extra cost for personnel are included in the cost function formulation, as it appears clear from Ogunyoye *et al.* (2011) that, in the UK, the specialised workers who deploy temporary flood barriers are full-time employees who are called during emergency, in case even outside their normal working hours. However, for transferability purposes, the RAO framework's cost function formulation allows the user to include the personnel cost for applications in different regions (e.g. outside the UK) or different applications (e.g. extraordinary circumstances in which personnel costs are not covered by government bodies' funding).

### *Cost function – fleet costs*

The Temporary and Demountable Flood Protection Guide (Ogunyoye *et al.*, 2011) also provides indications regarding transportation of emergency resources, in particular referring to the location of warehouses and their proximity to transportation companies or availability of lorries for barriers deployment close enough to the storing facility.

Several options are contemplated by Ogunyoye *et al.* (2011): a wide spectrum of vehicles ranging from small trailers to large shipping containers for transportation of strategic resources from warehouses to deployment sites. No matter what type of vehicle is adopted, a high relevance is given to the emergency strategy that should maximise transportation means accessibility to guarantee the success of emergency operations during flood events.

Similarly to the personnel cost assumption, there is no evidence to assume that vehicles are rented for single events and their cost does not directly influence the warehouse allocation, which is the main objective of the RAO framework. For transferability and scalability purposes, the user is able to set the value of  $n_l$  in equation (5.9), which represents the additional number of lorries to the existing fleet, but in the scenarios presented in section 5.5, the most reasonable assumption is to initialise this parameter to zero.

### *Cost function – temporary flood barriers unitary price*

Environment Agency's Temporary and demountable flood protection guide (Ogunyoye *et al.*, 2011) has an interesting appendix providing information on a wide range of commercially available temporary flood barriers, covering all the typologies presented in section 2.3.2.2 and Figure 5. For each barrier typology, several technical details are available, among which: product name, manufacturer, supplier details, description of the product, dimensions, structural details, adaptability to terrain conditions, operational details and financial details.

Every temporary flood barrier presented has a cost section containing information on installation requirements and costs, maintenance and cleaning requirements, reusability, warranty and deterioration details.

For instance, the "Mobile Flood Protection System", manufactured by Flood Protection Systems Sweden AB consists in a metal foldable frame covered with a waterproof plastic

membrane. The cost for the installation of 100m of barriers is estimated at £12,000 for a 0.8m height and it increases to £20,000 for a 1.2m height. According to the materials and the manufacturer, however the cost can vary considerably; as a matter of example, another Swedish manufacturer, Geodesign AB, produces barriers that cost between £30,000 and £50,000 for 100m long and 1.25m high barriers (according on barrier material and storage system) (Ogunyoye *et al.*, 2011).

In the Python formulation of the RAO framework, the linear cost of demountable barrier is represented by the variable “barriers\_lin\_cost”, which refers to the  $p_b$  parameter of equation (5.9). The user is able to choose any barrier typology that they deem appropriate to the case study terrain or the available budget, and set the linear price of the temporary flood barriers accordingly.

In the scenarios of section 5.5 the assumption for the parameter  $p_b$  is to consider it equal to zero. This assumption implies that no additional temporary barrier is going to be acquired in the case study scenarios: the RAO framework allocates warehouses to maximise their accessibility assuming that the amount of available demountable barriers in the Humber region suffices to cover the whole area. Nevertheless, to maximise the transferability of the methodology, even if initialised to zero,  $p_b$  is an integral part of the cost formulation and its input value can easily be adapted to the considered case study or scenario.

#### *Cost function – temporary flood barriers maintenance costs*

As anticipated in the previous section on barriers’ unitary price, Environment Agency’s Temporary and demountable flood protection guide (Ogunyoye *et al.*, 2011) annex provides useful information on maintenance costs of commercially available temporary flood barriers. The maintenance cost is strictly dependant on the typology of the chosen flood barrier. Some temporary measures require more maintenance than others; for instance freestanding barriers need to be clean, dried and packed before being stored, while impermeable containers do not require any maintenance at all.

In the scenarios presented in section 5.5, the parameter  $m_r$  of equation (5.9) representing the maintenance costs of demountable barriers is assumed equal to zero as it is assumed to be assimilated into the personnel cost: from Ogunyoye *et al.* (2011), it appears evident that the

costs related to the maintenance of temporary flood protections almost always pertain personnel costs to perform standard procedures like cleaning and packing. Such operations are likely to be carried out by the same personnel deploying the temporary barriers and for this reason, this cost is assumed to be covered by the personnel cost. However, to maximise transferability and scalability of the optimisation framework, the  $m_r$  parameter is kept independent to allow the modelling of non-standard implementations of temporary barriers requiring additional maintenance costs.

#### 5.4.5. Constraints

The chosen programming philosophy aims to leave the algorithm the most unconstrained as possible in order to let it free to explore the widest possible area of the solution space. Nevertheless, a few constraints are implemented in order to discard unrealistic solutions (see section 4.2.2.4 for a general definition of the RAO framework's constraints implementation).

Due to the nature of the evolutionary operators meant to modify solutions' spatial attributes (see Chapter 4.2.2), when mating and mutating individuals, it is possible to generate solutions that have a number of warehouses that is higher than the maximum allowed or lower than the minimum. This is why a constraint decorator is applied to the evolutionary operators' functions: it counts the number of warehouses present in the solutions after the application of the evolutionary operators and it discards those spatial plans that are outside the boundaries.

Moreover, to speed up run times, a distance constraint is applied when generating new spatial plans. This function measures the distance among the warehouses present in a potential solution and checks whether they are far apart from each other enough. If two warehouses are closer than a minimum distance set by the user, the solution is discarded; after a calibration process, a distance of 10 km resulted sufficient to decrease run times without heavily constraining the algorithm.

The definition of available locations for warehouses happens in the initialisation phase (see section 4.2.2.1), but it is itself based on meeting a series of constraints; locations are defined "available" if:



1. They are within the case study boundaries.
2. They are within 500 metres from a major road (constraint meant to avoid locations that are hard to be reached and to speed up the evolution process).
3. They are outside the flood zone.
4. They do not overlap protected green areas and/or parks.
5. They are on dry land.

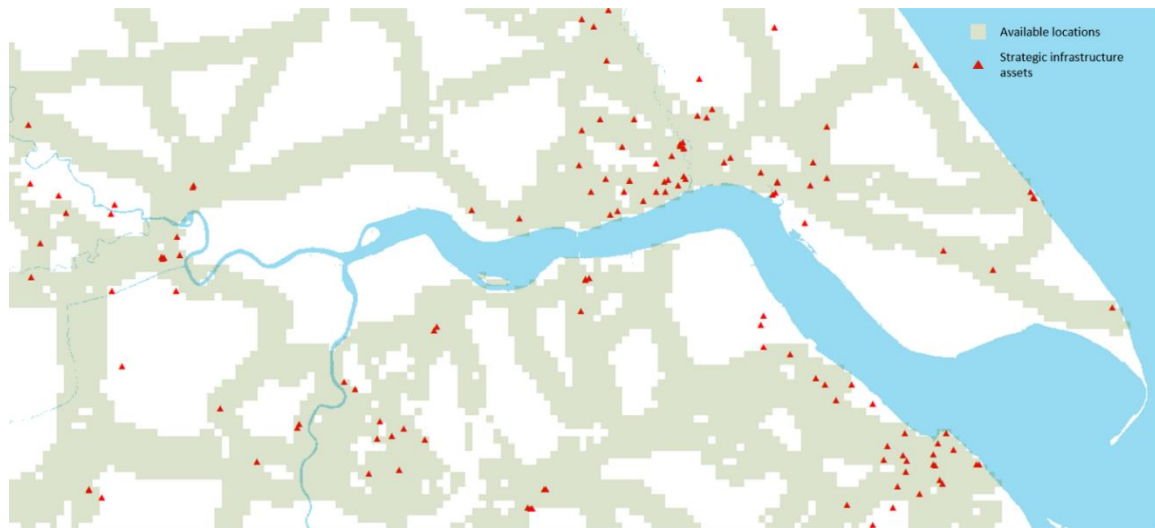


Figure 25 - Humber Estuary case study: available locations and strategic infrastructure assets.

Figure 26 shows the algorithm to determine how to label a location as “available” and Figure 25 shows all the locations that meet the criteria to be labelled as “available” and taken into consideration in the network analysis as origins. This is the result of the first phase of the optimisation framework: a raster dataset (500 m resolution) containing information about available locations. It is created and saved in the data folder, available to be open and used in the following phases of the process.

The 500 m resolution is itself another constraint dictated by run time necessities; higher resolutions necessarily imply more precision, but at the same time higher computational efforts. Another constraint related to the nature of the input datasets consists of the definition of travel times. As anticipated in section 4.2.2, travel times are evaluated based on the free flow speed on network edges. This implies neglecting the traffic variable and the consequential consideration of a best-case scenario. Besides, the free flow speed is evaluated basing on the average speed attributed to each road edge, which depends on the road type (e.g. Highways speed: 90 km/h; Secondary roads speed: 80 km/h).

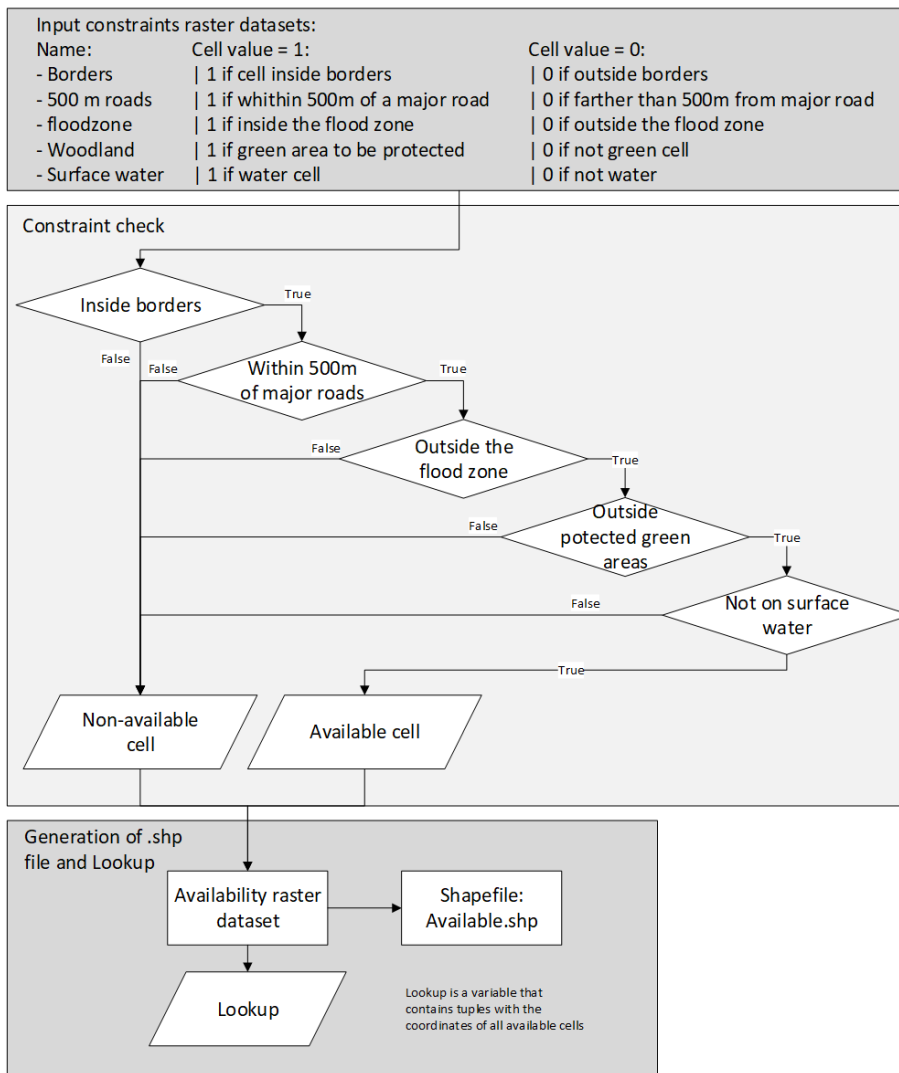


Figure 26 - Flowchart of the initialisation process for the Humber Estuary case study.

Finally, as anticipated (sections 2.3.2.2 and 5.4.4) current commercially available flood barriers cannot cope with water depth greater than 2 m and that only a few have been tested for water depths greater than 1 m (Cabinet Office and DEFRA, 2016). Hence, the choice to consider maximum flood depths of 1.5 m when estimating maximum volumes required for storing space.

#### 5.4.6. GA calibration

As anticipated in Chapter 4.4, the genetic algorithm chosen for the evolution of spatial plans is DEAP's  $\mu + \lambda$  strategy (Fortin *et al.*, 2012). Referring to DEAP Documentation (DEAP Project, 2009), the *eaMuPlusLambda* function evolves a population of spatial plans and returns the

optimised population together with a Logbook containing the statistics of the evolution process.

A general description of the main parameters of the *eaMuPlusLambda* formulation can be found in section 4.4. Regarding its application to the Humber Estuary case study, the choice of the values for the *lambda* (number of spatial plans to generate in each generation) and *ngen* (number of generations) parameters is the result of the calibration of the model. Calibrating the model means to perform different runs varying those parameters and understanding a proper combination that can guarantee an acceptable quality of results and feasible running times.

For this case study, the value of *lambda* is chosen to be 1000. That means that 1000 solutions are created at each generation. With this amount of generated children at each step of the iterative process, 50 generations (*ngen*) are enough to observe convergence in the Pareto-front, as shown in Figure 27.

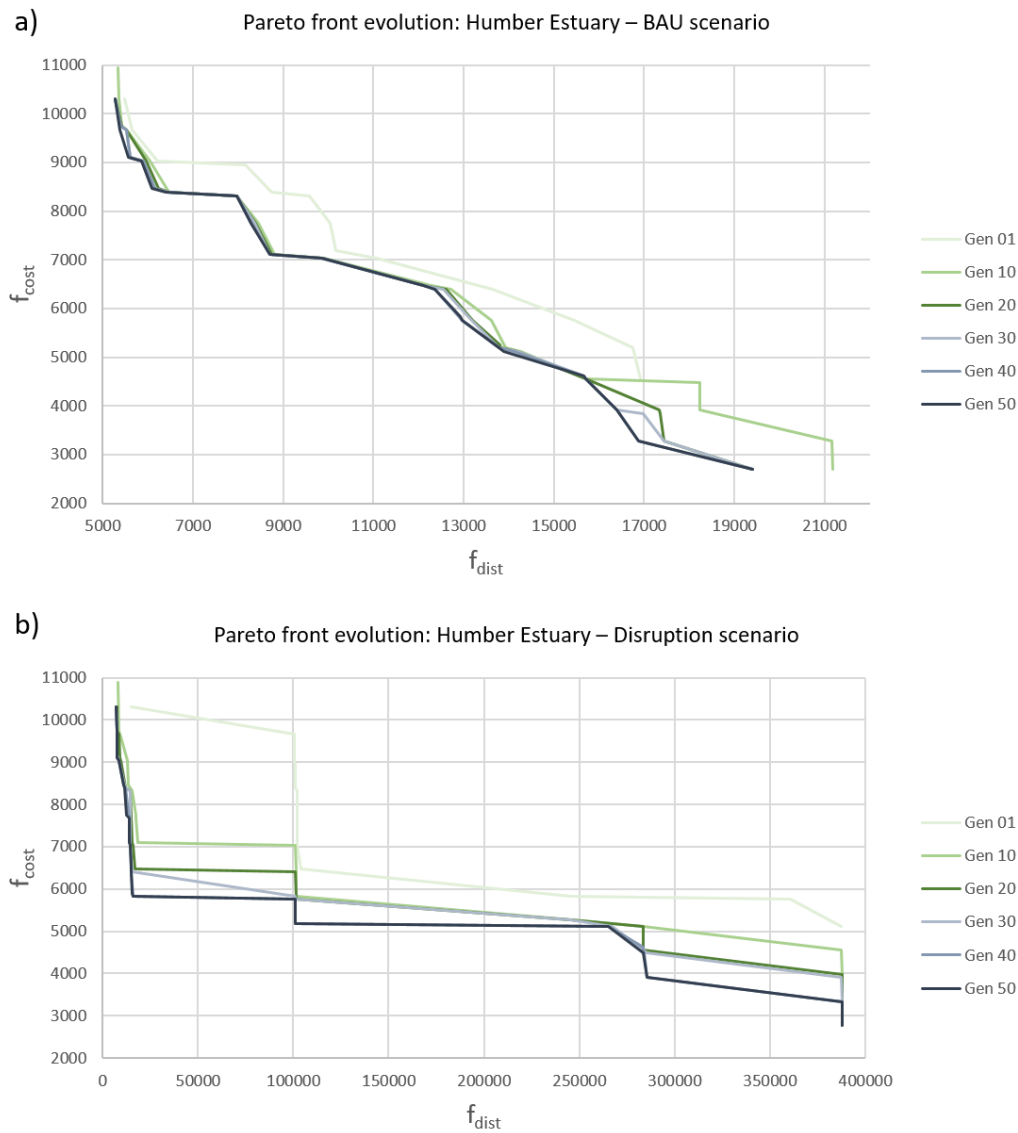


Figure 27 - Pareto fronts evolution of the Humber Estuary case study: a) Business as usual scenario; b) Disruption scenario.

#### 5.4.7. Output phase

The output creation phase relies on the Outputs module (see section 4.2.2.6). For the Humber Estuary case study, the output files are in the form of plots of Pareto-fronts (normalised and non-normalised) and in the form of shapefiles (.shp) containing the spatial references of Pareto-optimal solutions (spatial plans).

Pareto fronts are plotted in the solution space defined by the two objective functions; they provide a useful overview of all the solutions inspected by the GA and of the performance of Pareto-optimal plans (values of  $f_{dist}$  and  $f_{cost}$ ). On the other hand, shapefiles are convenient for direct visualisation of spatial plans in the form of maps in a GIS environment.

For more details, figures, graphs and maps concerning output and results for the Humber Estuary case study, see section 5.5.

## 5.5. Results

13 different scenarios have been investigated for the Humber Estuary case study inspecting different assumptions, testing different levels of emergency and assessing the sensitivity of the main parameters characterising the problem. These scenarios will be presented following the increasing level of complexity that can be modelled applying the RAO framework, starting from the most simplifying assumptions to the most complex formulations. In this case the complexity is given by both the considered number of variables and objective functions' equations (e.g. linear vs non-linear, discrete vs continuous etc.).

The following sections provide the details regarding the assumptions of each scenario and the results of the RAO framework applications. As specified in Chapter 4, the RAO framework's outputs consist in Pareto fronts composed by Pareto-optimal spatial plans. Each Pareto front contains on average 30 optimal spatial plans, which are all - by definition - optimally balancing the trade-off between accessibility and costs.

The results of the scenarios can be investigated in two ways: through the analysis of the Pareto fronts plotted in the solution spaces or using the maps representing Pareto-optimal spatial plans (see sections 5.5.1 -5.5.13). One of the advantages of this methodology is to provide the user with a wide portfolio of optimal solutions among which to choose; at the same time, though, this consists in a limitation in the results presentation when considering 13 different scenarios: since plotting maps for all the 340 optimal plans produced by the RAO framework would make this document unreadable, a selection of the most representative results will be presented in the following sections.

The final goal of the presentation of such a wide range of scenarios is the understating of the impacts and implications that different assumptions on the objective functions' formulations have on the results produced by the RAO framework application; and, at the same time, to provide a sensitivity analysis of the model's main parameters.

### 5.5.1. Scenario 1: Uniform rent price, discrete cost function

This scenario optimises the allocation of storing space for temporary flood defences considering a situation in which adequate warning is guaranteed before the flood event occurs. It is meant to explore the business as usual condition: the road network is considered perfectly functional and sufficient time to transport and deploy temporary flood defences is available. Table 8 presents a summary of the main assumptions at the base of the scenario.

*Table 8 - Scenario assumptions - Uniform rent price, discrete cost function*

Rent price	Uniform
Cost function	Discrete – proportional to warehouses’ dimensions
Distance function	GEUD formulation
Strategic infrastructure	All strategic infrastructure assets included

The rent price is considered uniform (average value: £55.00 per square metre per annum) in the whole Humber Estuary area and this value is used in the discrete cost function formulation presented in section 5.4.4; in this scenario, only capital costs for warehouses are taken into consideration, so the cost function formulation corresponds to Equation (5.5). The gEUD formulation of the distance function is proportional to the service area of each warehouse and it is presented in section 5.4.4 – Equation (5.1). Finally, regarding strategic infrastructure assets, they are all included in the scenario and no prioritisation is assumed.

The outputs of the RAO consist of Pareto-Fronts in the solution space and in spatial plans showing Pareto-optimal distributions of warehouses in the region according to different levels of costs and travel times.

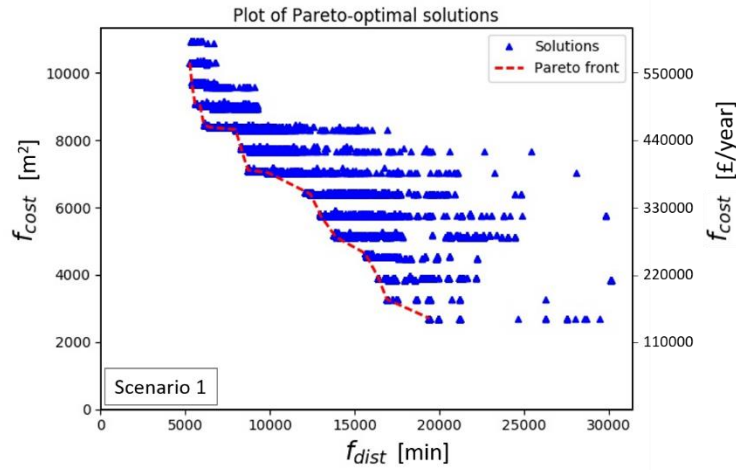


Figure 28 - Solution space and Pareto-front for Humber Estuary case study. Scenario 1.

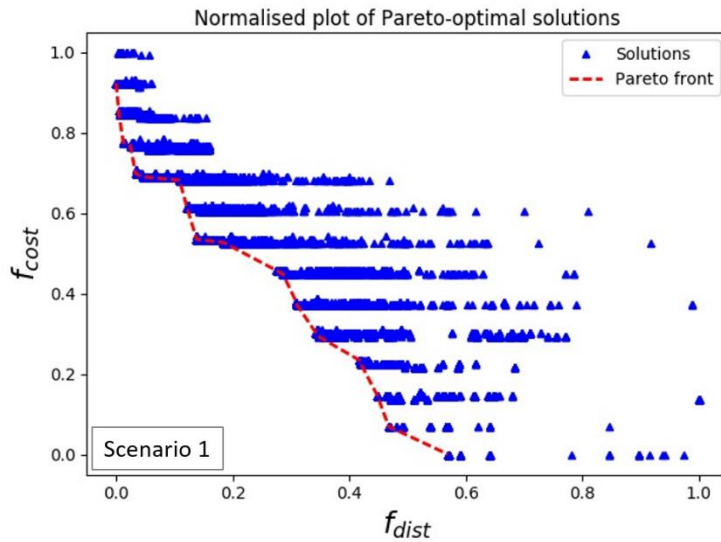


Figure 29 - Normalised solution space and Pareto-front for Humber Estuary case study. Scenario 1.

Figure 28 shows the solution space defined by the two objective functions  $f_{dist}$  (x-axis) and  $f_{cost}$  (y-axis). The blue triangles represent every solution inspected by the algorithm and the dashed red line is the Pareto-front: the solution lying on the Pareto-front are the ones that optimally balance the trade-off between the two conflicting objectives. The normalised representation showed in Figure 29 helps to better examine the solution space and analyse the distribution of the solutions inspected by the algorithm.

As described in Chapter 4.2.1, Pareto-optimality is based on the concept of domination: the solutions on the Pareto-front dominate all the other solutions in the simultaneous

minimisation of the two objective functions. This implies that they are not worse than the others in all the objectives and strictly better in at least one.

Every blue triangle in the graph represents a spatial plan of warehouses. This implies that each one has a correspondent map showing Pareto-optimal locations for temporary flood defences storing space. However, before analysing each Pareto-optimal solution, it could be useful to exploit the full potential of the solution space graph.

For complex case studies involving large regions or high resolutions, the number of Pareto-optimal spatial plans can be considerably high. However, despite all being optimal, some of them may be more significant than others.

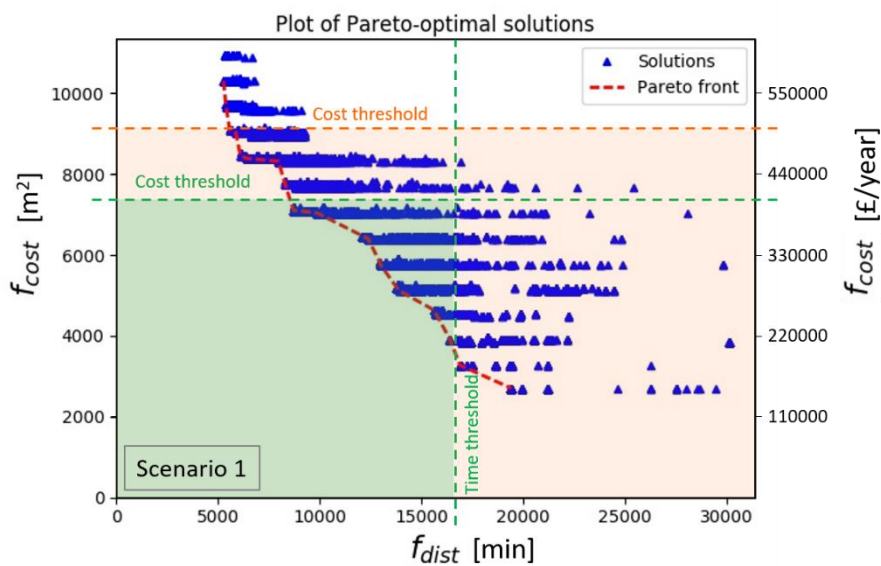


Figure 30 - Thresholds in the solution space for the Humber Estuary case study – Scenario 1. Orange threshold: result-driven. Green thresholds: objective-driven.

Figure 30 shows a way to narrow down the field of inspection of solutions. It is possible to define two different kinds of thresholds: one is result-driven, the other is objective-driven.

The first typology of threshold (in orange in Figure 30) can be defined simply analysing the results: it is possible to observe that beyond certain values there is a worsening in one objective without a significant improvement in the other. Analysing the cost function, for example, beyond the orange cost threshold there is an increase in costs without a significant decreasing of travel times. Similarly, it may happen that beyond a certain time threshold, relatively high travel times are considered without a significant decrease in costs.



On the other hand, a different kind of threshold can be set according to the user's needs (green in Figure 30). For instance, a limited budget would narrow the range of affordable solutions, or local authorities may not be interested in spatial plans that would require travel times from warehouses to deployment locations higher than a certain limit.

These constraints have deliberately not been implemented in the RAO algorithm because they can vary according to different needs. Even for the same case study, it is valuable for the user having a complete portfolio of solutions and decide which of them are feasible or not (according to available budget) and which ones are the most cost-effective.

The green cost and travel time thresholds shown in Figure 30 are exemplary. They are set assuming a hypothetical maximum available budget and a time threshold. Ideal time thresholds depend on the availability of staff for temporary flood defences deployment. In this particular context, it is important to bear in mind two considerations:

- 1) The time variable (in minutes) represented on the x-axis of the graph depends on the metric chosen to measure the performance of spatial plans against the distance function (for more details, see chapter 5.4.4).
- 2) In this scenario, travel times are evaluated on the road network for a single trip from each warehouse to the closest strategic infrastructure asset. Nevertheless, multiple trips from storing location to deployment site may be required according to the availability of staff and means of transport (dimension of the fleet of trucks available for transportation of temporary flood defences). These variables vary according to different situations that can involve many contingent factors and are explored in the next sections.

Once the area of interest of the solutions in the Pareto-front is identified, it is possible to analyse the spatial plans. They can be visualised in a GIS environment where further analyses can be performed if required. To be able to identify which spatial plans to inspect, it is useful to take a more in-depth look into the Pareto-front data. Table 9 shows all the solutions (spatial plans) that form the Pareto-front, with the respective fitnesses in terms of  $f_{dist}$  and  $f_{cost}$ . Figure 31, instead, is a highlight of the Pareto-front showed in Figure 28 with indications of the number of Pareto-optimal spatial plans.

Table 9 - Solutions forming the Pareto-front of the Humber Estuary – scenario 1.

<b>Solution</b>	<b>f<sub>dist</sub></b>	<b>f<sub>cost</sub> [m<sup>2</sup>]</b>	<b>f<sub>cost</sub> [£/year]</b>
Plan_18102	5268	10310	567050
Plan_42215	5392	9670	531850
Plan_40341	5571	9100	500500
Plan_46012	5871	9030	496650
Plan_48013	6097	8460	465300
Plan_42075	6415	8390	461450
Plan_7034	7967	8320	457600
Plan_6005	8292	7750	426250
Plan_37077	8699	7110	391050
Plan_29188	9862	7040	387200
Plan_25576	12103	6470	355850
Plan_39197	12371	6400	352000
Plan_45520	12936	5830	320650
Plan_33005	12977	5760	316800
Plan_37001	13781	5190	285450
Plan_44002	13881	5120	281600
Plan_25000	15663	4620	254100
Plan_14021	15697	4550	250250
Plan_24263	16393	3910	215050
Plan_34005	16881	3270	179850
Plan_17072	19408	2700	148500

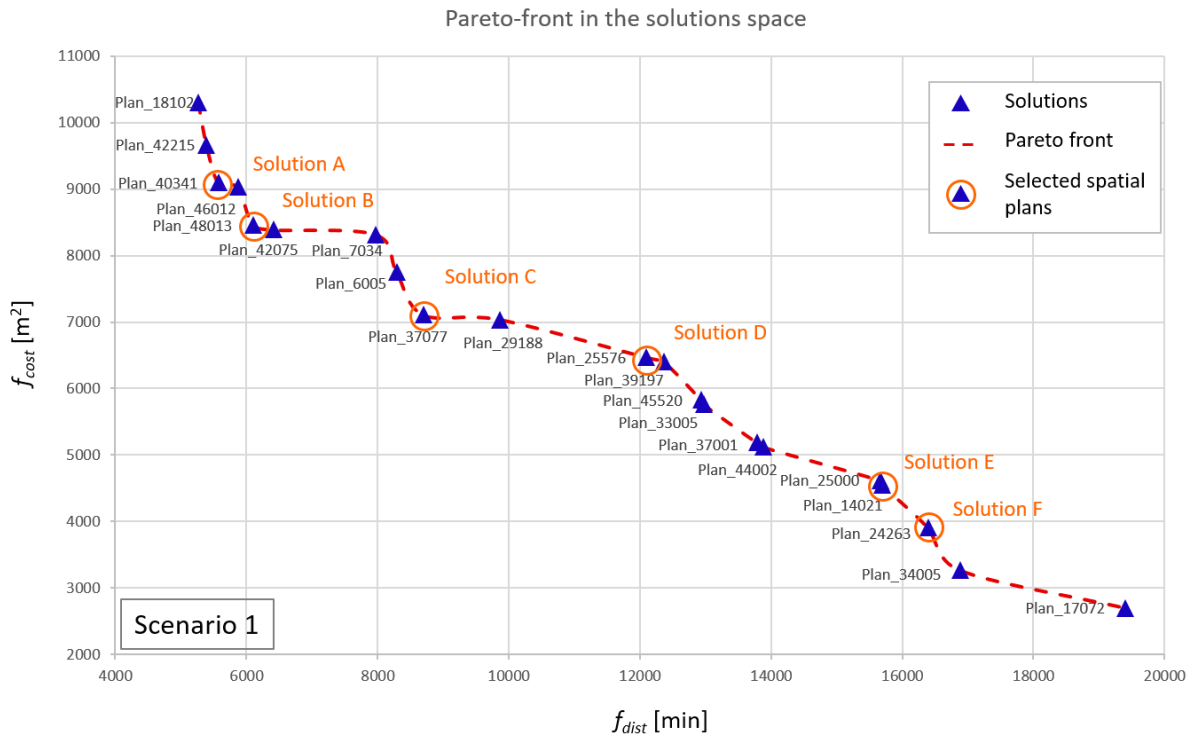


Figure 31 - Highlight of the Pareto-front for the Humber Estuary – Scenario 1 - with the indication of the number of Pareto-optimal spatial plans. Figures A, B, C, D, E and F are visualised respectively in Figure 32, Figure 33, Figure 34, Figure 35, Figure 36 and Figure 37.

The RAO provides a shapefile (.shp) for each Pareto-optimal solution. It is possible to import each one of them in a GIS environment and plot it as a map together with any other relevant spatial data regarding the case study.

For clarity and readability, only a selection of Pareto-optimal spatial plans will be reported in the following pages. The aim is to provide an example of how to handle this kind of outcomes, how to analyse them and draw conclusions out of them.

For this scenario, a higher number of solutions is presented (6) to provide the reader with an overview of the range of possibilities provided by each Pareto front. In the next sections, a narrower selection of Pareto-optimal spatial plans (the most significant) will be presented to ease readability. To provide solutions from all the areas of the Pareto-front (see Figure 31), six spatial plans are presented: Solutions A and B from the top-left side of the front (higher costs and lower travel times), Solutions C and D from the middle and Solutions E and F from the bottom-right side (lower costs and higher travel times).

The following pages present the six selected Pareto-optimal spatial plans: Solution A (Figure 32), Solution B (Figure 33), Solution C (Figure 34), Solution D (Figure 35), Solution E (Figure 36)

and Solution F (Figure 37). Every figure shows the location of the warehouses that are part of the plan, together with information about their size and travel times to reach the strategic infrastructure assets served by each storing location.

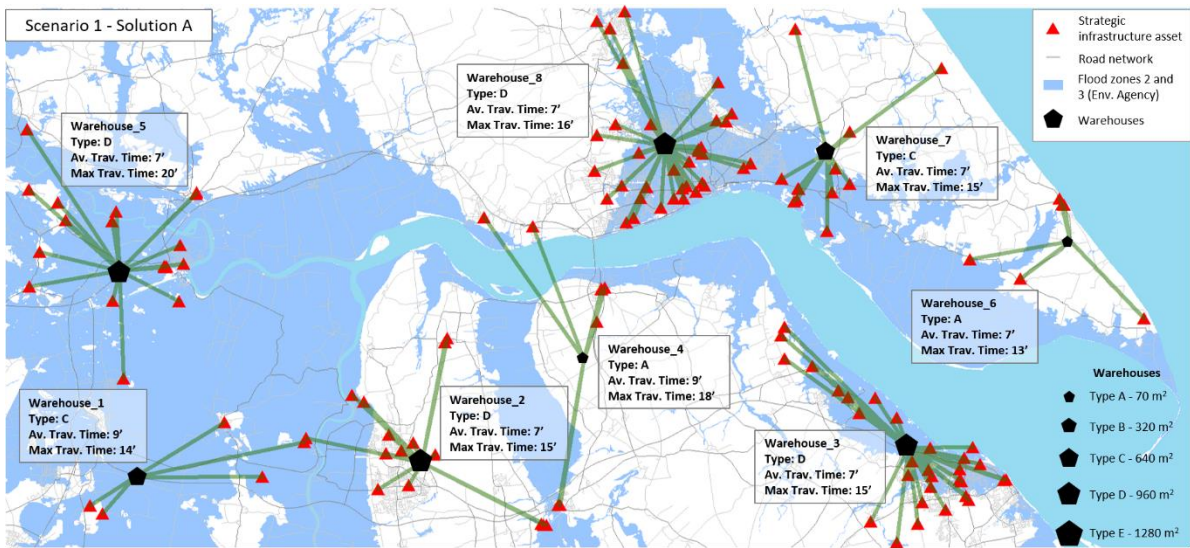


Figure 32 - Humber Estuary Scenario 1, Solution A. The green lines are for visualisation purposes: they connect each infrastructure asset to the closest warehouse. They do not represent distances, as distances are measured as travel times on the road network.

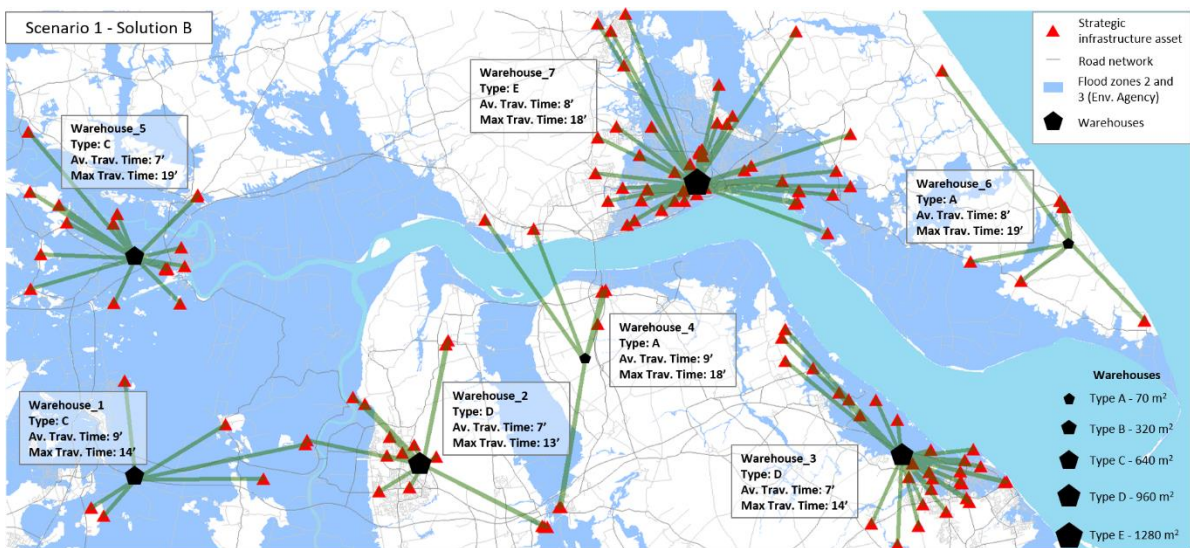


Figure 33 - Humber Estuary Scenario 1, Solution B. The green lines are for visualisation purposes: they connect each infrastructure asset to the closest warehouse. They do not represent distances, as distances are measured as travel times on the road network.

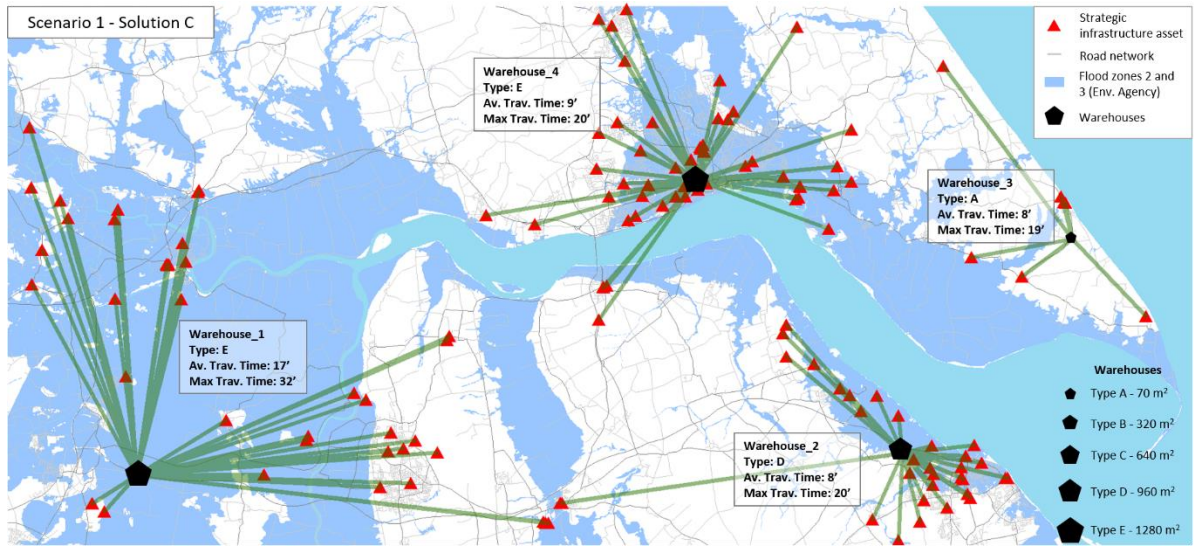


Figure 34 - Humber Estuary Scenario 1, Solution C. The green lines are for visualisation purposes: they connect each infrastructure asset to the closest warehouse. They do not represent distances, as distances are measured as travel times on the road network.

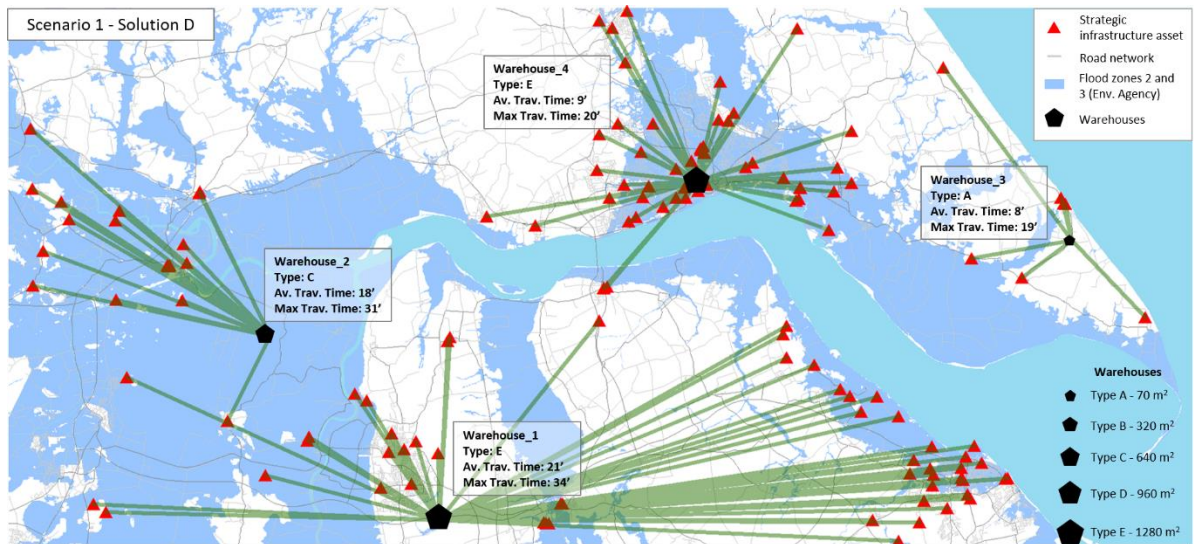


Figure 35 - Humber Estuary Scenario 1, Solution D. The green lines are for visualisation purposes: they connect each infrastructure asset to the closest warehouse. They do not represent distances, as distances are measured as travel times on the road network.

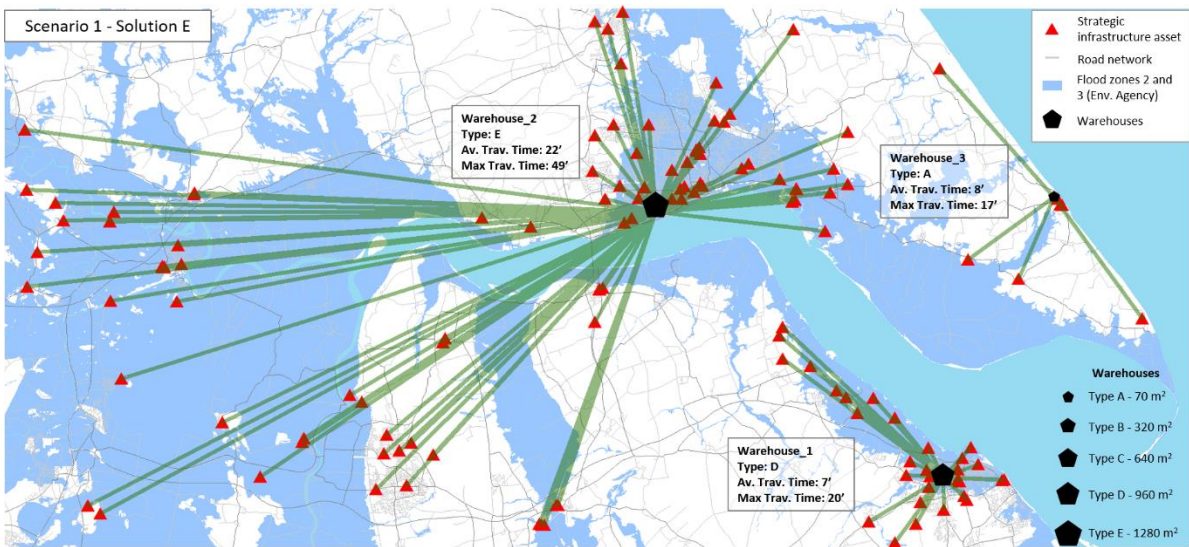


Figure 36 - Humber Estuary Scenario 1, Solution E. The green lines are for visualisation purposes: they connect each infrastructure asset to the closest warehouse. They do not represent distances, as distances are measured as travel times on the road network.

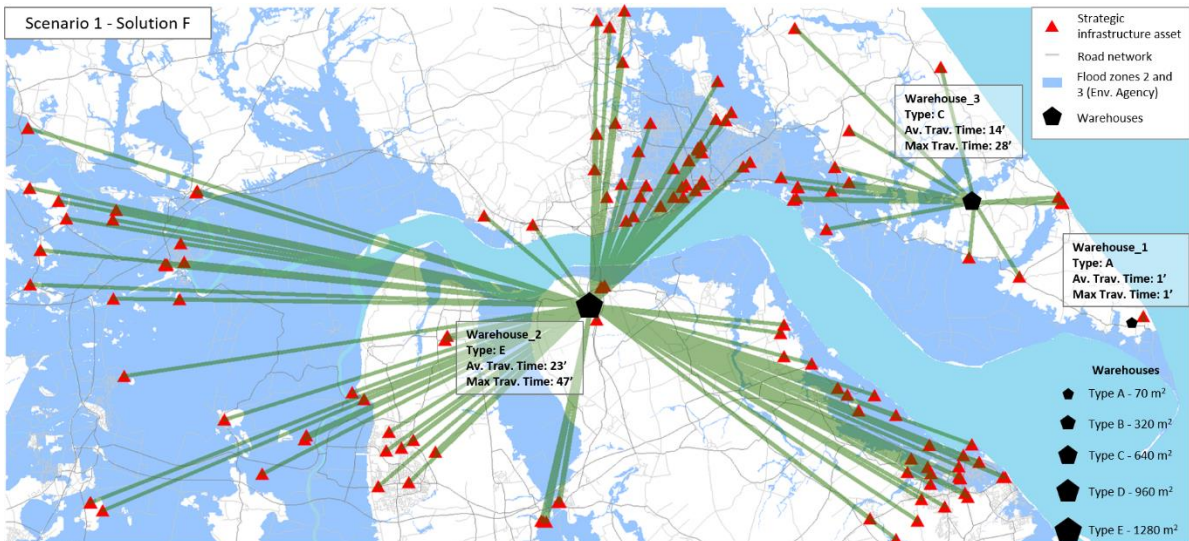


Figure 37 - Humber Estuary Scenario 1, Solution F. The green lines are for visualisation purposes: they connect each infrastructure asset to the closest warehouse. They do not represent distances, as distances are measured as travel times on the road network.

### 5.5.2. Scenario 2: Uniform rent price, discrete cost function with road network disruption

The second scenario refers to the same assumptions of the previous one with respect to objective functions' formulation, but it takes into account a disruption in which there might be not enough time to act before the beginning of the flood and some parts of the road network may be inaccessible due to the presence of floodwater. Table 10 presents a summary of the main assumptions at the base of the scenario.

Table 10 - Scenario assumptions - Uniform rent price, discrete cost function - disrupted road network.

Rent price	Uniform
Cost function	Discrete – proportional to warehouses' dimensions
Distance function	GEUD formulation
Strategic infrastructure	All strategic infrastructure assets included, but not all reachable from everywhere due to road network disruption.

A historic flood map has been considered: it represents the footprint of all past flood events in the area. This highlights how many routes are susceptible to blockage and disruption during a flood. The result is that two areas resulted disconnected from the rest of the region, as shown in Figure 38.

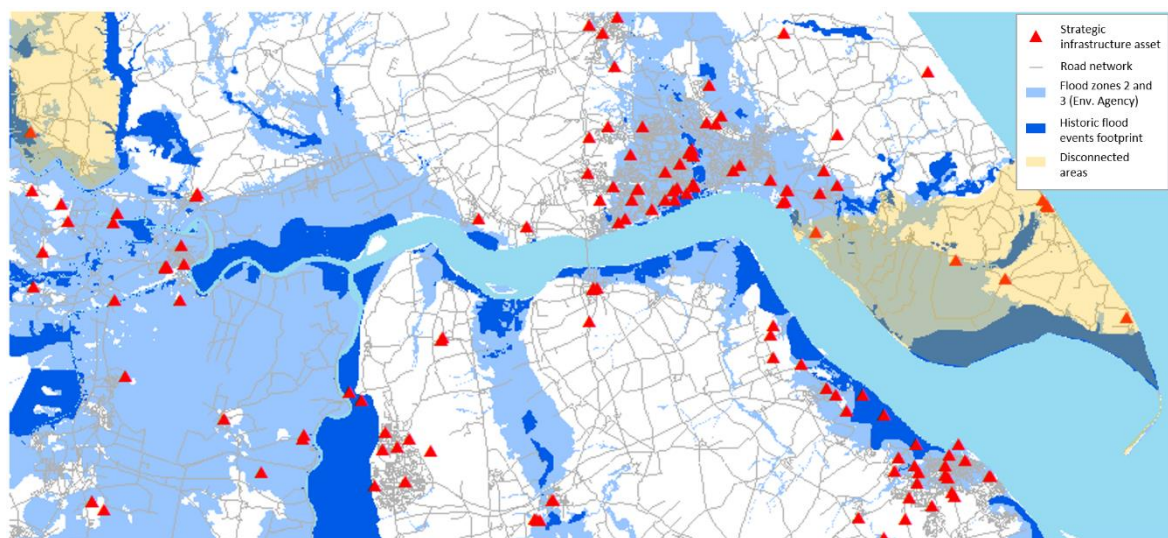


Figure 38 - Disconnected areas due to the flooded road network.

The disruption scenario shows the possibility of the optimisation methodology to explore extreme situations, like those in which there is not enough time to deploy all the required

flood defences before the flood begins. This could be due to insufficient warning time or a contingent insufficiency of the workforce to deploy all the resources.

In order to allow the RAO framework to perform the network analysis, a very high travel time value has been assigned to the flooded road edges (instead of deleting them). This simulates an obstacle on the network and allows NetworkX (Hagberg *et al.*, 2008) to always resolve a solution, disconnecting parts of the road network can lead to errors when trying to compile a new Origin/Destinations Matrix because shortest path calculations may not be possible.

As described in section 5.5.1, the outputs have a dual nature: Pareto-fronts in the solution space and georeferenced spatial plans. Figure 39 shows the solution space of the disruption scenario run of the RAO framework. At first glance, it is possible to observe two areas where the solutions are concentrated: there is a cluster of solutions in the left-hand side of the graph and there is a second group of more scattered solutions in the right-hand side of the solutions space.

This horizontal distribution of solutions indicates that the second group (right-hand side) has considerably high travel times (and generally low costs). This is due to the fact that when fewer warehouses are taken into consideration, it is less probable that at least one is present in each disconnected area of the case study. When there is not any storing location within the isolated area, it is necessary to cross one of the road edges with very high travel time assigned (i.e. flooded road), hence the very high travel times assigned to many solutions inspected by the algorithm and the resulting dispersion observed in Figure 39.

As a consequence, only the left-hand side of the Pareto-front will be taken into consideration in the analysis of the results, since only solutions that guarantee access to the isolated areas will be taken into consideration (see time threshold in Figure 39).

It is essential to highlight that this choice is up to the user and that the following analysis of the results is one of many possibilities. As for other design choices described in the previous chapters, this constraint can be a priori implemented with the result of producing only feasible solutions (i.e. with a warehouse in every disconnected area). Nevertheless, it seemed reasonable to show and highlight the versatility and adaptability of the RAO framework to different potential necessities and/or requirements of the ultimate user.



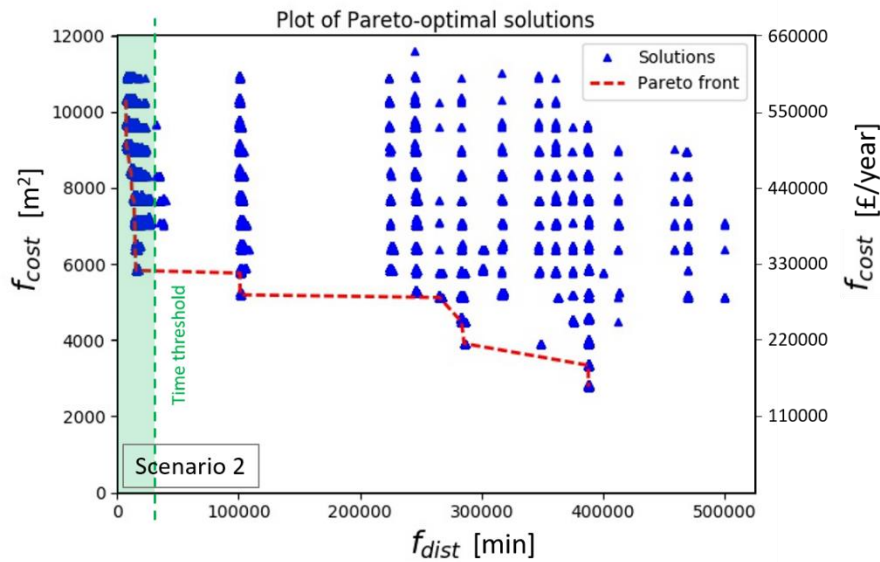


Figure 39 - Solution space and Pareto-front for Humber Estuary case study. Scenario 2.

Figure 40 shows a highlight of the left-hand part of the Pareto front of Figure 39, together with the indication of the solutions that are inspected. To ease the comparison of results among different scenarios, the same amount of Pareto-optimal spatial plant of section 5.5.1 is presented, Pareto-optimal solutions are chosen from all the parts of the Pareto-front in order to analyse results covering its entire range. Six plans are selected Solutions A (Figure 41) and B (Figure 42) from the top-left side of the front (higher costs and lower travel times), Solutions C (Figure 43) and D (Figure 44) from the middle and Solutions E (Figure 45) and F (Figure 46) from the bottom-right side (lower costs and higher travel times).

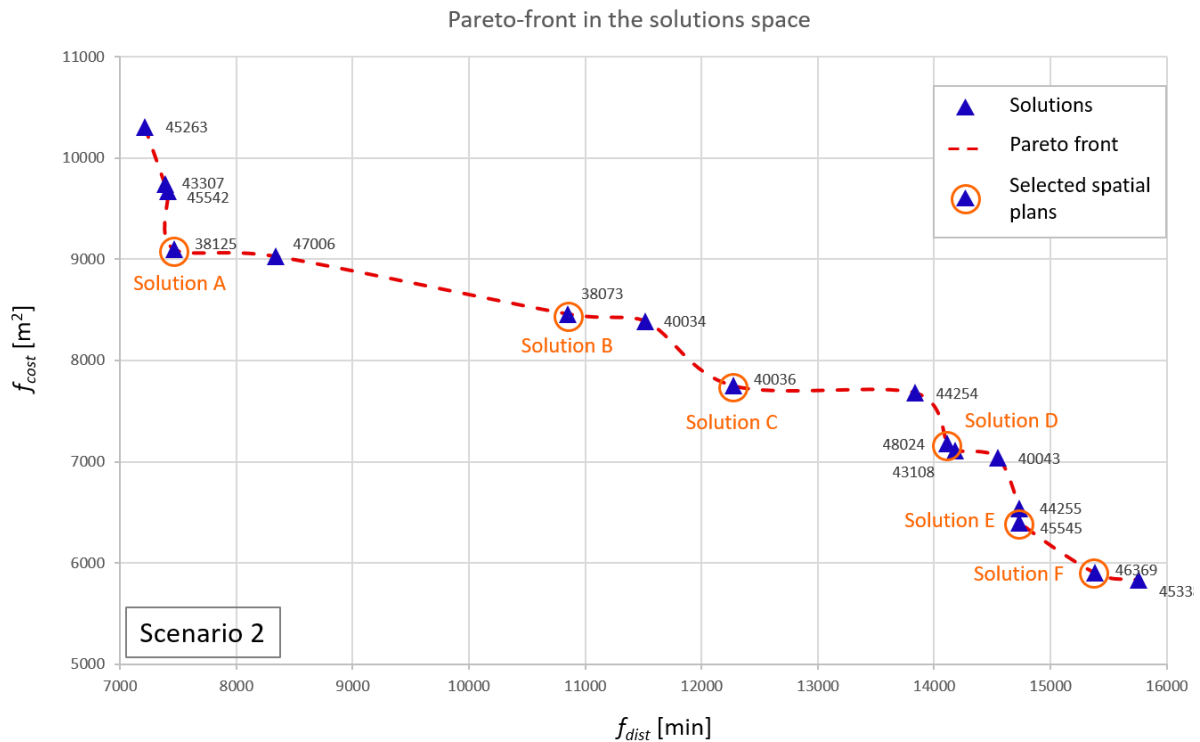


Figure 40 - Highlight of the Pareto-front for the Humber Estuary disruption scenario with the indication of the number of Pareto-optimal spatial plans. Solutions A, B, C, D, E and F are visualised respectively in Figure 41, Figure 42, Figure 43, Figure 44, Figure 45 and Figure 46.

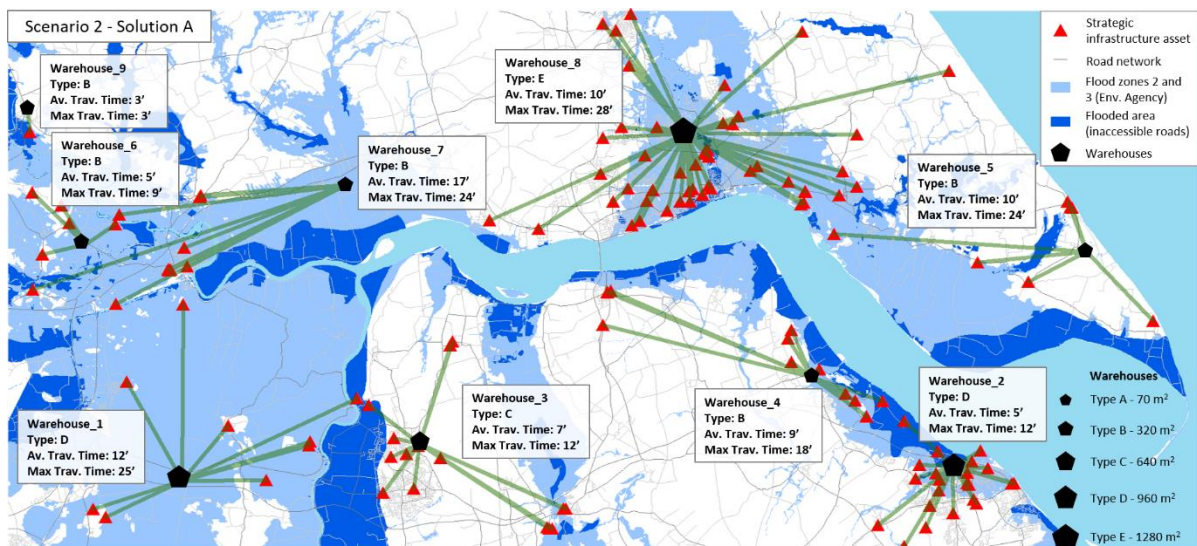


Figure 41 - Humber Estuary Scenario 2, Solution A. The green lines are for visualisation purposes: they connect each infrastructure asset to the closest warehouse. They do not represent distances, as distances are measured as travel time on the road network.

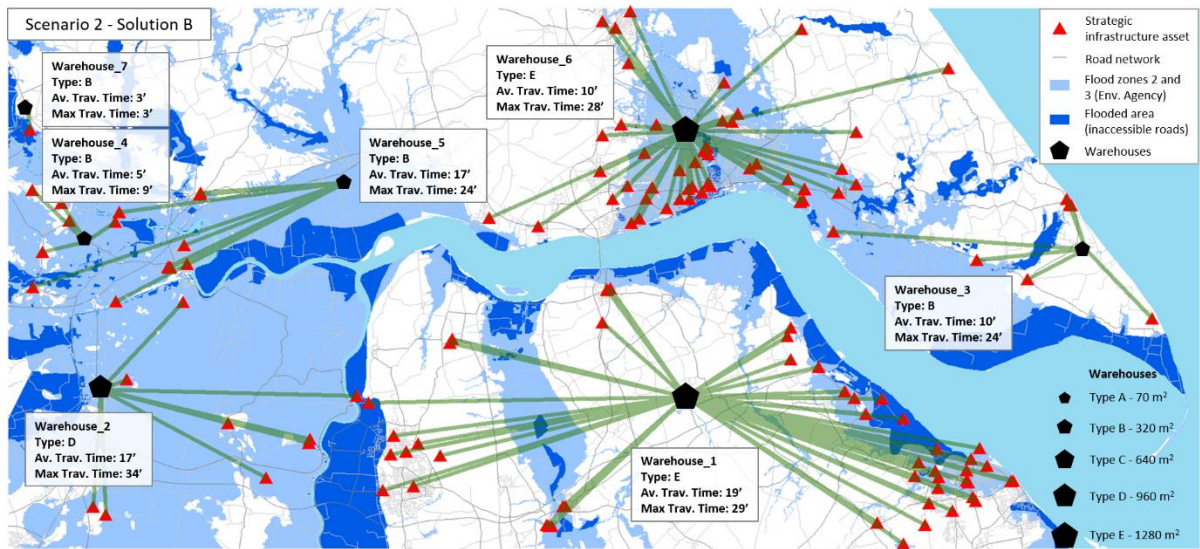


Figure 42 - Humber Estuary Scenario 2, Solution B. The green lines are for visualisation purposes: they connect each infrastructure asset to the closest warehouse. They do not represent distances, as distances are measured as travel time on the road network.

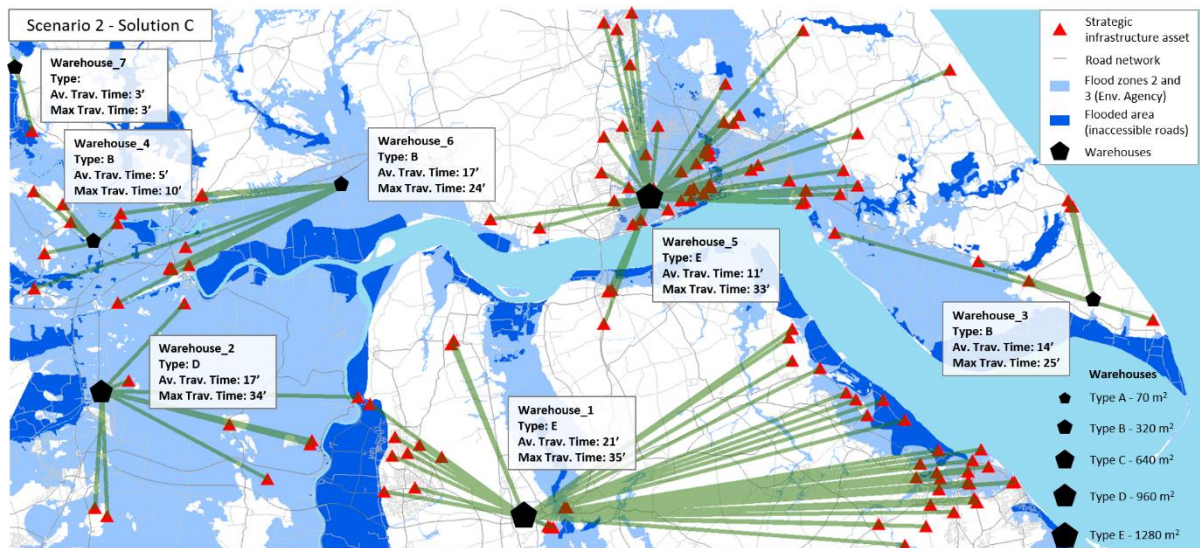


Figure 43 - Humber Estuary Scenario 2, Solution C. The green lines are for visualisation purposes: they connect each infrastructure asset to the closest warehouse. They do not represent distances, as distances are measured as travel time on the road network.

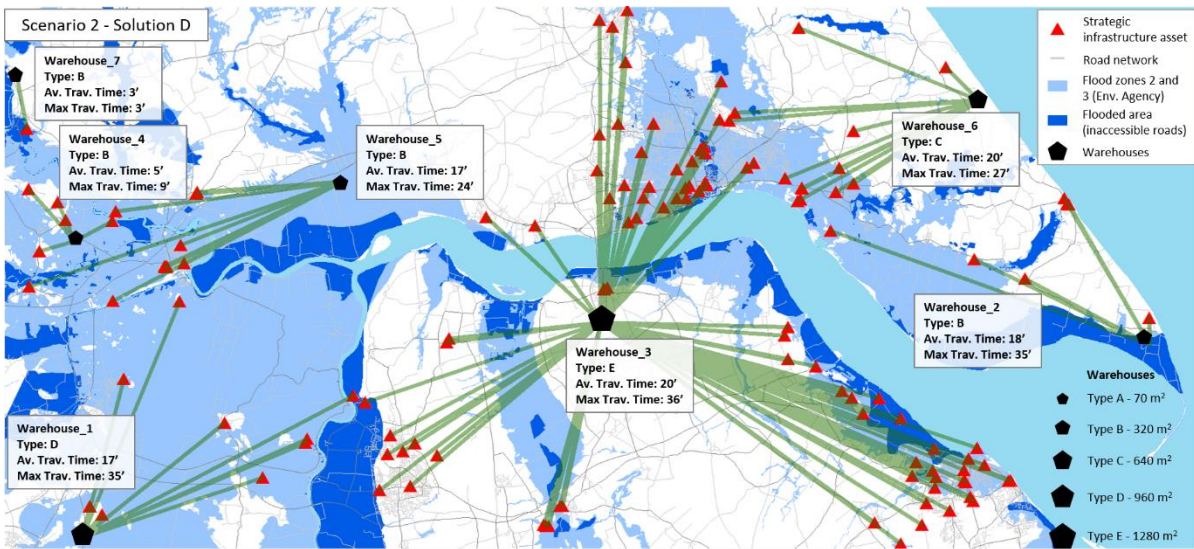


Figure 44 - Humber Estuary Scenario 2, Solution D. The green lines are for visualisation purposes: they connect each infrastructure asset to the closest warehouse. They do not represent distances, as distances are measured as travel time on the road network.

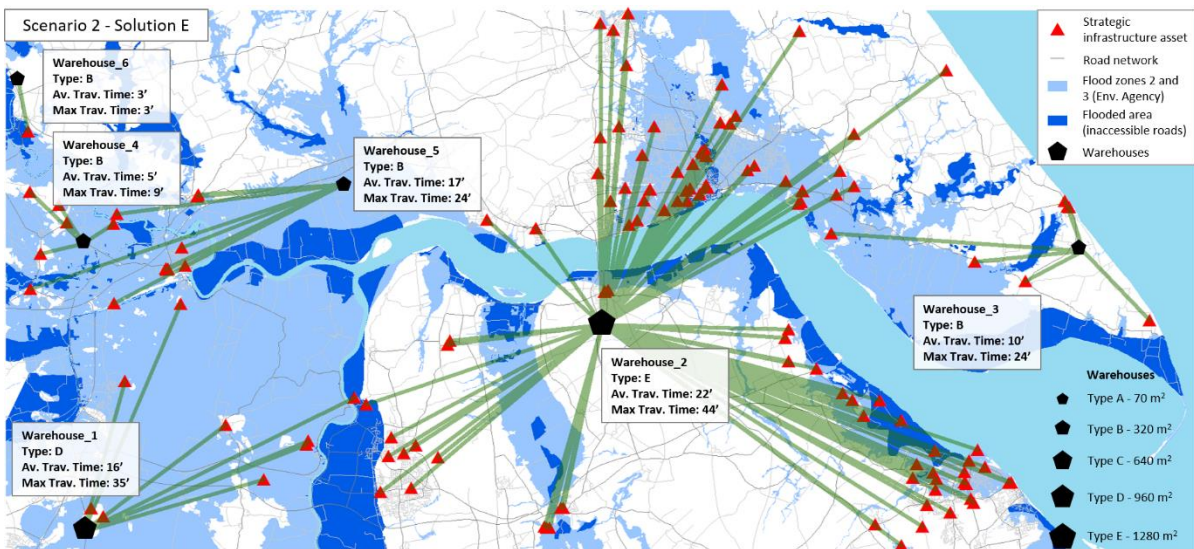


Figure 45 - Humber Estuary Scenario 2, Solution E. The green lines are for visualisation purposes: they connect each infrastructure asset to the closest warehouse. They do not represent distances, as distances are measured as travel time on the road network.

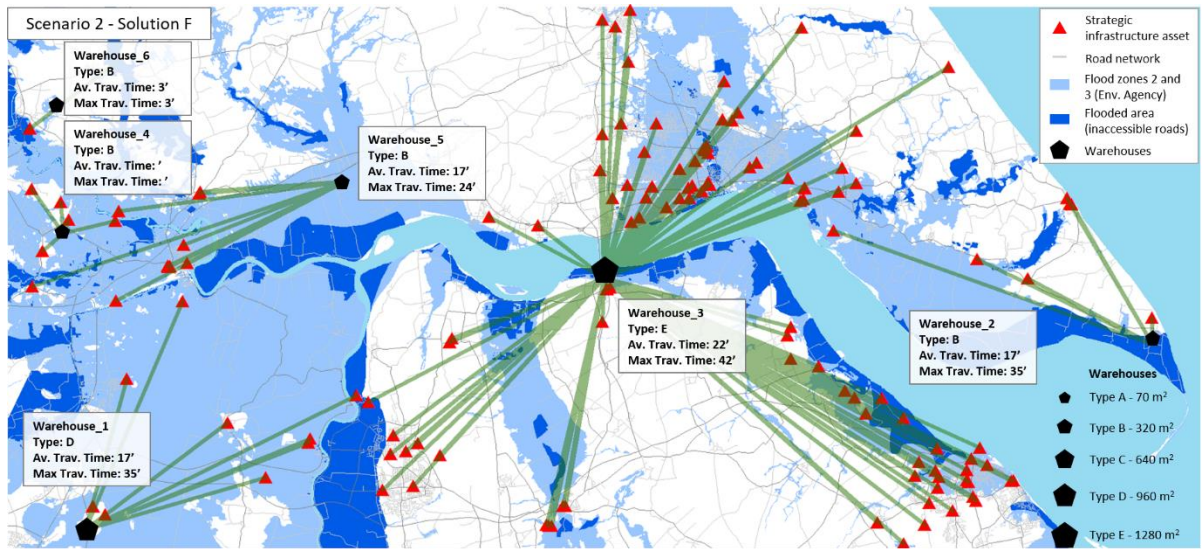


Figure 46 - Humber Estuary Scenario 2, Solution F. The green lines are for visualisation purposes: they connect each infrastructure asset to the closest warehouse. They do not represent distances, as distances are measured as travel time on the road network.

### 5.5.3. Scenario 3: Uniform rent price, linear continuous cost function

Scenario 3 introduces the first variation in terms of objective functions' formulation with respect to the previous scenarios. This scenario is meant as a starting point in the exploration of the impact that different assumptions regarding parameters and formulations have on the results of the RAO framework application to the Humber Estuary case study.

The distance function formulation refers to Equation (5.2), which takes into account the number of lorries necessary to transport emergency resources to deployment sites (fixed fleet dimension – assumption: 10 lorries) and the necessary number of trips.

Similarly to the previous scenarios, only the capital cost of warehouses is considered here, and again the warehouses' rent price per square metre in the case study region is considered uniform (average), but the cost function is considered continuous instead of discrete - refer to Equation (5.11).

$$\left\{ \begin{array}{l} f_{dist} = \frac{\sum_{i=1}^{SI} 2 \cdot TT_i}{n_{EF}} \\ f_{cost} = \sum_{i=1}^W f_i \cdot p_i \end{array} \right. \quad (5.11)$$

The problem of this formulation is the fact that, since the total amount of temporary flood defences to deploy is assumed constant, and since the warehouse dimension is directly proportional to the amount of strategic resources to store, the total sum of  $f_{cost}$  is constant, and the only variability is given by the distance function.

Consequently, given the absence of a trade off to balance, considering a continuous cost function under these assumptions reduces the optimisation problem from a multi-objective one to a single objective minimisation problem. The result is the absence of a Pareto front (see Figure 47) and the presence of a single solution which minimises the distance function.

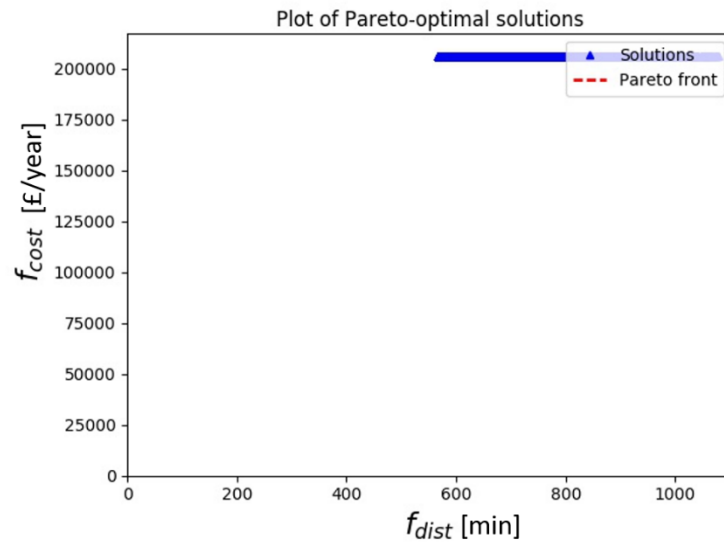


Figure 47 - Solution space for Scenario 3.

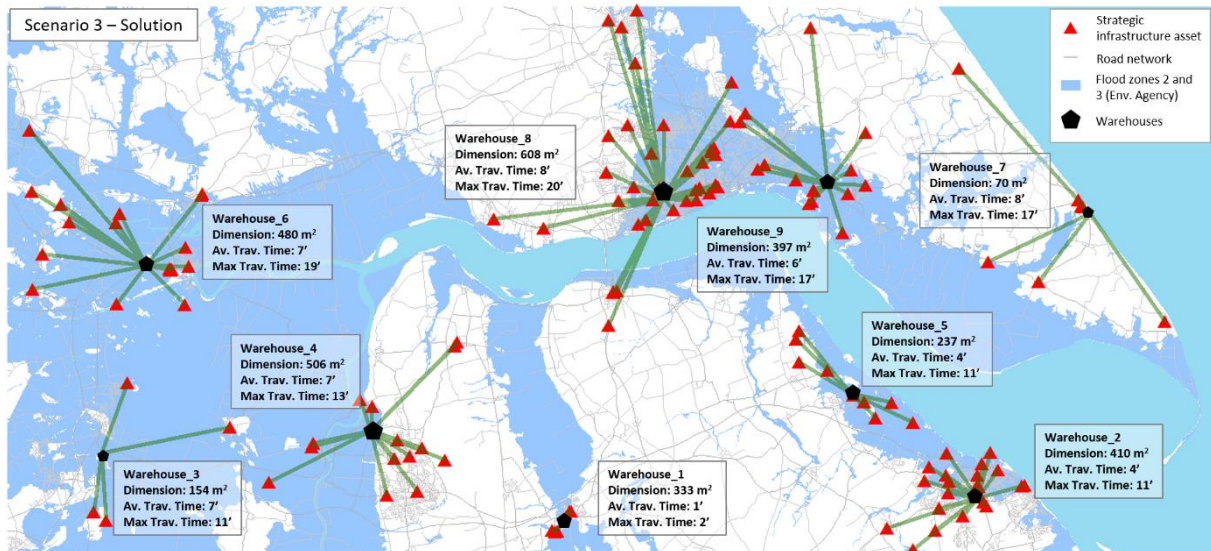


Figure 48 - Humber Estuary Scenario 3 Solution. The green lines are for visualisation purposes: they connect each infrastructure asset to the closest warehouse. They do not represent distances, as distances are measured as travel times on the shortest path on the road network.

#### 5.5.4. Scenario 4: Variable rent price (R/U), linear cost function with fixed number of lorries

Scenario 4 introduces a new element of spatial variability: a variable rent price function of the location of the warehouse. As explained in section 5.4.4, different available cells for warehouses allocation have different rent prices associated according to whether they are within an urban or a rural area. Scenario 4 subdivides the Humber Estuary region in two zones: rural and urban; consequently, equation (5.10) becomes:

$$p_i = p_{av} \cdot \gamma_u + p_{av} \cdot \gamma_r \quad (5.12)$$

Where:

- $p_i$  = annual rental price per square metre of i-th warehouse (see equation (5.9))
- $p_{av}$  = average rent price;
- $\gamma_u = 2$ , multiplier for urban areas;
- $\gamma_r = 1$ , multiplier for rural areas;

To assess the sensibility of this model to this parameter, the variable rent price is the only change in the formulation with respect to Scenario 3. This eases the comparison between different scenarios and allows to assess the impact on the model of the change of a single assumption.

Figure 49 shows the solution space defined by the two objective functions  $f_{dist}$  (x-axis) and  $f_{cost}$  (y-axis), with also the indication of the spatial plans inspected in Figure 50, Figure 51 and Figure 52.



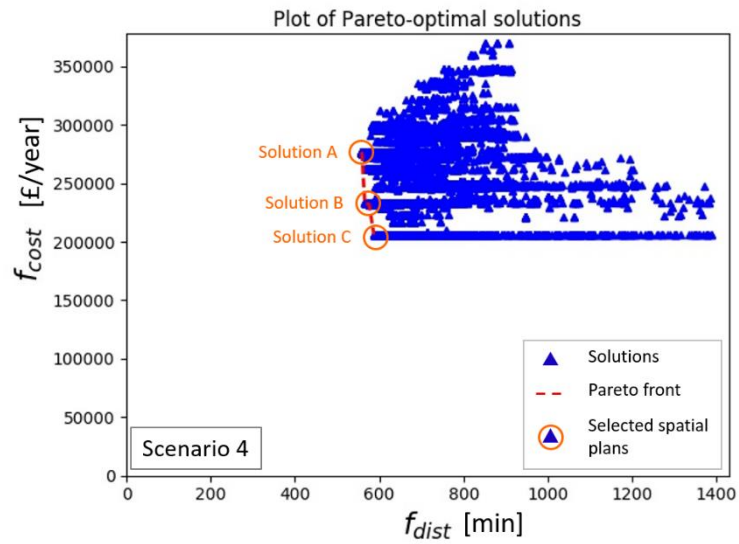


Figure 49 - Solution space and Pareto-front for Humber Estuary case study. Scenario 4. With the indication of Solutions A, B and C that are visualised respectively in Figure 50, Figure 51 and Figure 52.

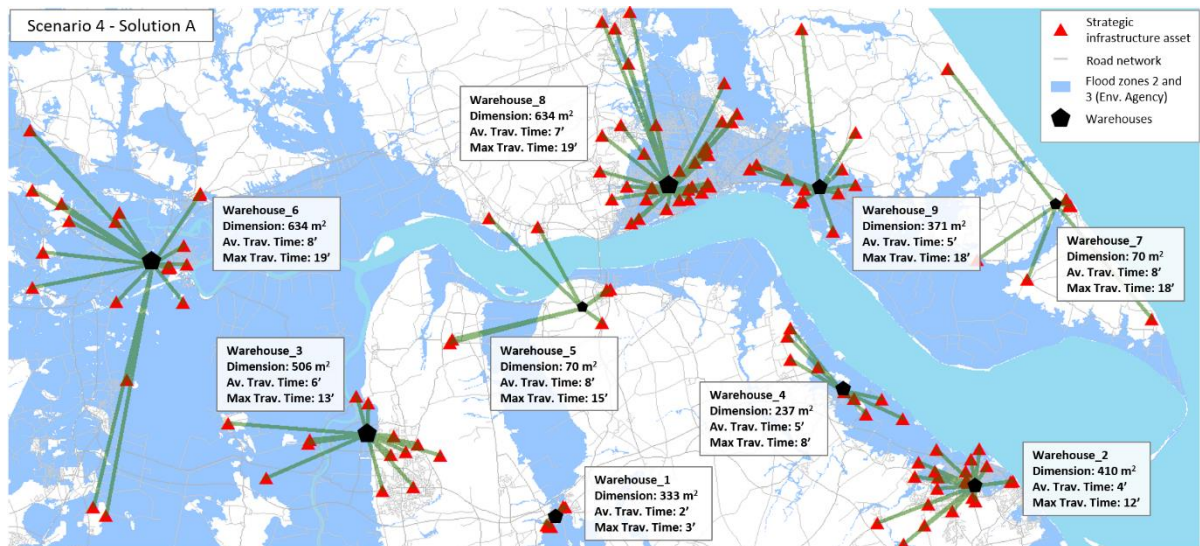


Figure 50 - Humber Estuary Scenario 4 Solution A. The green lines are for visualisation purposes: they connect each infrastructure asset to the closest warehouse. They do not represent distances, as distances are measured as travel times on the shortest path on the road network.

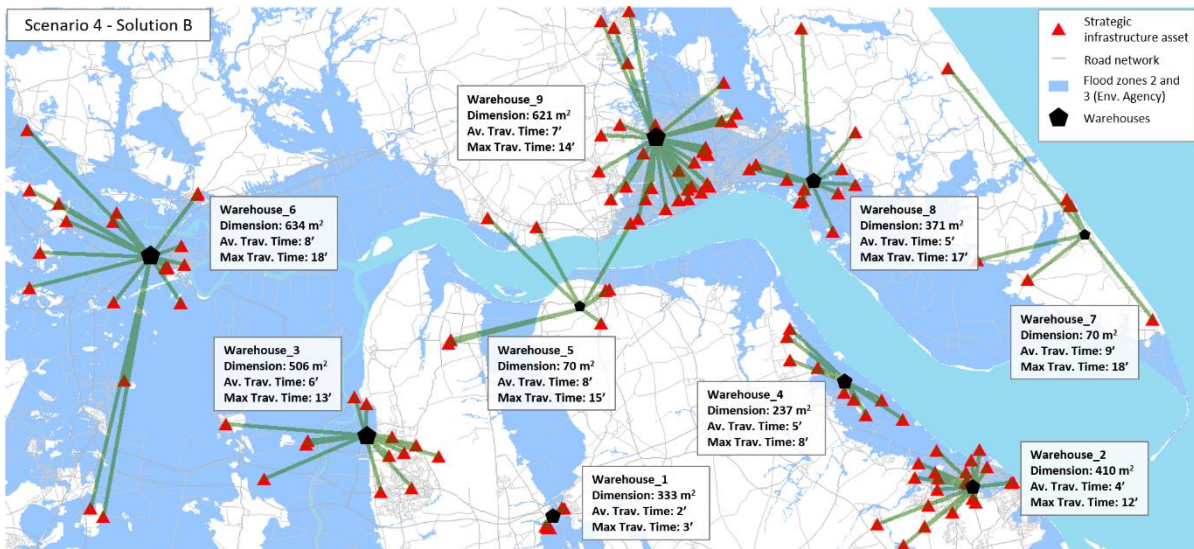


Figure 51 - Humber Estuary Scenario 4 Solution B. The green lines are for visualisation purposes: they connect each infrastructure asset to the closest warehouse. They do not represent distances, as distances are measured as travel times on the shortest path on the road network.

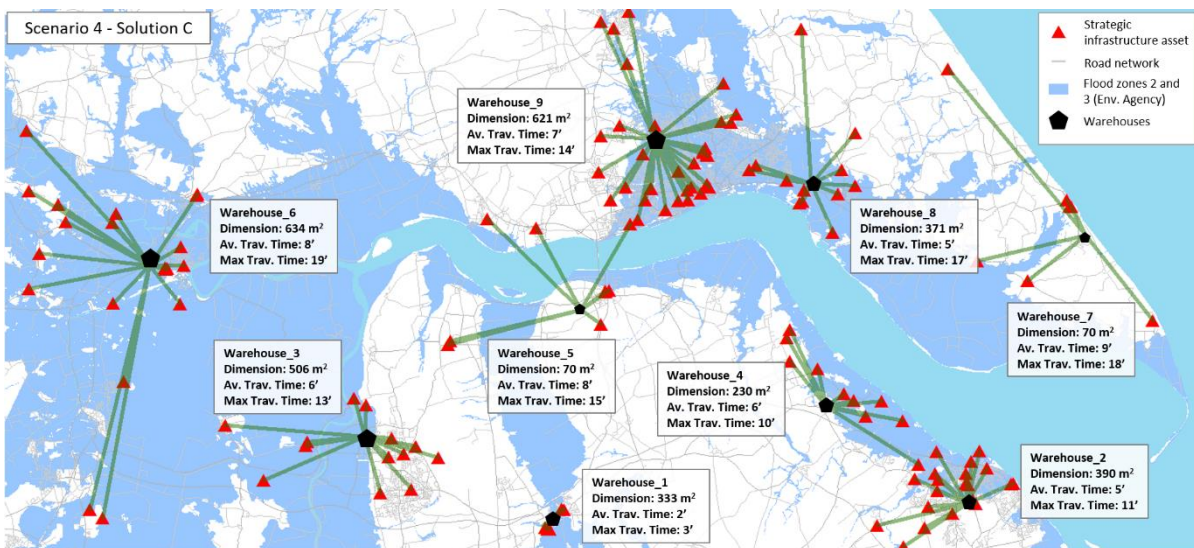


Figure 52 - Humber Estuary Scenario 4 Solution C. The green lines are for visualisation purposes: they connect each infrastructure asset to the closest warehouse. They do not represent distances, as distances are measured as travel times on the shortest path on the road network.

5.5.5. Scenario 5: Variable rent price (R/S/U), linear cost function with fixed number of lorries

Scenario 5 is built basing on the same assumptions and formulation of Scenario 4, with the only exception that an extra variable is included in the rent prices categories. As explained in section 5.4.4, and as anticipated in section 5.5.4, different available cells for warehouses allocation have different rent prices associated according to whether they are within an urban or a rural area. Scenario 5 subdivides the Humber Estuary region in three zones: rural, suburban and urban; consequently, equation (5.10) becomes:

$$p_i = p_{av} \cdot \gamma_u + p_{av} \cdot \gamma_s + p_{av} \cdot \gamma_r \quad (5.13)$$

Where:

- $p_i$  = annual rental price per square metre of i-th warehouse (see equation (5.9))
- $p_{av}$  = average rent price of the case study;
- $\gamma_u = 2$ , multiplier for urban areas;
- $\gamma_r = 1$ , multiplier for rural areas;
- $\gamma_s = 1.5$ , multiplier for suburban areas.

Figure 53 shows the solution space defined by the two objective functions  $f_{dist}$  (x-axis) and  $f_{cost}$  (y-axis). As can be observed, the Pareto front ranges between the same values of Scenario 4 (see Figure 49); since the three solutions of Scenario 4 (see Figure 50, Figure 51 and Figure 52) present a low spatial variability (but considerable in terms of costs), to avoid the plot of other almost identical maps, only a representative solution from the central part of the Pareto front is presented here (Figure 54). For a compared analysis of solutions from different scenarios, refer to section 5.6 and Chapter 7.

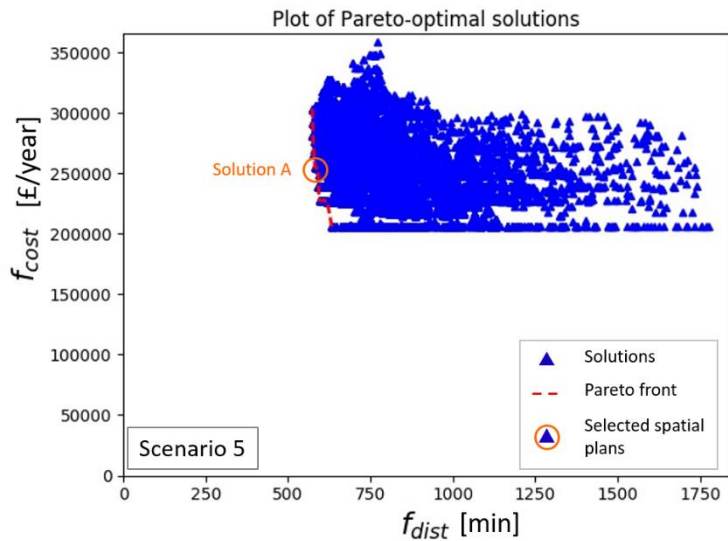


Figure 53 - Solution space and Pareto-front for Humber Estuary case study. Scenario 5. With the indication of the SolutionA that is visualised in Figure 54.

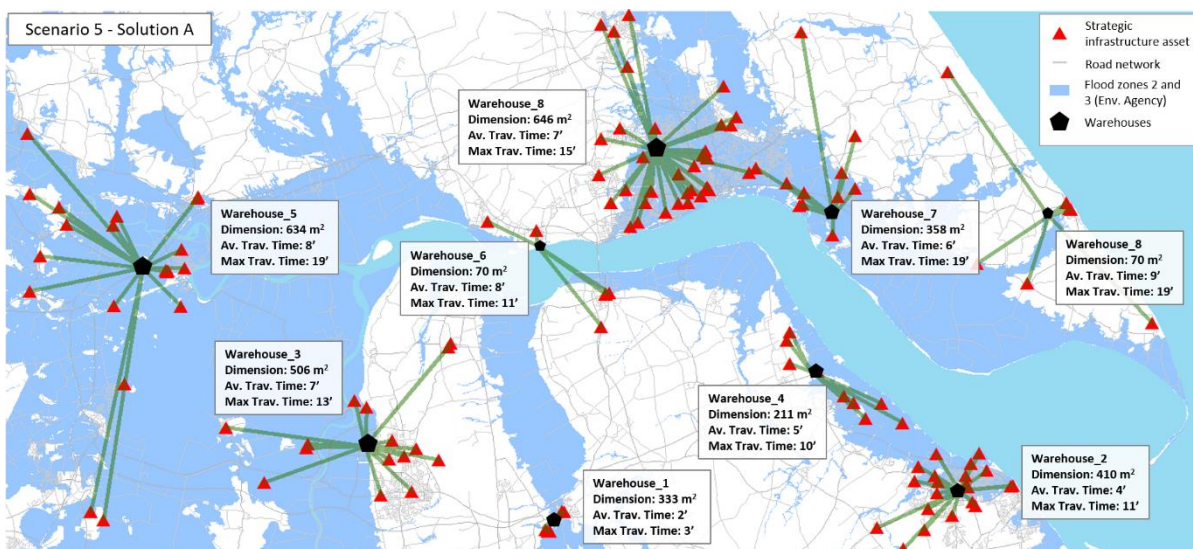


Figure 54 - Humber Estuary Scenario 5 Solution A. The green lines are for visualisation purposes: they connect each infrastructure asset to the closest warehouse. They do not represent distances, as distances are measured as travel times on the shortest path on the road network.

5.5.6. Scenario 6: Variable rent price (R/S/U), non-linear cost function with variable number of lorries (1)

Scenario 6 introduces a non-linear cost function for the evaluation of rent prices in different available cells for the allocation of warehouses. The formulation of the rent price follows the logarithmic function of Figure 23; therefore, the capex cost of warehouses becomes:

$$W_{capex} = \sum_{i=1}^W (\alpha \cdot \ln(f_i) + \beta) \cdot p_i \quad (5.14)$$

Scenario 6 also introduces the variability of the fleet dimension for the deployment of emergency resources (considered constant in the previous scenarios). The assumption is 1 lorry per warehouse; consequently, different Pareto-optimal spatial plans will have different fleet dimension even within the same Pareto front.

Figure 55 shows the solution space defined by the two objective functions  $f_{dist}$  (x-axis) and  $f_{cost}$  (y-axis), with also the indication of the spatial plans inspected in Figure 56, Figure 57 and Figure 58.

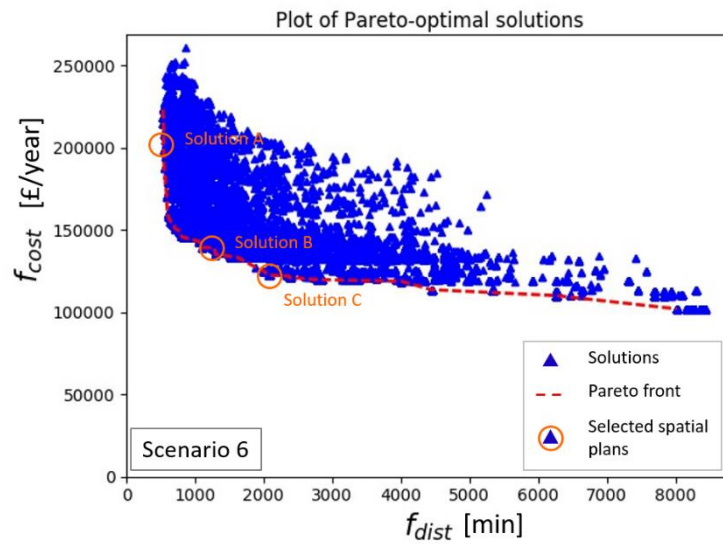


Figure 55 - Solution space and Pareto-front for Humber Estuary case study. Scenario 6. With the indication of Solutions A, B and C that are visualised respectively in Figure 56, Figure 57 and Figure 58.

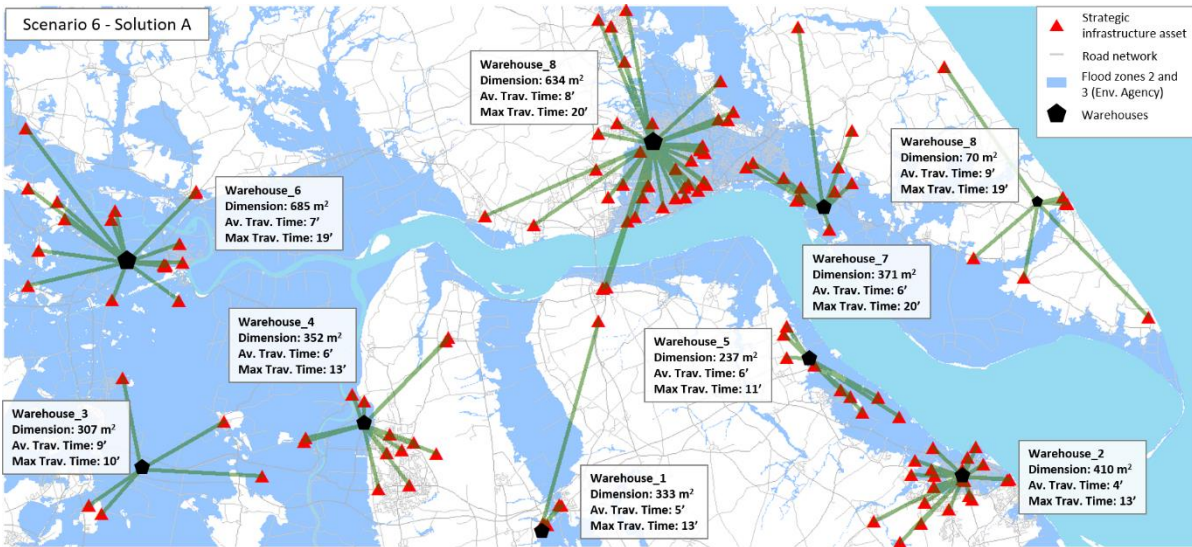


Figure 56 - Humber Estuary Scenario 6 Solution A. The green lines are for visualisation purposes: they connect each infrastructure asset to the closest warehouse. They do not represent distances, as distances are measured as travel times on the shortest path on the road network.

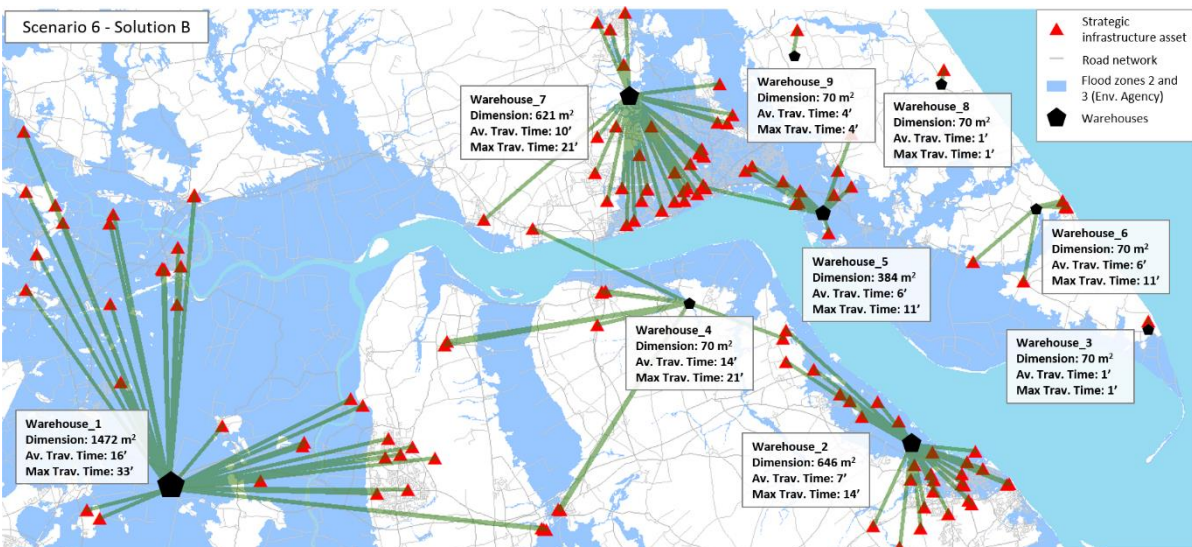


Figure 57 - Humber Estuary Scenario 6 Solution B. The green lines are for visualisation purposes: they connect each infrastructure asset to the closest warehouse. They do not represent distances, as distances are measured as travel times on the shortest path on the road network.

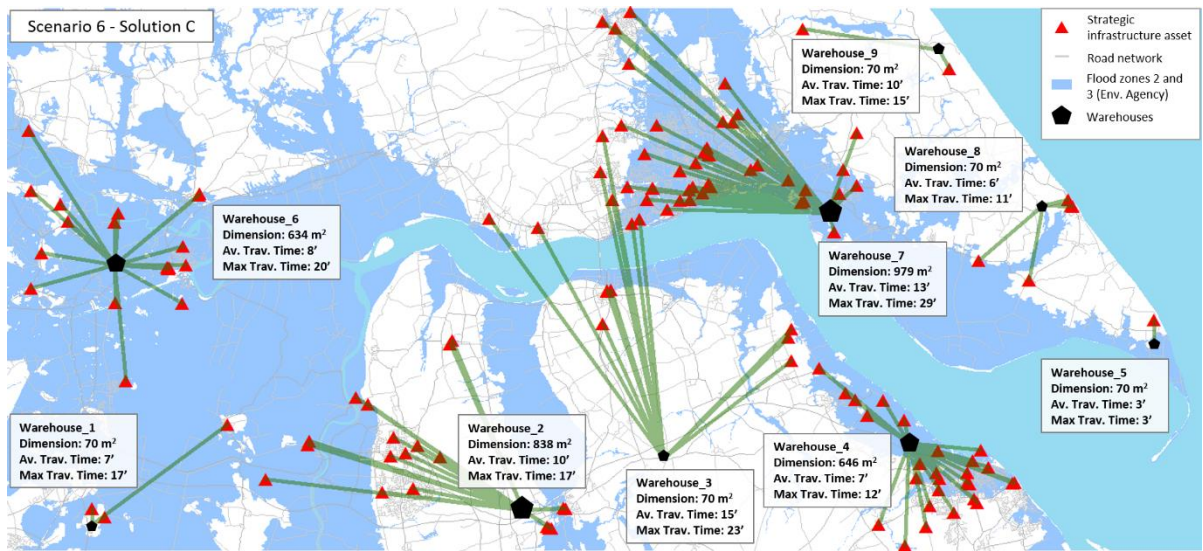


Figure 58 - Humber Estuary Scenario 6 Solution C. The green lines are for visualisation purposes: they connect each infrastructure asset to the closest warehouse. They do not represent distances, as distances are measured as travel times on the shortest path on the road network.

5.5.7. Scenario 7: Variable rent price (R/S/U), non-linear cost function with variable number of lorries (2)

Scenario 7 has the same formulation of Scenario 6, with the only exception of the fleet dimension: here the assumption is that each warehouse has 2 lorries for the deployment of emergency resources. For more specifics on the formulation of the objective functions, refer to section 5.5.6.

Figure 59 shows the solution space defined by the two objective functions  $f_{dist}$  (x-axis) and  $f_{cost}$  (y-axis), with also the indication of the spatial plans inspected in Figure 60, Figure 61 and Figure 62.

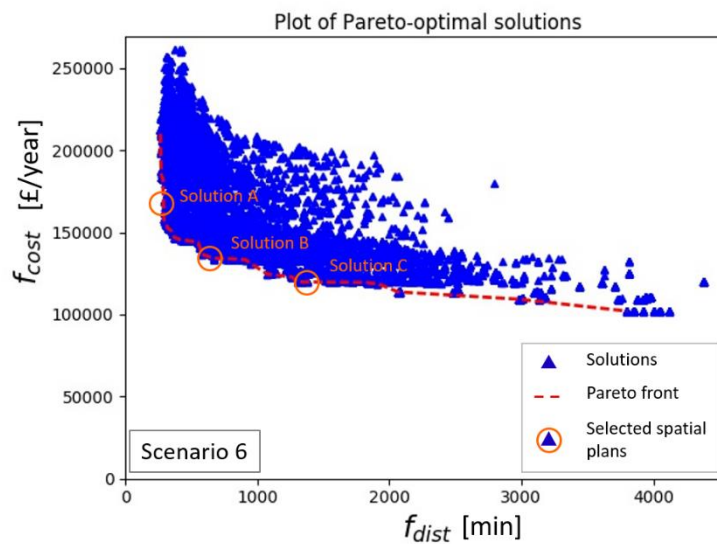


Figure 59 - Solution space and Pareto-front for Humber Estuary case study. Scenario 7. With the indication of Solutions A, B and C that are visualised respectively in Figure 60, Figure 61 and Figure 62.



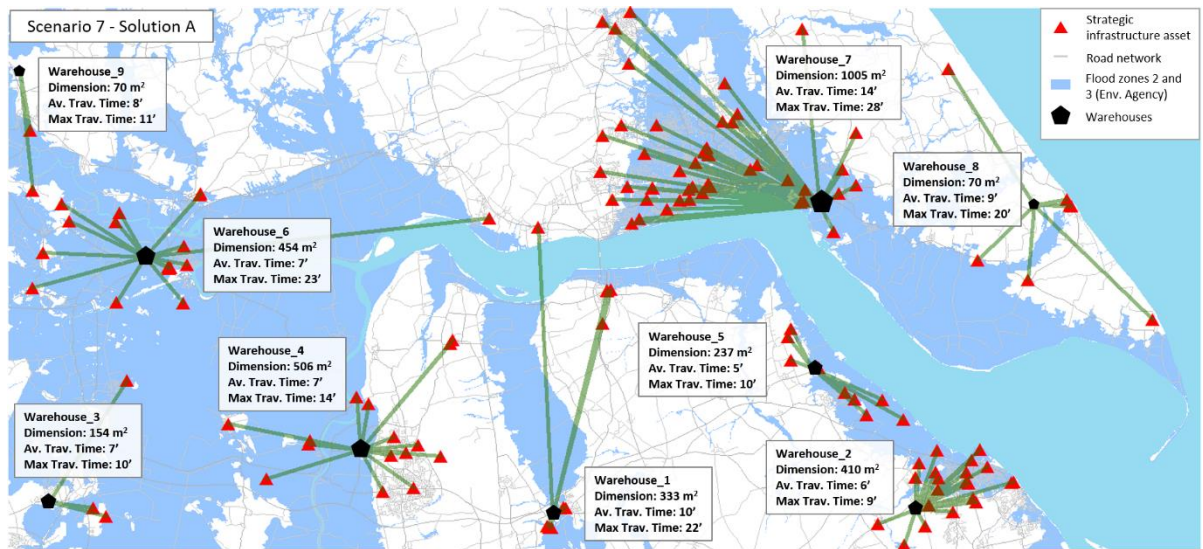


Figure 60 - Humber Estuary Scenario 7 Solution A. The green lines are for visualisation purposes: they connect each infrastructure asset to the closest warehouse. They do not represent distances, as distances are measured as travel times on the shortest path on the road network.

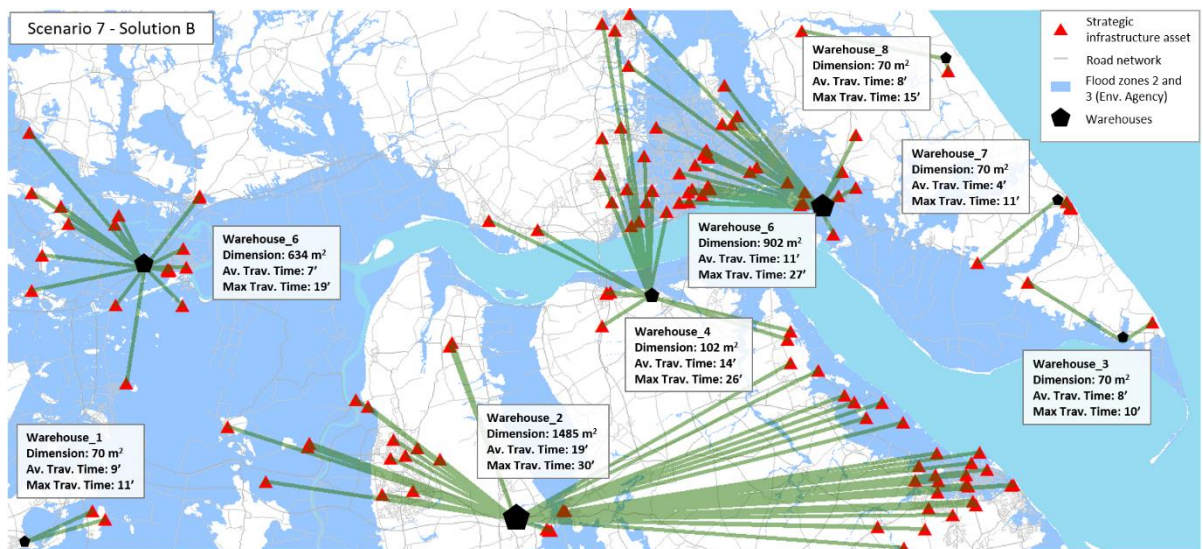


Figure 61 - Humber Estuary Scenario 7 Solution B. The green lines are for visualisation purposes: they connect each infrastructure asset to the closest warehouse. They do not represent distances, as distances are measured as travel times on the shortest path on the road network.



Figure 62 - Humber Estuary Scenario 7 Solution C. The green lines are for visualisation purposes: they connect each infrastructure asset to the closest warehouse. They do not represent distances, as distances are measured as travel times on the shortest path on the road network.

5.5.8. Scenario 8: Variable rent price (R/S/U), non-linear cost function with variable number of lorries (3)

Scenario 8 investigates the assumption of 3 lorries per warehouse to deploy emergency resources. The mathematical formulation of the objective functions is the same of Scenarios 6 and 7 presented in the previous sections (refer to section 5.5.6 for more details on the assumptions of this set of scenarios).

Figure 63 shows the solution space defined by the two objective functions  $f_{dist}$  (x-axis) and  $f_{cost}$  (y-axis), with also the indication of the spatial plans inspected in Figure 64, Figure 65 and Figure 66.

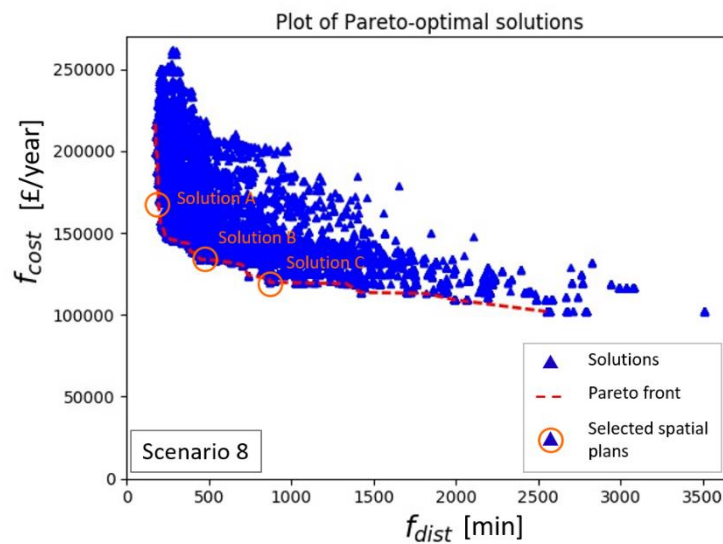


Figure 63 - Solution space and Pareto-front for Humber Estuary case study. Scenario 8. With the indication of Solutions A, B and C that are visualised respectively in Figure 64, Figure 65 and Figure 66

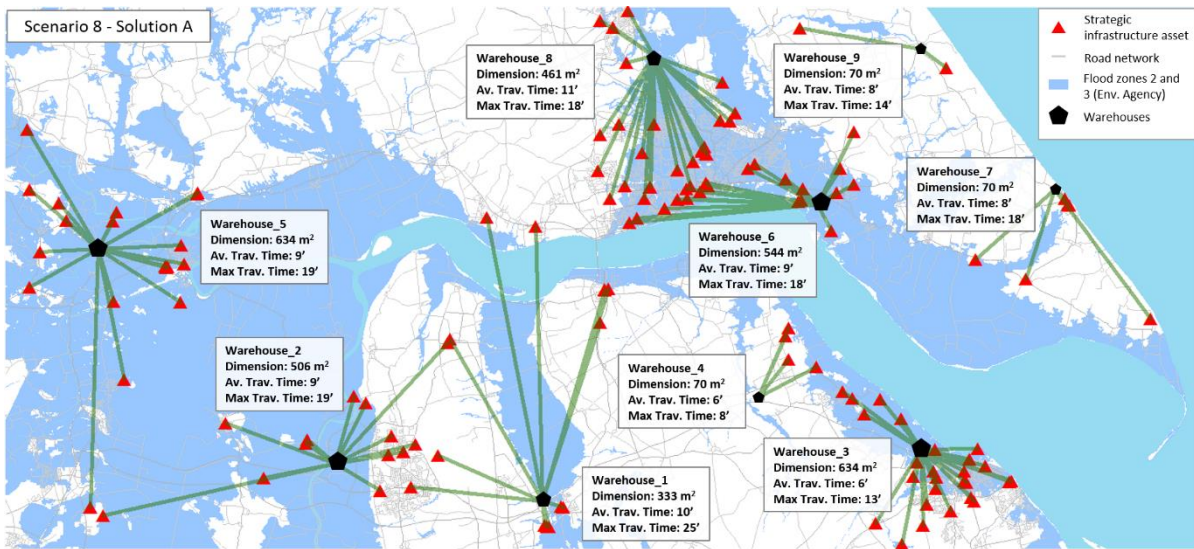


Figure 64 - Humber Estuary Scenario 8 Solution A. The green lines are for visualisation purposes: they connect each infrastructure asset to the closest warehouse. They do not represent distances, as distances are measured as travel times on the shortest path on the road network.

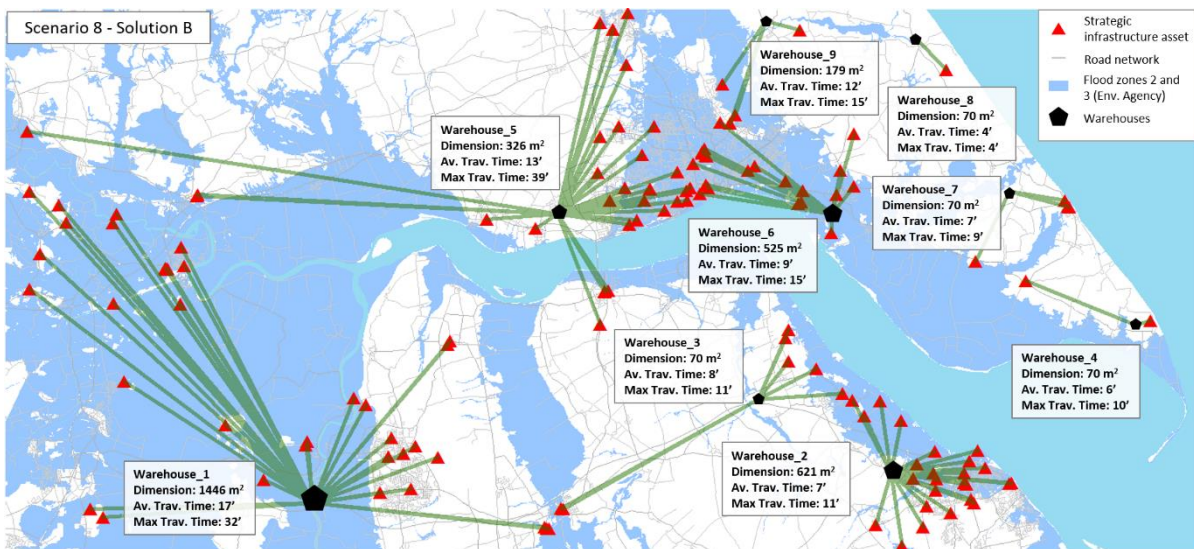


Figure 65 - Humber Estuary Scenario 8 Solution B. The green lines are for visualisation purposes: they connect each infrastructure asset to the closest warehouse. They do not represent distances, as distances are measured as travel times on the shortest path on the road network.

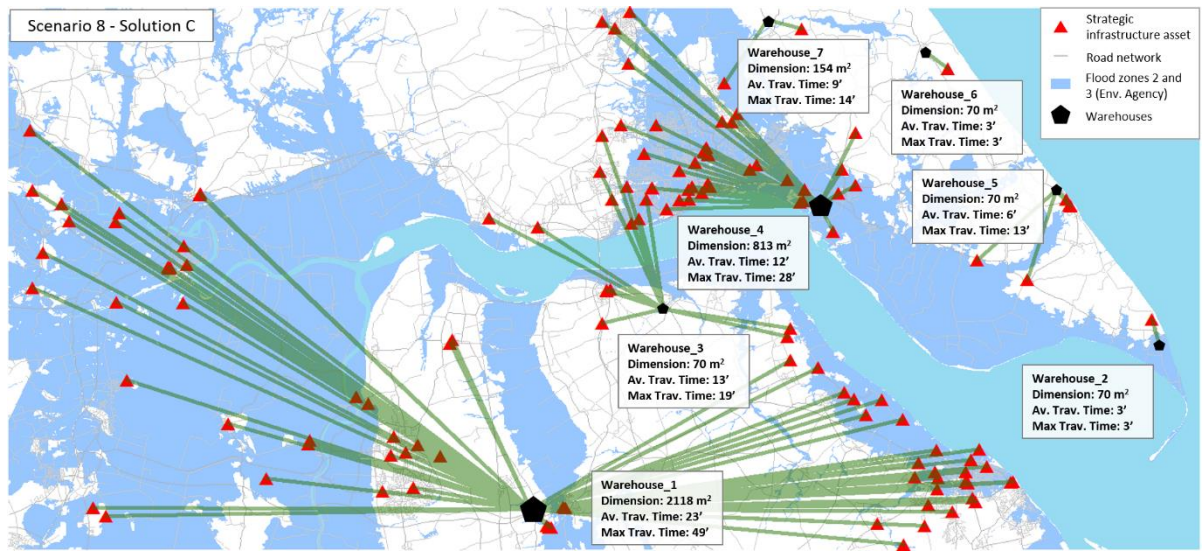


Figure 66 - Humber Estuary Scenario 8 Solution C. The green lines are for visualisation purposes: they connect each infrastructure asset to the closest warehouse. They do not represent distances, as distances are measured as travel times on the shortest path on the road network.

5.5.9. Scenario 9: Variable rent price (R/S/U), non-linear cost function with variable number of lorries (0.5)

Scenario 9 represents the last variation of the scenario formulation presented in section 5.5.6, with the assumption of a fleet dimension of 1 lorry every 2 warehouses.

Figure 67 shows the solution space defined by the two objective functions  $f_{dist}$  (x-axis) and  $f_{cost}$  (y-axis), with also the indication of the spatial plans inspected in Figure 68, Figure 69 and Figure 70.

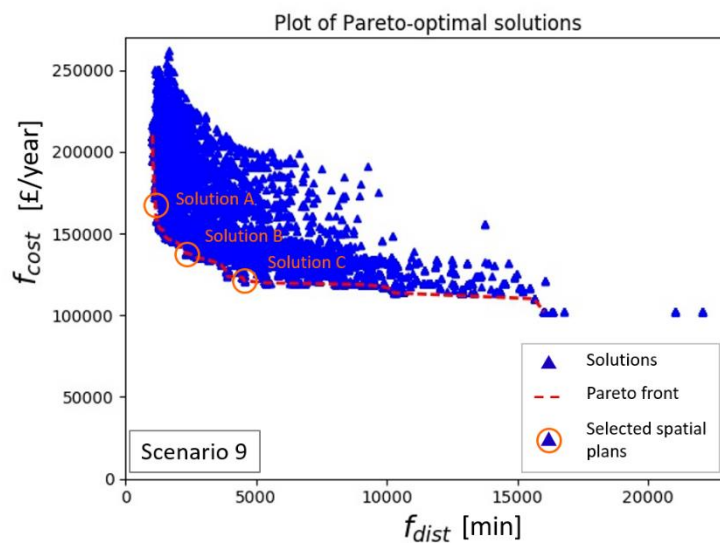


Figure 67 - Solution space and Pareto-front for Humber Estuary case study. Scenario 9. With the indication of Solutions A, B and C that are visualised respectively in Figure 68, Figure 69 and Figure 70.

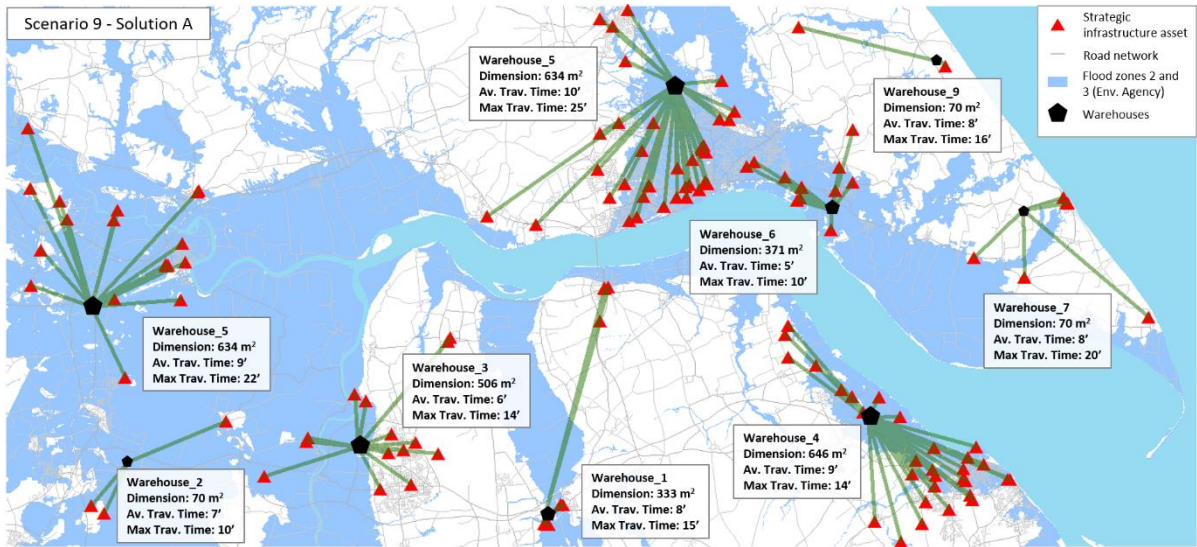


Figure 68 - Humber Estuary Scenario 9 Solution A. The green lines are for visualisation purposes: they connect each infrastructure asset to the closest warehouse. They do not represent distances, as distances are measured as travel times on the shortest path on the road network.

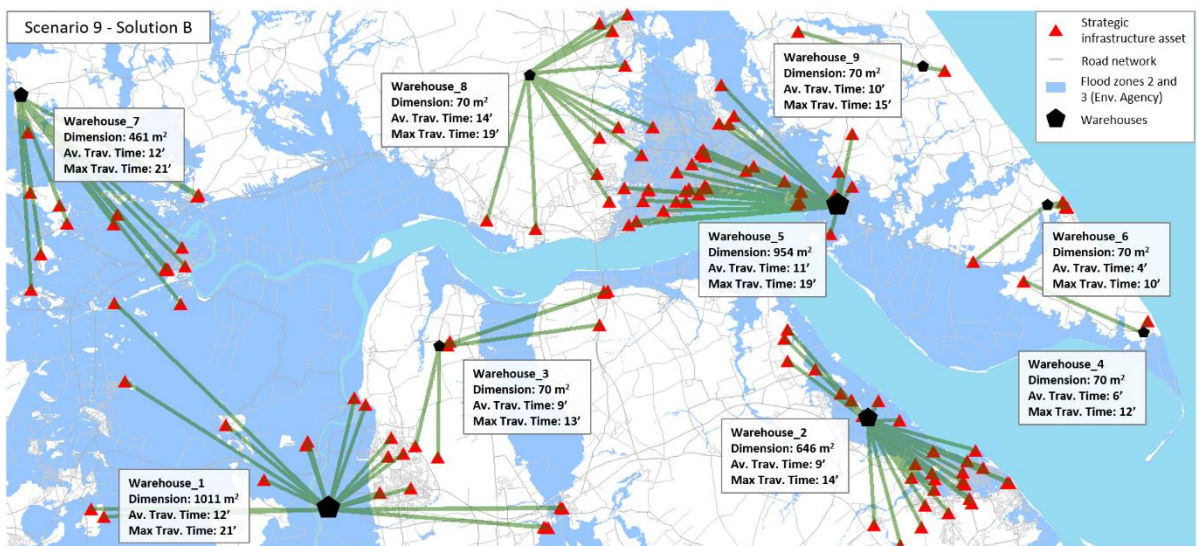


Figure 69 - Humber Estuary Scenario 9 Solution B. The green lines are for visualisation purposes: they connect each infrastructure asset to the closest warehouse. They do not represent distances, as distances are measured as travel times on the shortest path on the road network.

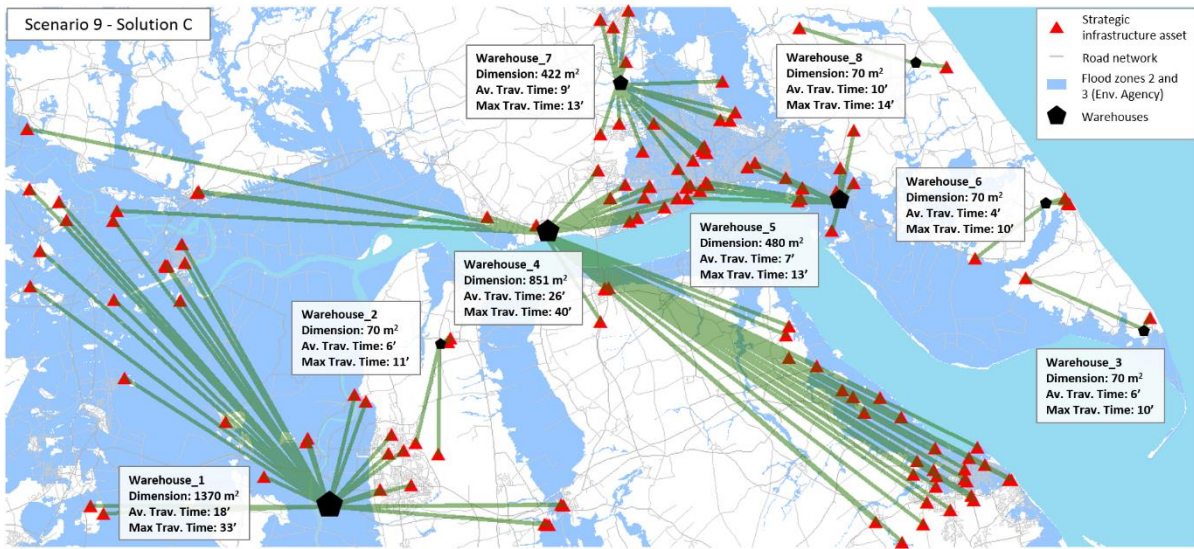


Figure 70 - Humber Estuary Scenario 8 Solution C. The green lines are for visualisation purposes: they connect each infrastructure asset to the closest warehouse. They do not represent distances, as distances are measured as travel times on the shortest path on the road network.



#### 5.5.10.Scenario 10: Variable rent price (R/S/U), non-linear cost function with variable number of lorries (1), SI priority (top 3)

Scenario 10 introduces a new concept: the prioritisation of the strategic infrastructure assets to protect in case of flooding. In case of limited budget or limited resources, in the previous scenarios the only option was to choose optimal spatial plans from the bottom-right part of the Pareto front; i.e. those plans with lower costs, but higher time fitness values. This implied lower costs at the price of a lower response time: for example, a smaller number of warehouses or a smaller fleet allow lower costs, but higher travel/deployment times for all the strategic infrastructure assets in the region. Scenario 10 (and the following ones) explore a different approach to reduce costs (or deal with limited resources): to maximise the service areas of warehouses only considering the most relevant assets from each category.

Scenario 10 maintains the same formulation of Scenario 6 (see section 5.5.6): the rent price of warehouse varies according to the location (rural, suburban, urban), the cost function consists in the non-linear formulation and the fleet dimension is variable, assuming one lorry per warehouse; the only extra assumption that only the top 3 assets of each strategic infrastructure category will be considered in the minimisation of costs and distances of the GA.

Each strategic infrastructure asset is ranked on the basis of the number of served buildings in the region; in absence of specific data for each infrastructure network, the attribution of service areas (and therefore of rank values) has been performed with Thiessen polygons in a GIS environment.

Figure 71 shows the solution space defined by the two objective functions  $f_{dist}$  (x-axis) and  $f_{cost}$  (y-axis), with also the indication of the spatial plans inspected in Figure 72. Figure 73 and Figure 74.

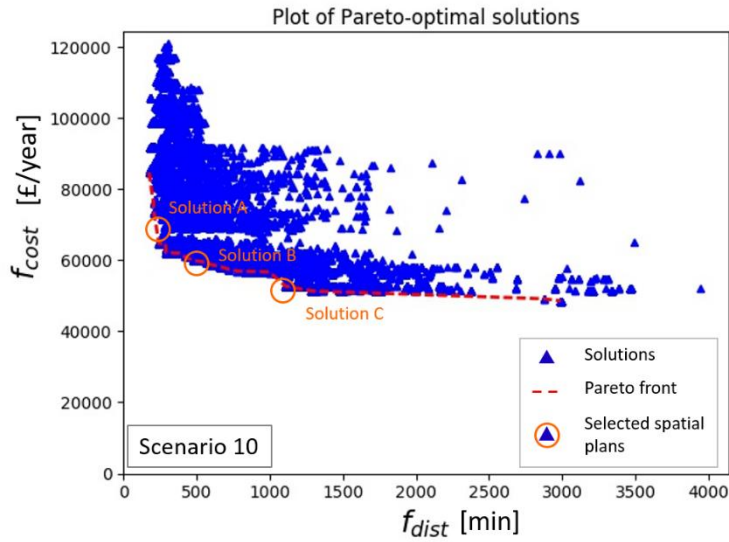


Figure 71 - Solution space and Pareto-front for Humber Estuary case study. Scenario 10. With the indication of Solutions A, B and C that are visualised respectively in Figure 72, Figure 73 and Figure 74.

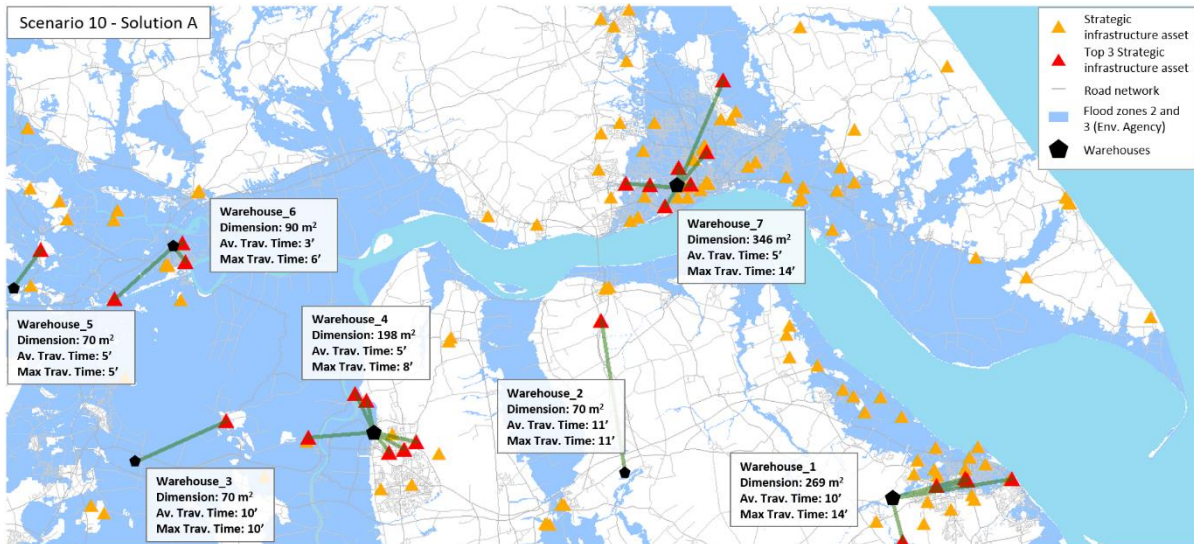


Figure 72 - Humber Estuary Scenario 10 Solution A. The green lines are for visualisation purposes: they connect each infrastructure asset to the closest warehouse. They do not represent distances, as distances are measured as travel times on the shortest path on the road network.

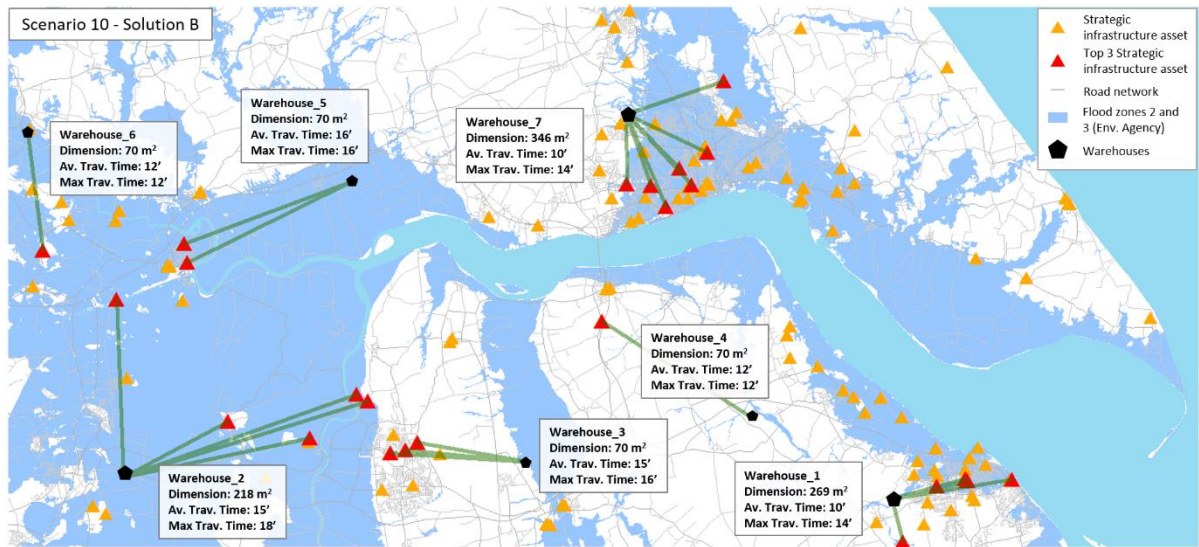


Figure 73 - Humber Estuary Scenario 10 Solution B. The green lines are for visualisation purposes: they connect each infrastructure asset to the closest warehouse. They do not represent distances, as distances are measured as travel times on the shortest path on the road network.

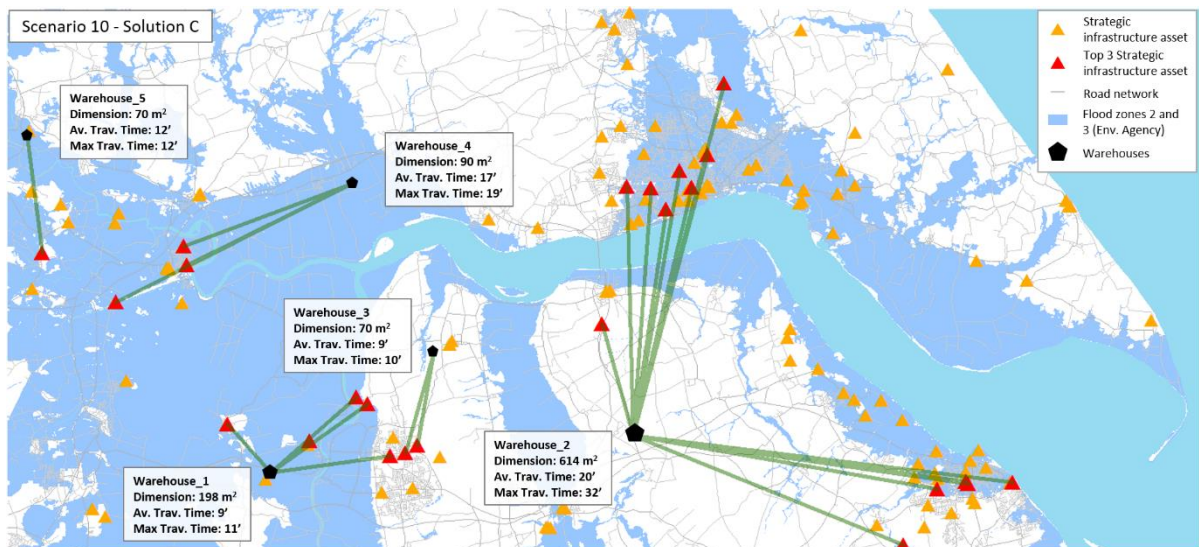


Figure 74 - Humber Estuary Scenario 10 Solution C. The green lines are for visualisation purposes: they connect each infrastructure asset to the closest warehouse. They do not represent distances, as distances are measured as travel times on the shortest path on the road network.

5.5.11.Scenario 11: Variable rent price (R/S/U), non-linear cost function with variable number of lorries (1), SI priority (top 5)

Scenario 11 investigates the assumption of prioritising the top5 assets for each strategic infrastructure category. The formulation and other assumptions are the same of the previous Scenario (see section 5.5.10 for more details).

Figure 75 shows the solution space defined by the two objective functions  $f_{dist}$  (x-axis) and  $f_{cost}$  (y-axis), with also the indication of the spatial plans inspected in Figure 76, Figure 77 and Figure 78.

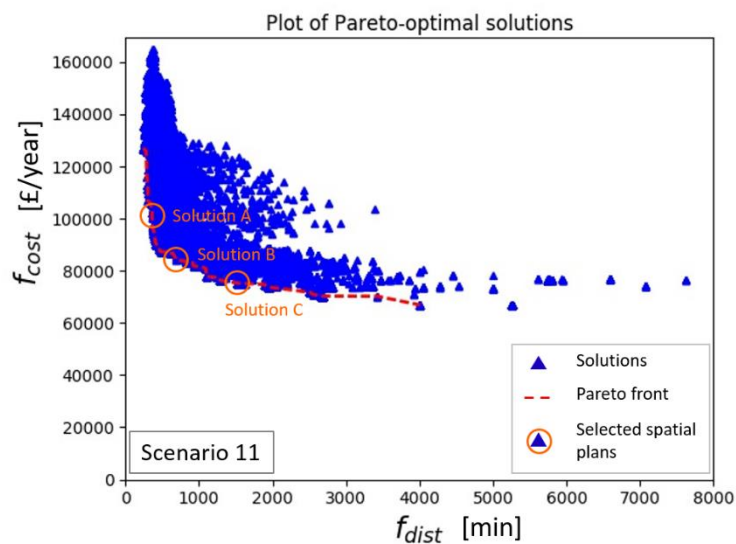


Figure 75 - Solution space and Pareto-front for Humber Estuary case study. Scenario 11. With the indication of Solutions A, B and C that are visualised respectively in Figure 76, Figure 77 and Figure 78.

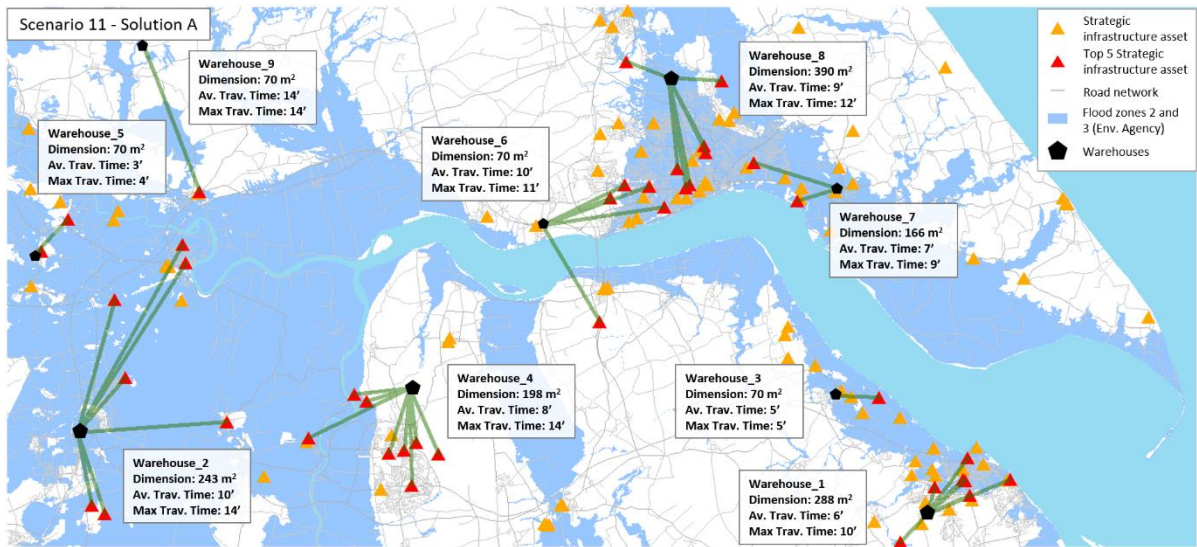


Figure 76 - Humber Estuary Scenario 11 Solution A. The green lines are for visualisation purposes: they connect each infrastructure asset to the closest warehouse. They do not represent distances, as distances are measured as travel times on the shortest path on the road network.

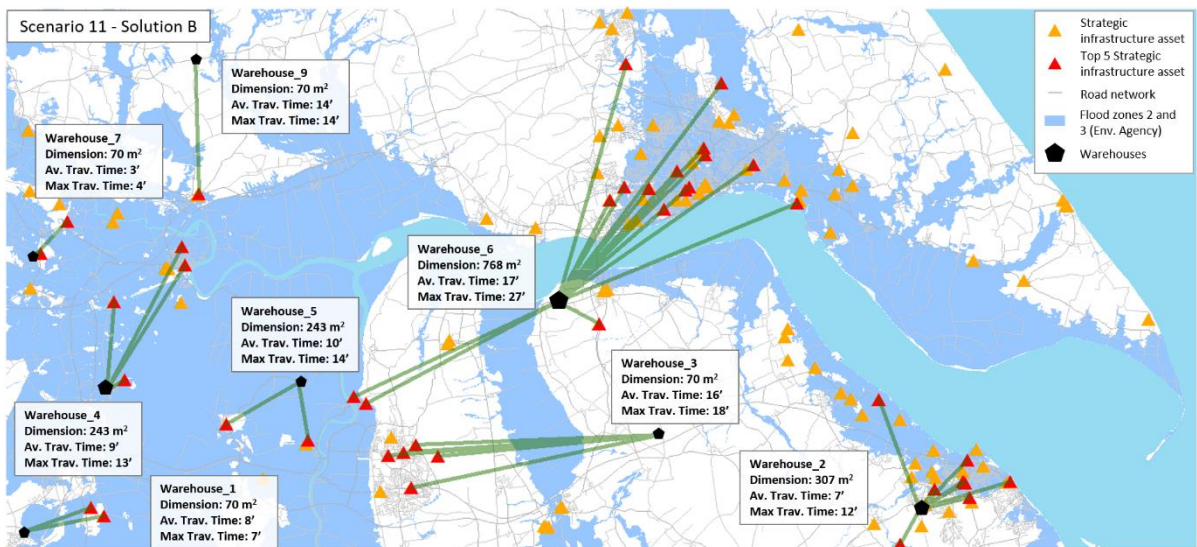


Figure 77 - Humber Estuary Scenario 11 Solution B. The green lines are for visualisation purposes: they connect each infrastructure asset to the closest warehouse. They do not represent distances, as distances are measured as travel times on the shortest path on the road network.

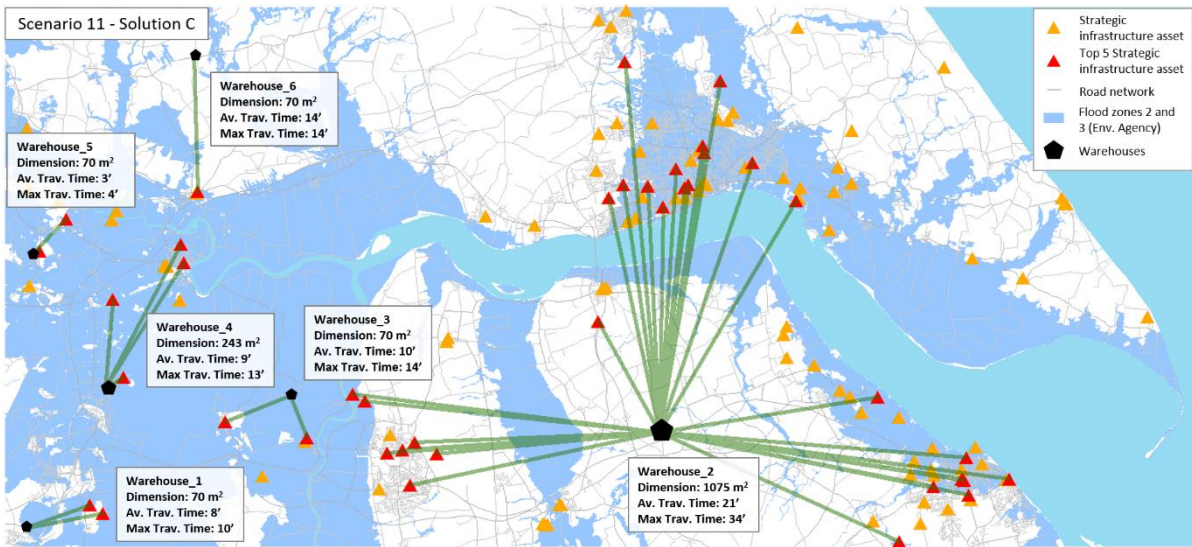


Figure 78 - Humber Estuary Scenario 11 Solution C. The green lines are for visualisation purposes: they connect each infrastructure asset to the closest warehouse. They do not represent distances, as distances are measured as travel times on the shortest path on the road network.

5.5.12.Scenario 12: Variable rent price (R/S/U), non-linear cost function with variable number of lorries (1), SI priority (top 10)

Like the previous one, in Scenario 12, the only variation with respect to Scenario 10's formulation is the prioritisation criterion: here the top 10 assets of each strategic infrastructure category are considered as a priority for flood protection.

Figure 79 shows the solution space defined by the two objective functions  $f_{dist}$  (x-axis) and  $f_{cost}$  (y-axis), with also the indication of the spatial plans inspected in Figure 80, Figure 81 and Figure 82.

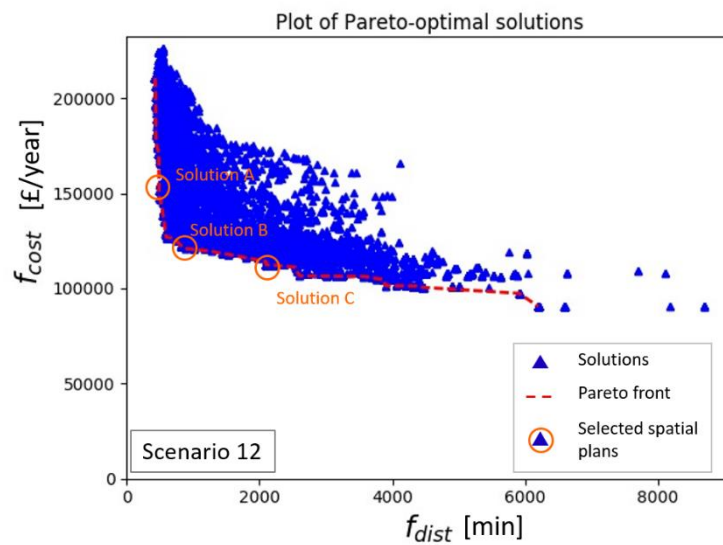


Figure 79 - Solution space and Pareto-front for Humber Estuary case study. Scenario 12. With the indication of Solutions A, B and C that are visualised respectively in Figure 80, Figure 81 and Figure 82.

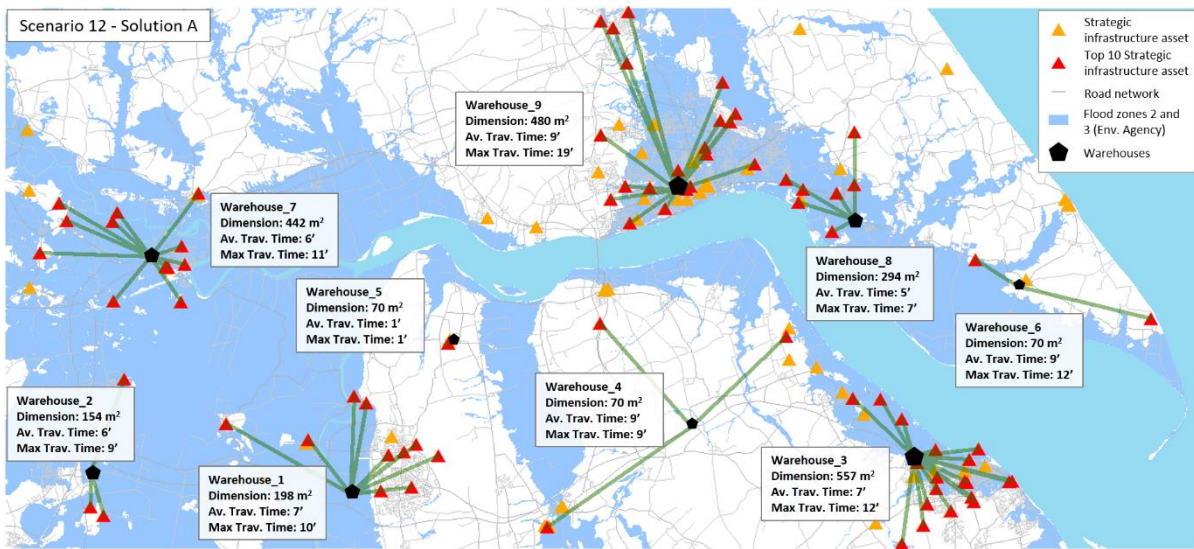


Figure 80 - Humber Estuary Scenario 12 Solution A. The green lines are for visualisation purposes: they connect each infrastructure asset to the closest warehouse. They do not represent distances, as distances are measured as travel times on the shortest path on the road network.

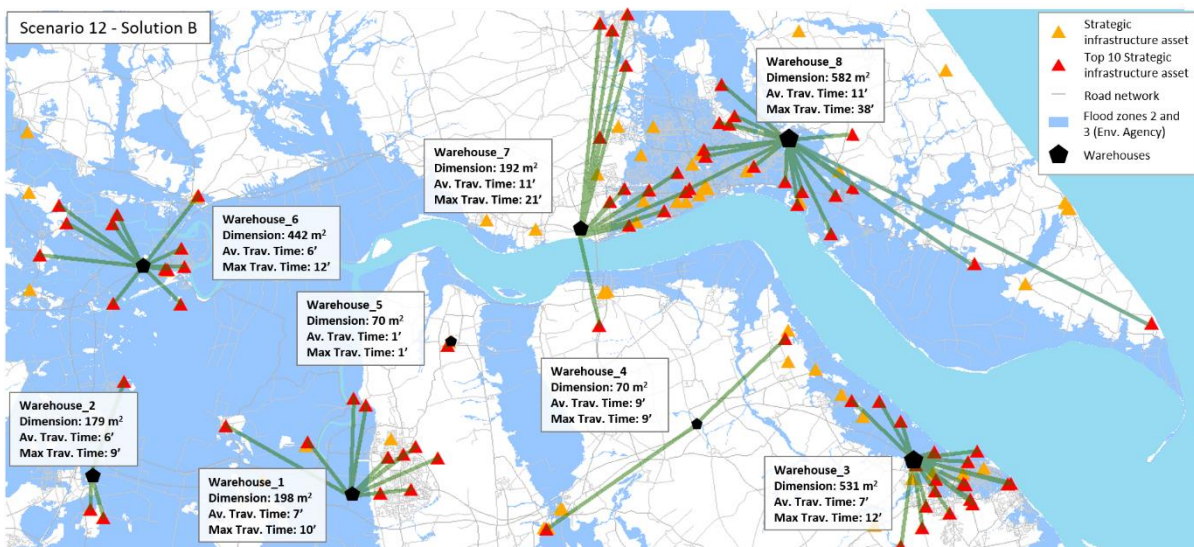


Figure 81 - Humber Estuary Scenario 12 Solution B. The green lines are for visualisation purposes: they connect each infrastructure asset to the closest warehouse. They do not represent distances, as distances are measured as travel times on the shortest path on the road network.



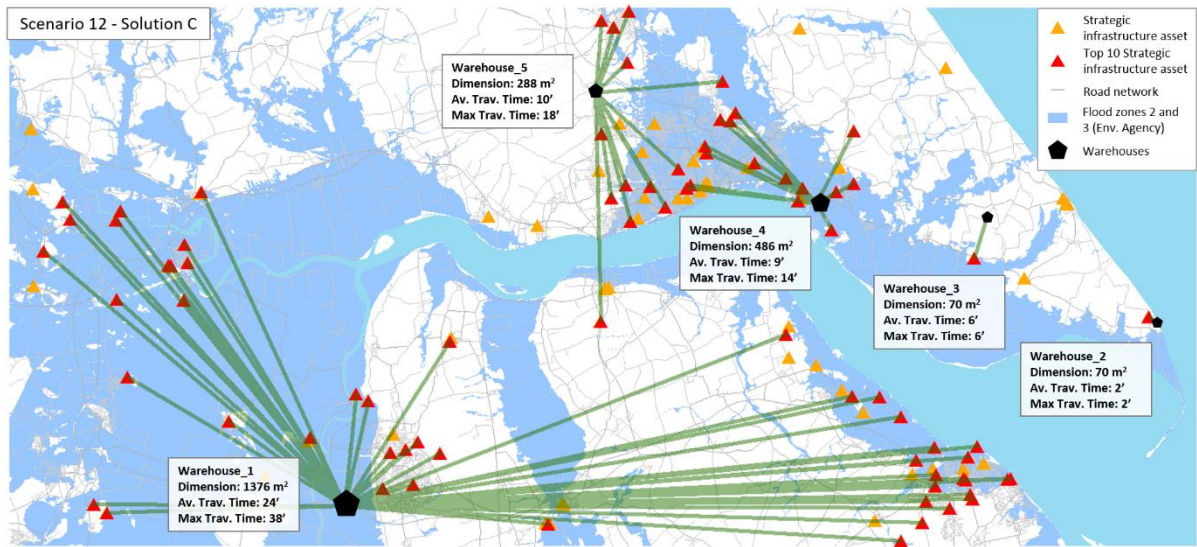


Figure 82 - Humber Estuary Scenario 12 Solution C. The green lines are for visualisation purposes: they connect each infrastructure asset to the closest warehouse. They do not represent distances, as distances are measured as travel times on the shortest path on the road network.

5.5.13.Scenario 13: Variable rent price (R/S/U), non-linear cost function with variable number of lorries (1), SI priority (top 10 – excluding police and fire stations)

Scenario 13 introduces a different prioritisation criterion: like in Scenario 12, the top 10 assets of each strategic infrastructure category are selected as priority targets to be protected in case of flood, but in this case police and fire stations are excluded, assuming that these categories already have in place flood protection resources.

The mathematical formulation of the objective functions and the assumptions regarding the other main parameters are not different with respect to the previous Scenarios (see section 5.5.10 for more details).

Figure 83 shows the solution space defined by the two objective functions  $f_{dist}$  (x-axis) and  $f_{cost}$  (y-axis), with also the indication of the spatial plans inspected in Figure 84, Figure 85 and Figure 86.

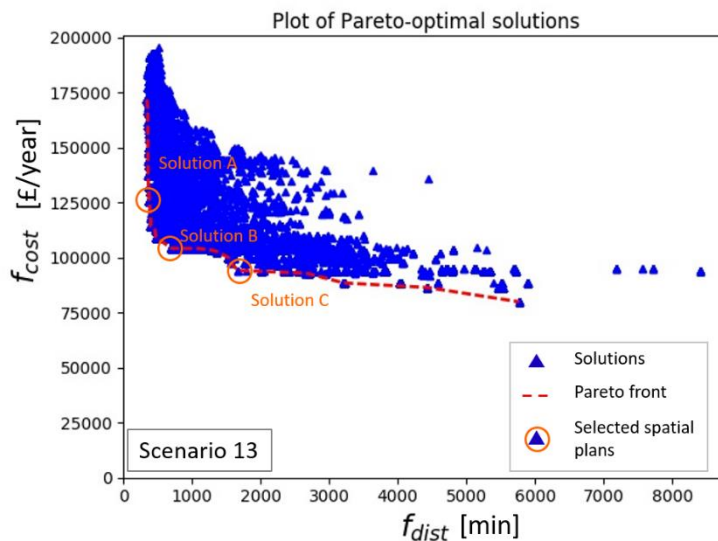


Figure 83 - Solution space and Pareto-front for Humber Estuary case study. Scenario 13. With the indication of Solutions A, B and C that are visualised respectively in Figure 84, Figure 85 and Figure 86.

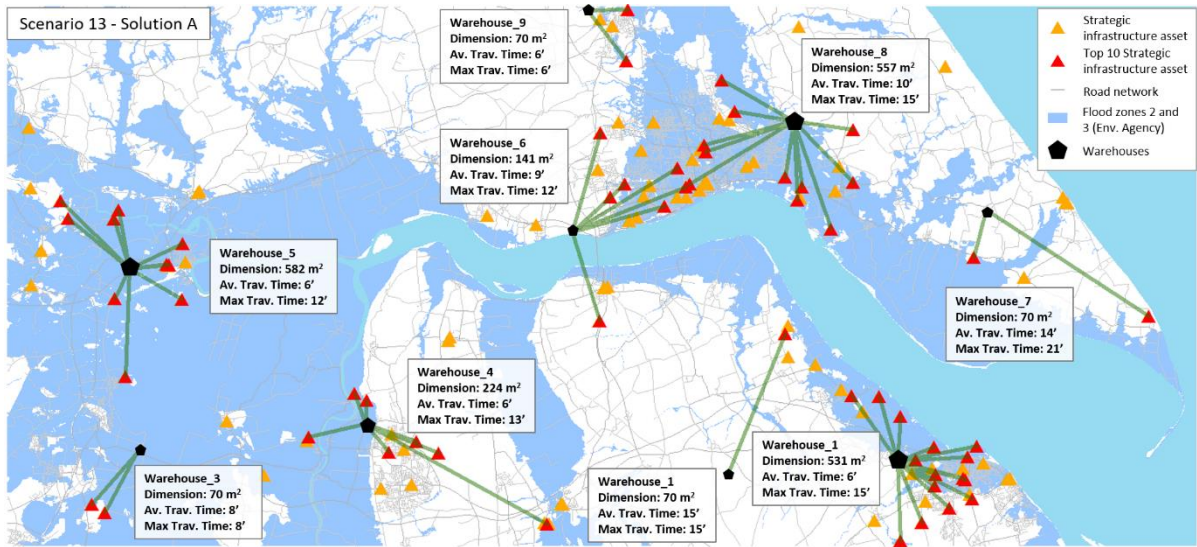


Figure 84 - Humber Estuary Scenario 13 Solution A. The green lines are for visualisation purposes: they connect each infrastructure asset to the closest warehouse. They do not represent distances, as distances are measured as travel times on the shortest path on the road network.

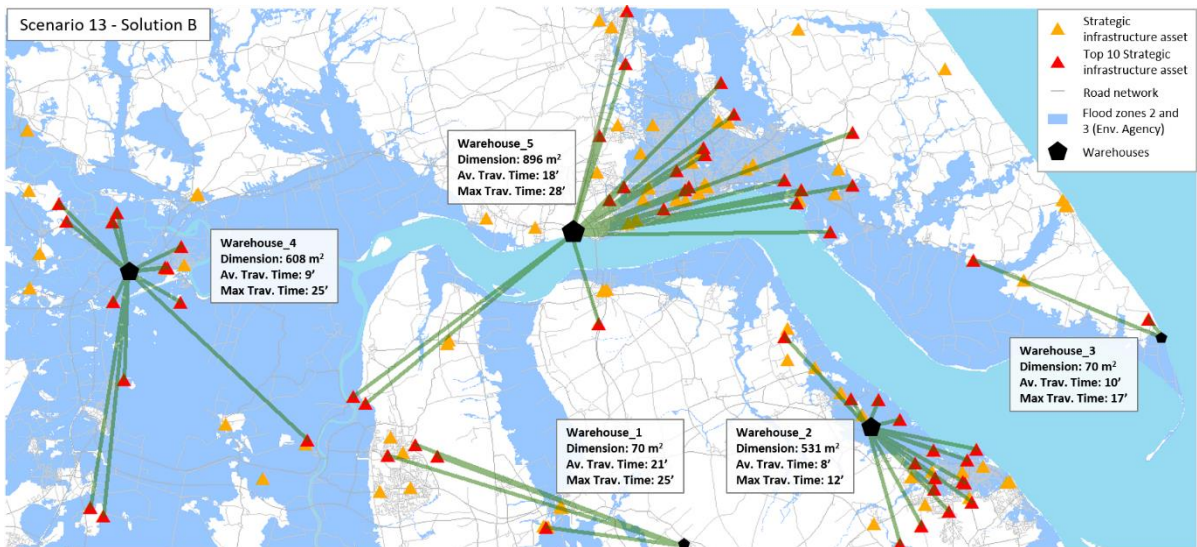


Figure 85 - Humber Estuary Scenario 13 Solution B. The green lines are for visualisation purposes: they connect each infrastructure asset to the closest warehouse. They do not represent distances, as distances are measured as travel times on the shortest path on the road network.

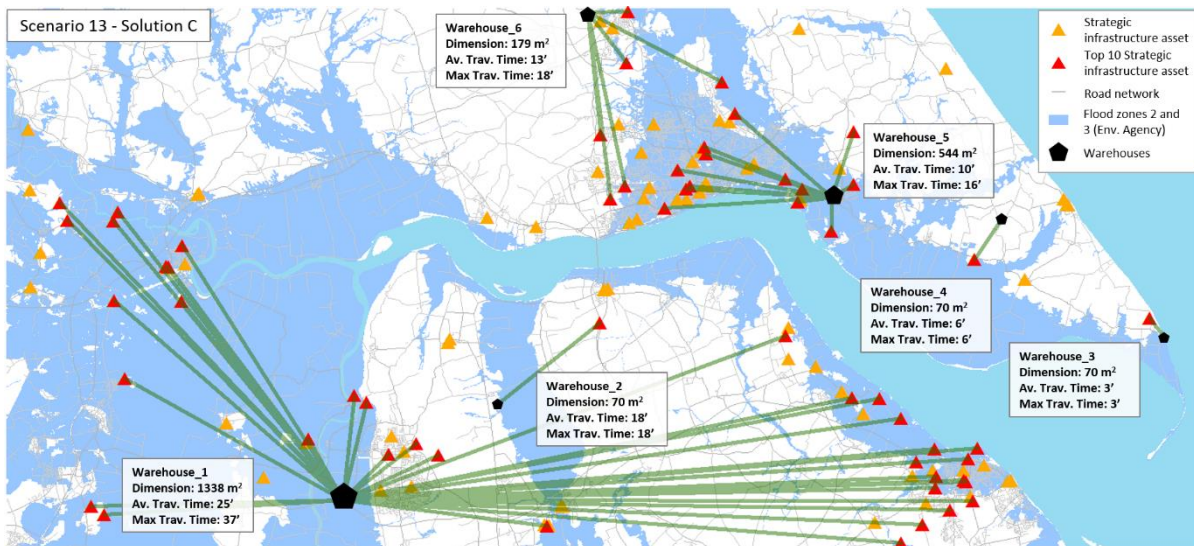


Figure 86 - Humber Estuary Scenario 13 Solution C. The green lines are for visualisation purposes: they connect each infrastructure asset to the closest warehouse. They do not represent distances, as distances are measured as travel times on the shortest path on the road network.

## 5.6. Discussion of Humber Estuary case study results

Analysing the Pareto-optimal spatial plans of the various scenarios, it is possible to visualise on a map the observations made on the solution space. Solutions A have higher costs (in terms of warehouses surface areas) and lower travel times: consequently, they will result in more numerous warehouses. A higher number of warehouses implies lower travel times due to higher coverage of the territory. Solutions B represent middle-ground solutions, while solutions C represent the other extreme of the spectrum. They are, in general, more centralised spatial plans; they have fewer warehouses, which entails lower costs, but higher travel times.

As well as solutions A-C, any other Pareto-optimal spatial plan can be represented as a map of warehouses. Ideally, for real-life applications, the RAO framework would provide not only three, but a complete portfolio of printed maps of Pareto-optimal solutions, on which to draw conclusions on how to plan the allocation of new warehouses or how to modify/improve the current assets' distribution. To ease the readability, only a selection of Pareto-optimal spatial plans are presented as maps in the scenarios of section 5.5, as most of the maps can result very similar to each other. For example, this is the case of Scenario 4: the three plotted spatial plans appear very similar to each other, all with 8 warehouses allocated in similar locations; however, observing the Pareto front, their respective costs are very different (quite steep Pareto front): this is due to the different costs associated to rural or urban locations – locating a warehouse just outside an urban area might slightly raise the value of  $f_{dist}$ , but considerably decrease the associated costs. This is why, despite apparent similarities in spatial distributions, solutions from all the areas of Pareto fronts have been plotted in all the scenarios results.

However, also with only three maps representing solutions from different areas of the Pareto-front, it is possible to draw some conclusions. For instance, no matter what formulation is adopted, a large warehouse is always present in the main town of the region (Kingston upon Hull) because a cluster of strategic infrastructure assets is present in this densely populated area.

Perhaps less intuitive is the constant allocation of a warehouse in the most eastern part of the estuary. A lower number of strategic infrastructure assets is present here, but due to the remoteness of the area, not allocating a warehouse here would imply very high travel times.

High travel times are highly penalised in the optimisation process because multiple trips may be necessary according to staff availability and/or truck fleet's dimensions.

Due to the more restrictive constraints, a lower variability is observed in Scenario 2, where the disruption of the road network due to floodwater is simulated. As anticipated in section 5.5.2, only solutions that include a warehouse in each isolated area are considered (refer to Figure 39). This necessarily requires, on average, a higher number of warehouses to be considered in Pareto-optimal solutions.

To better assess the impact of the roads closure assumption, it is useful to consider the entire portfolio of spatial plans that form the Pareto front (as opposed to single solutions) of Scenarios 1 and 2 (presented in sections 5.5.1 and 5.5.2) as these scenarios have the same objective functions' formulation and the only variation consists in the road network analysis. Figure 87 shows a heatmap which represents the probability of a warehouse allocation by the RAO framework of scenarios 1 and 2. All the storing facilities of all the spatial plans that form the Pareto front are considered when drawing the heatmap. Darker areas represent higher probabilities that a storing facility is allocated in that zone.

The results presented in Figure 87 differ according to the considered scenario. When the road network is not affected by flooding (Figure 87.a), Scenario 1 presents higher probability of warehouse allocations indicatively correspond to higher concentrations of strategic infrastructure assets. Consequently, to avoid flood-related disruptions whilst maximising accessibility under normal conditions, temporary flood defences storing facilities should be allocated in the areas of Hull, Grimsby, Scunthorpe and Thorne, with a warehouse dimension varying according to how many other facilities are present in the spatial plan. In Scenario 1, the RAO framework also provides the user with potentially unintuitive insights like the necessity of a warehouse allocation in Withernsea for the reasons explained before.

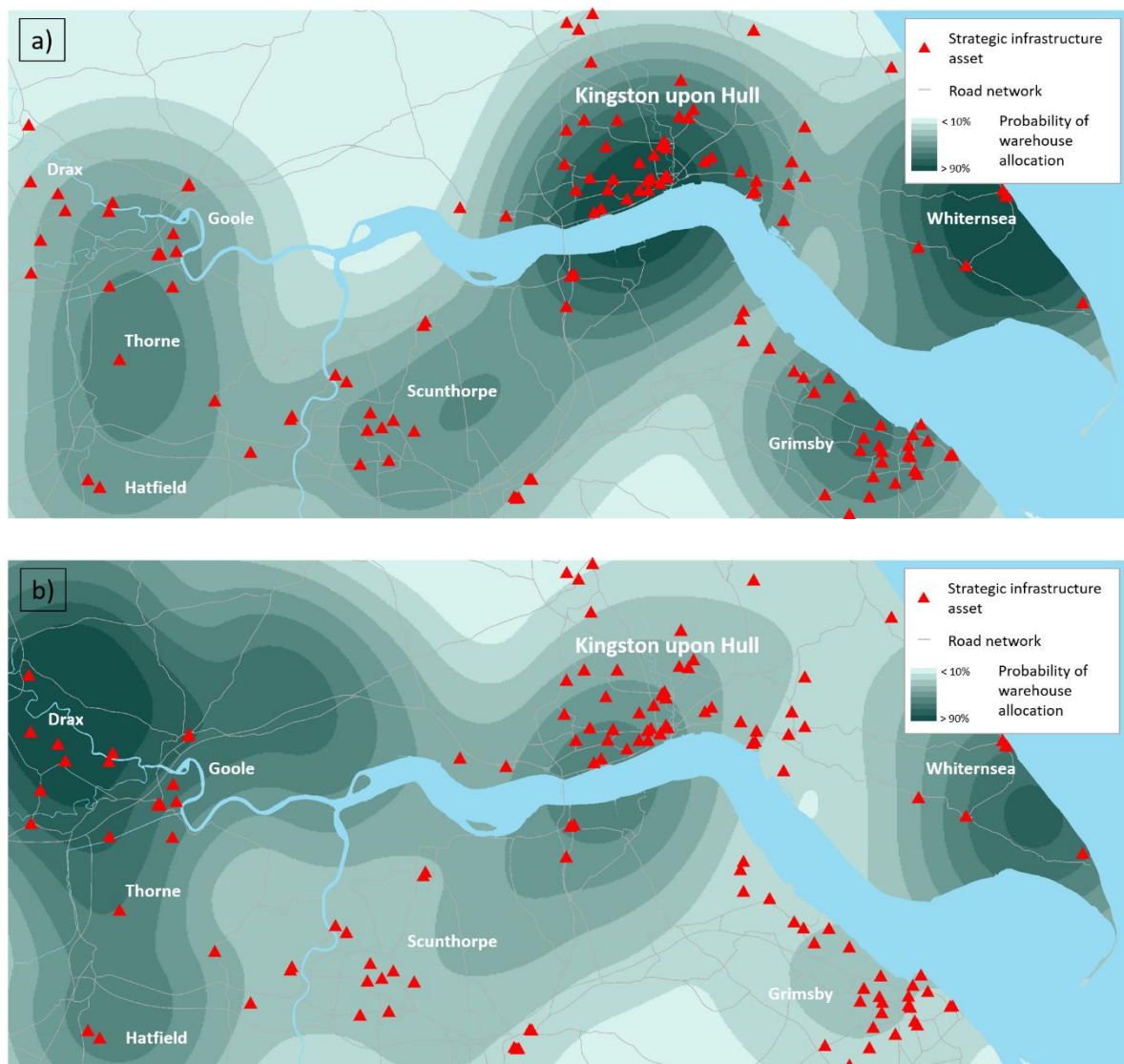


Figure 87 - Pareto front heatmap representing the probability of allocation of a warehouse by the RAO framework. a) BAU scenario. b) Disruption scenario.

However, the full potential of the RAO framework is exploited when testing different scenarios and situations and when comparing their results. Figure 87.b shows the solutions' density of Scenario 2 (i.e. with road closures due to floodwater). Here the situation changes as the highest probability of warehouse allocation is located where road network disruptions increase the isolation/remoteness of certain areas (refer to map in Figure 38).

In terms of results interpretations, different solution densities (i.e. allocation probabilities) correspond to different priorities that vary according to the evaluated scenarios: in Scenario 1, as the road network is perfectly functioning, the driving factor in terms of accessibility is the number of infrastructure assets to protect. Spatially, it is translated as a higher probability of warehouse allocation where the more significant number of infrastructure is present. On the

contrary, in the Scenario 2, the driving factor in terms of accessibility is travel time. Since isolated areas are more complicated (or even impossible) to reach due to the disrupted condition of the road network, and since areas with a higher number of strategic infrastructure assets are also the most interconnected, accessibility of most remote locations is the parameter that governs the problem. Therefore, a higher probability of warehouses allocation will correspond to difficult-to-reach locations (like Drax or Withernsea); while densely populated areas (like Kingston upon Hull or Scunthorpe) have a more dispersed allocation probability as their spatial variability is less significant due to their high interconnection.

When considering scenarios involving road closures, particular attention is due to the Humber Bridge as it represents a crucial asset in the region's transport system. Due to its nature of suspension bridge (its clearance is around 30 meters from the water below), it cannot be affected by the presence of floodwater on the road section, and for this reason it has been considered fully operative in Scenario 2; however, bridges are vulnerable from many different perspectives (e.g. scour) (Pregolato, 2019) and the potential closure of the Humber Bridge would have dramatic consequences for the connection of different areas of the Estuary. This is highlighted by the results of Scenario 2 (Solutions D, E and F shown in Figure 44, Figure 45 and Figure 46 ): when considering spatial plans with lower costs (and therefore lower number of warehouses), relying on the Humber Bridge becomes an absolute necessity as in all the solutions at least one warehouse serves both the city of Hull and the southern bank of the Humber. Therefore, the results of the case study highlight that it is crucial for decision-makers and final users of the RAO framework to assess the Humber Bridge's risk of closure when designing flood protection strategies involving temporary flood defenses.



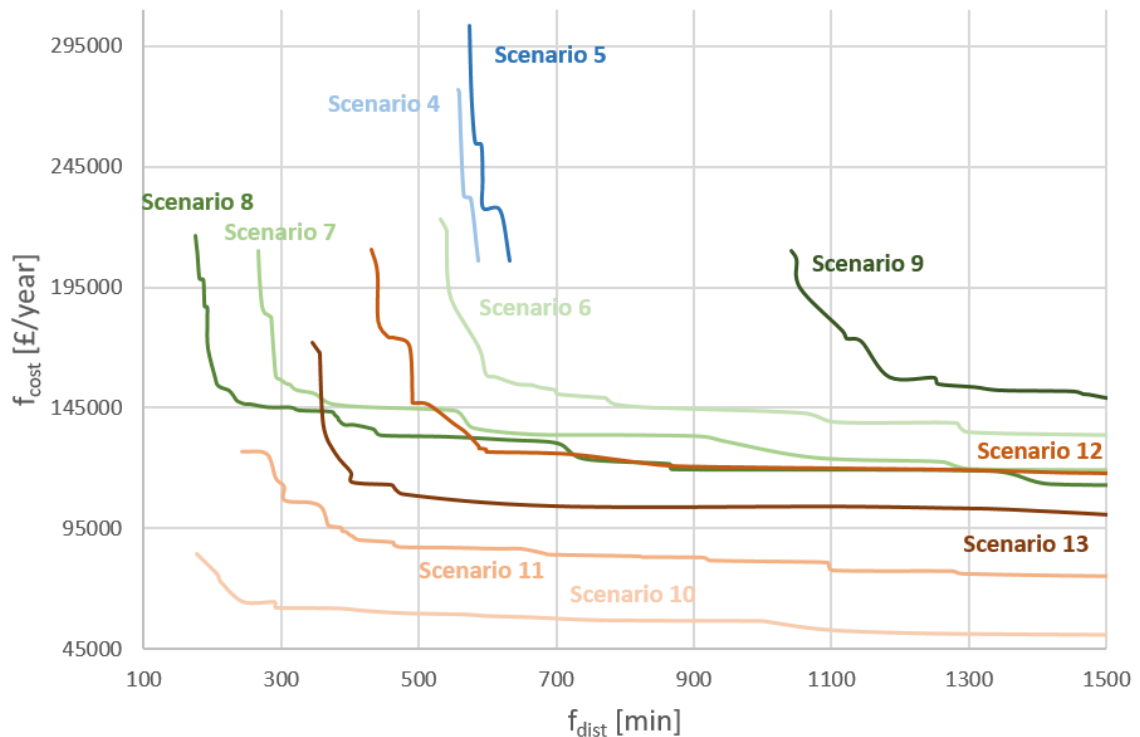


Figure 88 - Comparison of Pareto fronts from different scenarios.

In addition to the analysis of the road network functionality assumption, it is possible to assess the sensitivity of the model also to the other assumptions explored in the other scenarios. To facilitate the analysis, the scenarios can be clustered in three groups:

1. Scenarios 4 and 5: linear cost function & fixed number of lorries (blue Pareto fronts in Figure 88).
2. Scenarios 6-9: non-linear cost function & variable number of lorries (green Pareto fronts in Figure 88).
3. Scenarios 10-13: Strategic infrastructure prioritisation (orange Pareto fronts in Figure 88).

Figure 88 shows the Pareto fronts of scenarios 4-13. The orange Pareto fronts represent the SI prioritisation scenarios and entail lower costs as the infrastructure assets to protect are fewer and therefore less storing space is required and a smaller fleet is necessary to deploy temporary flood defences. Scenarios 10 and 11 (respectively considering the top 3 and top 5 assets for each strategic infrastructure category) can correspond up to a 50% decrease of costs with respect to considering all the assets of the region, while Scenario 12 (top 10 assets) has comparable costs to the green Pareto fronts (considering the full set of strategic infrastructure

in the Humber Estuary region), but lower deployment times when compared to Scenario 6, which has the same assumption with respect to the fleet dimension (i.e. 1 lorry per warehouse).

Referring to Figure 88, when observing the orange Pareto fronts it is possible to observe a general vertical shift corresponding to an increase of costs when the range of SI assets to be protected in case of flood expands. On the other hand, in the green Pareto fronts the shift is generally horizontal, corresponding to a decrease of deployment time when the dimension of the fleet increases. Of course more SI assets to protect imply higher travel times and a larger fleet corresponds to higher costs, however, the observation of the Pareto fronts indicates that the assumption on the fleet dimension as major repercussion on travel times rather than on costs, while the model is more sensitive on the costs side regarding the assumption on the number of SI to protect.

The blue Pareto fronts of Figure 88, instead, allow to assess the sensitivity of the model to the land use category assumption: Scenario 4 considers two categories: “urban” and “rural”, while Scenario 5 also includes the “suburban” category. The system appears to be less sensitive to this assumption with respect to the previous one as the differences in terms of costs and travel times are smaller. Costs appear to be lower when considering only two categories, but this is due to an oversimplification of the spatial variability of the land uses: since the Humber Estuary region has a low level of urbanisation, when considering only two categories, most of the available cells are classified as “rural”. Introducing a third category decreases the number of “rural” cells and inevitably increases the average costs, this is aimed at a better representation of the land values/rent prices of the region.

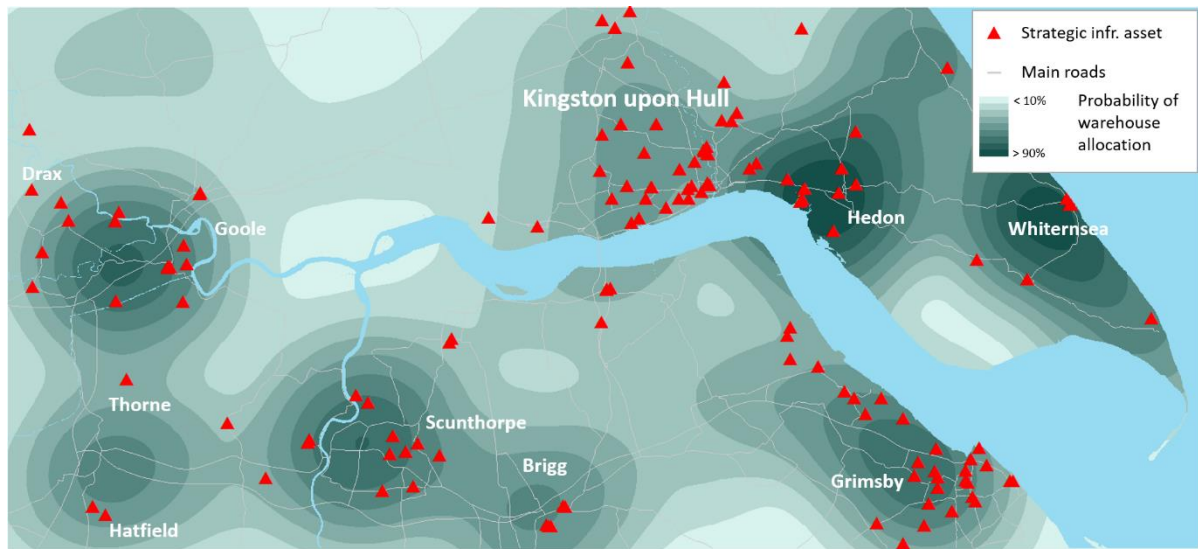


Figure 89 - Pareto front heatmap representing the probability of allocation of a warehouse by the RAO framework in all scenarios with a fully functional road network.

Regarding the spatial variability, similarly to Figure 87, Figure 89 shows a heatmap of the spatial allocation of warehouses in the Scenarios that consider a fully functional road network. With respect to Figure 87.a, which refers to a Scenario with simplifying assumptions like a uniform rent price across the region and a discrete cost function, Figure 89 presents a more spatially variable panorama. This is helpful to assess the sensitivity of the system to the parameters governing the optimisation equations: more refined cost and time functions correspond to a more detailed identification of hotspots for warehouses allocations. These hotspots are 8: Hedon, Whiternsea, Scunthorpe and Goole/Drax with allocation probabilities >70% and Kingston upon Hull, Grimsby, Brigg and Hatfield with allocation frequencies >60%. These statistics have been calculated considering all the Pareto-optimal spatial plans of each Scenario and plotted using ArcGIS Kernel Density function.

## 5.7. Summary

Chapter 5 presented a case study in the Humber Estuary. The RAO framework introduced in Chapter 4 was applied to a case study regarding emergency planning. The main objective was the optimisation of warehouse allocation for the storage of flood emergency resources. Optimally allocated storing locations allow to minimise travel times for the deployment of temporary flood defences and simultaneously minimise construction and management costs. Initially, an overview of the datasets and initial settings of the framework was presented, followed by a detailed description of the problem formulation and the adaptation of the

general optimisation methodology to this particular case study. Thirteen different scenarios were investigated to show how the same case study area can be investigated from different perspectives and taking into consideration different variables using the RAO framework. The scenarios investigated both a business as usual situation with a fully functional road network and a disrupted road network scenario.

The business as usual Scenarios investigated the normal situation in which adequate warning before the flood event is guaranteed, while the disruption scenario examined a situation in which such a warning may not be enough to deploy all the required temporary defences effectively. That could also be due to a temporary/contingent lack of available staff or insufficiency in the truck fleet necessary to transport the emergency resources into place.

Assessing 13 different scenarios with different assumptions and optimisation functions formulations demonstrates the flexibility of the approach and the adaptability of the methodology to potential different a priori knowledge of the case study or data availability. The different scenarios also constitute a sensitivity analysis of the governing parameters of the problem as explained in the previous sections (see Figure 88).

Results showed how the first scenario allows more room for different possibilities, while a reduced variability in Pareto-optimal solutions is observable in the second one due to its more constrained nature. In fact, in the disruption scenario, the disrupted road network isolated three different areas, each of which would require at least one warehouse to store the temporary defences needed for the strategic infrastructure assets present in those areas. Furthermore, as shown in Figure 89, exploring Scenarios with more complex formulations allows to draw more precise conclusions on the spatial allocation of warehouses in the Humber Estuary, also with higher confidence in the cost valuation.

The scenarios of the Humber Estuary case study represent an example of how this methodology can be applied to produce results to support planning decisions on behalf of emergency planners. Section 5.5 demonstrated how versatility and adaptability are major drivers in the design of the RAO framework by presenting different applications and solving different real-life problems (e.g. allocation of storing space for flood defences and allocation of healthcare services – Chapters 5 and 6) with the same conceptual approach.

## 6. Northland (NZ) case study

### 6.1. Introduction Chapter 6

Chapter 6 introduces the Northland (New Zealand) case study. The RAO framework introduced in Chapter 4 is applied to solve an allocation problem concerning the healthcare infrastructure of the Northland region (New Zealand). The multi-objective spatial optimisation aims to find Pareto-optimal locations for clinics (and doctors) to maximise accessibility and simultaneously optimise the ratio between doctors and patients.

Two different scenarios are investigated: one under normal conditions and another one involving a disrupted road network due to natural disasters such as floods and landslides. For both the scenarios, a Greenfield approach is adopted; this means that the results are to be intended as guidelines for future investments in this sector or the improvement of the current healthcare infrastructure in Northland.

The chapter is structured with an introduction to the case study at the beginning (section 6.2), followed by the presentation of the sources and the datasets involved (section 6.3). Section 6.4 presents the problem formulation and the details concerning the application of the methodology to this particular case study; sections 6.5 and 6.6, instead, present the results of different investigated scenarios.

Table 11 presents a summary of the key information regarding the nature of the case study.

*Table 11 - Northland case study problem definition summary table.*

Case study	Northland (NZ)
Hazard	Flooding and landslides
Objectives	<ul style="list-style-type: none"> <li>- Minimisation of travel times between households and GP clinics.</li> <li>- Minimisation of costs (i.e. number of clinics and doctors).</li> </ul>
Scenarios	<ul style="list-style-type: none"> <li>- BAU – Target ratio patients/doctors 1500</li> <li>- BAU – Target ratio patients/doctors 2500</li> <li>- Disruption – Target ratio patients/doctors 1500</li> <li>- Disruption – Target ratio patients/doctors 2500</li> <li>- Additional scenarios for sensitivity analysis: BAU – TR = 1000, 1500, 2000, 2500, 3000 and <math>\gamma_c = 2, 4, 6</math> (13 in total)</li> </ul>
Main constraints	<ul style="list-style-type: none"> <li>- Minimum and maximum number of allowed clinics</li> <li>- Minimum and maximum number of GPs according to served population</li> <li>- Clinics aggregated per village/town</li> <li>- 20 minutes driving time catchment areas</li> </ul>

## 6.2. Introduction to case study

A significant number of countries worldwide face (or are predicted to face in the near future) a shortage of general practitioners (GP). In rural areas, this problem is particularly hard to tackle due to a series of factors like wider areas to cover (because of low population densities) and low attractiveness for doctors (in terms of profit and/or lifestyle). Solving this problem means to balance a trade-off between conflicting objectives, since on one side patients need accessible healthcare facilities, but, on the other hand, GPs need a sufficient number of patients for their activity to be remunerative. The nature of rural areas exacerbates the conflict between these two objectives: population densities are typically low and that implies either a small number of patients or high travel times.

The multi-objective RAO framework presented in Chapter 4 is here applied to the region of Northland (New Zealand). Northland constitutes the northern part of the North Island of New Zealand (Figure 90). Its population is around 150.000 inhabitants, and its capital is Whangarei.

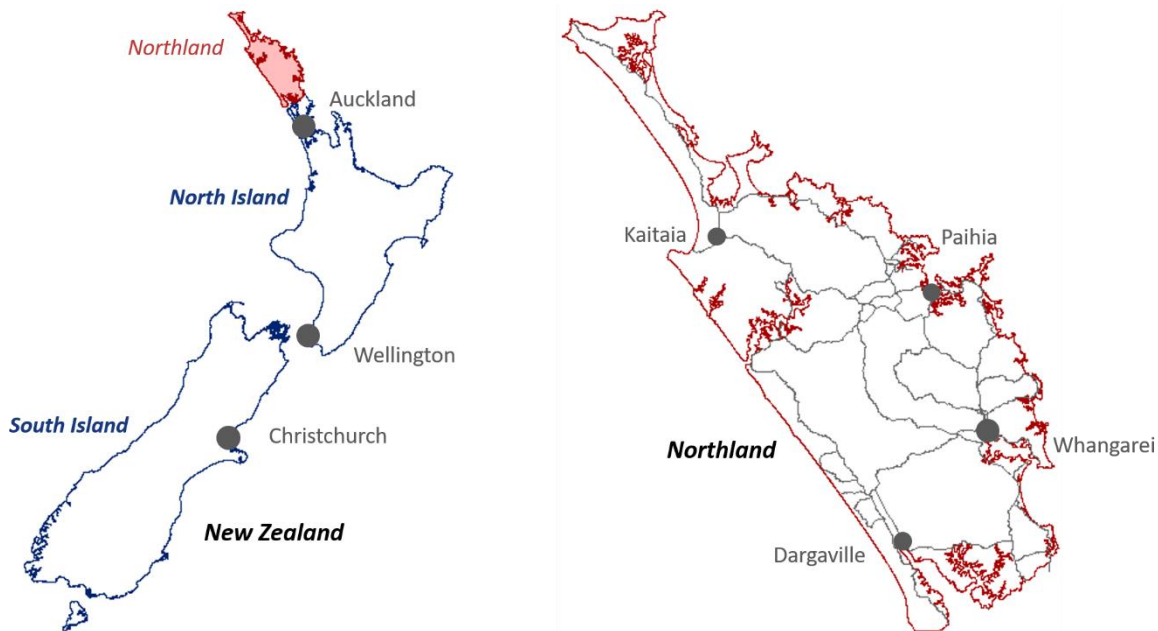


Figure 90 - New Zealand and Northland maps.

Before the application of the RAO framework, an analysis of the current situation of Northland GP practices system is performed to produce a baseline against which to measure any potential improvement provided by the RAO framework results. Figure 91 and Table 12 show the results of this analysis: currently, there are 31 clinics with 90 doctors practising in the area.

Different locations have different levels of service with considerable discrepancies in terms of the average number of patients per doctor and different (average) travel times to reach the closest clinic.

Attribution of patients to clinics has been performed on a distance basis: in the absence of more detailed information - and due to the rural nature of the region - it has been assumed that the average patient would go to the closest clinic to access primary healthcare services.

*Table 12 - Result of the preliminary analysis of primary healthcare accessibility in Northland.*

Location ID	Town	N. of clinics	FTE GPs	N. of patients	Av. Patients per GP	Av. Travel time	Travel time 75° quantile	Travel time 95° quantile	Max. Travel time
01	Te Kao	1	0.50	1437	2874	17'	21'	29'	41'
02	Kaitaia	2	5.25	11742	2237	13'	16'	39'	65'
03	Mangonui	1	2.00	3969	1985	11'	17'	31'	34'
04	Kaero	1	2.00	3531	1766	16'	23'	30'	31'
05	Kerikeri	2	6.75	10737	1591	9'	10'	16'	27'
06	Okaihau	1	2.25	3927	1745	28'	40'	77'	88'
07	Kaikohe	1	2.25	9660	4293	18'	31'	46'	55'
08	Moerewa	1	4.00	2826	707	7'	10'	21'	36'
09	Kawakawa	2	3.00	3345	1115	10'	17'	23'	31'
10	Paihia	2	3.50	3804	1087	8'	12'	16'	27'
11	Russell	1	2.00	1767	884	11'	19'	29'	30'
12	Dargaville	1	13.00	11262	866	17'	25'	41'	53'
13	Ngunguru	1	2.50	2664	1066	8'	9'	15'	43'
14	Waipu	1	2.00	15120	7560	19'	25'	32'	46'
15	Whangarei	13	39.00	65847	1688	9'	12'	29'	42'

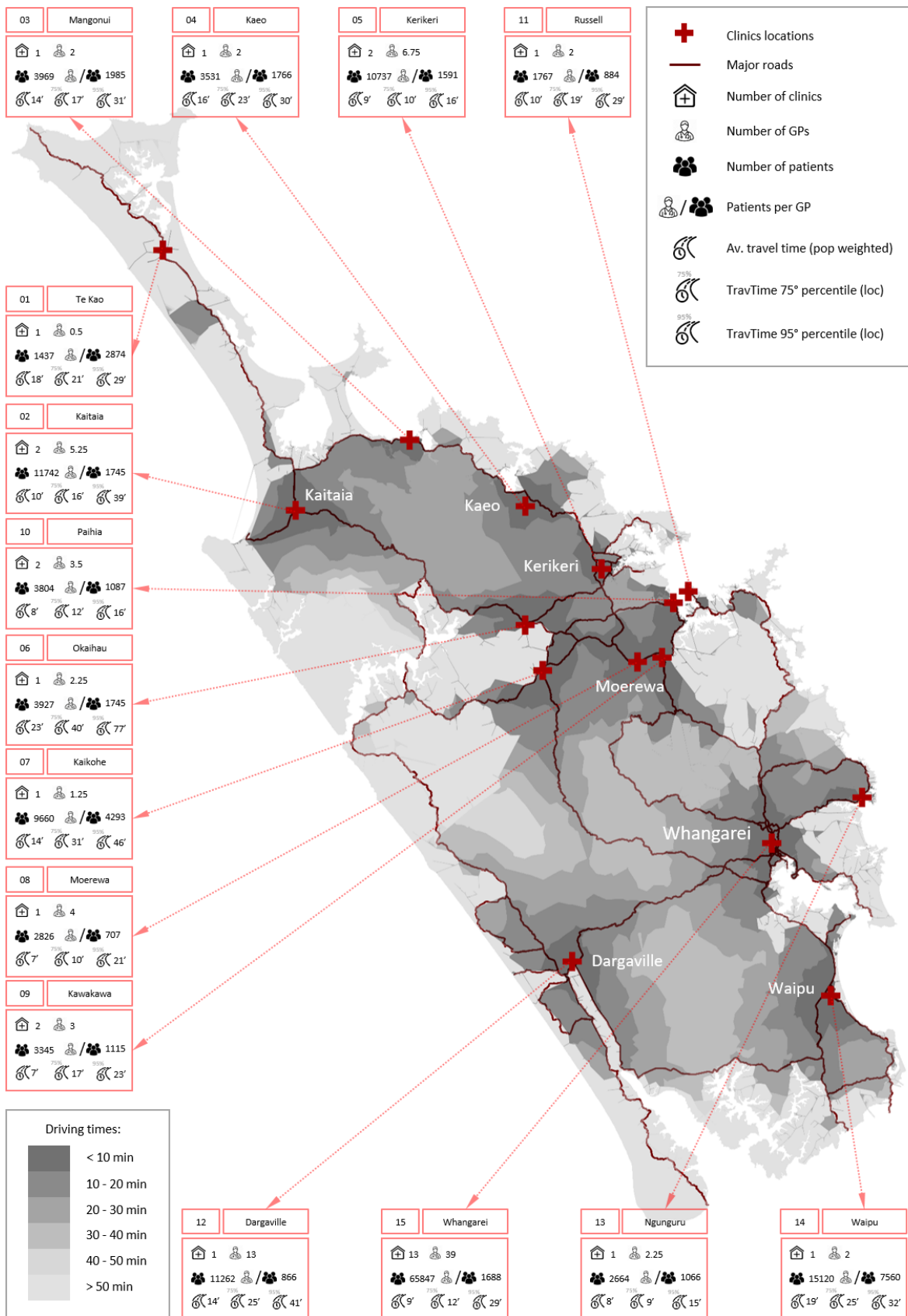


Figure 91 - Current distribution of clinics and general practitioners in Northland.



Based on this preliminary analysis, and with the perspective of a future shortage of doctors in the region, the RAO framework has been applied in a Greenfield approach to investigate Pareto-optimal distributions (spatial plans) of clinics and GPs. The results are meant to be guidelines to support future decisions, investment and/or policies in terms of allocation of clinics and doctors in the region.

### 6.3. Data

The source of the georeferenced data used in the Northland case study is the Land Information New Zealand (LINZ) service available at [data.linz.govt.nz](http://data.linz.govt.nz). Among all the available information of the open dataset, the ones of interest are the road network and the meshblock dataset. Meshblocks constitute the smallest census geographic unit produced by Statistics New Zealand (NZ Government department for statistics related to the economy, population and society). Meshblocks vary in size (from city blocks to large rural areas) and population (varying from around 60 people in rural areas to an average of 110 in urban areas) and can be aggregated to form larger units like area units, urban areas, territorial authorities and regional councils.

The road network is used to calculate distances and travel times in the optimisation process; the meshblock dataset is used as origins in the travel time evaluation while the available locations for clinics represent the destinations.

Regarding available locations for clinics, all the towns/villages (37 in total) of the region are considered to be potential locations for clinics and doctors. Although rural sites may represent efficient locations from an accessibility point of view, they are not considered as potential available locations because of the remoteness of rural Northland. This region presents vast wild areas, very different from rural Europe (to make a comparison with the Humber Estuary case study presented in Chapter 5); a GP clinic outside a town or a village in this region would not represent a realistic assumption. Figure 92 shows all the available locations for clinics and all the meshblock centroids. Every meshblock centroid has a population assigned (census data), and distances from meshblock centroids to available locations are measured as travel times on the road network. In the optimisation process, these data are combined when assessing the performance of spatial plans: i.e. travel times from origins and destinations are

weighted with the served population in order to prioritise shorter distances serving a higher population (consequently penalising higher distances serving a lower population).

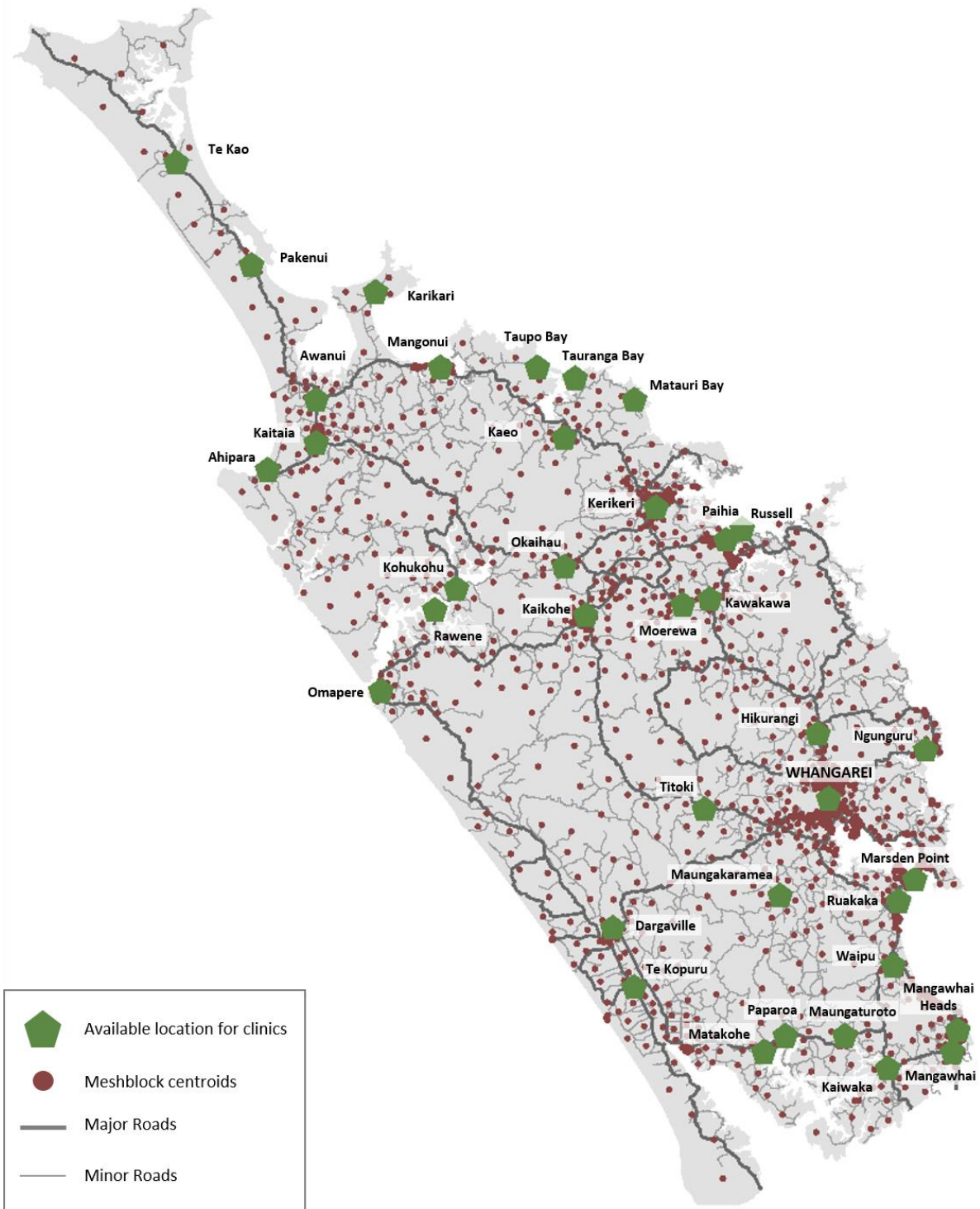


Figure 92 - Available locations for clinics and meshblock centroids in Northland.

Table 13 - Input data for the Northland case study.

Input data	Format	Source
Road network edges	Line shapefile	LINZ
Road network nodes	Point shapefile	LINZ
Meshblocks	Polygon shapefile	Stats NZ
Available locations for GP clinics	Point shapefile	Original
GP clinics	Point shapefile	Healthpoint.co.nz
FTE general practitioners	csv	Healthpoint.co.nz
Road network risk areas	Point shapefile	Northland Regional Council

#### 6.4. RAO applied to Northland case study

The RAO framework described in Chapter 4 is applied to the Northland case study introduced in chapter 6.2 to produce Pareto-optimal spatial plans of clinics and doctors practising in this region.

##### 6.4.1. Input phase

Referring to the several phases of the framework described in Figure 8 (Section 4.2), the RAO initially takes a series of datasets as input and on the base of such datasets defines available locations for clinics and doctors. The variable “Lookup” is then created, containing the coordinates of all available locations. Saving the coordinates in a lookup list rather than keeping a raster/vector format is a standard procedure meant to reduce run time (see Chapter 4 for more details).

##### 6.4.2. Problem formulation

In this phase, the user can set lower and upper bounds to the number of clinics that can be taken into consideration in the solutions. The term “clinic” is used hereafter to indicate “locations for clinics”, meaning that the number of clinics at each location is not prescribed like the number of GPs is. As an example, if in a single location 30 doctors are allocated, that does not mean that they are practising in the same clinic. Given the rural nature of the area though, with the only exception of Whangarei and a few other towns, one clinic per town is

generally enough to accommodate the number of doctors generally allocated - hence the adopted terminology.

Regarding the range of considered locations, a minimum of 5 and a maximum of 25 clinics have been explored in the results presented in the following paragraphs. The upper bound of 25 clinics is chosen because it corresponds to almost one clinic in each available location; choosing to cut off the extremes (i.e. less than 5 and more than 25 clinics) is a procedure meant to speed up the run time excluding “extreme” solutions we would not be interested in anyway. This is an input parameter that can be modified by the end-user according to different necessities. However, for lower numbers and limited ranges (low variability), the RAO can produce Pareto-optimal solutions, but the problem is sufficiently tractable to be solvable using simpler methods; for more details about solutions variability and approach efficiency see chapter 5.4.2.

In this phase, the user must define another fundamental parameter: the target ratio (TR) patients/doctors and the accepted level of variability around such target ratio. This parameter defines how many patients should ideally be assigned to every doctor. This ratio should represent a good balance between a trade-off defined as the following: on one side, a GP would aspire to have as many patients as possible to have a profitable activity; on the other hand, too many patients would imply long waiting lists with a consequential worsening of the provided service.

Finally, the user must define an acceptable level of variability around the target ratio: this implies the definition of two thresholds (upper bound and lower bound) below or beyond which spatial plans are not considered. This procedure is implemented both in the initialisation and constraint phase and it is meant to speed up the evolutionary process. Different factors for upper and lower bounds are applied to define the minimum and maximum allowed number of doctors for each clinic and the minimum and maximum number of doctors in the entire region.

#### 6.4.3. Initialisation

The initialisation module is used at the beginning of the iterative process to generate the first generation of solutions. Spatial plans are randomly generated selecting locations from the

Lookup variable (containing available locations for clinics), with a number of clinics within the allowed range and with a number of doctors assigned to each clinic within the defined variability around the target ratio doctors/patients.

The allowed range for the number of doctors assigned to each clinic is the result of a pre-processing of the input data. For every available location, the living population within a 20 minutes radius has been calculated and, according to the defined target ratio, an ideal number of doctors has been assigned. Then, a variability range is applied to this number. The user can set the variability range by the definition of two factors: a lower bound and an upper bound. For the results presented in the following chapters, the lower bound has been chosen as 75% of the ideal number of doctors and the upper bound as 125%.

#### 6.4.4. Evaluation

After the creation of the initial population, individuals (spatial plans) are evaluated against the objective functions, then the evolutionary operators are applied and the following generation is created. The procedure is repeated again in the iterative process: at every stage, the individuals of each generation are evaluated and assigned fitness values for each objective function.

The objective functions are two: 1) a distance function:  $f_{dist}$  and 2) a cost function:  $f_{cost}$ .

##### *Distance function*

The distance function attributes a distance fitness to each spatial plan. This fitness is minimised in the optimisation process. The fitness is a measure of the performance of the spatial plan with regards to a particular function. In this study, distance is evaluated as travel time on the road network.

The distance function is defined as a weighted average of travel times between meshblock centroids and the closest clinic, where the number of the population living in each meshblock represents the weight of the function. The formulation is the following:

$$f_{dist} = \frac{\sum_{i=1}^M TT_i \cdot p_i}{p_{TOT}} \quad (6.1)$$

Where:

- $i$  = single meshblock,
- $M$  = total number of meshblocks,
- $TT_i$  = travel time from  $i$ -th meshblock to closest clinic,
- $p_i$  = population living in the  $i$ -th meshblock,
- $p_{TOT}$  = total population of the case study area.

### Cost function

The cost function attributes a cost fitness ( $f_{cost}$ ) to each spatial plan. Similarly to the distance function, this fitness is minimised in the optimisation process. This function measures the cost of each spatial plan intended as a weighted sum of the number of clinics and doctors. In the minimisation process, plans with high numbers of clinics and doctors are penalised. The formulation is the following:

$$f_{cost} = \gamma_C \cdot n_C + \gamma_{GP} \cdot n_{GP} \quad (6.2)$$

Where:

- $\gamma_C$  = weighting factor for clinics,
- $n_C$  = number of clinics in the spatial plan.
- $\gamma_{GP}$  = weighting factor for GPs,
- $n_{GP}$  = number of GPs in the entire spatial plan.

The weighting factors have been assumed equal to 1 for GPs and 4 for clinics. This assumption implies that the allocation of a new clinic will not be cost-effective for less than four doctors; the algorithm, instead, will privilege solutions with allocations of extra doctors to close by clinics. This means that, for example, for target ratios patients/doctors equal to 1500, the allocation of a new clinic will not be cost-efficient for less than 6000 patients. Nevertheless, clinics with less than four doctors will be present in the Pareto-optimal solution as in remote areas having only clinics with many practitioners would imply too long travel times (the distance function mitigates this).

The value of  $\gamma_C = 4$  was chosen taking as a reference the medium size of New Zealand GP practices (Goodyear-Smith and Janes, 2008; Leitch *et al.*, 2018), which is comparable with the average dimension of UK practices (Kelly and Stoye, 2014) and small-sized US practices (Casalino *et al.*, 2003). However, other values of  $\gamma_C$  have been explored in the sensitivity

analysis presented in section 6.6, as  $\gamma_C$  is one of the governing parameters of the optimisation problem and its choice can actually be considered a policy scenario by itself. The additional values of  $\gamma_C$  that have been considered are  $\gamma_C = 2$  and  $\gamma_C = 6$ , in combination with the variation of the other main parameter of the optimisation formulation: the target ratio patients/doctors, whose additional explored values are  $TR = 1000, 1500, 2000, 2500, 3000$ .

#### 6.4.5. Constraints

As explained in chapter 5.4.5, the aim of the presented methodology is to leave the algorithm the most unconstrained as possible (to allow it to explore the whole space of solutions), yet the implementation of some constraints can be beneficial to reduce the computational effort.

Due to the nature of the evolutionary operators meant to modify solutions' spatial attributes (see Chapter 4), when mating and mutating individuals, it is possible to generate solutions that have a number of assigned GPs that is higher than the maximum allowed or lower than the minimum.

This is why a constraint decorator is applied to the evolutionary operators' functions: it counts the number of GPs present in the solutions after the application of the evolutionary operators and it discards those spatial plans that have less than the minimum or more than the maximum allowed number of GP sites.

The constraint functions are two: one for counting the total number of doctors in the whole case study region and another one to check if the number of doctors assigned to each clinic is within the acceptable range.

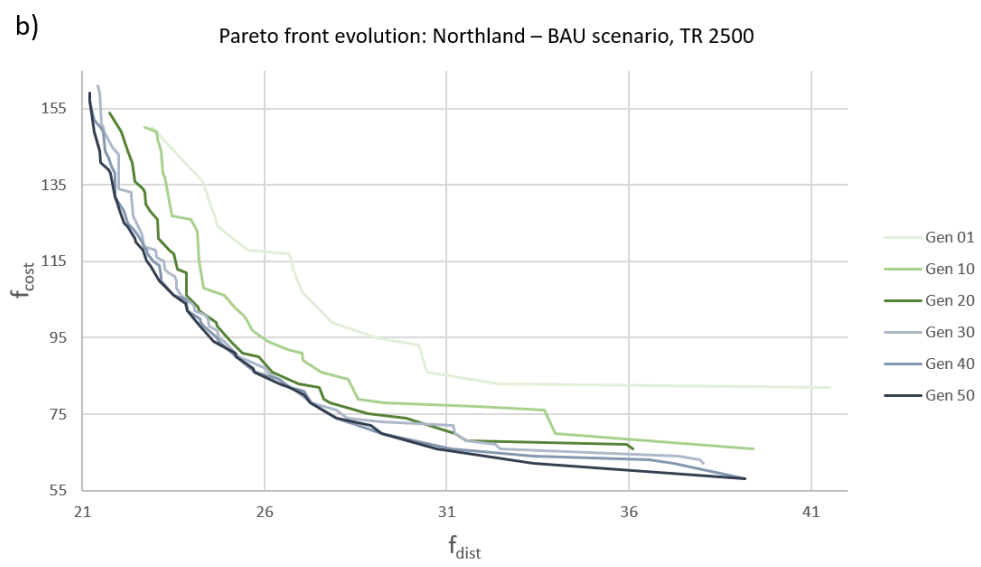
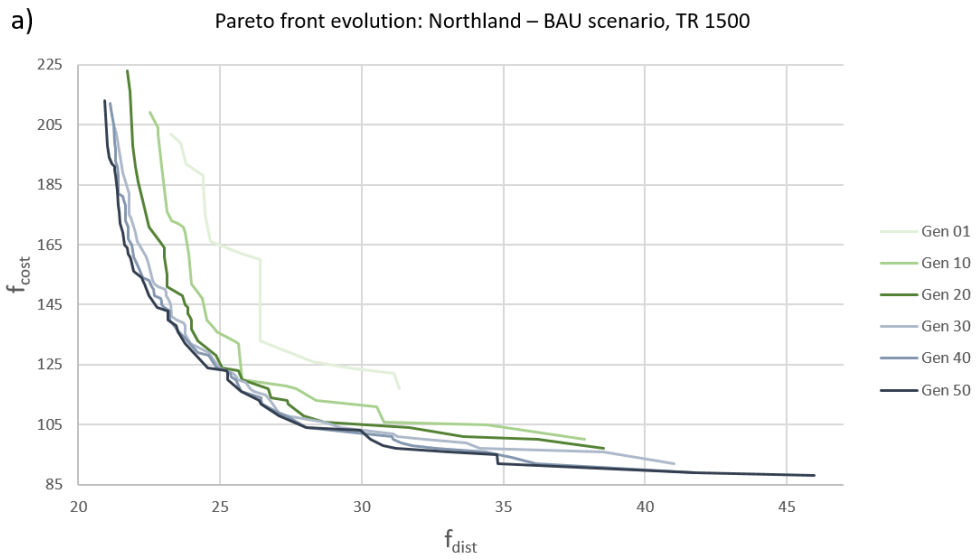
As in the case of the Humber Estuary case study (see section 5.4.5), several implicit constraints are present; these constraints are due to both the initialisation phase and the nature of spatial input data. The definition of available locations for clinics and doctors (section 6.3) constitutes a spatial constraint regarding the location of potential solutions. Also, as in the UK case study, another implicit constraint is represented by the evaluation of travel times. They are evaluated in a best-case scenario since the traffic variable is not taken into account. Average allowed speeds are deduced from road types. Based on this assumption, free-flow speeds are evaluated for each edge of the road network and travel times are consequently calculated.

Finally, the weighting factors of the cost function defined in the previous section are also a priori determined. This parameter is somewhat arbitrary and, in fact, it constitutes a medical policy scenario. For this reason, it is treated as the target ratio patients/doctors: it is an input variable of the framework, and different values can be explored according to the user's needs/purposes.

#### 6.4.6. GA applied to the Northland case study

As anticipated in Chapter 4.4, and exactly like in the Humber Estuary case study (see chapter 5.4.6), the genetic algorithm chosen for the evolution of spatial plans is DEAP's  $\mu + \lambda$  strategy (Fortin *et al.*, 2012). Referring to DEAP Documentation (DEAP Project, 2009), the *eaMuPlusLambda* function evolves a population of spatial plans and returns the optimised population together with a Logbook containing the statistics of the evolution process.





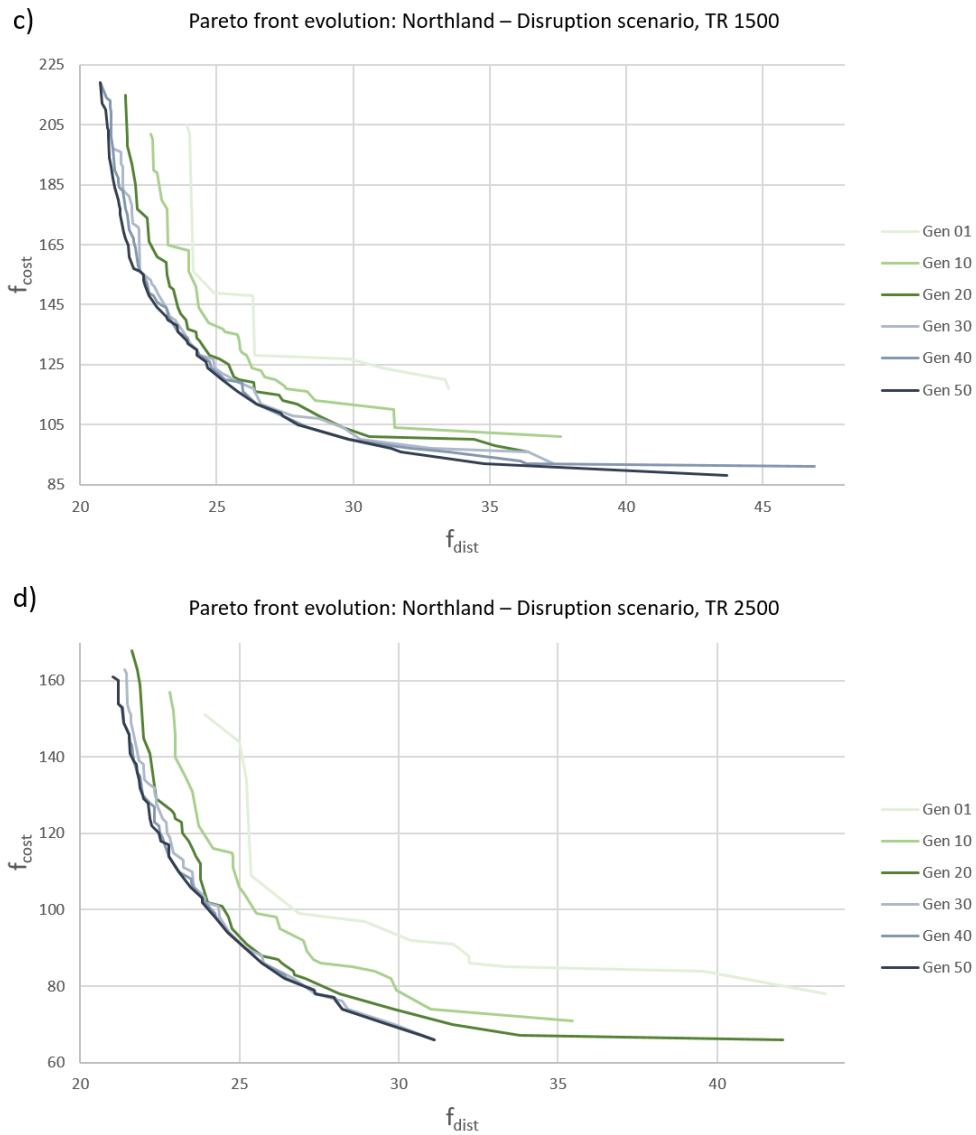


Figure 93 - Pareto fronts evolution of the Northland case study: a) Business as usual scenario, target ratio patients/GPs 1500; b) Business as usual scenario, target ratio 2500; c) Disruption scenario, target ratio 1500; d) Disruption scenario, target ratio 2500.

The framework architecture is the same as the previous case study and the same notation is adopted (refer to Chapters 0 and 5 for details and specifics related to the application of the  $\mu + \lambda$  strategy). For this case study, the value of lambda is chosen to be 1000. That means that 1000 solutions are created at each generation. With this amount of generated children at each step of the iterative process, 50 generations (*ngen*) are enough to observe convergence in the Pareto-front, as shown in Figure 93.

## 6.5. Results

Two different scenarios are investigated:

- 1) a business as usual (BAU) scenario, with a completely functional road network;
- 2) a disruption scenario, where the road network is partially disrupted due to potential natural disasters.

To understand the most critical sections of the road network, reference is made to the Regional Land Transport Plan 2015-2021 (Northland Regional Council, 2018), where “Major Risk Areas in Northland” are identified and mapped (Figure 94). Table 14 summarises the reasons why road sections are identified as critical in Northland’s Regional Land Transport Plan.

*Table 14 - Risks on critical road sections in Northland.*

Road number	Road section	Risk
-	Brynderwyn Hill	No easy alternative routes
-	Te Hana Bridges	No easy alternative routes
SH1	North Cape Road at Mitimiti Stream Bridge	Flooding and landslips
	Waihou River (Rangiahua) Bridge	
	Mangamuka	
	Lemons Hill	
	North Larmers Rd	
	Kamo bypass	
	Otiria Stream (Moerewa)	
	Whakapara	
	Otonga Flats	
	Waipu to Whangarei	
	Kawakawa	
SH10	Bulls Gorge	Flooding and landslips
	Kaeo	
	Kaingaroa Bridge	
SH11	Tirohanga Stream Bridge	Flooding
	Kawakawa	
SH12	through Dargaville	Flooding and landslips
	Mangatoa	
SH14	Kirikopuni River Bridge	Flooding
-	Paparoa – Oakleigh	Landslips



Figure 94 - Major risk areas in Northland. Map developed from Northland Regional Council (2018).

### 6.5.1. Business as usual (BAU) scenario

Business as usual (BAU) scenario investigates the typical situation with a completely functional road network. It is meant to explore Pareto-optimal clinics and doctors spatial plans with a Greenfield approach: the current distribution of clinics and practitioners is neglected in the spirit of finding ideal solutions and critically comparing them with the current situation and future plans.

Like in the UK case study presented in chapter 5, the outputs of the RAO framework are in the form of Pareto-fronts plotted in the solution space and georeferenced spatial plans displayable in a GIS environment.

Two different target ratios between patients and GPs are investigated: 1500 and 2500 (i.e. 1500 patients per GP and 2500 patients per GP), resulting in a reasonable average patient number per GP in rural New Zealand to guarantee profit for the clinic and simultaneously avoid overcrowding (Goodyear-Smith and Janes, 2008).

The methodology is easily adaptable to inspect different ratios between patients and doctors according to the user's needs (by changing a single input variable). In other words, different motivations could drive the final user of the RAO framework: this tool can be used to make the most out of some available resources (i.e. doctors and clinics) or, on the other hand, use the optimisation framework to support future investments aimed at the improvement of the current health infrastructure.

#### 6.5.1.1. BAU scenario – Target ratio patients/GPs: 1500

Figure 95 shows the plot of the solutions inspected by the algorithm in the solution space defined by the two objective functions. On the x-axis,  $f_{dist}$  represents the average travel times weighted by the served population of each clinic. On the y-axis,  $f_{cost}$  represents the weighted sum of clinics and doctors (for more details on the objective functions, see section 6.4.4).

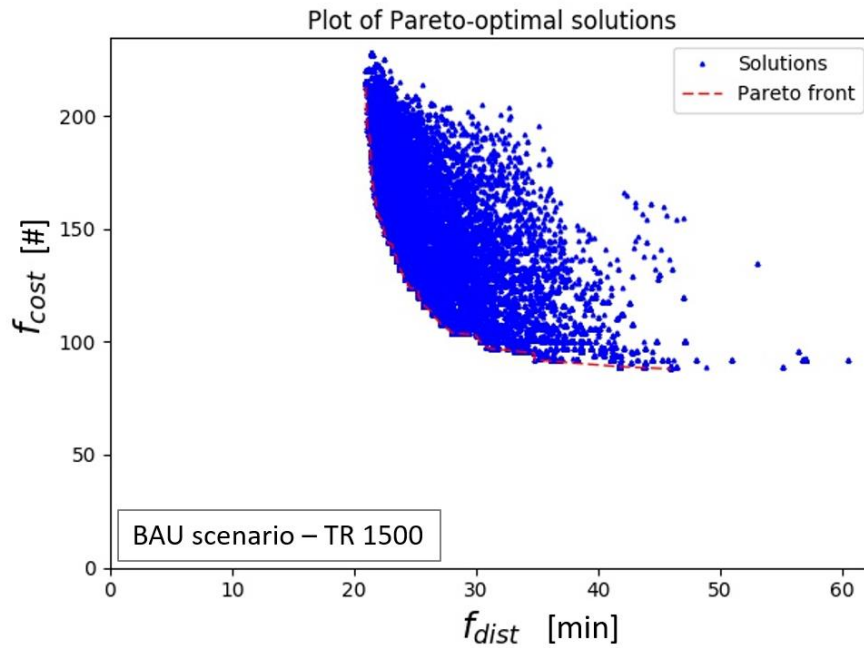


Figure 95 - Solution space and Pareto-front for Northland case study. BAU scenario, target ratio 1500.

Every blue triangle of Figure 95 represents a solution inspected by the GA, the dashed red line, instead, connects the Pareto-optimal solutions, i.e. the ones that are non-dominated by all the others. “Domination” is the concept on which Pareto-optimality is based on: a solution is not dominated if it is not worse than all the others in all the objectives and it is strictly better in at least one. The non-dominated solutions form the Pareto-front.

As observed in chapter 5.5.1, a first analysis of the results consists in understanding the area of interest of the solution space. A time and a cost threshold can be set in a preliminary qualitative analysis of the Pareto-front. As shown in Figure 96, beyond the time threshold, we have an increase in travel times without a significant decreasing of the cost fitness and vice versa beyond the cost threshold.

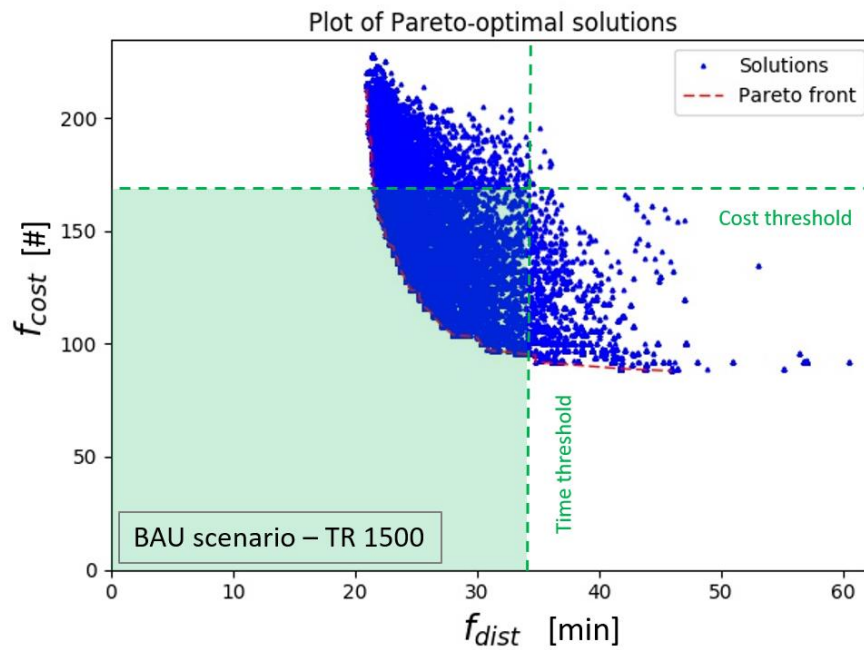


Figure 96 - Thresholds in the solution space for Northland case study. BAU scenario, target ratio 1500.

The green area of Figure 96 represents the area of interest of our results; from this area, the solutions plotted in the remaining part of this section are selected and identified in Figure 97. For clarity and readability, not all the spatial plans forming the Pareto-front are going to be plotted. Only a selection of them, covering different areas of the Pareto-front are showed and analysed:

- Solution A (Figure 98 and Table 15) from the top-left side of the Pareto-front (lower travel times, but a high number of clinics and doctors);
- Solution B (Figure 99 and Table 16) from the bottom-right side (lower costs, but higher travel times).

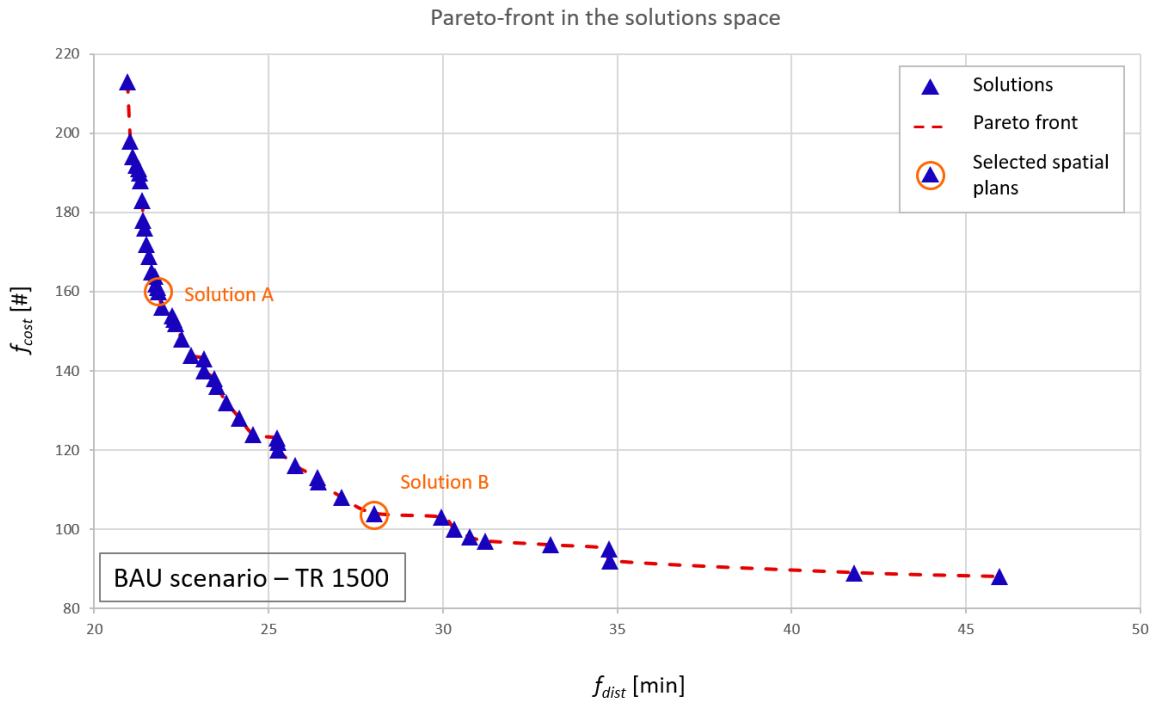


Figure 97 - Highlight of the Pareto-front for the Northland BAU scenario (target ratio 1500) with the indication of the number of Pareto-optimal spatial plans. Solutions A and B are visualised in Figure 98, Figure 99, Table 15 and Table 16.



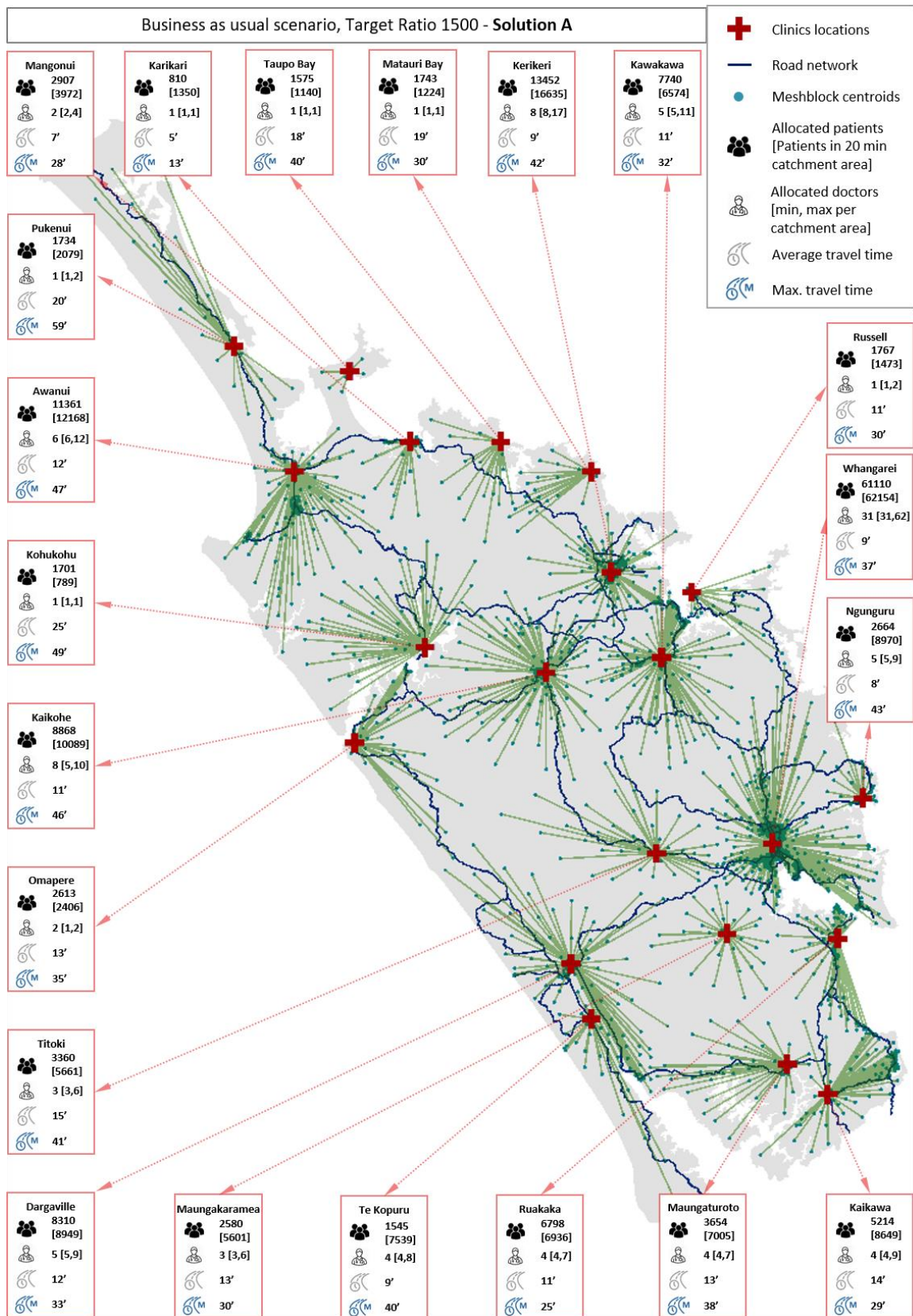


Figure 98 - Northland Case study, BAU scenario, Target ratio patients/GPs: 1500, Solution A (from Figure 97). The green lines are for visualisation purposes: they connect each meshblock centroid to the closest GP clinic. They do not represent distances, as distances are measured as travel times on the shortest path on the road network.

Table 15 - Northland case study, BAU scenario, target ratio patients/GPs: 1500, solution A (from Figure 97). Accessibility table.

Town	FTE GPs	N. of patients	Av. Patients per GP	Av. Travel time	Max. Travel time
Kaiwaka	4	5214	1304	14'	29'
Maungaturoto	4	3654	914	13'	38'
Te Kopuru	4	1545	386	9'	40'
Dargaville	5	8310	1662	12'	33'
Ruakaka	4	6798	1700	11'	25'
Maungakaramea	3	2580	860	13'	30'
Titoki	3	3360	1120	15'	41'
Whangarei	31	61110	1971	9'	37'
Ngunguru	5	2664	533	8'	43'
Omapere	2	2613	1307	13'	35'
Kaikohe	8	8868	1109	11'	46'
Kawakawa	5	7740	1548	11'	32'
Kohukohu	1	1701	1701	25'	49'
Russell	1	1767	1767	11'	30'
Kerikeri	8	13452	1682	9'	42'
Awanui	6	11361	1894	20'	59'
Matauri Bay	1	1743	1743	19'	30'
Mangonui	2	2907	1454	7'	28'
Taupo Bay	1	1575	1575	18'	40'
Karikari	1	810	810	5'	13'
Pukenui	1	1734	1734	20'	59'

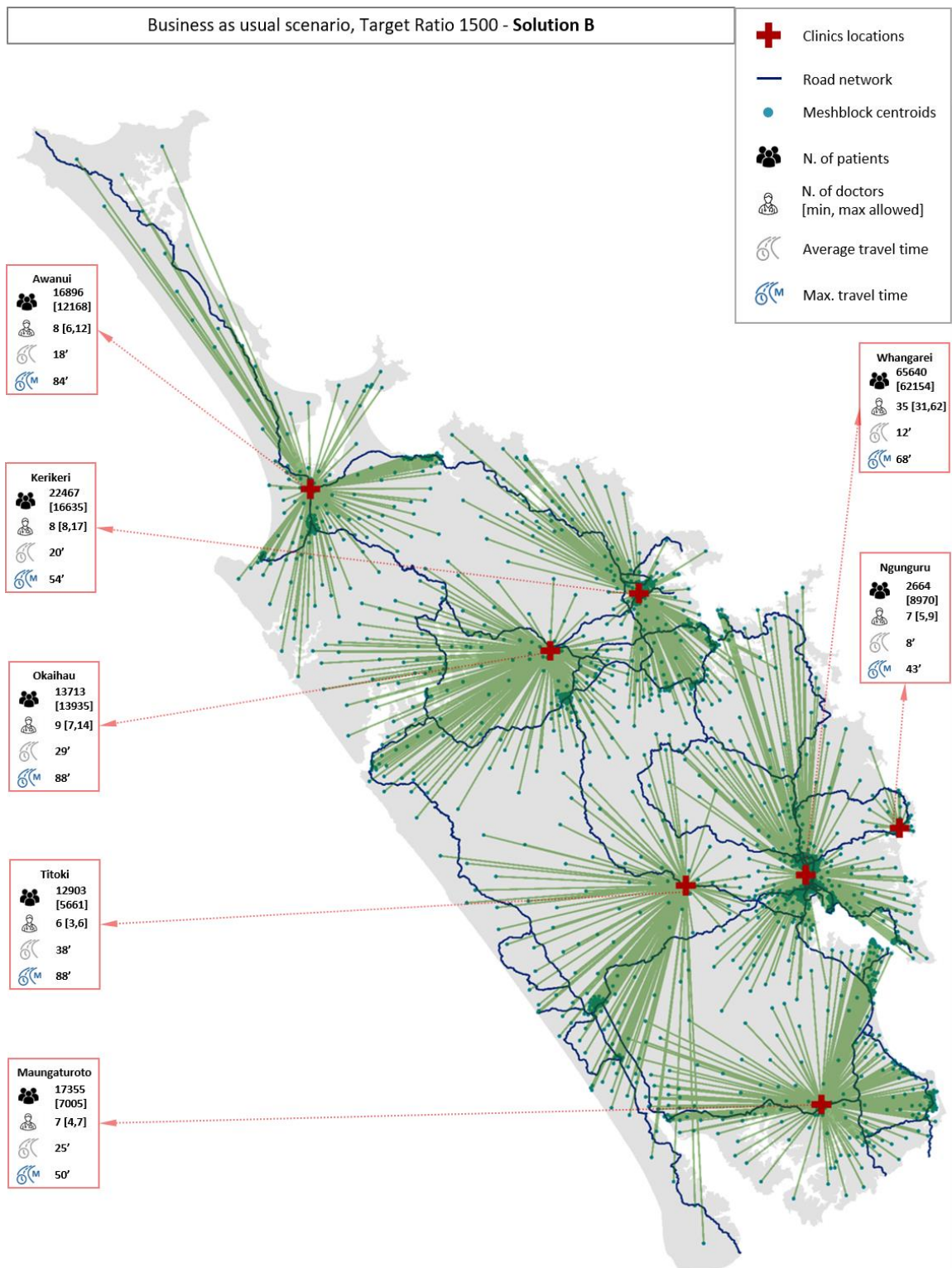


Figure 99 - Northland Case study, BAU scenario, Target ratio patients/GPs: 1500, Solution B (from Figure 97). The green lines are for visualisation purposes: they connect each meshblock centroid to the closest GP clinic. They do not represent distances, as distances are measured as travel times on the shortest path on the road network.

Table 16 - Northland case study, BAU scenario, target ratio patients/GPs: 1500, solution B (from Figure 97). Accessibility table.

Town	FTE GPs	N. of patients	Av. Patients per GP	Av. Travel time	Max. Travel time
Maungaturoto	7	17355	2479	25'	50'
Titoki	6	12903	2151	38'	88'
Whangarei	35	65640	1875	12'	68'
Ngunguru	7	2664	381	8'	43'
Okaihau	9	13713	1524	29'	88'
Kerikeri	8	22467	2808	20'	54'
Awanui	8	16896	2112	18'	84'

### 6.5.1.2. BAU scenario – Target ratio patients/GPs: 2500

The same methodology with the same parameters of section 6.5.1.1 is applied one more time, with the only difference of the input datum “target ratio patients/GPs”. In this run, the ratio is 2500 (for more details see 6.5.1). As shown in the previous section, in Figure 100, the solutions inspected by the algorithm are plotted in the solution space defined by the two objective functions (x-axis:  $f_{dist}$  - average travel times weighted by the served population of each clinic; y-axis:  $f_{cost}$  - weighted sum of number of clinics and doctors).

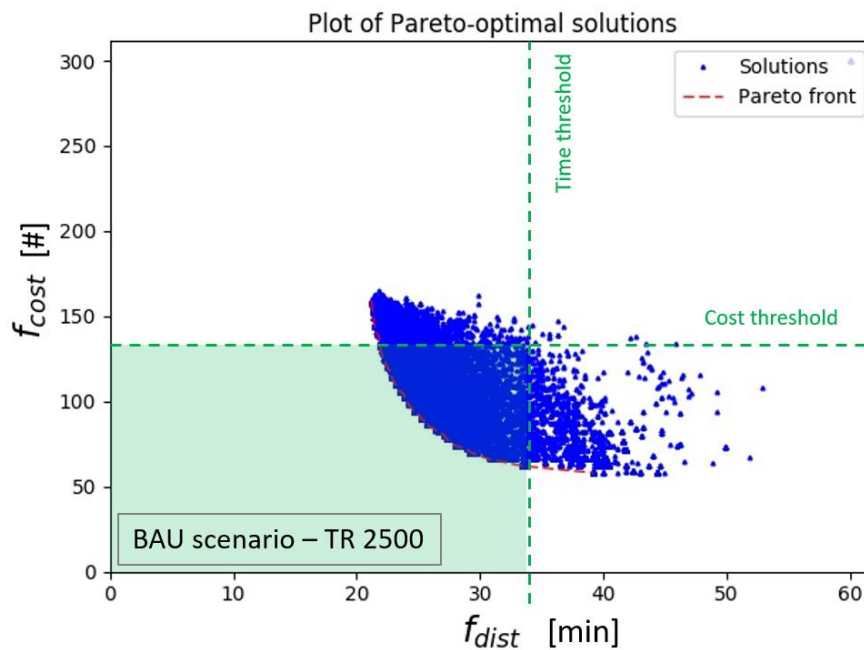


Figure 100 - Solution space and Pareto-front for Northland case study. BAU scenario, target ratio 2500.

Figure 100 represents all the solutions inspected by the GA (blue triangles), and the dashed red line is the Pareto-front, where Pareto-optimal solutions lie. The green lines represent a time and a cost threshold (see previous sections for thresholds definitions) beyond which there is a worsening of one objective without a significant improvement of the other. This is a preliminary qualitative analysis aimed at understanding the area of interest of the Pareto-front.

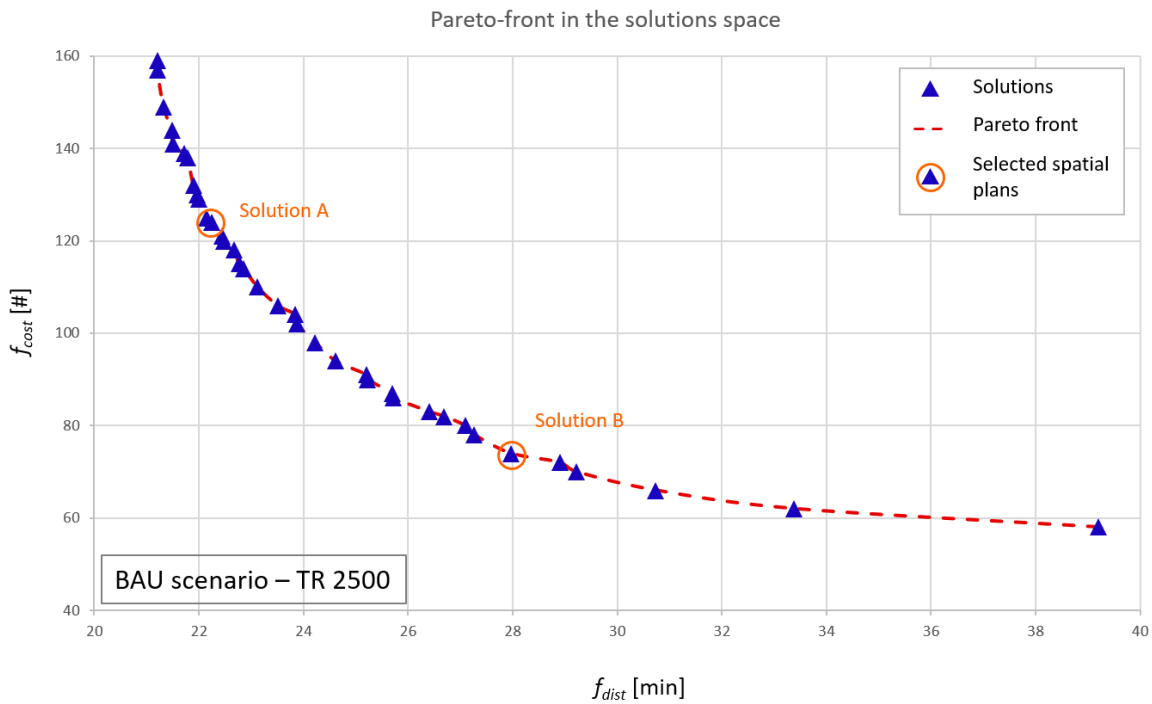


Figure 101 - Highlight of the Pareto-front for the Northland BAU scenario (target ratio 2500) with the indication of the number of Pareto-optimal spatial plans. Solution A and B are visualised in Figure 102, Figure 103, Table 17 and Table 18.

The green area of Figure 100 represents the area of interest of our results, from the same area, two spatial plans are selected (Figure 101) and plotted in the remaining part of this section. For clarity and readability, not all the spatial plans forming the Pareto-front are plotted. Only a selection of them, covering different areas of the Pareto-front are showed and analysed:

- Solution A (Figure 102 and Table 17) from the top-left side of the Pareto-front (lower travel times, but higher cost);
- Solution B (Figure 103 and Table 18) from the bottom-right side (lower cost, but higher travel times).

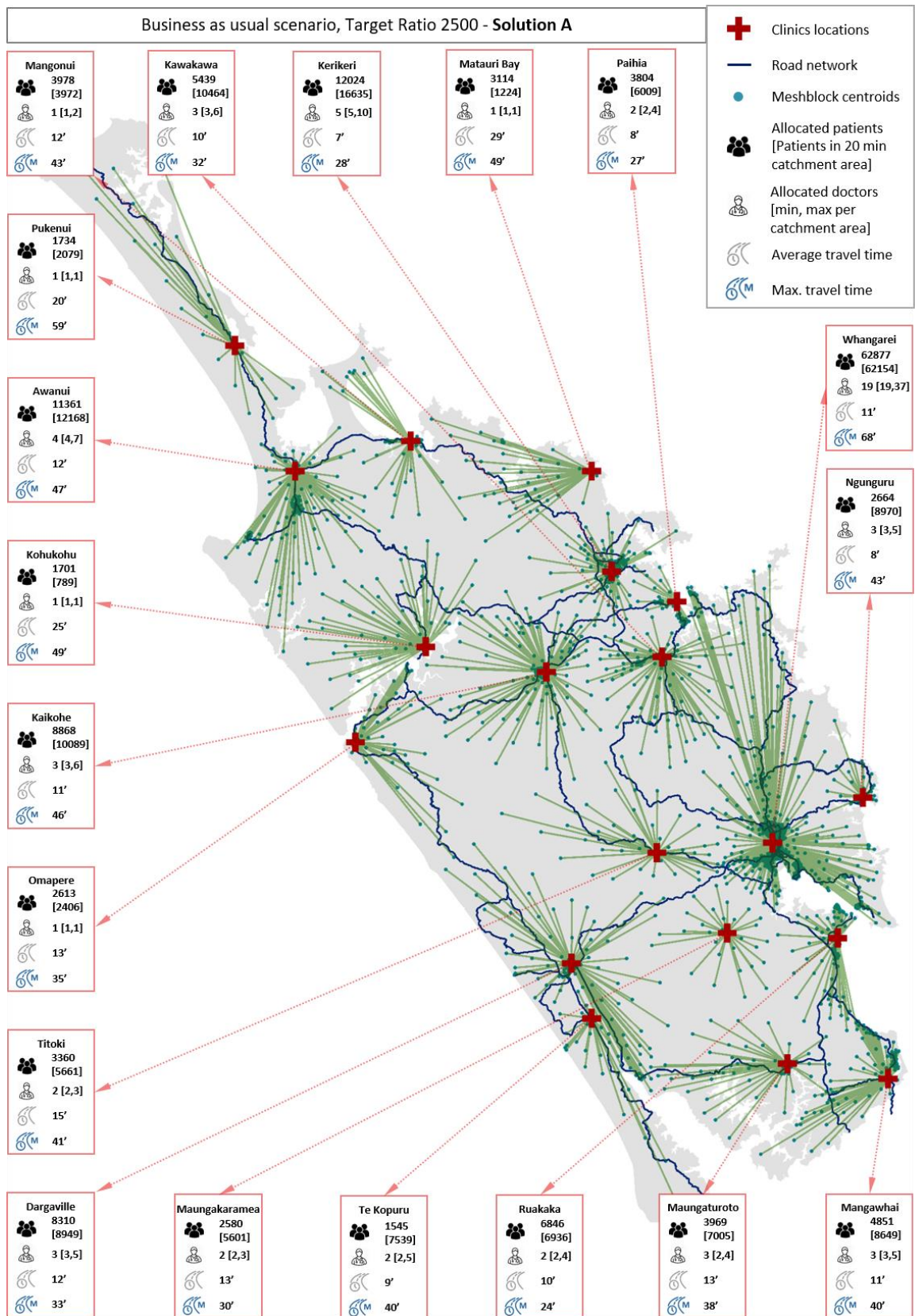


Figure 102 - Northland Case study, BAU scenario, Target ratio patients/GPs: 2500, Solution A (from Figure 101). The green lines are for visualisation purposes: they connect each meshblock centroid to the closest GP clinic. They do not represent distances, as distances are measured as travel times on the shortest path on the road network.

Table 17 - Northland case study, BAU scenario, target ratio patients/GPs: 2500, solution A (from Figure 101). Accessibility table.

Town	FTE GPs	N. of patients	Av. Patients per GP	Av. Travel time	Max. Travel time
Mangawhai	3	4851	1617	11'	40'
Maungaturoto	3	3969	1323	13'	38'
Te Kopuru	2	1545	773	9'	40'
Dargaville	3	8310	2770	12'	33'
Ruakaka	2	6846	3423	10'	24'
Maungakaramea	2	2580	1290	13'	30'
Titoki	2	3360	1680	15'	41'
Whangarei	19	62877	3309	11'	68'
Ngunguru	3	2664	888	8'	43'
Omapere	1	2613	2613	13'	35'
Kaikohe	3	8868	2956	11'	46'
Kawakawa	3	5439	1813	10'	32'
Kohukohu	1	1701	1701	25'	49'
Paihia	2	3804	1902	8'	27'
Kerikeri	5	12024	2405	7'	28'
Awanui	4	11361	2840	12'	47'
Matauri Bay	1	3114	3114	29'	49'
Mangonui	1	3978	3978	12'	43'
Pukenui	1	1734	1734	20'	59'



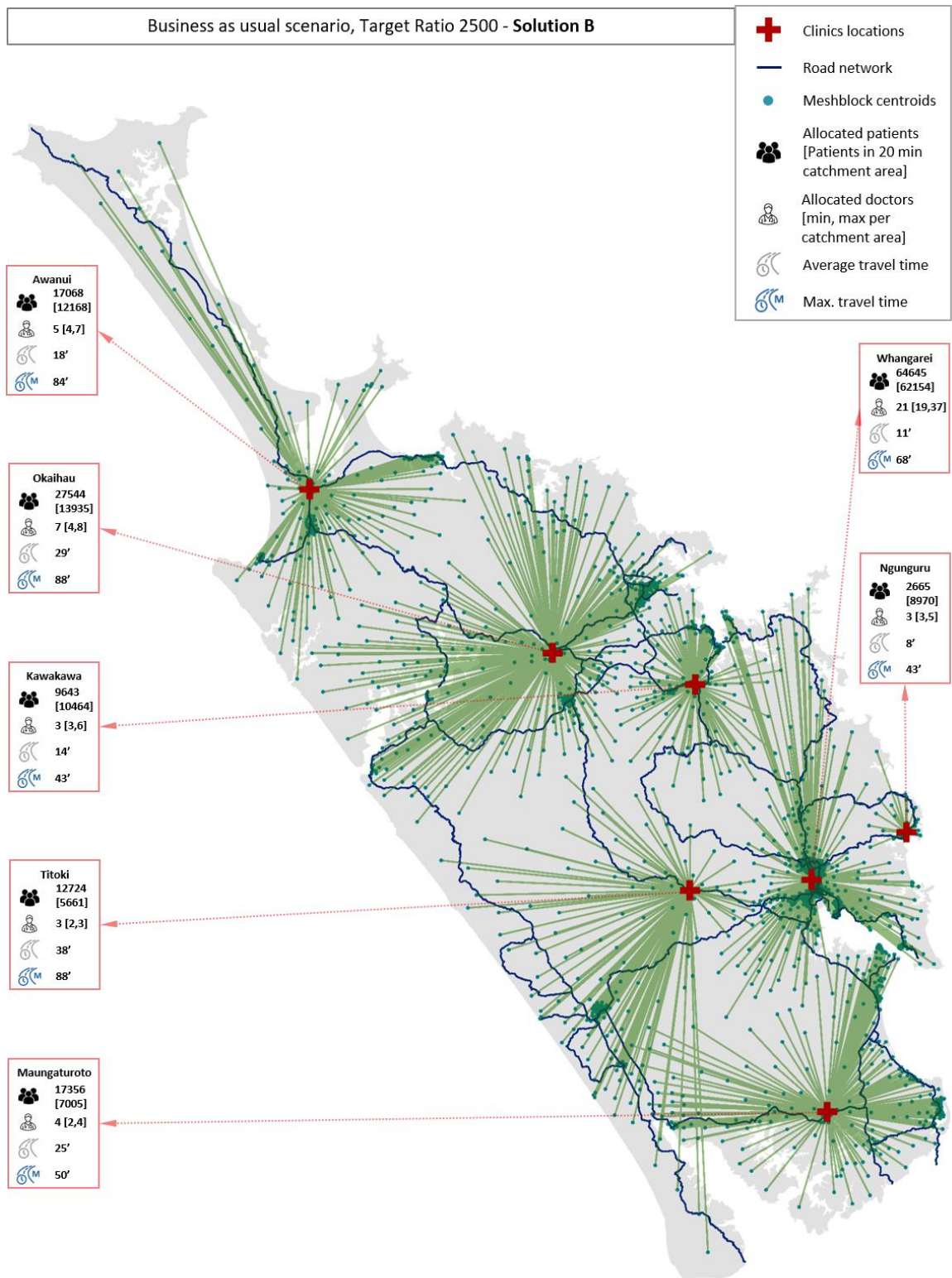


Figure 103 - Northland Case study, BAU scenario, Target ratio patients/GPs: 2500, Solution B (form Figure 101). The green lines are for visualisation purposes: they connect each meshblock centroid to the closest GP clinic. They do not represent distances, as distances are measured as travel times on the shortest path on the road network.

Table 18 - Northland case study, BAU scenario, target ratio patients/GPs: 2500, solution B (from Figure 101). Accessibility table.

Town	FTE GPs	N. of patients	Av. Patients per GP	Av. Travel time	Max. Travel time
Maungaturoto	4	17356	4339	25'	50'
Titoki	3	12724	4241	38'	88'
Whangarei	21	64645	3078	11'	68'
Ngunguru	3	2665	888	8'	43'
Kawakawa	3	9643	3214	14'	43'
Okaihau	7	27544	3935	29'	88'
Awanui	5	17068	3414	18'	84'

### 6.5.2. Disruption scenario

As explained in section 6.5, the second scenario is the one that takes into consideration the possibility of road closures due to natural disasters. To understand the vulnerabilities of Northland's road network, reference is made to the Regional Land Transport Plan 2015-2021 (Northland Regional Council, 2018), from which Figure 94 is extracted. To simulate road closures due to landslides and/or floods, the road edges of Table 14 are removed from the network and not considered in the road network analysis.

Subsequently, the same analysis of section 6.5.1 is performed: two different target ratios between patients and GPs are considered: 1500 and 2500. The choice of the same parameters allows comparing the results in the different scenarios, but as stated in the previous section, different numbers can be set as inputs to produce richer portfolios of results for more in-depth analyses.

#### 6.5.2.1. Disruption scenario – Target ratio patients/GPs: 1500

Figure 104 shows the solutions inspected by the genetic algorithm (blue triangles) and the Pareto-front on which Pareto-optimal solutions lie. It also represents the result of a preliminary qualitative analysis regarding the area of interest of Pareto-optimal solutions. Beyond the cost threshold, there is a considerable worsening of  $f_{cost}$  without any relevant

improvement in the travel time performance. Similarly, beyond the time threshold, there is no improvement in the cost performance of solutions despite higher travel times.

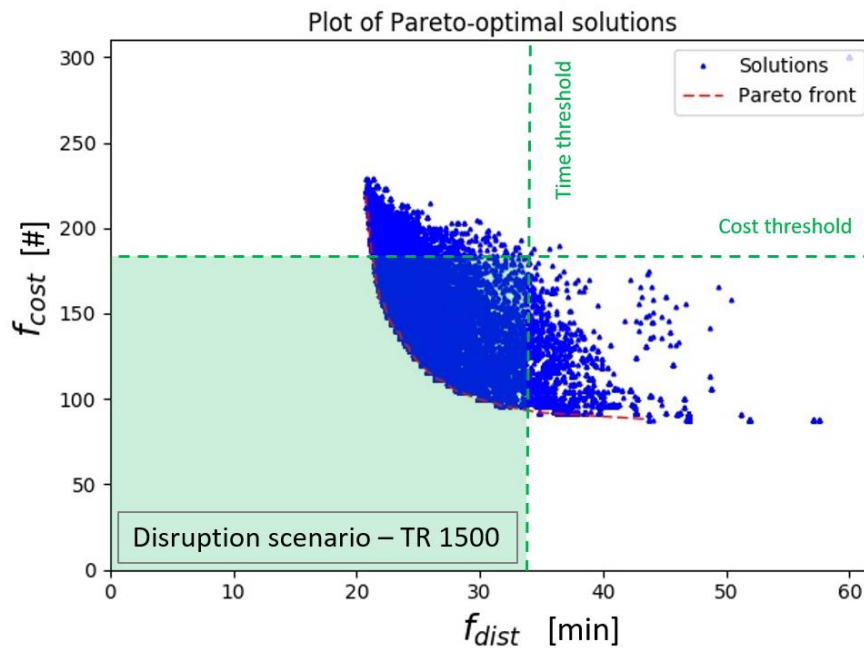


Figure 104 - Thresholds in the solution space for Northland case study. Disruption scenario, target ratio 1500.

The green area of Figure 104 represents the area of interest of Pareto-optimal solutions. Figure 105 shows the solutions selected from the area of interest that will be plotted in the following pages. A selection of Pareto-optimal solutions is imported in a GIS environment to produce maps for georeferenced visualisation. These solutions cover different areas of the Pareto-front:

- Solution A (Figure 106 and Table 19) from the top-left side of the Pareto-front (lower travel times, but higher cost);
- Solution B (Figure 107 and Table 20) from the bottom-right side (lower cost, but higher travel times).

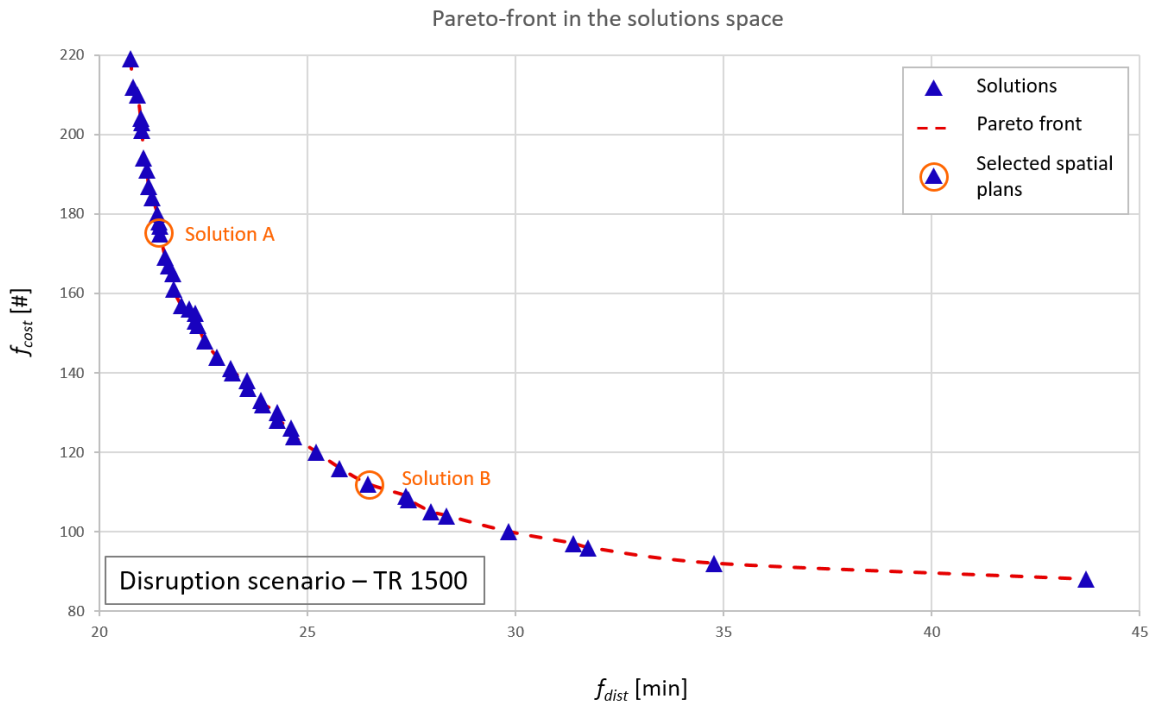


Figure 105 - Highlight of the Pareto-front for the Northland disruption case study (target ratio 1500) with the indication of the number of Pareto-optimal spatial plans. Solutions A and B are visualised in Figure 106, Figure 107, Table 19 and Table 20.

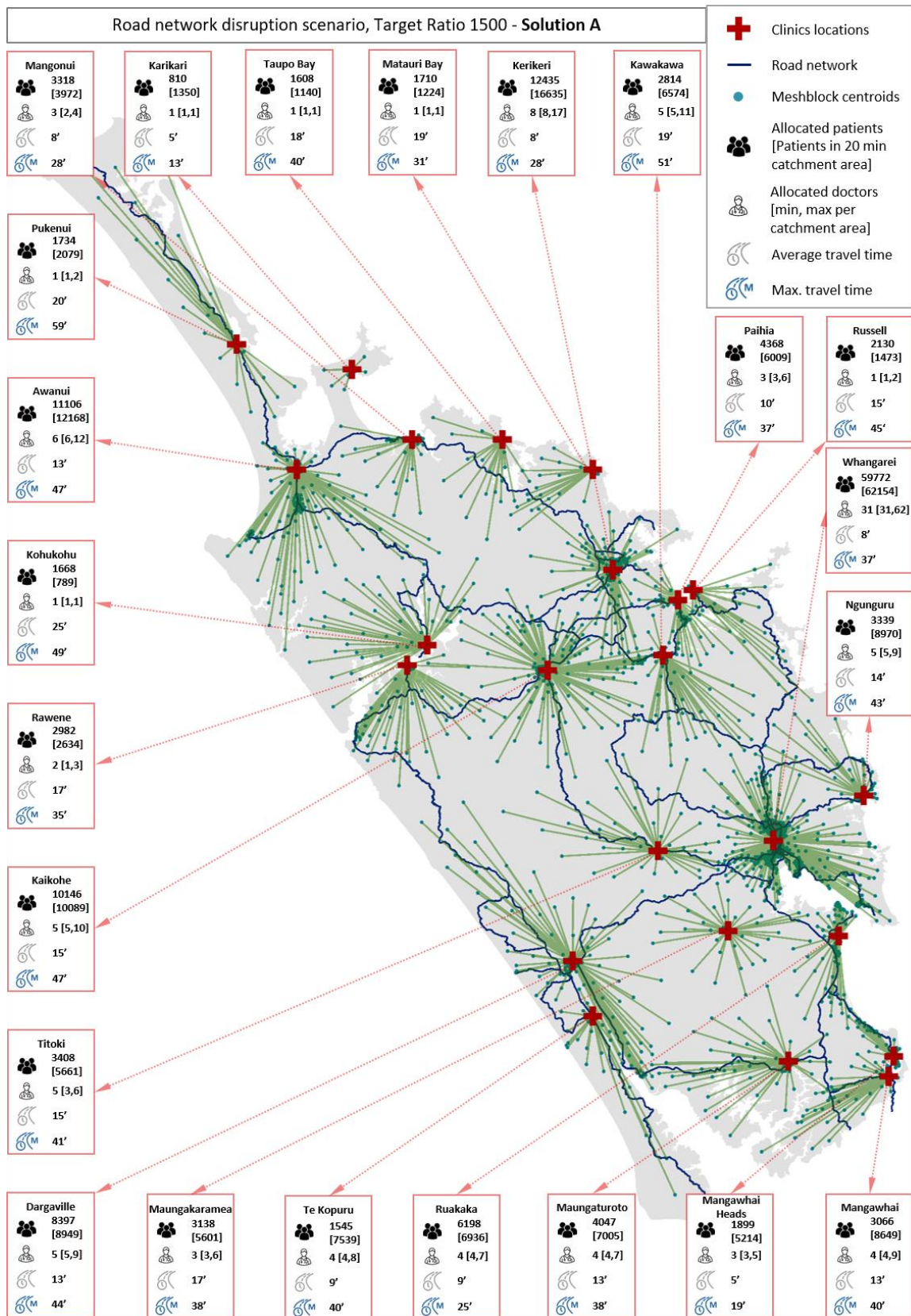


Figure 106 - Northland Case study, disruption scenario, Target ratio patients/GPs: 1500, Solution A (from Figure 105). The green lines are for visualisation purposes: they connect each meshblock centroid to the closest GP clinic. They do not represent distances, as distances are measured as travel times on the shortest path on the road network.

Table 19 - Northland case study, Disruption scenario, target ratio patients/GPs: 1500, solution A (from Figure 105).  
Accessibility table.

Town	FTE GPs	N. of patients	Av. Patients per GP	Av. Travel time	Max. Travel time
Mangawhai	4	3066	767	13'	40'
Maungaturoto	4	4047	1012	13'	38'
Mangawhai Heads	3	1899	633	5'	19'
Te Kopuru	4	1545	386	9'	40'
Dargaville	5	8397	1679	13'	44'
Ruakaka	4	6198	1550	9'	25'
Maungakaramea	3	3138	1046	17'	38'
Titoki	5	3408	682	15'	41'
Whangarei	31	59772	1928	8'	37'
Ngunguru	5	3339	668	14'	43'
Kaikohe	5	10146	2029	15'	47'
Rawene	2	2982	1491	17'	35'
Kawakawa	5	2814	563	19'	51'
Kohukohu	1	1668	1668	25'	49'
Paihia	3	4368	1456	10'	37'
Russell	1	2130	2130	15'	45'
Kerikeri	8	12435	1554	8'	28'
Awanui	6	11106	1851	13'	47'
Matauri Bay	1	1710	1710	19'	31'
Mangonui	3	3318	1106	8'	28'
Taupo Bay	1	1608	1608	18'	40'
Karikari	1	810	810	5'	13'
Pukenui	1	1734	1734	20'	59'

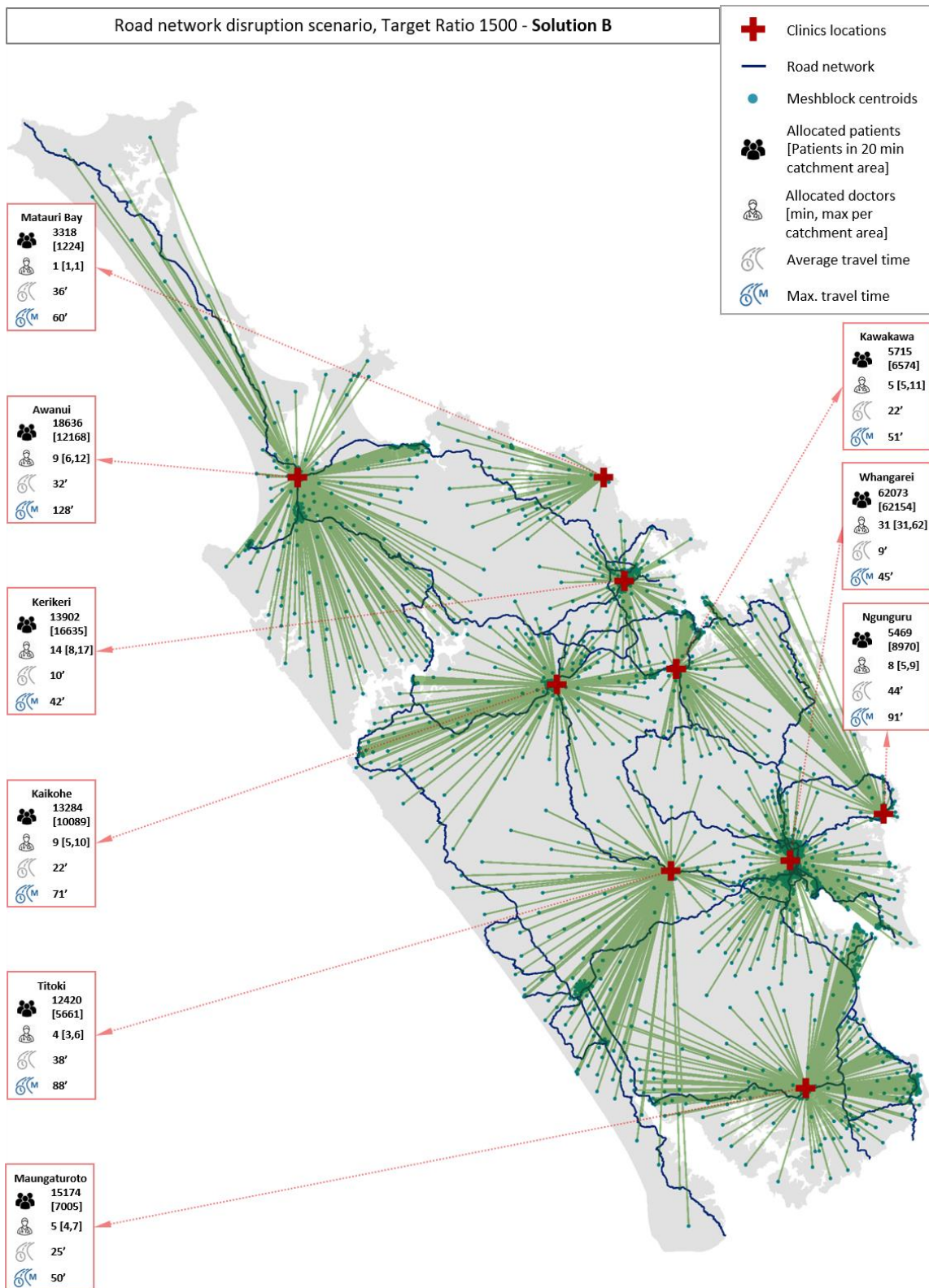


Figure 107 - Northland Case study, disruption scenario, Target ratio patients/GPs: 1500, Solution B (from Figure 105). The green lines are for visualisation purposes: they connect each meshblock centroid to the closest GP clinic. They do not represent distances, as distances are measured as travel times on the shortest path on the road network.

Table 20 - Northland case study, Disruption scenario, target ratio patients/GPs: 1500, solution B (from Figure 105).  
Accessibility table.

Town	FTE GPs	N. of patients	Av. Patients per GP	Av. Travel time	Max. Travel time
Maungaturoto	5	15174	3035	25'	50'
Titoki	4	12420	3105	38'	88'
Whangarei	31	62073	2002	9'	45'
Ngunguru	8	5469	684	44'	91'
Kaikohe	9	13284	1476	22'	71'
Kawakawa	5	5715	1143	22'	51'
Kerikeri	14	13902	993	10'	42'
Awanui	9	18636	2071	32'	128'
Matauri Bay	1	3318	3318	36'	60'

#### 6.5.2.2. Disruption scenario – Target ratio patients/GPs: 2500

The same methodology with the same parameters of section 6.5.2.1 is applied one more time, with the only difference of the input datum “target ratio patients/GPs”. In this run, the ratio is 2500 (for more details see 6.5.2).

As shown in the previous section, in Figure 108, the solutions inspected by the algorithm are plotted in the solution space defined by the two objective functions (x-axis:  $f_{dist}$  - average travel times weighted by the served population of each clinic; y-axis:  $f_{cost}$  - weighted sum of number of clinics and doctors).



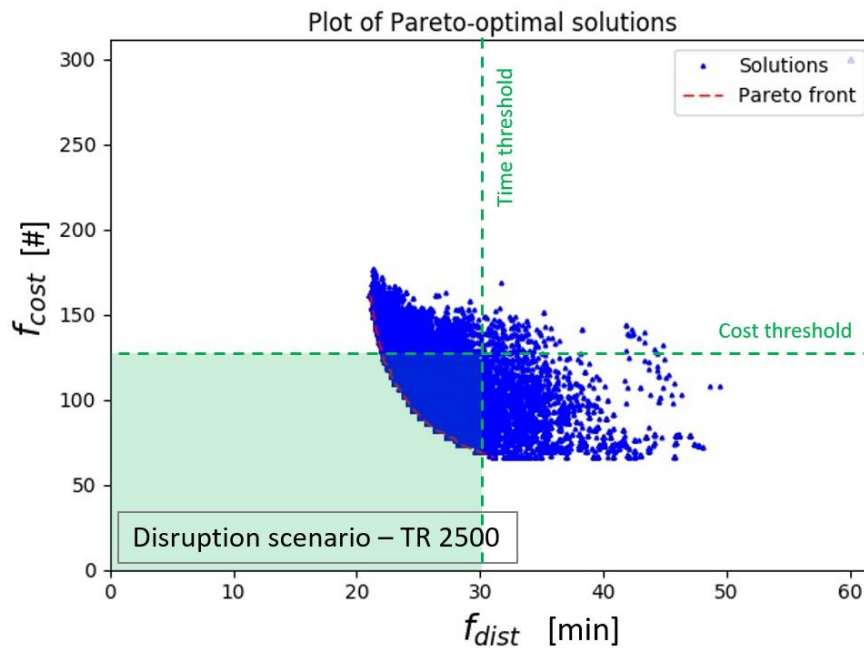


Figure 108 - Solution space and Pareto-front for Northland case study. Disruption scenario, target ratio 2500.

As explained in the previous section, Figure 108 represents all the solutions inspected by the GA (blue triangles) and the dashed red line is the Pareto-front, where Pareto-optimal solutions lie. The green area represents the area of interest of Pareto-optimal solutions (see the previous section for more details on time and cost thresholds). This is a preliminary qualitative analysis aimed at understanding the area of interest of the Pareto-front. Figure 109 shows the spatial plans plotted in the remaining part of this section. For clarity and readability, not all the spatial plans forming the Pareto-front are plotted. Only a selection of them, covering different areas of the Pareto-front are showed and analysed:

- Solution A (Figure 110 and Table 21) from the top-left side of the Pareto-front (lower travel times, higher cost);
- Solution B (Figure 111 and Table 22) from the bottom-right side (lower cost, but higher travel times).

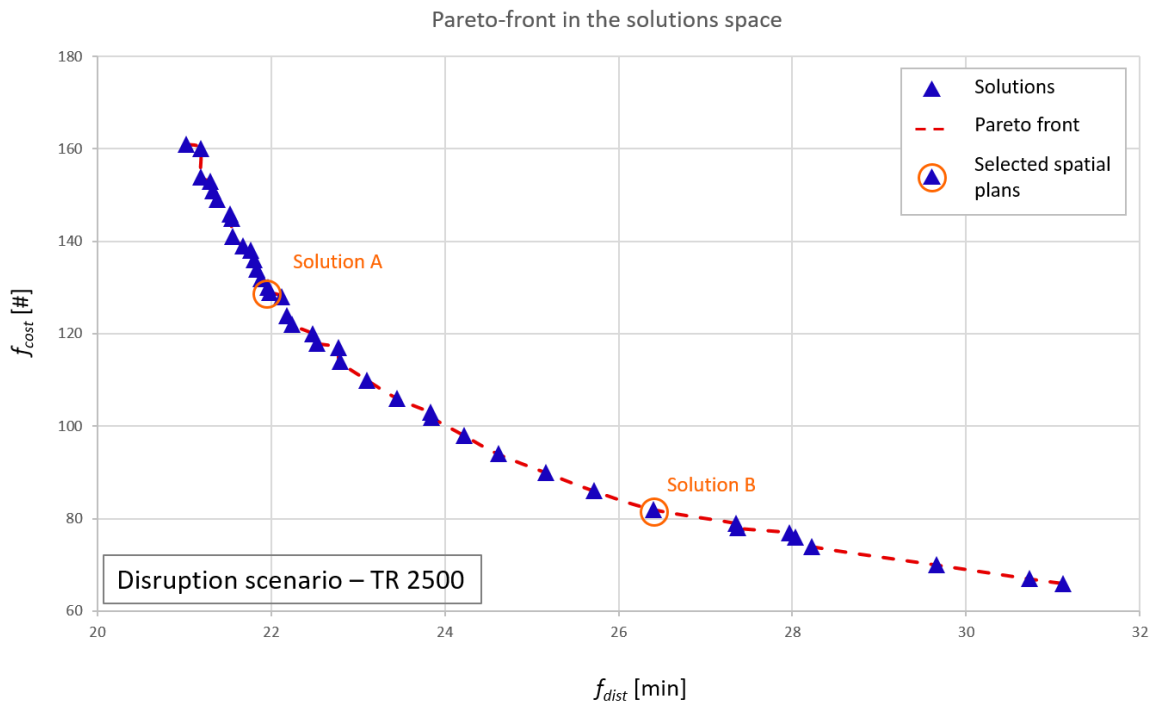


Figure 109 - Highlight of the Pareto-front for the Northland disruption scenario (target ratio 2500) with the indication of the number of Pareto-optimal spatial plans. Solutions A and B are visualised in Figure 110 Figure 111, Table 21 and Table 22.

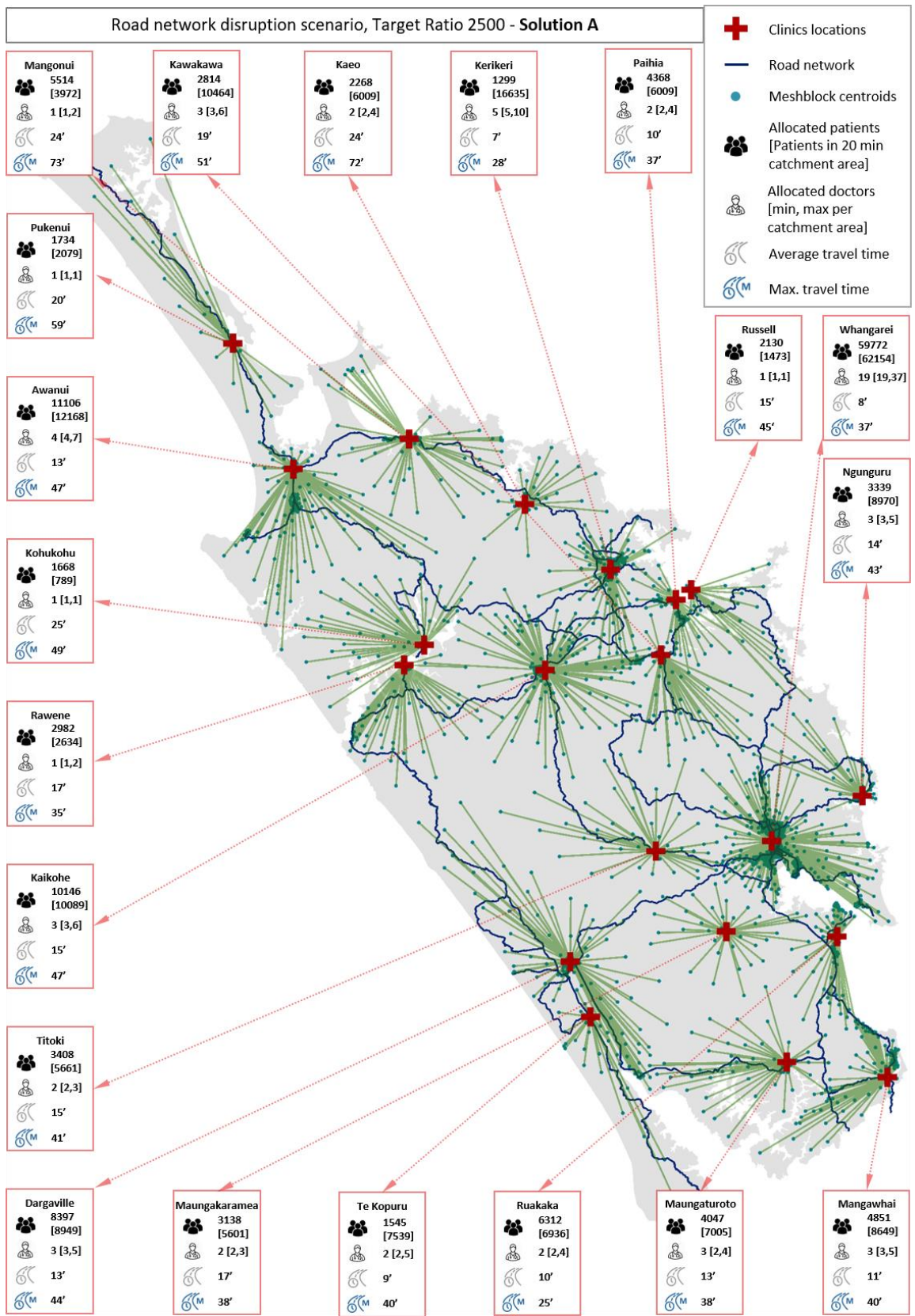


Figure 110 - Northland Case study, disruption scenario, Target ratio patients/GPs: 2500, Solution A (from Figure 109). The green lines are for visualisation purposes: they connect each meshblock centroid to the closest GP clinic. They do not represent distances, as distances are measured as travel times on the shortest path on the road network.

Table 21 - Northland case study, Disruption scenario, target ratio patients/GPs: 2500, solution A (from Figure 109).  
Accessibility table.

Town	FTE GPs	N. of patients	Av. Patients per GP	Av. Travel time	Max. Travel time
Mangawhai	3	4851	1617	11'	40'
Maungaturoto	3	4047	1349	13'	38'
Te Kopuru	2	1545	773	9'	40'
Dargaville	3	8379	2793	13'	44'
Ruakaka	2	6312	3156	10'	25'
Maungakaramea	2	3138	1569	17'	38'
Titoki	2	3408	1704	15'	41'
Whangarei	19	59772	3146	8'	37'
Ngunguru	3	3339	1113	14'	43'
Kaikohe	3	10146	3382	15'	47'
Rawene	1	2982	2982	17'	35'
Kawakawa	3	2814	938	19'	51'
Kohukohu	1	1668	1668	25'	49'
Paihia	2	4368	2184	10'	37'
Russell	1	2130	2130	15'	45'
Kerikeri	5	1299	260	7'	28'
Kaero	2	2268	1134	24'	72'
Awanui	4	11106	2777	13'	47'
Mangonui	1	5514	5514	24'	73'
Pukenui	1	1734	1734	20'	59'

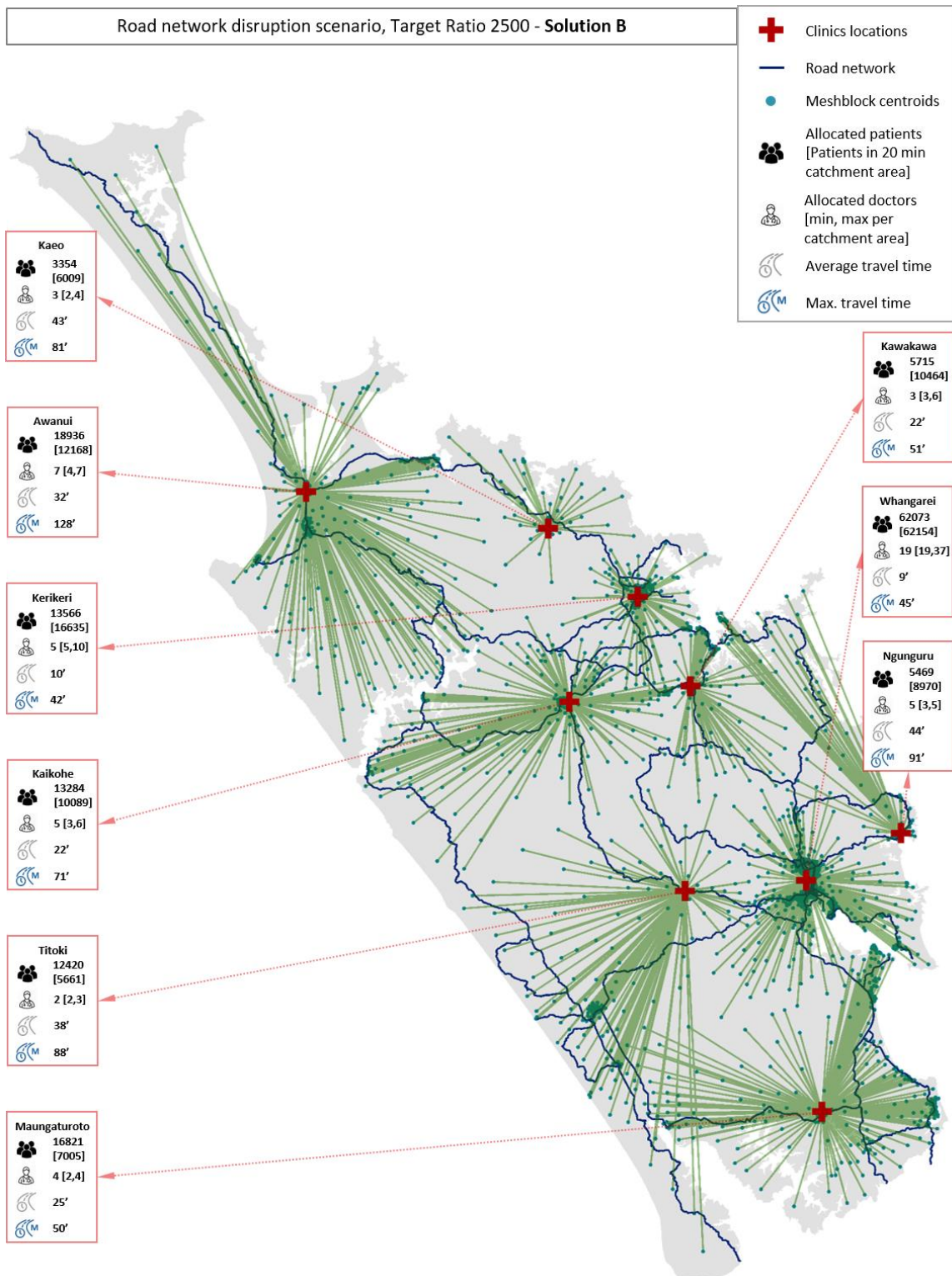


Figure 111 - Northland Case study, disruption scenario, Target ratio patients/GPs: 2500, Solution B (from Figure 109). The green lines are for visualisation purposes: they connect each meshblock centroid to the closest GP clinic. They do not represent distances, as distances are measured as travel times on the shortest path on the road network.

Table 22 - Northland case study, Disruption scenario, target ratio patients/GPs: 2500, solution B (from Figure 109).  
Accessibility table.

Town	FTE GPs	N. of patients	Av. Patients per GP	Av. Travel time	Max. Travel time
Maungaturoto	4	16821	4205	25'	50'
Titoki	2	12420	6210	38'	88'
Whangarei	19	62073	3267	9'	45'
Ngunguru	5	5469	1094	44'	91'
Kaikohe	5	13284	2657	22'	71'
Kawakawa	3	5715	1905	22'	51'
Kerikeri	5	13566	2713	10'	42'
Kaero	3	3314	1105	43'	81'
Awanui	7	18936	2705	32'	128'

## 6.6. Discussion of Northland case study results

BAU scenario's maps allow the visualisation of what observed in the solution space plots: a portfolio of solutions spanning from one edge of the spectrum of investigated spatial plans to the other. On the first edge, solutions with lower travel times and lower target ratios present more spread clinics with higher accessibility, on the other, as expected, more concentrated clinics plans with higher travel times, but clinics and doctors limited to the main towns. The same variability of solutions is observed in the disruption scenario, where there is a similarity in the nature of the solutions, but a difference in the average travel times due to road network disruptions.

A particular mention is due to the cost function formulation and the consequent results. As explained in section 6.4.3, the attribution of the number of doctors to each clinic happens randomly within an allowed range. This allowed range is a priori determined considering the population living within a 20 minutes' drive radius from the potential clinic location. It may happen, though, that in the final solutions clinics are assigned to adjacent towns that may share the same served population in the 20 minutes' drive radius. This overlapping problem results in possible over-attribution of doctors in close-by clinics. This is why the maps showing the Pareto-optimal spatial plans also have the indication of the allowed range of doctors for each clinic and the residing population in the catchment area. It is up to the final user to

critically analyse the spatial plans and draw conclusions concerning possible overlapping of service areas of close-by clinics. Possible solutions can be either choosing to “merge” close enough locations or keeping them separate but considering a reduction in the number of doctors.

To ease the comparison of different spatial plans, maps like the ones in Figure 112 help understanding the differences among different solutions with respect to a single parameter. As a matter of example, Figure 112 shows the different levels of accessibility in two solutions that represent the extremes of the spectrum of solutions presented in section 6.5. Here travel times are compared in two very different situations; Figure 112.a shows an accessibility map for the solution represented in Figure 98. In the BAU scenario, the road network is fully functional, and Solution A lies in the top-left area of the Pareto front associated with lower travel times. On the other hand, Figure 112.b presents the overall lower accessibility associated with the disrupted road network of the disruption scenario. In addition to the variability due to the different scenario conditions, Solution B represents the spatial plan illustrated in Figure 107, a solution lying in the bottom-right area of the Pareto front associated with higher travel times (but lower costs).

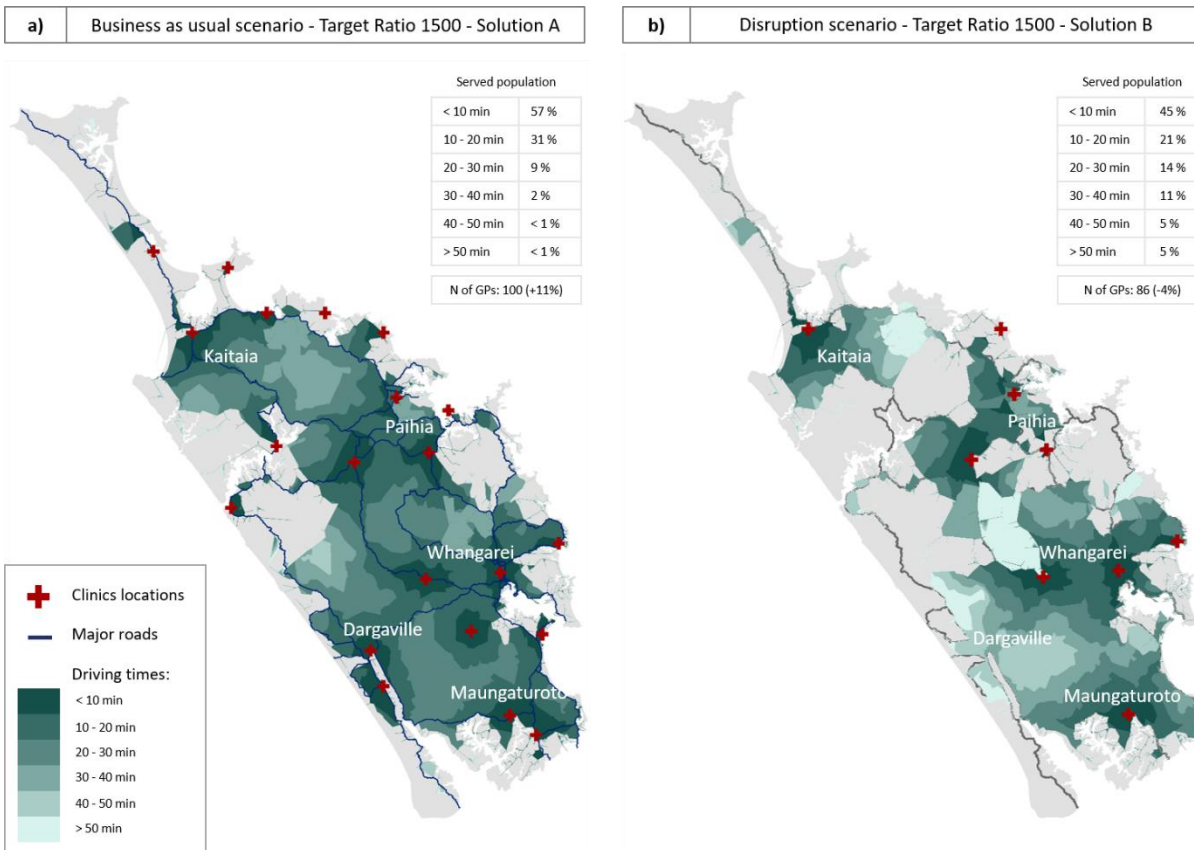


Figure 112 - Comparison of different levels of accessibility in different scenarios: a) BAU scenario, b) Disruption scenario.

Figure 112 is just one of the many possible examples in terms of comparison of results. The RAO framework provides georeferenced solutions that can be easily processed in any GIS environment to address any kind of analysis of interest to the final user.



Table 23 - Northland scenarios accessibility comparison. The current distribution of clinics and GPs in Northland is considered as the baseline for the assessment of the improvements provided by the different Pareto-optimal solutions in terms of accessibility and costs.

Travel time		< 10 min	10-20 min	20-30 min	30-40 min	40-50 min	> 50 min	
Current situation	Pop served	83277	39423	18750	7554	1557	1077	<b>N of GPs</b>
	% Pop	55%	26%	12%	5%	1%	1%	90
BAU TR 1500 Sol A	Pop served	86385	46905	14094	3513	657	84	<b>N of GPs</b>
	% Pop	57	31	9	2	0	0	100
	± %	+2%	+5%	-3%	-3%	-1%	-1%	(+11%)
BAU TR 1500 Sol B	Pop served	61791	36840	24105	16512	6768	5622	<b>N of GPs</b>
	% Pop	41	24	16	11	4	4	80
	± %	-14%	-2%	+4%	+6%	+3%	+3%	(-11%)
BAU TR 2500 Sol A	Pop served	88221	42948	13494	3558	1818	1599	<b>N of GPs</b>
	% Pop	58	28	9	2	1	1	61
	± %	+3%	+2%	-3%	-3%	+0.2%	+0.3%	(-32%)
BAU TR 2500 Sol B	Pop served	57424	38001	28314	14232	7026	6648	<b>N of GPs</b>
	% Pop	38	25	19	9	5	4	46
	± %	-17%	-1%	+6%	+4%	+4%	+4%	(-49%)
Disruption TR 1500 Sol A	Pop served	88257	41967	13233	6546	1452	183	<b>N of GPs</b>
	% Pop	58	28	9	4	1	0	110
	± %	+3%	+2%	-4%	-1%	-0.1%	-1%	(+22%)
Disruption TR 1500 Sol B	Pop served	67512	31521	20976	16524	7473	7632	<b>N of GPs</b>
	% Pop	45	21	14	11	5	5	86
	± %	-10%	-5%	+1%	+6%	+4%	+4%	(-4%)
Disruption TR 2500 Sol A	Pop served	87456	41289	12708	6609	1929	1647	<b>N of GPs</b>
	% Pop	58	27	8	4	1	1	63
	± %	+3%	+1%	-4%	-1%	+0.2%	+0.4%	(-30%)
Disruption TR 2500 Sol B	Pop served	67764	31365	20526	16230	7296	8457	<b>N of GPs</b>
	% Pop	45	21	14	11	5	6	53
	± %	-10%	-5%	+1%	+6%	+4%	+5%	(-41%)

Table 23 provides an overview of the solutions of sections 6.5.1 and 6.5.2. Here, the served population's travel times are compared to the current clinics and doctors layout in Northland, which is taken as a baseline for the assessment of the improvements provided by the different

Pareto-optimal solutions. Relative percentage increments (or reductions) are measured against the current service in Northland (see Figure 91 and Table 12).

In the business as usual scenario, we can observe that solutions A (top-left area of Pareto fronts, i.e. high accessibility and high costs) present increments in accessibility (i.e. more people served in less than 20 minutes). This is achieved with an increment of 11% in the number of doctors when considering a target ratio patients/doctors of 1500, and with a reduction of almost a third of the number of doctors when considering a ratio of 2500. The same trend is observed in the disruption scenario, with the only difference consisting in the fact that maintaining the same level of service would require an extra 10% increment in the number of doctors when considering the 1500 ratio. This means that the higher is the number of doctors, the higher is the extra expense to maintain the service provision in case of disruption.

Solutions B, instead, are those spatial plans from the bottom-right area of the Pareto fronts. This implies lower accessibility and lower costs. These solutions are useful to understand the consequences of potential reductions in the number of available GPs. They necessarily imply reductions in the served population in less than 20 minutes, but provide useful information regarding optimal allocations of a reduced number of resources.

The disruption scenario takes into account the simultaneous disruption of all the most critical sites of Northland's road network. This represents a quite unlikely worst-case scenario; nevertheless, it provides the opportunity to find and focus on the most resilient solutions generated by the RAO framework.

As stated in the introduction of this chapter, a Greenfield approach has been adopted for this case study. This makes these results not applicable to the reality tout court; instead, they need to be analysed and then taken as a reference for the improvement of the current situation of the health service provided in Northland. This is why the overlapping of catchments areas does not appear as a conceptual obstacle to the interpretation of the RAO framework results.

Moreover, highlighting interconnections and implications between infrastructure design and natural disasters is one of the main objectives of this research. In this spirit, the results of the disruption scenario are meant to highlight potential criticalities putting together two aspects of infrastructure design that may not always be taken into consideration at the same time.

The main drivers behind the opening or relocation of GP clinics are usually related to the personal motivations of the practitioners as small entrepreneurs. This study aims at proposing a new perspective on this particular infrastructure planning, a top-down approach in which the main drivers are not (just) the personal interests of singular professionals, but also a collective perspective that takes into account a higher level of optimisation of the healthcare service provision. This is why the presented results are meant not as a prescription, but as guidance for future investments in the area or a reorganisation of the status quo.

The attribution of weighting factors to general practitioners and clinics in the evaluation phase presented in section 6.4.4 represents a final discussion point. These weighting factors are an input parameter adjustable by the end-user, however, rather than an assumption, this must be considered as an actual medical policy scenario. Assigning different weighting factors has repercussions on the final optimal spatial plans, and their determination is unquestionably arbitrary. Nevertheless, in case of lack of data regarding costs and profits of the private healthcare business (in terms of clinics and practitioners), it is necessary to make a reasonable assumption to obtain sensible results.

Additional values of clinics' weighting factors are explored in Table 24 together with additional values of target ratios patients/doctors to assess the sensitivity of the problem to the two main parameters defining the optimisation formulation. The assessed values in this sensitivity analysis are:  $\gamma_C = 2, 4, 6$  and  $TR = 1000, 1500, 2000, 2500, 3000$ .

To allow the comparison among different scenarios and combinations of  $\gamma_C$  and  $TR$ , Table 24 considers different spatial plans with the same  $f_{time}$  fitness; therefore, it is not surprising to observe small differences in accessibility fitnesses: between +2% and +4% of served population under 10 minutes with respect to current situation in Northland for  $f_{time} = 22$  min. However, it is interesting to observe how the infrastructure cost varies (i.e. number of FTE GPs and clinics) to achieve such an improvement in terms of accessibility (i.e. % of population served under 10, 20, 30 etc. minutes).

Table 24 - Accessibility analysis of BAU scenario for different values  $\gamma_c$  of and TR for a fixed value of  $f_{time}$ .

Travel time				< 10'	10'-20'	20'-30'	30'-40'	40'-50'	>50'		
Current situation				Pop	83277	39423	18750	7554	1557	1077	GPs
				% Pop	55	26	12	5	1	1	90
$\gamma_c$	TR	Sol ID	$f_{time}$	Pop	86811	45114	13680	3543	891	1599	GPs
2	1000	49201	22'	% Pop	57	30	9	2	1	1	114
				$\pm$ %	+2	+4	-3	-3	-0.4	+0.3	+27%
				$\gamma_c$	TR	Sol ID	$f_{time}$	Pop	86871	44943	15312
2	1500	43040	22'	% Pop	57	30	10	2	< 1	< 1	80
				$\pm$ %	+2	+4	-2	-3	+0.1	+0.3	-11%
				$\gamma_c$	TR	Sol ID	$f_{time}$	Pop	86232	45600	13044
2	2000	39062	22'	% Pop	57	30	9	2	1	1	57
				$\pm$ %	+2	+4	-4	-3	+0.1	+0.3	-37%
				$\gamma_c$	TR	Sol ID	$f_{time}$	Pop	88248	45276	13899
2	2500	49149	22'	% Pop	58	30	9	2	0	0	48
				$\pm$ %	+3	+4	-3	-3	-1	-1	-47%
				$\gamma_c$	TR	Sol ID	$f_{time}$	Pop	89175	43374	13866
2	3000	41995	22'	% Pop	59	29	9	2	1	0	40
				$\pm$ %	+4	+3	-3	-3	+0.04	-1	-56%
				$\gamma_c$	TR	Sol ID	$f_{time}$	Pop	86973	45651	14079
4	1000	47192	22'	% Pop	57	30	9	3	1	0	117
				$\pm$ %	+2	+4	-3	-2	-1	-1	+30%
				$\gamma_c$	TR	Sol ID	$f_{time}$	Pop	86385	46905	14094
4	1500	48254	22'	% Pop	57	31	9	2	0	0	100
				$\pm$ %	+2	+5	-3	-3	-1	-1	+11%
				$\gamma_c$	TR	Sol ID	$f_{time}$	Pop	86988	45507	14433
4	2000	42010	22'	% Pop	57	30	10	3	0	0	64
				$\pm$ %	+2	+4	-3	-2	-1	-1	-29%
				$\gamma_c$	TR	Sol ID	$f_{time}$	Pop	88221	42948	13494
4	2500	41222	22'	% Pop	58	28	9	2	1	1	61
				$\pm$ %	+3	+2	-3	-3	+0.2	+0.3	-32%
				$\gamma_c$	TR	Sol ID	$f_{time}$	Pop	89268	43398	13524
4	3000	43489	22'	% Pop	59	29	9	2	1	0	43
				$\pm$ %	+4	+3	-3	-3	+0.1	-1	-52%
				$\gamma_c$	TR	Sol ID	$f_{time}$	Pop	87720	44886	13842
6	1000	48080	22'	% Pop	58	30	9	2	1	0	117
				$\pm$ %	+3	+4	-3	-3	+0.04	-1	+30%
				$\gamma_c$	TR	Sol ID	$f_{time}$	Pop	86988	45507	14433
6	1500	42003	22'	% Pop	57	30	10	3	0	0	88
				$\pm$ %	+2	+4	-3	-2	-1	-1	-2%
				$\gamma_c$	TR	Sol ID	$f_{time}$	Pop	87159	45594	14229
6	2000	41211	22'	% Pop	57	30	9	3	0	0	67
				$\pm$ %	+3	+4	-3	-2	-1	-1	-26%
				$\gamma_c$	TR	Sol ID	$f_{time}$	Pop	86811	45114	13680
6	2500	46014	22'	% Pop	57	30	9	2	1	1	50
				$\pm$ %	+2	+4	-3	-3	-0.4	+0.3	-44%
				$\gamma_c$	TR	Sol ID	$f_{time}$	Pop	87894	44571	13464
6	3000	35209	22'	% Pop	58	29	9	3	1	0	50
				$\pm$ %	+3	+3	-3	-2	+0.1	-1	-44%

Figure 113 shows the comparison of infrastructure costs (i.e. relative increment of number of GPs) with respect to the current Northland situation presented in section 6.2 corresponding to different TR and  $\gamma_C$  values (and for a fixed value of  $f_{time} = 22'$ ).

When considering 1000 patients per GP, an increment in the number of GPs of nearly 30% is necessary for all the inspected  $\gamma_C$  values. Increasing the value of TR (i.e. allowing more patients per GP), it is possible to achieve the same accessibility (i.e.  $f_{time} = 22'$ ) with less doctors and therefore with a lower infrastructure cost, even with less GPs than the current Northland situation.

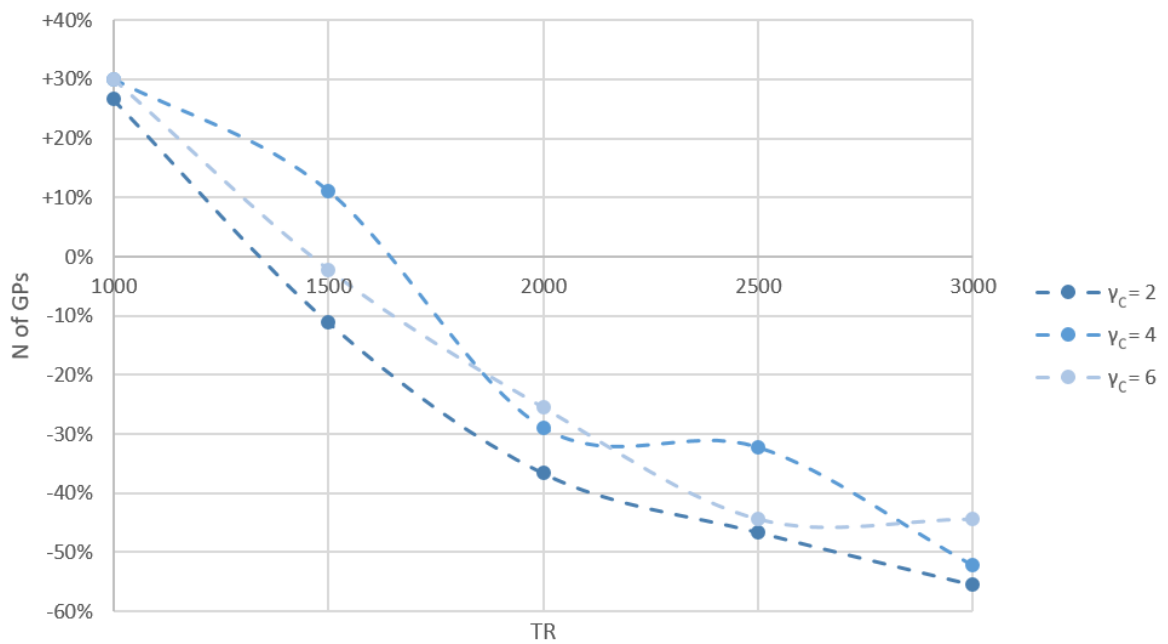


Figure 113 - Comparison of infrastructure cost with respect to current Northland situation for different values of  $\gamma_C$  and TR for a fixed value of  $f_{time}$ .

Different values of  $\gamma_C$  imply different numbers of employed doctors, since lower values of  $\gamma_C$  correspond to lower costs in opening new clinics compared to adding GPs to existing ones. The mathematical formulation of the infrastructure cost function involves  $\gamma_C$  as a parameter to capture the competition between close-by available locations for clinics, therefore its value is not directly proportional to the cost fitness. Moreover, a general trend is observable from Figure 113: increasing the value of TR always corresponds to a lowering of the total number of GPs in the region; therefore,  $\gamma_C$  does not influence the behaviour of the Pareto-optimal solution as much as TR. The target ratio patients/doctors is the governing parameter of the problem, since its variations have greater influence on the global costs of the regional case study, while  $\gamma_C$  is a secondary modelling parameter meant to capture local competition.

## 6.7. Summary

Chapter 6 presented the Northland case study. Here the RAO framework has been applied to the healthcare infrastructure of the Northland region (New Zealand). The focus is general practitioners' clinics' optimal allocation. A Greenfield approach is applied for the determination of Pareto-optimal locations in the multi-objective spatial optimisation process. The two objectives are: 1) maximisation of accessibility (translated as minimisation of travel times on the road network) and 2) minimisation of costs (number of clinics and doctors).

After an introduction to the case study (section 6.2), a description of the sources and the datasets taken into consideration (section 6.3) and a description of the problem formulation (section 6.4), the results are presented and discussed in sections 6.5 and 6.6.

Two different scenarios are investigated: a BAU scenario and a disruption scenario. The first one aims at optimising the healthcare service in Northland under normal circumstances; the second one investigates a disrupted road network condition due to natural disasters. The simulations otherwise use the parameters in order to allow a comparison between the different situations.

As highlighted in section 6.6, the results of this case study do not have a prescriptive nature, but the final user should consider them as a reference for future investments or a reorganisation of the current situation for more cost-effective management of the healthcare infrastructure of the region.

Since the visualisation of single spatial plans does not facilitate the comparison between different solutions and scenarios, Figure 112 provides an example of accessibility comparison between different spatial plans belonging to different scenarios. Figure 112 is meant to show the variability in terms of a particular parameter (travel time) between solutions that are at different extremes of the spectrum provided by the RAO framework. Of course, travel time is not the only significant parameter, and other comparison maps can be produced according to different potential particular needs of the end-user.

Figure 112 confirms some information already evidenced from the previous maps: for example, no matter what number of clinics are part of a solution, the area around Whangarei (the capital and most populated centre) always has a quite constant good coverage; together with the area around Kaitaia, in the northern part of the region. Higher variability, as expected,

is encountered in more remote and less populated areas. This happens for two reasons: first, the population works as a weighting factor in the evaluation phase; meaning that solutions that better serve bigger portions of the population are always prioritised. Secondly, because of the lower grade of interconnection of remote areas: when a disruption occurs, remote areas have less network redundancy to count on, making them ultimately less resilient to network disruptions.





## 7. Discussion

### 7.1. Introduction

The increase of climate risks in urban areas, coupled with increasing global urban population, continuous development of urban environments and the generally limited availability of resources to cope with natural disasters are the drivers behind new system scale approaches to urban planning and infrastructure management (Caparros-Midwood, 2015). The literature review of Chapter 2 explored the current flood management approaches, and Chapter 4 highlighted the challenges in achieving different (and conflicting) objectives in the same strategy.

The overall goal of the present research is the improvement of infrastructure services' resilience through the spatial optimisation of resources allocation. To achieve this goal, a Resource Allocation Optimisation (RAO) framework is presented in Chapter 4. The formulation of the framework's structure, the choice of the methodology and the nature of the different components are based on the review of optimisation techniques presented in Chapter 3.

The RAO framework represents the core of this research work; it is meant as a both theoretical and practical spatial methodology aimed at balancing the typical trade-offs in urban and emergency planning like accessibility maximisation and cost optimisation. It is designed to optimally allocate multiple facilities to improve infrastructure services in the two case study areas, focussing respectively on reducing flood impacts (UK case study – Chapter 5) and improving access to healthcare infrastructure (NZ case study – Chapter 6).

This section will explore the results of the RAO framework concerning the two applications developed for the flood emergency response problem (Humber Estuary case study) and the healthcare infrastructure accessibility problem (Northland case study). Section 7.2 frames the case studies within the general subject of trade-off balancing in spatial problems, presenting its rationale and highlighting the main issues to address in this particular context. Section 7.3, instead, explores the evidence from the case studies results providing details on their interpretation and implications. Section 7.5 presents the main assumptions and model limitations, together with the indication of potential starting points for the future development of this research work. Finally, section 7.6 focusses on the software implementation of the RAO framework and its implications.

## 7.2. Balancing conflicts and trade-offs in spatial planning

Accessibility maximisation vs cost minimisation is a typical trade-off in spatial optimisation. Both public administrative authorities and private companies perform location-allocation analyses when they need to determine optimal locations for facilities with a catchment area. The spatial (and mathematical) problem to solve is the same whether the facility to allocate is a hospital, a school, a power plant or a shopping centre. It is relatively straightforward to determine optimal locations for single facilities with ordinary network solvers embedded in most GIS software packages (like ArcGIS or QGIS). It is less trivial when more than one facility is to be allocated, but still quite easily achievable (depending on the case study) if the number of facilities is a fixed number.

This research work addresses the case in which the number of multiple facilities to be optimally allocated is variable. Adding an extra variable transforms the problem from a single-objective spatial optimisation problem to a multi-objective one. The new extra variable is the number of facilities to be allocated, which is directly proportional to the cost invested. Allocating more facilities means improving accessibility but at the same time it entails investing more resources. According to how this cost is evaluated (i.e. proportional to the number of facilities or to the floor space of each facility, etc. – see section 5.5 for different cost function formulations) more refined analyses can be performed. Moreover, the advantages of considering different locations are not necessarily related only to accessibility, since different locations can provide different benefits. For instance, different infrastructure assets can serve different shares of the population according to their dimension (e.g. a transformer could serve either 100 or 1000 houses – sections 5.5.10-5.5.13 explore a critical infrastructure protection prioritisation based on the served population of each asset).

The case study presented in Chapter 5 describes the allocation of storing space for temporary flood defences, based upon the problem defined by the UK National Flood Resilience Review (Cabinet Office and DEFRA, 2016). In this document, the UK government committed £2.3 billion to be invested in a 6-year time frame to improve flood protection throughout the country. Part of this funding - namely £12.5 million - is explicitly allocated for temporary flood defences with the aim to improve the Environment Agency's stock. These new temporary defences need to be allocated in strategic locations to allow a prompt and efficient deployment when needed. For this reason, the RAO framework has been developed and then

applied to the Humber Estuary region to test the spatial optimisation framework and produce spatial plans of warehouses that optimally balance the trade-off between the maximisation of accessibility and minimisation of costs.

The case study presented in Chapter 6 is a different application of the RAO framework. The case study is different, but the mathematical formulation of the problem is the same. This proves the versatility and transferability of the optimisation methodology: the RAO framework has been originally developed for the emergency response scenario, but its flexible design makes it suitable to a series of spatial multi-objective optimisation problems and applications in different fields and locations. Here the RAO framework is applied to solve the optimal allocation of healthcare facilities (and personnel) in a rural area of New Zealand. The balanced trade-off is once again between the maximisation of facilities' accessibility and the minimisation of costs, which in this case is translated as a Pareto-optimal number of clinics and practising doctors.

As these examples illustrate, the presented RAO framework has the potential to support the decision-making process when spatially allocating multiple resources or facilities. Optimal allocation is directly translated as resilience and cost-efficiency, which, in turn, are directly linked to sustainability as expressed in Chapter 2. Planning future resilient sustainable infrastructure cannot disregard holistic approaches given the complex nature of cities and urban areas and the level of interconnection and interdependencies of different infrastructure networks. The digital revolution provides us with unprecedented tools to model and try to manage this complexity.

This work aims to be beneficial to the scientific community on two different levels: first, by setting the ground for a new conceptual approach in emergency planning based on new digital tools with a rigorous mathematical and scientific background. Second, being a pilot and a reference for the future development of support digital tools for decision-makers and urban planners dealing with spatial optimisation and resource allocation.

### 7.3. Flood Incident Management

The outcomes of the RAO framework applied to the different case studies are presented in section 5.5 and 6.5. The optimisation methodology produces a set of different outputs: 1)

Pareto-fronts in the solution space showing the performance of all the inspected solutions (diagram) and the ones that optimally balance the trade-off between the conflicting objectives; 2) georeferenced spatial plans (either in shape or CSV format) presenting the Pareto-optimal plans in the form of a map. These datasets can be handled in any GIS environment to produce maps containing any relevant information together with the Pareto-optimal location of assets/facilities of interest to the particular case study.

The combination of locations and attributes of the Pareto-optimally allocated facilities allows the final user to make comparisons and draw conclusions on otherwise unintuitive cost-benefits analyses of different spatial plans. While allocating a single warehouse or a GP clinic may be a rather quick and intuitive process, the allocation of 10 or 20 facilities at a regional scale against conflicting objectives (simultaneously meeting boundaries and constraints and with non-linear cost formulations) is a process that requires automation and a discrete amount of computational power.

Information like the Pareto-optimal spatial plans presented in sections 5.5 and 6.5 represents a good example of numerical support in the decision-making process of resources allocation. If this kind of information was available in all the processes that require a choice of where to spatially allocate a variable number of facilities, more informed, cost-effective and ultimately sustainable strategies could be produced.

The Humber Estuary case study is an example of how the RAO framework can be applied to solve the optimal spatial allocation of warehouses to store temporary flood defences. The analysis of thirteen different scenarios allows exploring and implementing different strategies according to different boundary conditions and different cost formulations (that can be implemented according to the scope of the final user, or according to the data availability of the case study). Approaching the problem with a perfectly functional road network or considering potential road closures due to the presence of floodwater are both valid choices. They are directly proportional to the level of confidence that the final user has concerning factors like a reliable alert system or the dimension of the fleet (and staff) available to transport and deploy the flood defences. When there are uncertainties regarding such a level of confidence, it can be valuable to consider both the scenarios to explore the variability of the solutions. This variability is strictly case-dependent. Different regions may present very different variabilities due to their geography, which in the RAO framework is translated as

network redundancy. In general, the more the road network is interconnected, the more resilient it will be to potential road closures. Also, comparing the outcomes of different scenarios considering different assumptions (e.g. cost functions, fleet dimension, strategic infrastructure prioritisation etc.) allows a wider range of insights on the strategic planning of critical infrastructure's resilience to natural hazards, with socio-economic benefits related to costs optimisation, safety measures implementation and economic and environmental sustainability.

Figure 87, Figure 89 and Figure 112 are examples of accessibility comparisons between different scenarios. While spatial plans maps allow visualising different data in the same place (e.g. locations, dimensions, travel times, etc.), heatmaps allow to efficiently visualise just one variable at a time (for example accessibility) providing an effective way to compare different scenarios or set of multiple spatial plans at a glance.

The BAU and the disruption scenarios explored in both Chapters 5 and 6 represent respectively a best-case and a worst-case scenario; intermediate situations could also be considered (see the section on future development). Flooding is a dynamic phenomenon: together with the preparation time guaranteed by alert systems, an extra amount of time is necessary to reach the flood peak; this allows to evaluate the promptness and efficiency of emergency response and, in case, consider middle ground scenarios (e.g. partially flooded road network with consequent reduced allowed speeds). However, in the absence of detailed information, it is recommended to consider the worst-case scenario as during emergencies it is usually difficult to guarantee a perfectly functional road network and, by definition, risks can be minimised, but not eliminated.

The Humber Estuary results allow drawing some conclusions and drafting some recommendations. For example, Figure 89 identifies eight hotspots for warehouses allocation: Hedon, Whiternsea, Scunthorpe and Goole/Drax with allocation probabilities >70% and Kingston upon Hull, Grimsby, Brigg and Hatfield with allocation frequencies >60%. As explained in section 5.6, the reasons why these locations are hotspots for storing space allocations are different, like the presence of a cluster of strategic infrastructure assets or the remoteness/accessibility of the area.

When considering a disrupted road network due to the presence of floodwater, the Pareto-optimal solutions' pattern changes because of the presence of isolated areas. If at least one warehouse must be accessible from the whole region's territory, the mandatory allocation of warehouses to this potentially isolated areas results in very different spatial plans if compared to the business as usual scenario. For example, in the Humber Estuary case study, this is the case of Drax (Figure 87).

In addition to the analysis of the road network functionality assumption, Figure 88 allows the assessment of the model's sensitivity to the other assumptions explored in the several scenarios of Chapter 5. The Pareto fronts of different scenarios can be clustered in three groups according to the different cost function formulations or to other assumptions (e.g. fleet dimension or strategic infrastructure assets prioritisation) and compared in the solution space in terms of costs and accessibility. This is valuable to the final user when assessing different assumptions on missing data (e.g. when applying the methodology to other regions, data on rent prices in different locations or details regarding the costs of operating a fleet of lorries might not be available) or different cost functions (e.g. when deciding whether to consider the expansion of the available fleet of lorries or only using the already in-place resources, different cost functions are taken into consideration in the RAO framework application).

The novelty of the presented approach makes it hard to compare the RAO framework's results with a current in-place strategy, because a strategy for temporary flood defences storing and deployment has not been found in the literature or policy documents. This is because the Humber Estuary region is divided into different local authorities: the East Riding of Yorkshire, Kingston upon Hull and North Lincolnshire. As explained in Chapter 2, these different local governments are autonomous in terms of flood management strategies and, to date, they have not produced a joint flood protection strategy that considers the whole Humber Estuary at a regional level. Moreover, their local flood protection strategies do not take into account temporary flood defences.

Together with considering temporary flood defences as a viable tool for effective flood management in a region (see section 2.3.2), the novelty of the presented approach resides also in the scale of the studied instances; in fact, it optimises the emergency response infrastructure at a regional level, with the aim to overcome local authorities boundaries for more efficient and cost-effective flood management strategies.

#### 7.4. Embedding infrastructure network vulnerability into strategic planning

The recommendations emerging from the RAO framework results' analysis are valuable for both planning future emergency response strategies and comparing already-in-place infrastructure. In fact, in real-life problems, the Greenfield approach adopted in the case study of section 5 is hardly ever a realistic option. Rather a current in-place strategy is usually assessed and, in case, options to improve it are evaluated and implemented. The RAO framework provides a support tool for this kind of situations. This means that, in this regard, for the Humber Estuary case study, the recommendations for the temporary measures will need to be integrated with the already-in-place structural measures and with the ones currently under development.

This is true also for the Northland instance. The Greenfield approach does not allow drawing direct conclusions concerning the Pareto-optimal spatial plans of clinics and doctors, as it will never be the case that all the GP clinics of the region will be relocated at the same time. Nevertheless, the results of the spatial analysis are valuable for different reasons. First, they allow assessing the Pareto-optimality of the current distribution of healthcare facilities in the region with respect to accessibility and cost (intended as the number of clinics, doctors and number of patients per GP). Besides, they allow making useful considerations in terms of policymaking and in terms of resilience to road network disruptions in different areas (e.g. allocation of clinics in vulnerable locations – either on a permanent base or as temporary solutions during emergencies).

The different scenarios of the maps produced by the RAO framework allow local authorities to understand which areas are more resilient to potential natural disasters (like floods or landslides) and which ones are more vulnerable. The diversity of Northland with respect to population densities and infrastructure distribution on the territory necessarily implies profound differences in terms of accessibility to GPs. The RAO framework's results help to understand which are the critical locations for clinics for the provision of an adequate level of service at the minimum cost.

The RAO framework's results can be compared to the baseline provided by the current distribution of clinics and general practitioners in Northland. In this regard, Table 23 and Table 24 provide an overview of all the solutions of the different scenarios analysed for the Northland case study. Here, the served population's travel times are compared to the current

clinics and doctors layout, i.e. the baseline for the assessment of the improvements provided by the different Pareto-optimal solutions. Relative percentage increments (or reductions) are measured against the current service in Northland (see Figure 91 and Table 12).

A detailed analysis of these results is presented in section 6.6; improvements with respect to the baseline are evaluated in terms of accessibility, i.e. percentages of the population served below different travel time thresholds. The Pareto fronts provide portfolios of solutions ranging from one extreme (many clinics, short travel times) to the other (few clinics, higher travel times). The closer the solutions are to the top-left extreme of the Pareto-front (i.e. high costs, short travel times), the higher the improvement is in terms of accessibility with respect to the baseline. This improvement comes at a cost though; Table 23 and Table 24 provide information regarding how much it is necessary to invest (in terms of clinics and doctors) to achieve such improvements. The same results can also be read from the opposite perspective: when exploring results from the bottom-right extreme of the Pareto front, they can be interpreted as the effects of a reduction of the number of clinics and general practitioners in the region. In this case, Table 23 and Table 24 show the reduction of the number of doctors from 5% up to 50% (according to the different target ratios doctors/patients considered). As a matter of example, for the BAU scenario, solutions in the top-left area of Pareto fronts present increments in the served in less than 20 minutes around 5-7%. This is achieved with an increment of 11% in the number of GPs when considering a target ratio patients/doctors of 1500 and with a reduction of almost 30% of the number of doctors when considering a ratio of 2500.

The disruption scenario presents the same trend observed in the BAU scenario; however, when considering the 1500 ratio, maintaining the same level of service implies an extra 10% increment in the number of doctors. This means that the higher is the number of doctors, the higher is the extra expense to maintain the service provision in case of disruption.

Moreover, Figure 113 allows the observation of a general trend of all the inspected scenarios and to draw conclusions on the governing parameters of the model: increasing the value of the patients/doctors ratio always corresponds to a lowering of the total number of GPs in the region; therefore, the  $\gamma_C$  parameter does not influence the behaviour of the Pareto-optimal solution as much as TR. The target ratio patients/doctors is the governing parameter of the



problem, since its variations have greater influence on the global costs of the regional case study, while  $\gamma_C$  is a secondary modelling parameter meant to capture local competition.

Ultimately, based on these results, local authorities may outline policies (or foster investments) to encourage general practitioners to open (or relocate) clinics in key locations in terms of accessibility or natural hazards vulnerability.

### 7.5. Model limitations and future development

Heuristic approaches are very powerful tools to address complex problems; they allow solving problems involving big data and/or high resolutions with reasonable run times. As seen in the previous sections, they are also extremely useful when handling a high number of variables like in multi-objective spatial optimisation problems. However, their significant efficacy comes at a cost; and this cost is precision. By nature, heuristic approaches do not provide exact solutions as not all the possible solutions to the problem are actually inspected/assessed.

This limitation has repercussions on the concept of optimality. Solutions achieved with heuristic approaches are not mathematically optimal, but they can be close enough to the mathematical solution of the problem, according to how strong the mathematical formulation is and how good the calibration process is. Mathematically optimal solutions can be achieved with exact methods, which, in turn, would imply incredibly high run times when addressing complex problems. This is why, despite their intrinsic margin of error, heuristic approaches are very popular in engineering applications like shown in the literature review section (Chapter 3).

Being heuristics, genetic algorithms inherit this kind of uncertainty. However, with proper calibrations, the margin of error can be minimised with a good level of confidence. To achieve this, a sensitivity analysis with respect to the governing parameters is sufficient to understand how many iterations are necessary to reach the convergence of the Pareto-front. In both the case studies presented, 50 iterations were more than enough to observe this convergence. Moreover, the assessment of several scenarios testing different assumptions in both the case studies allowed to test the sensitivity of the models to different parameters and formulations (see sections 5.5 and 6.5). This is valuable because through the RAO framework it is possible to build models that, by nature, are data driven models, and since data are not always

available for all the potential applications where the RAO framework might be implemented, it is fundamental to have a clear idea of what are the capabilities and limitations of different assumptions and objective functions formulations.

The RAO methodology relies on several assumptions that necessarily imply some limitations. An exhaustive enumeration of these assumptions can be found in Chapter 4, here below are the more relevant:

- Accessibility is evaluated through the means of travel times. Travel times, in turn, are based on free-flow speeds on the road network. This necessarily implies that what is evaluated is a best-case scenario in terms of traffic.
- The resolution of GIS input data necessarily constrains the precision of results. The RAO framework does not present any restriction with respect to this parameter; it only has repercussions on run times.
- The definition of available locations for facilities allocation is an a priori choice. The two case studies present different variations of this: in the Humber Estuary case study, the RAO framework automatically determines available locations for warehouses, but the user has to provide a set of physical constraints to be met. Alternatively, in the Northland case study, no physical constraints are required, but a list of potential clinics location is taken as an input.
- The a priori choice that more heavily influence the spatial optimisation process is the definition of the optimisation functions. This must necessarily be a modeller choice; how to evaluate the performances of different spatial plans in terms of accessibility or cost is a delicate matter. For example, concerning accessibility, there is not a best choice in absolute terms. Choosing to consider the average travel time over the 75<sup>th</sup> quantile may be the right choice or the wrong one according to the mathematical formulation of the problem. Chapters 5.4.4 and 6.4.4 provide explanations of why in this work different metrics have been chosen for different case studies. Similarly, assuming different cost function formulations lead to different outcomes in terms of Pareto-optimal allocations as explored in the several scenarios of sections 5.5 and 6.5.

These assumptions imply some limitations of the optimisation methodology, but, at the same time, they provide a good starting point for the future development of this research. In terms of accessibility evaluation, better input data regarding the road networks could provide a

better evaluation of travel times. For instance, if allowed speeds for each network edge were available instead of relying on the road type information, more accurate input data would lead to more reliable results. The inclusion of the traffic variable would also provide added value to the methodology, providing a more precise simulation of the emergency situation and allowing the formulation of more accurate assumptions.

Regarding the network disruption scenarios, the presented results explore the case of road closures due to floodwater presence. Additional scenarios may be explored, for instance, considering speed reductions instead of complete closures. Adding a dimension to the flood risk analysis (for instance considering water depth) would allow a better modelling of the flood hazard and more sensible assumptions on road closures or speed reductions due to the presence of floodwater on the road.

As mentioned in the previous section, in both the case studies, the disruption scenarios consider all road network disruptions happening simultaneously. This represents a worst-case scenario worth investigating; however, a more refined scenario evaluation could be developed in the future development of this work. An interesting development of the disruption scenario could involve a better evaluation of the flood hazard, for instance considering not only fluvial but also pluvial flooding and their coupled effect, like explored in Zhang *et al.* (2010). Moreover, considering the dynamic nature of floods would improve the quality of the hazard evaluation. Time is a fundamental factor in emergency management, and a dynamic flood simulation would allow better consideration of the temporal dimension in the RAO framework. This would expand the current range of objectives, including the analysis of dynamic phenomena and their potential effects on complex systems of infrastructure networks.

In the Northland case study, the disruption scenario takes into account the simultaneous disruption of all the most critical sites of Northland's road network. This represents a quite unlikely worst-case scenario; nevertheless, it provides the opportunity to find and focus on the most resilient solutions generated by the RAO framework. This represents an interesting potential future development of this research: it would be interesting to evolve this approach considering the likelihood of individual disruptions and optimise against all possible events (e.g. either optimising all individually or in combination or otherwise randomly selecting different disruptions in the optimisation routine).

Future development of this research would involve the application of the RAO framework to different areas, at different scales and for different applications. The UK and NZ case studies presented in Chapters 5 and 6 already demonstrated the transferability of the methodology to different areas of different countries with different data availabilities, and also the flexibility of the methodology to be applied to different optimisation problems (from flood defences storing space to general practitioners allocation). Particular attention would require the application at different scales as building national scale models would pose different challenges. Maintaining the same resolution would simply imply too big data to be handled and consequently not reasonable run times. Changing the resolution would imply a redefinition of the problem formulation because of the impossibility to represent the physical constraints that limit the definition of available locations (e.g. distance from main roads, surface water, urban vs suburban etc.) as low resolutions would not be able to capture the spatial variability of the studied area unless changing the evaluation criteria for the determination of available locations. Different solutions could be explored to address this issue: like considering vector files instead of raster data to reduce the computational effort or considering parallel programming subdividing the national territory into sub-regions to be analysed in parallel.

Finally, another potentially interesting improvement would be including the current situation as a starting point of the RAO framework instead of considering a Greenfield approach. An interesting perspective would include further expanding the range of objectives by exploring how to evolve the current distribution of facilities to achieve the best possible solution at the smallest possible cost. This problem would have a quite different nature (and thus mathematical formulation), but this work could provide a solid background on which to base this further research.

In conclusion, this research aimed at widening the scale of analysis of infrastructure resilience to natural hazards. Both the analysed case studies areas constitute regional level analyses. As seen for the Humber Estuary case study, a regional-scale analysis already goes beyond the current flood management approaches, which only considers smaller areas. Future development of this approach will ideally consider even bigger scales (e.g. national scale), which would imply the simultaneous consideration of multiple regions allowing a better

optimisation process and ultimately allowing making consideration on resources and fund allocations.

#### 7.6. Software challenges for spatial optimisation

Chapter 4 presents the software architecture of the RAO framework (see also Figure 9). All the different components of the optimisation framework are developed in Python. This development environment has been chosen for its flexibility and its rich range of mathematical and optimisation modules (Fortin *et al.*, 2012). The programming language represents a strong assumption in the modelling phase; R and MATLAB represent viable potential alternatives for the development of a multi-objective spatial optimisation framework; however, Python's accessibility and ease of interface with ArcGIS and GDAL make it the best choice for the presented RAO framework development. Also, the use of Python for optimisation applications is well-grounded in the literature, like in Caparros-Midwood *et al.* (2019), Beham *et al.* (2014), Matott *et al.* (2011), Hebrard *et al.* (2010), Ligmann-Zielinska *et al.* (2008) and Bröker *et al.* (2005).

In terms of code performance, the network analyses are performed using NetworkX, which requires quite high run times. This is the reason why this process has been separated from the GA (for more details, see Chapter 4) and run beforehand. This separation allows the network analysis to be performed just once, at the beginning of the process, allowing multiple scenarios evaluations using the same network. Alternative potentially more efficient solutions in terms of computational effort may be explored in future development of this research (e.g. [igraph - https://igraph.org/](https://igraph.org/)) to try and improve run times of the network analysis.

Another significant methodological assumption and novel feature of the methodology consists in using the K-means clustering algorithm (Ostrovsky *et al.*, 2013) for the generation of spatial plans to seed the GA at the beginning of the iterative process. The module aims to perform a K-means clustering of the target assets (destinations of the network analysis) and determine the centroids of the identified clusters. This information is useful for seeding the algorithm with not-randomly generated initial spatial plans.

K-means clustering is a machine learning technique aimed at partitioning a series of  $n$  data into  $k$  clusters. This is implemented through the Python module "SciKit-learn" (Pedregosa *et*

*al.*, 2011; Buitinck *et al.*, 2013) that allows the K-means clustering of all the available locations and finding the centroids of these clusters. Network analysis is then performed to calculate travel times from each available location and the closest cluster centroid (Figure 21). Subsequently, the available locations are ranked according to their proximity to the centroid of their cluster.

When the initial population of solutions is created, available cells close to their cluster centroids are selected with a certain probability (set by the user), while the other locations are randomly selected from the Lookup variable. This procedure is meant to speed up the iterative process, and it is based on the assumption that cluster centroids are good locations in terms of accessibility. This is generally true; however, this procedure is only meant as a starting point in the search of Pareto-optimal solutions as it alone does not take into consideration any cost factor. The true value and the novelty of the methodology does not consist in the employment of one approach or the other (GA vs K-means), but in their coupling to make the most out of each technique exploiting their respective strengths and mitigating their shortcomings.

Moreover, in addition to the innovative coupling of K-means clustering to enhance the performance of the Genetic Algorithm, other steps forward with respect to traditional spatial optimisation frameworks – and in particular with respect to Caparros-Midwood (2015)'s approach – consist in both methodological and technical aspects. From the software perspective, the RAO framework allows a better management of scenarios and input choices on behalf of the final user because of its flexibility and ease in switching from one scenario to another in the main module (refer to Figure 9 and to the GitHub main RAO script: [github.com/fdlopane/RAO\\_HumberEstuary/blob/master/RAO.py](https://github.com/fdlopane/RAO_HumberEstuary/blob/master/RAO.py)). Also, the RAO framework provides a richer range of possible outputs datatypes (see the Outputs.py module in the GitHub repository [github.com/fdlopane/RAO\\_HumberEstuary](https://github.com/fdlopane/RAO_HumberEstuary)), a wider range of optimisation functions from which to choose (as shown in sections 5.5 and 6.5) which translate into additional Python functions available to the user in the Evaluation module. The case studies of Chapters 5 and 6 also showcased the wider range of possibilities in terms of acceptable input data formats that the RAO framework offers to the final user: according to the user's a priori knowledge/data availability, the RAO framework is flexible enough to allow the user to decide whether to provide the available locations for resources allocation as an input csv file or

to allow the RAO framework to automatically define an availability raster providing shapefiles as input datasets to model the physical constraints of the studied area. The flexibility and transferability of the RAO frameworks translates into a methodological novelty: traditionally the spatial optimisation frameworks present in the literature (refer to Chapter 3) consist in bespoke models to solve a particular engineering problem; the RAO framework's novelty, in this context, consists in its level of abstraction which allows its applicability to quite different real life problems as shown in this thesis' case studies: from emergency resources in the UK to healthcare facilities in New Zealand.

Despite addressing complex spatial problems involving different modelling assumptions and allowing several options, the RAO framework is quite straightforward to run. To apply the framework to real-life problems, the final user has to perform 3 steps:

1. Upload the data in the data folder;
2. Run the Network analysis module;
3. Set up the input variables and run the Main module.

The first step involves uploading all the spatial data that are necessary to represent the case study, its constraints, the infrastructure networks and the potential disruptions to the road network that they might want to investigate. To ease the operation on behalf of the user, all the input data can be uploaded in the same "Data" folder even if they have different formats (e.g. shapefiles, csv, txt etc.).

The second step is to run the Network analysis module. To do this, a Python compiler is used, and provided that the user uploaded the road network shapefile in the data folder, the only operation required is to hit the "run" button. No input parameters are required in this phase, as this module will produce a lookup txt file containing the travel times (in minutes) of all the road network nodes pairs evaluated using Dijkstra's shortest path algorithm implemented through NetworkX (Hagberg *et al.*, 2008).

The third and final step consists in defining the input parameters and running the Main module. The input parameters are those defining the scenarios of each case study (e.g. see sections 5.5 and 6.5), but also those defining some constraints and inspection ranges (e.g. minimum and maximum number of warehouses/clinics/doctors, minimum distance between allocated assets etc.). Once all the input parameters are defined by typing their values in the

first section of the Python script, the user can select which scenario to considerate and run the code with the Python compiler.

To evaluate different scenarios of the same case study, the user only has to repeat the final step (step 3) modifying the input parameters. A subfolder of the “Results” folder will be created for each run, avoiding overwriting or mixing up results from previous runs.

The methodological choice to adopt a genetic algorithm for the multi-objective spatial optimisation procedure is explained in section 3.4.5. Regarding the software implementation, DEAP (Distributed Evolutionary Algorithms in Python) (Fortin *et al.*, 2012) has been chosen over Pyevolve (Perone, 2009) and Pygene (McNab, 2011) (for more details, see section 4.4). Consequently, the evolution of the solutions is performed through DEAP by the application of the three evolutionary operators: selection (`tools.selNSGA2`), crossover (`tools.cxTwoPoint`) and mutation (`tools.mutUniformInt`) (as explained in Chapter 4).

A limitation of this approach is the predetermined number of iterations of the algorithm. For the case studies analysed in Chapter 5 and 6, the model calibration showed that after 50 generations, a convergence of the Pareto front was achieved. However, running the code several times to determine the appropriate number of iterations to implement is acceptable in a research context and for geographically limited case studies. For applications that would involve higher resolutions or bigger areas, longer run times would complicate the calibration process. Future development of the RAO framework would include the automatic termination of the iteration upon the achieving of the Pareto front’s convergence.

Finally, another significant potential improvement on the software implementation front is represented by the development of a user interface that would allow the setting of input parameters and bring together the outputs in a single platform. In his regard, PyQt could represent a valid option for the development of a bespoke UI in Python (Harwani, 2018).



## 8. Conclusions

The focus of this research work is strategic infrastructure services. The primary goal of this research is the development and demonstration of an optimisation-based decision support tool to help infrastructure operators and urban planners to identify strategies that improve the resilience of infrastructure services during disruptive natural hazards.

As introduced in Chapter 1, In order to achieve this aim, the work has been structured around five objectives. The review of these objectives will be the focus of the following sections of this chapter. Finally, a conclusive section summarises the implications of this research basing on the discussion chapter and the analyses of the outcomes of the case studies presented in Chapters 5 and 6.

### 8.1. Review of Objective 1: flood risk management and infrastructure resilience

Objective 1 includes the review of flood risk management practice, to identify the conflicts and barriers that can occur in the allocation of resources to enhance infrastructure resilience.

Objective 1 has been achieved in Chapter 2, which highlighted how natural disasters' impacts on cities and infrastructure are predicted to increase as disastrous events are foreseen to increase in frequency and severity and because of the fact that global urban population is continuously arising (Global Commission on Adaptation, 2019; United Nations, 2019).

Urban areas are therefore key locations in terms of vulnerability and resilience to natural disaster due to their concentration of residing population and infrastructure. Strategic infrastructure, in particular, is crucial for the normal functioning of urban environments in business as usual scenarios and even more so during emergencies (Cabinet Office and DEFRA, 2016).

Therefore, this research's focus is on strategic infrastructure resilience to natural disasters (in particular floods) by proposing a multi-objective spatial optimisation methodology for urban planning and the allocation of resources in emergency response.

The UK National Flood Resilience Review (Cabinet Office and DEFRA, 2016) explores the potential role of temporary flood defences not only as a 'backup' solution, but also as a valid

alternative to structural measures to take into consideration when designing flood mitigation strategies. It also explicitly declares the intention of the Environment Agency not only to increase the currently available stock of temporary flood defences, but also to identify “further strategic storage sites across the country, enabling temporary barrier deployment anywhere in England within 12 hours” (Cabinet Office and DEFRA, 2016). This is the focus of the main case study of this research work: the optimal allocation of storing space for temporary flood defences (see Objective 4).

A second case study is also explored to test the versatility and transferability of the optimisation methodology. The RAO framework (see Objective 3) is applied to a different kind of resource allocation problem: clinics and general practitioners in rural areas. Also in this instance, a business as usual scenario is compared to a disruption scenario to assess infrastructure’s resilience to potential disruptions due to floods or landslides (most common natural hazards in the case study region).

## 8.2. Review of Objective 2: optimisation techniques

The review optimisation techniques, in particular their application to spatial resource allocation problems, to identify a suitable approach constitutes Objective 2 of this research. This has been addressed in Chapter 3, where the mathematical formulation of optimisation problems is initially presented, followed by a review of different techniques available for spatial problems.

The literature presents a wide range of different optimisation applications developed to solve different problems. The focus of the review presented in Chapter 3 is on spatial applications as this is the main interest of this work. Even narrowing down the field only to spatial problems, the available approaches are numerous; this is why section 3.3 further limits the research to multi-objective optimisation problems and section 3.4 presents an overview of the most popular solutions adopted in the past to solve this kind of problems.

In light of this review, heuristics appeared as the most suitable technique for spatial problems involving big data and/or high resolutions (as the one intended to be explored in this research). For this reason, Pareto optimisation has been identified as the most appropriate approach to address the multi-objective spatial optimisation problem of this work. Then,

Genetic Algorithms (section 3.4.5) have been identified as one of the best available tools to address the Pareto multi-objective spatial optimisation.

### 8.3. Review of Objective 3: the RAO framework

Objective 3 consists in the development of a RAO framework that generates optimal spatial plans, to support infrastructure and urban planners to meet criteria identified in objective 2.

The Resources Allocation Optimisation framework is presented in Chapter 4. Initially, the multi-objective spatial nature of the optimisation is declared and defined. Section 4.2 then presents the framework architecture. The structure is summarised in the diagram represented in Figure 8; here, all the different components and stages are shown in a flow chart.

In order to ease its handling, clarity and intelligibility, the RAO framework has been structured in six phases: 1) the initialisation phase, 2) the iterator, 3) the evolutionary operator, 4) the constraints and evaluation phase, 5) the MOPO set maintenance and finally 6) the output phase. The relationship among these components is not linear, as phases 3, 4, and 5 can be considered as sub-components of the iterator. However, they are presented separately to ease the comprehension of the structure and the understanding of each component's function.

Sections 4.3 and 4.4 focus on the choice of the development environment and the type of adopted genetic algorithm. Python is chosen as the reference programming language because of its accessibility, its ease of interface with ArcGIS and its instrumental Geospatial Data Abstraction Library (GDAL), together with the fact that it has been used in a wide part of the literature on optimisation applications in general and in particular on spatial allocation optimisation. Python also offers the Distributed Evolutionary Algorithms in Python (DEAP) module that is used for the implementation of the  $\mu+\lambda$  strategy (Fortin *et al.*, 2012) adopted by the RAO framework.

The RAO framework formulation represents the theoretical core of this research as it embodies the optimisation methodology for solving multi-objective optimisation problems addressed in the case studies (Objective 4).

#### 8.4. Review of Objective 4: case studies

Objective 4 entails the application and demonstration of the RAO approach to different case studies to demonstrate its utility and transferability. This is addressed in Chapters 5 and 6. Chapter 5 presents a UK case study regarding temporary flood defences storing space optimisation in the Humber Estuary region. For this case study, the RAO provides solutions that balance the trade-off between accessibility to emergency resources maximisation and costs minimisation. The RAO framework is applied to identify Pareto-optimal warehouses locations for temporary flood defences storing space. The focus is on strategic infrastructure networks as they are identified as priority assets to be protected in case of flooding. The results consist of spatial plans showing different options with a different number of facilities for storing emergency response resources. Distances are evaluated as travel times on the road network, and the warehouses' locations are optimised to minimise transportation and deployment times together with the simultaneous minimisation of costs (i.e. number and dimension of storing facilities).

Chapter 6 presents a New Zealand case study, where the RAO is applied to a different problem with a similar mathematical formulation: the spatial optimisation of healthcare infrastructure assets allocation in Northland. The RAO framework here provides Pareto-optimal spatial plans of locations for GP clinics to maximise accessibility and resilience in case of road closures due to natural disasters.

The Northland instance proves the transferability of the methodology to different case study areas and different multi-objective spatial optimisation problems. Further development of this work could either improve the performance and refine the case studies analysed or apply the RAO framework to new case studies in different regions, at different scales or to solve different problems.

#### 8.5. Review of Objective 5: cases studies' results analysis

The final objective is the analysis of the results from case studies and discussion of the utility of spatial optimisation to help improve infrastructure resilience. The results of the RAO framework come in two forms: Pareto fronts in the solution space and maps representing the different spatial plans forming the Pareto front.

The Pareto fronts are useful as all the inspected solutions are plotted in the solution space defined by the two objective functions (i.e. minimisation of costs and minimisation of travel times). The solutions that form the Pareto front are the ones that outperform all the others in at least one objective. In fact, Pareto-optimisation produces a portfolio of equally optimal solutions, and it is up to the end-user to choose which one to adopt or which part of the Pareto front to inspect.

Maps allow analysing every single Pareto-optimal solution. In general, solutions from the top-left area of the Pareto-front will result in maps with many allocated assets with short travel times (but in general higher costs) while the solutions from the bottom-right area of the Pareto-front result in more centralised spatial plans with higher associated travel times (but lower costs).

In terms of results interpretation, as highlighted in section 7.3, the Humber Estuary case study represents a novel approach for flood management in this area for three main reasons. First, temporary flood defences are not considered in current flood management strategies if not for sandbags in emergency situations, which, however, are deprecated by the National Resilience Review (Cabinet Office and DEFRA, 2016) and, in case, as optional citizens' private initiative to protect their dwellings. Second, this research work provides the only regional analysis of this area, as there is no unique flood management strategy for this region at this scale because the Humber Estuary is divided into three different local authorities with autonomous and independent policies in terms of flood protection. Furthermore, the novelty also resides in considering strategic infrastructure as priorities in flood management strategies - as advocated by Cabinet Office and DEFRA (2016) - as dwellings are very often prioritised in this context.

For the Northland case study, it is easier to measure the benefits of the application of the RAO framework as it is possible to compare the results with the baseline represented by the current distribution of clinics and general practitioners in the area. In this regard, Table 23 and Table 24 provide an overview of all the solutions of the different analysed scenarios. The served population's travel times are compared to the current clinics and doctors layout, i.e. the baseline for the assessment of the improvements provided by the different Pareto-optimal solutions. Relative percentage increments (or reductions) are measured against the current service in Northland (see Figure 91 and Table 12).

The analysis of these results is presented in section 6.6 and 7.3; improvements with respect to the baseline are evaluated in terms of accessibility, in fact, it is possible to observe the percentage increases (or decreases) of the population served below different travel time thresholds (i.e. 10 min, 20 min, 30 min, 40 min and 50 min). According to how many doctors and clinics are allocated (Table 23 and Table 24 also show this information in terms of percentage increment), the served population percentages change, and they can be compared to the baseline. These analyses are summarised in the form of heatmaps in Figure 112. This information is not meant to have a prescriptive nature, but the final user should consider it as a reference for future investments or a reorganisation of the current situation for more cost-effective management of the healthcare infrastructure of the region.

### 8.6. Implications of the research

As explored in Chapter 3, a series of available optimisation techniques are currently available and extensive literature provides methodologies and applications to different problems. However, a spatial optimisation framework explicitly designed to solve resources allocation in an emergency response context is not present in the literature.

The focus of this piece of research is strategic infrastructure services, as they underpin every human and economic activity in urban areas under normal conditions; they are also even more crucial when facing natural disasters or in any kind of emergency response situation. For this reason, different scenarios have been evaluated considering a business as usual condition of the road network and its potential disruption due to natural disasters like floods or landslides. This allows us to make comparisons among the different conditions and draw conclusions on the resilience of different infrastructure services.

The digital revolution provides us with unprecedented tools for complex analyses involving big data, together with a likewise unprecedented computational power availability. Nonetheless, some problems still involve too big data or too complex analyses to be solved with mathematical exact methods in a reasonable time. This is why this work makes use of a heuristic approach that allows addressing multi-objective spatial optimisation problems exploring different scenarios.

This work applies spatial optimisation to infrastructure resilience and sustainability in emergency planning problems. It addresses problems by proposing a RAO framework meant as a potential support tool for urban planners and decision-makers when designing emergency management strategies. Spatial optimisation has the potential to support planning decisions that efficiently make use of the available means, ultimately saving money and resources, which implicitly implies cost-efficiency and sustainability.

The beneficiaries of the presented support tool are local authorities facing spatial planning decisions in the presence of multiple conflicting objectives. Engineers and infrastructure operators can benefit from this research as the RAO framework is designed to be flexible enough to adapt to different case studies and different situations. The outcomes in the form of diagrams and maps ease the comparison between different optimal solutions and allow visualising sensitivity analyses of particular parameters (for example, comparing accessibility maps when varying a single - or even multiple - parameter of interest).

This study will benefit planners and public agencies because it represents a novel perspective in infrastructure management strategies involving a wide-scale spatial optimisation approach to assess multiple scenarios to improve current infrastructure services (as in the Northland instance) or even implement new ones (like in the case of the Humber Estuary, where no in-place strategy is present at this scale for temporary flood defences).

In addition to the practical benefits to the potential end-users of the RAO framework, this work also aims at representing an inspiration for the development of other support tools for decision-making processes. We, as engineers and researchers, have now the means to build digital tools to help to undertake better decisions. When these tools are applied to infrastructure improvements, the whole society benefits for having more resilient infrastructure services for two main reasons: higher safety levels, which imply lower impacts of natural disasters on people and economies, and more sustainable emergency response systems, since, as highlighted in Chapter 2, resilient systems require fewer resources and efforts to recover after the occurrence of natural disasters.

Optimality is a concept that can hardly ever be achieved in real-life problems because they are typically open systems; nevertheless, it should be our duty at least to do our best to identify and design solutions that provide the best possible outcomes. For complex and

computationally demanding problems such as the urban planning and emergency response problem presented here, this thesis has shown how application of spatial optimisation algorithms can lead to more cost-effective strategies and ultimately more resilient and sustainable infrastructure.



## 9. References

- Aarts, E., Korst, J. and Michiels, W. (2005) 'Simulated Annealing', in Burke, E.K. and Kendall, G. (eds.) *Search Methodologies: Introductory Tutorials in Optimization and Decision Support Techniques*. Boston, MA: Springer US, pp. 187-210.
- Adachi, T. (2009) 'Flood damage mitigation efforts in Japan'. April 2020. Available at: [https://www.mlit.go.jp/river/basic\\_info/english/pdf/conf\\_09-0.pdf](https://www.mlit.go.jp/river/basic_info/english/pdf/conf_09-0.pdf).
- Adshead, D., Thacker, S., Fuldauer, L.I. and Hall, J.W. (2019) 'Delivering on the Sustainable Development Goals through long-term infrastructure planning', *Global Environmental Change*, 59, p. 101975.
- Aerts, J., Botzen, W., Bowman, M., Dircke, P. and Ward, P. (2011) *Climate Adaptation and Flood Risk in Coastal Cities*. London: Routledge.
- Aerts, J., Van Herwijnen, M., Janssen, R. and Stewart, T. (2005) 'Evaluating Spatial Design Techniques for Solving Land-use Allocation Problems', *Journal of Environmental Planning and Management*, 48(1), pp. 121-142.
- Aerts, J.C.J.H., Eisinger, E., Heuvelink, G.B.M. and Stewart, T.J. (2003) 'Using Linear Integer Programming for Multi-Site Land-Use Allocation', *Geographical Analysis*, 35(2), pp. 148-169.
- Aerts, J.C.J.H. and Heuvelink, G.B.M. (2002) 'Using simulated annealing for resource allocation', *International Journal of Geographical Information Science*, 16(6), pp. 571-587.
- Agnolucci, P., Akgul, O., McDowall, W. and Papageorgiou, L.G. (2013) 'The importance of economies of scale, transport costs and demand patterns in optimising hydrogen fuelling infrastructure: An exploration with SHIPMod (Spatial hydrogen infrastructure planning model)', *International Journal of Hydrogen Energy*, 38(26), pp. 11189-11201.
- Alhamwi, A., Medjroubi, W., Vogt, T. and Agert, C. (2019) 'Development of a GIS-based platform for the allocation and optimisation of distributed storage in urban energy systems', *Applied Energy*, 251, p. 113360.
- Álvarez-Miranda, E., Salgado-Rojas, J., Hermoso, V., Garcia-Gonzalo, J. and Weintraub, A. (2020) 'An integer programming method for the design of multi-criteria multi-action conservation plans', *Omega*, 92, p. 102147.
- American Society of Civil Engineers (2017) *Levees - Infrastructure Report Card*. [Online]. Available at: <https://www.infrastructurereportcard.org/cat-item/levees/>.
- Arrighi, C. and Castelli, F. (2020) Cham. Springer International Publishing.
- Arthur, J.L. and Nalle, D.J. (1997) 'Clarification on the use of linear programming and GIS for land-use modelling', *International Journal of Geographical Information Science*, 11(4), pp. 397-402.
- Australian Emergency Management Institute (2013) *Managing the floodplain: a guide to best practice in flood risk management in Australia*.

Axelrod, R.M. and Cohen, M.D. (2000) *Harnessing complexity : organizational implications of a scientific frontier*. New York (USA): Basic Books.

Bai, Q. (2010) 'Analysis of Particle Swarm Optimization Algorithm', *Computer and Information Science*, 3(1), pp. 180-184.

Baskent, E.Z. and Keles, S. (2005) 'Spatial forest planning: A review', *Ecological Modelling*, 188(2), pp. 145-173.

Batty, M. (2018) *Inventing future cities*. MIT Press.

Beham, A., Karder, J., Kronberger, G., Wagner, S., Kommenda, M. and Scheibenpflug, A. (2014) 'Scripting and Framework Integration in Heuristic Optimization Environments', *2014 Annual Conference on Genetic and Evolutionary Computation*. Vancouver. pp. 1109–1116.

Berardi, L., Giustolisi, O., Savic, D.A. and Kapelan, Z.S. (2009) 'An effective multi-objective approach to prioritisation of sewer pipe inspection', *Water Science and Technology*, 60(4), pp. 841-850.

Bieupoude, P., Azoumah, Y. and Neveu, P. (2012) 'Optimization of drinking water distribution networks: Computer-based methods and constructal design', *Computers, Environment and Urban Systems*, 36(5), pp. 434-444.

Bivand, R., Keitt, T., Rowlingson, B., Pebesma, E., Sumner, M., Hijmans, R., Rouault, E., Warmerdam, F., Ooms, J. and Rundel, C. (2019) *Bindings for the 'Geospatial' Data Abstraction Library, 1.4-6* [Computer program].

Blake, E.S. and Zelinsky, D.A. (2018) *National Hurricane Center Tropical Cyclone Report: Hurricane Harvey*. U.S. Department of Commerce.

Bonabeau, E., Dorigo, M. and Theraulaz, G. (1999) *From Natural to Artificial Swarm Intelligence*. Oxford University Press, Inc.

Bröker, O., Chinellato, O. and Geus, R. (2005) 'Using Python for large scale linear algebra applications', *Future Generation Computer Systems*, 21(6), pp. 969-979.

Buitinck, L., Louppe, G., Blondel, M., Pedregosa, F., Mueller, A., Grisel, O., Niculae, V., Prettenhofer, P., Gramfort, A., Grobler, J., Layton, R., Vanderplas, J., Joly, A., Holt, B. and Varoquaux, G. (2013) 'API design for machine learning software: experiences from the scikit-learn project', *European Conference on Machine Learning and Principles and Practices of Knowledge Discovery in Databases*.

Cabinet Office (2011) *Keeping the Country Running: Natural Hazards and Infrastructure*. London (UK): Civil Contingencies Secretariat, Cabinet Office. [Online]. Available at: [https://assets.publishing.service.gov.uk/government/uploads/system/uploads/attachment\\_data/file/61342/natural-hazards-infrastructure.pdf](https://assets.publishing.service.gov.uk/government/uploads/system/uploads/attachment_data/file/61342/natural-hazards-infrastructure.pdf).

Cabinet Office and DEFRA (2016) *National flood resilience review*. Department for Environment, Food & Rural Affairs, Cabinet Office, The Rt Hon Ben Gummer MP, The Rt Hon Andrea Leadsom MP.

- Cabrera, J.S. and Lee, H.S. (2018) 'Impacts of climate change on flood-prone areas in Davao Oriental, Philippines', *Water (Switzerland)*, 10(7).
- Cao, K., Batty, M., Huang, B., Liu, Y., Yu, L. and Chen, J. (2011) 'Spatial multi-objective land use optimization: extensions to the non-dominated sorting genetic algorithm-II', *International Journal of Geographical Information Science*, 25(12), pp. 1949-1969.
- Cao, K., Huang, B., Wang, S. and Lin, H. (2012) 'Sustainable land use optimization using Boundary-based Fast Genetic Algorithm', *Computers, Environment and Urban Systems*, 36(3), pp. 257-269.
- Caparros-Midwood, D. (2015) *Spatial optimization of multiple planning objectives for sustainable urban development*. PhD thesis. Newcastle University.
- Caparros-Midwood, D., Barr, S. and Dawson, R. (2017) 'Spatial Optimization of Future Urban Development with Regards to Climate Risk and Sustainability Objectives', *Risk Analysis*.
- Caparros-Midwood, D., Dawson, R. and Barr, S. (2016) 'Optimization of urban spatial development against flooding and other climate risks, and wider sustainability objectives', *FLOODrisk 2016 - 3rd European Conference on Flood Risk Management*. Lyon.
- Caparros-Midwood, D., Dawson, R. and Barr, S. (2019) 'Low Carbon, Low Risk, Low Density: Resolving choices about sustainable development in cities', *Cities*, 89, pp. 252-267.
- Casalino, L.P., Devers, K.J., Lake, T.K., Reed, M. and Stoddard, J.J. (2003) 'Benefits of and barriers to large medical group practice in the United States', *Arch Intern Med*, 163(16), pp. 1958-64.
- Chen, A.S., Hammond, M.J., Djordjević, S., Butler, D., Khan, D.M. and Veerbeek, W. (2016) 'From hazard to impact: flood damage assessment tools for mega cities', *Natural Hazards*, 82(2), pp. 857-890.
- Chuvieco, E. (1993) 'Integration of linear programming and GIS for land-use modelling', *International Journal of Geographical Information Systems*, 7(1), pp. 71-83.
- Climate Central and ICF International (2015) *States At Risk: America's Preparedness Report Card 2015*.
- Coello Coello, C.A. (1999) *A Survey of Constraint Handling Techniques used with Evolutionary Algorithms*. Laboratorio Nacional de Informatica Avanzada Rébsamen 80, Xalapa, Veracruz 91090, México.
- Comber, A., Brunsdon, C., Hardy, J. and Radburn, R. (2009) 'Using a GIS—Based Network Analysis and Optimisation Routines to Evaluate Service Provision: A Case Study of the UK Post Office', *Applied Spatial Analysis and Policy*, 2(1), pp. 47-64.
- Costamagna, E., Fanni, A. and Giacinto, G. (1998) 'A Tabu Search algorithm for the optimisation of telecommunication networks', *European Journal of Operational Research*, 106(2), pp. 357-372.

Coulthard, T.J. and Frostick, L.E. (2010) 'The Hull floods of 2007: implications for the governance and management of urban drainage systems', *Journal of Flood Risk Management*, 3(3), pp. 223-231.

CRED and UNISDR (2015) *The human cost of weather-related disasters 1995-2015*.

Cromley, R.G. and Hanink, D.M. (1999) 'Coupling land use allocation models with raster GIS', *Journal of Geographical Systems*, 1(2), pp. 137-153.

Czyżżak, P. and Jaskiewicz, A. (1998) 'Pareto simulated annealing—a metaheuristic technique for multiple-objective combinatorial optimization', *Journal of Multi-Criteria Decision Analysis*, 7(1), pp. 34-47.

D'Acci, L. (2019) 'Quality of urban area, distance from city centre, and housing value. Case study on real estate values in Turin', *Cities*, 91, pp. 71-92.

Dawson, R. (2007) 'Re-engineering cities: a framework for adaptation to global change', *Philosophical Transactions of the Royal Society A: Mathematical, Physical and Engineering Sciences*, 365(1861), pp. 3085-3098.

DEAP Project (2009) *DEAP 1.3.0 Documentation*. Available at: <https://deap.readthedocs.io/en/master/> (Accessed: Oct 28, 2019).

Deb, K. (2000) 'An efficient constraint handling method for genetic algorithms', *Computer Methods in Applied Mechanics and Engineering*, 186(2), pp. 311-338.

Deb, K. (2001) *Multi-objective optimization using evolutionary algorithms*. 1st ed.. edn. Chichester: Chichester : John Wiley & Sons.

Deb, K., Pratap, A., Agarwal, S. and Meyarivan, T. (2002) 'A fast and elitist multiobjective genetic algorithm: NSGA-II', *Evolutionary Computation, IEEE Transactions on*, 6(2), pp. 182-197.

Dijkstra, L., Hamilton, E., Lall, S. and Wahba, S. (2020) 'How do we define cities, towns, and rural areas?', *World Bank Blogs*.

Dijkstra, L. and Poelman, H. (2014) 'A harmonised definition of cities and rural areas: the new degree of urbanisation'.

Dowland, K.A. (1993) 'Some experiments with simulated annealing techniques for packing problems', *European Journal of Operational Research*, 68(3), pp. 389-399.

Dowland, K.A. (1996) 'Genetic Algorithms-a Tool for OR?', *Journal of the Operational Research Society*, 47(4), p. 550.

Du, J., Cai, Z. and Chen, Y. (2007) 'A Sorting Based Algorithm for Finding a Non-dominated Set in Multi-objective Optimization'. pp. 436-440.

East Reading of Yorkshire Council (2015) *Local flood risk management strategy 2015-2027*. [Online]. Available at: <https://www.eastriding.gov.uk/council/plans-and-policies/other-plans-and-policies-information/flood-risk/local-flood-risk-management-strategy/>.

Eastman, J.R., Jin, W., Kyem, P.A.K. and Toledano, J. (1995) 'Raster procedures for multi-criteria/multi-objective decisions', *Photogrammetric Engineering & Remote Sensing*, (61), pp. 539-547.

Environment Agency (2014) *Flood and coastal erosion risk management. Long-term investment scenarios (LTIS) 2014*.

Environment Agency (2015) *NAFRA April 2015 - Appendix K people at risk*.

Environment Agency (2016) *Humber river basin district flood risk management plan 2015 to 2021*.

Environment Agency (2019) *Flood and coastal risk management: Long-term investment scenarios (LTIS) 2019*.

Environment Agency and DEFRA (2011) 'Understanding the risks, empowering communities, building resilience: the national flood and coastal erosion risk management strategy for England'.

ESRI (2011) *ArcGIS Desktop: Release 10* [Computer program].

European Commission, Eurostat, Directorate-General for Regional and Urban Policy, International Labour Organization, Food and Agriculture Organization, Organisation for Economic Co-operation and Development, UN-Habitat and Bank, W. (2020) *A recommendation on the method to delineate cities, urban and rural areas for international statistical comparisons*.

FEMA (online) 'The National Flood Insurance Program'. April 2020. Available at: <https://www.fema.gov/national-flood-insurance-program>.

Feng, C.-M. and Lin, J.-J. (1999) 'Using a genetic algorithm to generate alternative sketch maps for urban planning', *Computers, Environment and Urban Systems*, 23(2), pp. 91-108.

Feng, X., Zhu, X., Qian, X., Jie, Y., Ma, F. and Niu, X. (2019) 'A new transit network design study in consideration of transfer time composition', *Transportation Research Part D: Transport and Environment*, 66, pp. 85-94.

Ferranti, E., Chapman, L. and Whyatt, D. (2017) 'A Perfect Storm? The collapse of Lancaster's critical infrastructure networks following intense rainfall on 4/5 December 2015', *Weather*, 72(1), pp. 3-7.

Fogel, L.J., Owens, A.J. and Walsh, M.J. (1966) *Artificial intelligence through simulated evolution*. Oxford, England: John Wiley & Sons.

Folke, C., Carpenter, S.R., Walker, B., Scheffer, M., Chapin, T. and Rockström, J. (2010) 'Resilience Thinking: Integrating Resilience, Adaptability and Transformability', *Ecology and Society*, 15(4).

Fortin, F.-A., De Rainville, F.o.-M., Gardner, M.-A., Parizeau, M. and Gagné, C. (2012) 'DEAP: Evolutionary algorithms made easy', *Journal of Machine Learning Research*, 13, pp. 2171-2175.

Fourer, R., Gay, D.M. and Kernighan, B.W. (2003) *AMPL: A Modeling Language for Mathematical Programming: second edition*. Brooks/Cole Publishing Company.

Fu, G., Kapelan, Z.S., Kasprzyk, J. and Reed, P. (2012) 'Optimal Design of Water Distribution Systems Using Many-Objective Visual Analytics', *Journal of Water Resources Planning and Management*, 139(6), pp. 624-633.

Garschagen, M. and Romero-Lankao, P. (2015) 'Exploring the relationships between urbanization trends and climate change vulnerability', *Climatic Change*, 133(1), pp. 37-52.

GDAL/OGR contributors (2019) *GDAL/OGR Geospatial Data Abstraction software Library* [Computer program]. Available at: <https://gdal.org>.

Gencer, E. (2017) *Local government powers for disaster risk reduction: A study on local-level authority and capacity for resilience*.

Gibson, M.J., Chen, A.S., Khoury, M., Vamvakeridou-Lyroudia, L.S., Stewart, D., Wood, M., Savić, D.A. and Djordjević, S. (2019) 'Case study of the cascading effects on critical infrastructure in Torbay coastal/pluvial flooding with climate change and 3D visualisation', *Journal of Hydroinformatics*, 22(1), pp. 77-92.

Global Commission on Adaptation (2019) *Adapt now: a global call for leadership on climate resilience*.

Glover, F. (1986) 'Future paths for integer programming and links to artificial intelligence', *Computers & Operations Research*, 13(5), pp. 533-549.

Glover, F. (1989) 'Tabu Search—Part I', *ORSA Journal on Computing*, 1(3), pp. 190-206.

Glover, F. (1990) 'Tabu Search—Part II', *ORSA Journal on Computing*, 2(1), pp. 4-32.

Goldberg, D.E. (1989) *Genetic algorithms in search, optimization, and machine learning*. Reading, Mass.: Reading, Mass. : Addison-Wesley Pub. Co.

Goldberg, D.E. and Deb, K. (1991) 'A comparison of selection schemes used in genetic algorithms', in *Foundations of Genetic Algorithms*. San Mateo, Calif. : M. Kaufmann Publishers, pp. 69-93.

Goodyear-Smith, F. and Janes, R. (2008) 'New Zealand rural primary health care workforce in 2005: more than just a doctor shortage', *Aust J Rural Health*, 16(1), pp. 40-6.

Greater London Authority (2021) *The London Plan: The Spatial Development Strategy for Greater London*. London (UK): Greater London Authority. [Online]. Available at: [https://www.london.gov.uk/sites/default/files/the\\_london\\_plan\\_2021.pdf](https://www.london.gov.uk/sites/default/files/the_london_plan_2021.pdf).

Hagberg, A.A., Schult, D.A. and Swart, P.J. (2008) *7th Python in Science Conference (SciPy 2008)*. Pasadena, CA.

Harwani, B.M. (2018) *Qt5 Python GUI Programming Cookbook: Building Responsive and Powerful Cross-Platform Applications with PyQt*. Birmingham: Birmingham: Packt Publishing, Limited.

Hebrard, E., O'Mahony, E. and O'Sullivan, B. (2010) 'Constraint programming and combinatorial optimisation in numberjack', in *Integration of AI and OR techniques in Constraint Programming for Combinatorial Optimization Problems.*, pp. 181-185.

Hendrickson, C.T. (1989) *Project management for construction / Chris Hendrickson, Tung Au*. Englewood Cliffs, N.J.: Englewood Cliffs, N.J. : Prentice Hall.

Henríquez, F.C. and Castrillón, S.V. (2011) 'A quality index for equivalent uniform dose', *Journal of medical physics*, 36(3), pp. 126-132.

Heymann, Y., Steenmans, C., Croisille, G., Bossard, M., Lenco, M., Wyatt, B., Weber, J.-L., O'Brian, C., Cornaert, M.-H. and Sifakis, N. (1994) *Corine land cover : guide technique / ed. Commissions of the European Communities, Brussels*. Communities, C.o.t.E.

Holland, J.H. (1992) *Adaptation in Natural and Artificial Systems: An Introductory Analysis with Applications to Biology, Control and Artificial Intelligence*. MIT Press.

Holling, C.S. (1973) 'Resilience and Stability of Ecological Systems', *Annual Review of Ecology and Systematics*, 4(1), pp. 1-23.

Holling, C.S. (1996) 'Engineering Resilience versus Ecological Resilience', in Engineering, N.A.o. (ed.) *Engineering Within Ecological Constraints*. Washington, DC: The National Academies Press.

Hu, X., Pant, R., Hall, J.W., Surminski, S. and Huang, J. (2019) 'Multi-Scale Assessment of the Economic Impacts of Flooding: Evidence from Firm to Macro-Level Analysis in the Chinese Manufacturing Sector', *Sustainability*, 11(7).

Huang, G. (2014) 'A Comparative Study on Flood Management in China and Japan', *Water*, 6(9), pp. 2821-2829.

Hull City Council (2015) *Local flood risk management strategy*.

Hunter, J.D. (2007) 'Matplotlib: A 2D Graphics Environment', *Computing in Science & Engineering*, 9(3), pp. 90-95.

IPCC (2012) *Managing the Risks of Extreme Events and Disasters to Advance Climate Change Adaptation*. Cambridge, UK, and New York, NY, USA: The Intergovernmental Panel on Climate Change (IPCC) Press, C.U.

IPCC (2014) *Climate Change 2014: Synthesis Report. Contribution of Working Groups I, II and III to the Fifth Assessment Report of the Intergovernmental Panel on Climate Change*. Geneva, Switzerland: IPCC.

Jaeggi, D.M., Parks, G.T., Kipouros, T. and Clarkson, P.J. (2008) 'The development of a multi-objective Tabu Search algorithm for continuous optimisation problems', *European Journal of Operational Research*, 185(3), pp. 1192-1212.

Jiang-Ping, W. and Qun, T. (2009) *ISECS International Colloquium on Computing, Communication, Control, and Management*.

Jones, D.F., Mirrazavi, S.K. and Tamiz, M. (2002) 'Multi-objective meta-heuristics: An overview of the current state-of-the-art', *European Journal of Operational Research*, 137(1), pp. 1-9.

Jordahl, K., Van den Bossche, J., Fleischmann, M., Wasserman, J., McBride, J., Gerard, J., Tratner, J., Perry, M., Garcia Badaracco, A., Farmer, C., Hjelle, G.A., Snow, A.D., Cochran, M., Gillies, S., Culbertson, L., Bartos, M., Eubank, N., maxalbert, Bilogur, A., Rey, S., Ren, C., Arribas-Bel, D., Wasser, L., Wolf, L.J., Journois, M., Wilson, J., Greenhall, A., Holdgraf, C., Filipe and Leblanc, F. (2020) *geopandas/geopandas: v0.8.1* (Version v0.8.1) [Computer program]. Zenodo. Available at: <https://doi.org/10.5281/zenodo.3946761>.

Kapelan, Z.S., Savic, D.A. and Walters, G.A. (2005) 'Multiobjective design of water distribution systems under uncertainty', *Water Resources Research*, 41.

Kaufmann, M., van Doorn-Hoekveld, W., Gilissen, H.K. and van Rijswijk, M. (2016) *Analysing and evaluating flood risk governance in the Netherlands*.

Kelly, E. and Stoye, G. (2014).

Kelman, I. (2017) 'Linking disaster risk reduction, climate change, and the sustainable development goals', *Disaster Prevention and Management: An International Journal*, 26(3), pp. 254-258.

Kennedy, J. and Eberhart, R. (1995) *Proceedings of ICNN'95 - International Conference on Neural Networks*. 27 Nov.-1 Dec. 1995.

Kepaptsoglou, K. and Karlaftis, M. (2009) 'Transit Route Network Design Problem: Review', *Journal of Transportation Engineering*, 135(8), pp. 491-505.

Khalili-Damghani, K., Aminzadeh-Goharrizi, B., Rastegar, S. and Aminzadeh-Goharrizi, B. (2014) 'Solving land-use suitability analysis and planning problem by a hybrid meta-heuristic algorithm', *International Journal of Geographical Information Science*, pp. 1-27.

Kirkpatrick, S., Gelatt, C.D. and Vecchi, M.P. (1983) 'Optimization by Simulated Annealing', *Science*, 220(4598), pp. 671-680.

Knowles, J.D. and Corne, D.W. (2000) 'Approximating the nondominated front using the Pareto Archived Evolution Strategy', *Evolutionary computation*, 8(2), p. 149.



- Konak, A., Coit, D.W. and Smith, A.E. (2006) 'Multi-objective optimization using genetic algorithms: A tutorial', *Reliability Engineering and System Safety*, 91(9), pp. 992-1007.
- Larrue, C., Bruzzone, S., Lévy, L., Gralepois, M., Schellenberger, M., Trémorin, J.-B., Fournier, M., Manson, C. and Thuillier, T. (2016) *Analysing and evaluating Flood Risk Governance in France: from State Policy to Local Strategies*. Rapport national.
- Leitch, S., Dovey, S.M., Samaranayaka, A., Reith, D.M., Wallis, K.A., Eggleton, K.S., McMenemy, A.W., Cunningham, W.K., Williamson, M.I., Lillis, S. and Tilyard, M.W. (2018) 'Characteristics of a stratified random sample of New Zealand general practices', *J Prim Health Care*, 10(2), pp. 114-124.
- Li, L.J., Huang, Z.B. and Liu, F. (2009) 'A heuristic particle swarm optimization method for truss structures with discrete variables', *Computers & Structures*, 87(7), pp. 435-443.
- Li, X. and Parrott, L. (2016) 'An improved Genetic Algorithm for spatial optimization of multi-objective and multi-site land use allocation', *Computers, Environment and Urban Systems*, 59, pp. 184-194.
- Liang, L.Y., Thompson, R.G. and Young, D.M. (2004) 'Optimising the design of sewer networks using genetic algorithms and tabu search', *Engineering, Construction and Architectural Management*, 11(2), pp. 101-112.
- Ligmann-Zielinska, A., Church, R. and Jankowski, P. (2006) 'Development Density-Based Optimization Modeling of Sustainable Land Use Patterns', in Riedl, A., Kainz, W. and Elmes, G.A. (eds.) *Progress in Spatial Data Handling: 12th International Symposium on Spatial Data Handling*. Berlin, Heidelberg: Springer Berlin Heidelberg, pp. 881-896.
- Ligmann-Zielinska, A. and Jankowski, P. (2007) 'Agent-Based Models as Laboratories for Spatially Explicit Planning Policies', *Environment and Planning B: Planning and Design*, 34(2), pp. 316-335.
- Ligmann-Zielinska, A., Church, R. and Jankowski, P. (2005) 'Sustainable Urban Land Use Allocation With Spatial Optimization', *8th ICA Workshop on Generalisation and Multiple Representation*.
- Ligmann-Zielinska, A., Church, R.L. and Jankowski, P. (2008) 'Spatial optimization as a generative technique for sustainable multiobjective land-use allocation', *International Journal of Geographical Information Science*, 22(6), pp. 601-622.
- Liu, Y., Tang, W., He, J., Liu, Y., Ai, T. and Liu, D. (2015) 'A land-use spatial optimization model based on genetic optimization and game theory', *Computers, Environment and Urban Systems*, 49, pp. 1-14.
- Lofberg, J. (2004) 'YALMIP : a toolbox for modeling and optimization in MATLAB', *2004 IEEE International Symposium on Computer Aided Control Systems Design*. Taipei, Taiwan. pp. 284-289.
- Loonen, W., Heuberger, P. and Kuijpers-Linde, M. (2007) 'Spatial Optimisation in Land-Use.', in *Modelling Land Use Change: Progress and Applications*.

Lopane, F.D., Barr, S., James, P. and Dawson, R. (2019) 'Optimization of resource storage location for managing flood emergencies', *2nd International Conference on Natural Hazards & Infrastructure*. Chania (GR).

Lorenzo-Lacruz, J., Amengual, A., Garcia, C., Morán-Tejeda, E., Homar, V., Maimó-Far, A., Hermoso, A., Ramis, C. and Romero, R. (2019) 'Hydro-meteorological reconstruction and geomorphological impact assessment of the October 2018 catastrophic flash flood at Sant Llorenç, Mallorca (Spain)', *Nat. Hazards Earth Syst. Sci.*, 19(11), pp. 2597-2617.

Lu, Q., Chang, N.-B., Joyce, J., Chen, A.S., Savic, D.A., Djordjevic, S. and Fu, G. (2018) 'Exploring the potential climate change impact on urban growth in London by a cellular automata-based Markov chain model', *Computers, Environment and Urban Systems*, 68, pp. 121-132.

Luke, S. (2015) 'Essentials of metaheuristics'.

Ma, S., He, J., Liu, F. and Yu, Y. (2011) 'Land-use spatial optimization based on PSO algorithm', *Geo-spatial Information Science*, 14(1), pp. 54-61.

Maliszewski, P.J., Kuby, M.J. and Horner, M.W. (2012) 'A comparison of multi-objective spatial dispersion models for managing critical assets in urban areas', *Computers, Environment and Urban Systems*, 36(4), pp. 331-341.

Maoh, H. and Kanaroglou, P. (2009) 'A tool for evaluating urban sustainability via integrated transportation and land use simulation models', *Environnement Urbain / Urban Environment*, 3, pp. 28-46.

Masoomi, Z., Mesgari, M.S. and Hamrah, M. (2013) 'Allocation of urban land uses by Multi-Objective Particle Swarm Optimization algorithm', *International Journal of Geographical Information Science*, 27(3), pp. 542-566.

Matott, L.S., Leung, K. and Sim, J. (2011) 'Application of MATLAB and Python optimizers to two case studies involving groundwater flow and contaminant transport modeling', *Computers and Geosciences*, 37(11), pp. 1894-1899.

McNab, D. (2011) *pygene* [Computer program].

Meyer, V. and Schwarze, R. (2019) 'The Economics and Management of Flood Risk in Germany', in Köster, S., Reese, M. and Zuo, J.e. (eds.) *Urban Water Management for Future Cities: Technical and Institutional Aspects from Chinese and German Perspective*. Cham: Springer International Publishing, pp. 473-495.

Ministère de L'Écologie, du Développement durable et de l'Énergie, (2011) 'National preliminary flood risk assessment'.

Ministère de l'Écologie, du Développement Durable, des Transports et du Logement, (2017) 'Programmes d'action de prévention des inondations (PAPI)'.

Ministère de l'Écologie, du Développement Durable, des Transports et du Logement, Ministère de l'Intérieur, de l'Outre-mer, des Collectivités Territoriales et de l'Immigration, Ministère de l'Économie, des Finances et de l'industrie, and Ministère du Budget, des

Comptes Publics,, de la Fonction Publique et de la Réforme de l'État, (2010) 'Plan submersions rapides'.

Ministry of Land, Infrastructure,, Transport and Tourism, (online) 'Flood management in Japan'. April 2020. Available at: [http://www.mlit.go.jp/river/basic\\_info/english/pdf/conf\\_01-6.pdf](http://www.mlit.go.jp/river/basic_info/english/pdf/conf_01-6.pdf).

Mishra, G. (2021) 'Types of Construction Project Costs – Direct and Indirect Costs'. The Constructor. Available at: <https://theconstructor.org/construction/construction-project-costs-direct-indirect-costs/7677/>.

Mishra, K.K. and Harit, S. (2010) 'A Fast Algorithm for Finding the Non Dominated Set in Multi objective Optimization', *International Journal of Computer Applications*, Volume 1(25), pp. 35–39.

Mitchell, M. (1998) *An introduction to genetic algorithms*. London: London : MIT.

Moeini, R. and Afshar, M.H. (2017) 'Arc Based Ant Colony Optimization Algorithm for optimal design of gravitational sewer networks', *Ain Shams Engineering Journal*, 8(2), pp. 207-223.

Molina Bacca, E.J., Knight, A. and Trifkovic, M. (2020) 'Optimal land use and distributed generation technology selection via geographic-based multicriteria decision analysis and mixed-integer programming', *Sustainable Cities and Society*, 55, p. 102055.

Monsef, H., Naghashzadegan, M., Jamali, A. and Farmani, R. (2019) 'Comparison of evolutionary multi objective optimization algorithms in optimum design of water distribution network', *Ain Shams Engineering Journal*, 10(1), pp. 103-111.

Moreno-Benito, M., Agnolucci, P. and Papageorgiou, L.G. (2017) 'Towards a sustainable hydrogen economy: Optimisation-based framework for hydrogen infrastructure development', *Computers & Chemical Engineering*, 102, pp. 110-127.

Murray, A.T. and Church, R.L. (1996) 'Applying simulated annealing to location-planning models', *Journal of Heuristics*, 2(1), pp. 31-53.

Nam, D. and Park, C.H. (2000) 'Multiobjective Simulated Annealing: A Comparative Study to Evolutionary Algorithms', *International Journal of Fuzzy Systems* 2(2).

Niemierko, A. (1997) 'Reporting and analyzing dose distributions: A concept of equivalent uniform dose', *Medical Physics*, 24(1), pp. 103-110.

Niroshinie, M.A.C., Ohtuski, K. and Nihei, Y. (2016) 'Effect of Small Rivers for the Inundations Due to Levee Failure at Kinu River in Japan', *Procedia Engineering*, 154, pp. 794-800.

North Lincolnshire Council (2019) *Flood defence work gathers pace on south Humber bank*. [Online]. Available at: <https://www.northlincs.gov.uk/news/flood-defence-work-gathers-pace-on-south-humber-bank/>.

Northland Regional Council (2018) *Regional Land Transport Plan 2015-2021 - Three year review*.

Ogunyoye, F., Stevens, R. and Underwood, S. (2011) *Temporary and demountable flood protection guide*. Environment Agency, Horizon House, Deanery Road, Bristol, BS1 5AH.

Oléron-Evans, T.P. and Salhab, M. (2021) 'Optimal land use allocation for the Heathrow opportunity area using multi-objective linear programming', *Land Use Policy*, 105(C).

Orsi, F., Church, R.L. and Geneletti, D. (2011) 'Restoring forest landscapes for biodiversity conservation and rural livelihoods: A spatial optimisation model', *Environmental Modelling & Software*, 26(12), pp. 1622-1638.

Ostrovsky, R., Rabani, Y., Schulman, L.J. and Swamy, C. (2013) 'The effectiveness of Lloyd-type methods for the k-means problem', *J. ACM*, 59(6), pp. 1-22.

Papadimitriou, C.H. and Steiglitz, K. (1998) *Combinatorial optimization : algorithms and complexity*. Mineola, N.Y: Mineola, N.Y : Dover Publications.

Pascual, M.S. (2011) 'GIS Data: A Look at Accuracy, Precision, and Types of Errors' [Article]. May 2020. GIS Lounge. Available at: <https://www.gislounge.com/gis-data-a-look-at-accuracy-precision-and-types-of-errors/>.

PBL Netherlands Environmental Assessment Agency (online) 'Correction wording flood risks for the Netherlands in IPCC report'. April 2020. Available at: <https://www.pbl.nl/en/correction-wording-flood-risks>.

Pedregosa, F., Varoquaux, G., Gramfort, A., Michel, V., Thirion, B., Grisel, O., Blondel, M., Prettenhofer, P., Weiss, R., Dubourg, V., Vanderplas, J., Passos, A., Cournapeau, D., Brucher, M., Perrot, M. and Duchesnay, É. (2011) 'Scikit-learn: Machine Learning in Python', *Journal of Machine Learning Research*, 12, pp. 2825-2830.

Perone, C.S. (2009) 'Pyevo: a Python open-source framework for genetic algorithms', *SIGEVolution*, 4(1), pp. 12-20.

Pitt, M. (2008) *Learning lessons from the 2007 floods*. London: London : Pitt Review.

Poo, C.P. (2020) *Climate change adaptation for seaports and airports*. Liverpool John Moores University [Online]. Available at: <http://researchonline.ljmu.ac.uk/id/eprint/13421/>.

Prasad, T. and Park, N. (2004) 'Multiobjective genetic algorithms for design of water distribution networks', *J. Water Resour. Plan. Manage.-ASCE*, 130(1), pp. 73-82.

Pregolato, M. (2017) *Risk analysis of the disruption to urban transport networks from pluvial flooding*. Newcastle University.

Pregolato, M. (2019) 'Bridge safety is not for granted – A novel approach to bridge management', *Engineering Structures*, 196, p. 109193.

Pulido, G.T. and Coello Coello, C.A. (2004) *Proceedings of the 2004 Congress on Evolutionary Computation (IEEE Cat. No.04TH8753)*. 19-23 June 2004.

Python Software Foundation (2010) *Python Language Reference, version 2.7* [Computer program]. Available at: <http://www.python.org>.

Qian, M., Pu, L., Zhu, M. and Weng, L. (2010) *18th International Conference on Geoinformatics*. 18-20 June 2010.

Ramos, D. (2017) 'Construction Cost Estimating: The Basics and Beyond'. Available at: <https://www.smartsheet.com/construction-cost-estimating>.

Rechenberg, I. (1973) 'Evolutionsstrategie — Optimierung technischer Systeme nach Prinzipien der biologischen Evolution.', *Feddes Repertorium*, 86(5), pp. 337-337.

Reddy, M.J. and Nagesh Kumar, D. (2007) 'Multi-objective particle swarm optimization for generating optimal trade-offs in reservoir operation', *Hydrological Processes*, 21(21), pp. 2897-2909.

Reeves, C.R. (1995) *Modern Heuristic Techniques for Combinatorial Problems*.

Rinaldi, S.M., Peerenboom, J.P. and Kelly, T.K. (2001) 'Identifying, understanding, and analyzing critical infrastructure interdependencies', *IEEE Control Systems Magazine*, 21(6), pp. 11-25.

Romero, C., Tamiz, M. and Jones, D.F. (1998) 'Goal programming, compromise programming and reference point method formulations: linkages and utility interpretations', *Journal of the Operational Research Society*, 49(9), pp. 986-991.

Rothlauf, F. (2011) *Design of modern heuristics principles and application*.

RStudio Team (2015) *RStudio: Integrated Development for R* [Computer program]. Available at: <http://www.rstudio.com/>.

Saad, D.A., Mansour, H. and Osman, H. (2018) 'Concurrent bilevel multi-objective optimisation of renewal funding decisions for large-scale infrastructure networks', *Structure and Infrastructure Engineering*, 14(5), pp. 594-603.

Samaniego, L. and Treuner, P. (2006) 'Optimisation of Infrastructure Location', *Jahrbuch für Regionalwissenschaft*, 26(2), pp. 119-145.

Santé-Riveira, I., Boullón-Magán, M., Crecente-Maseda, R. and Miranda-Barrós, D. (2008) 'Algorithm based on simulated annealing for land-use allocation', *Computers & Geosciences*, 34(3), pp. 259-268.

Sayers, P., Li, Y., Le Quesne, T., Fuxin, S., Galloway, G., Penning-Rowsell, E., Wen, K. and Chen, Y. (2013) *Flood risk management: a strategic approach*.

Sayers, W., Savić, D., Kapelan, Z. and Kellagher, R. (2014) 'Artificial Intelligence Techniques for Flood Risk Management in Urban Environments', *Procedia Engineering*, 70, pp. 1505-1512.

Schlager, K.J. (1965) 'A LAND USE PLAN DESIGN MODEL', *Journal of the American Institute of Planners*, 31(2), pp. 103-111.

Schouwenaars, T., Moor, B.D., Feron, E. and How, J. (2001) *2001 European Control Conference (ECC)*. 4-7 Sept. 2001.

Scrucca, L. (2013) 'GA : A Package for Genetic Algorithms in R', *Journal of Statistical Software*, 53(4).

Sean Gillies and others (2013) *Rasterio: geospatial raster I/O for Python programmers* [Computer program]. Available at: <https://github.com/mapbox/rasterio>.

Shakti, P.C., Nakatani, T. and Misumi, R. (2018) 'Analysis of flood inundation in ungauged mountainous river basins: A case study of an extreme rain event on 5–6 July 2017 in Northern Kyushu, Japan', *Journal of Disaster Research*, 13(5), pp. 860-872.

Shimamoto, H., Murayama, N., Fujiwara, A. and Zhang, J. (2010) 'Evaluation of an existing bus network using a transit network optimisation model: a case study of the Hiroshima City Bus network', *Planning - Policy - Research - Practice*, 37(5), pp. 801-823.

Siau, T. and Bayen, A.M. 1 (2014) 'An Introduction to MATLAB Programming and Numerical Methods for Engineers'. Beaverton: Ringgold Inc.

Sidiropoulos, E. and Fotakis, D. (2009) 'Cell-based genetic algorithm and simulated annealing for spatial groundwater allocation', *WSEAS Transactions on Environment and Development*, 5(4), pp. 351-360.

Sigmund, O. (2001) 'A 99 line topology optimization code written in Matlab', *Structural and Multidisciplinary Optimization*, 21(2), pp. 120-127.

Stewart, T.J. and Janssen, R. (2014) 'A multiobjective GIS-based land use planning algorithm', *Computers, Environment and Urban Systems*, 46, pp. 25-34.

Sung, Y.-H., Lin, M.-D., Lin, Y.-H. and Liu, Y.-L. (2007) 'Tabu Search Solution of Water Distribution Network Optimization', *J. Environ. Eng. Manage.*, 17(3), pp. 177-187.

Suppasri, A., Shuto, N., Imamura, F., Koshimura, S., Mas, E. and Yalciner, A.C. (2013) 'Lessons Learned from the 2011 Great East Japan Tsunami: Performance of Tsunami Countermeasures, Coastal Buildings, and Tsunami Evacuation in Japan', *Pure and Applied Geophysics*, 170(6), pp. 993-1018.

Tainter, J.A. and Taylor, T.G. (2014) 'Complexity, problem-solving, sustainability and resilience', *Building Research & Information*, 42(2), pp. 168-181.

Tarp, P. and Helles, F. (1997) 'Spatial optimization by simulated annealing and linear programming', *Scandinavian Journal of Forest Research*, 12(4), pp. 390-402.

Tasseff, B., Bent, R. and Van Hentenryck, P. (2016) *Integration of AI and OR Techniques in Constraint Programming*. Cham, 2016//. Springer International Publishing.

Tasseff, B., Bent, R. and Van Hentenryck, P. (2019) 'Optimization of Structural Flood Mitigation Strategies', *Water Resources Research*, 55(2), pp. 1490-1509.

The Countryside Agency, DEFRA, Office of the Deputy Prime Minister, Office for National Statistics and Welsh Assembly Government (2004) *Rural and Urban Area Classification 2004 - An Introductory Guide*.

The MathWorks Inc. (2010) *MATLAB version 7.10.0 (R2010a)* [Computer program].

The Parliamentary Office of Science and Technology (2020) *Natural mitigation of flood risk*. London, UK: UK Parliament. [Online]. Available at: <https://post.parliament.uk/research-briefings/post-pn-0623/>.

Thieken, A.H., Mariani, S., Longfield, S. and Vanneuville, W. (2014) 'Preface: Flood resilient communities - managing the consequences of flooding', *Natural hazards and earth system sciences*, 14(1), pp. 33-39.

Triantafyllidis, C.P., Koppelaar, R.H.E.M., Wang, X., van Dam, K.H. and Shah, N. (2018) 'An integrated optimisation platform for sustainable resource and infrastructure planning', *Environmental Modelling & Software*, 101, pp. 146-168.

UN General Assembly (2015) *Transforming our world: the 2030 Agenda for Sustainable Development*. UN General Assembly. [Online]. Available at: <https://www.refworld.org/docid/57b6e3e44.html>.

UNFCC (2015) *Paris Agreement from the Conference of Parties 21 (COP21)*. Paris: United Nations.

UNISDR (2015) *Sendai Framework for Disaster Risk Reduction 2015-2030*. United Nations - Headquarters, (UNDRR), U.N.O.f.D.R.R.

United Nations, D.o.E.a.S.A., Population Division, (2019) *World Urbanization Prospects: The 2018 Revision*. New York (USA).

US President's Commission on Critical Infrastructure Protection (1997) *Critical Foundations: Protecting America's Infrastructures*. Protection, U.S.P.s.C.o.C.I.

Vamvakeridou-Lyroudia, L., Walters, G. and Savic, D.A. (2005) 'Fuzzy Multiobjective Optimization of Water Distribution Networks', *Journal of Water Resources Planning and Management*, 131(6), pp. 467-476.

Vamvakeridou-Lyroudia, L.S., Chen, A.S., Khoury, M., Gibson, M.J., Kostaridis, A., Stewart, D., Wood, M., Djordjevic, S. and Savic, D.A. (2018) 'Enhancing the resilience of interconnected critical infrastructures to urban flooding: an integrated approach', *1st International WDSA / CCWI 2018 Joint Conference*. Kingston, Ontario, Canada.

Vamvakeridou-Lyroudia, L.S., Chen, A.S., Khoury, M., Gibson, M.J., Kostaridis, A., Stewart, D., Wood, M., Djordjevic, S. and Savic, D.A. (2020) 'Assessing and visualising hazard impacts to enhance the resilience of Critical Infrastructures to urban flooding', *Science of The Total Environment*, 707, p. 136078.

Vergouwe, R., Sarink, H.M. and Bisschop, C. (2016) *The national flood risk analysis for the Netherlands: final report*. Rijkswaterstaat VNK Project Office.

Wang, L., Shi, H. and Gan, L. (2018) 'Healthcare Facility Location-Allocation Optimization for China's Developing Cities Utilizing a Multi-Objective Decision Support Approach', *Sustainability*, 10(12).

Weise, T. (2011) *Global Optimization Algorithms - Theory and Application*. Third edn.

Wenger, C., Hussey, K. and Pittock, J. (2013) *Living with floods: Key lessons from Australia and abroad*. Facility, N.C.C.A.R. [Online]. Available at: [https://www.nccarf.edu.au/sites/default/files/attached\\_files\\_publications/Wenger\\_2013\\_Living\\_with\\_floods.pdf](https://www.nccarf.edu.au/sites/default/files/attached_files_publications/Wenger_2013_Living_with_floods.pdf).

Woodward, M., Kapelan, Z. and Gouldby, B. (2014) 'Adaptive Flood Risk Management Under Climate Change Uncertainty Using Real Options and Optimization', *Risk Analysis*, 34(1), pp. 75-92.

Woolhouse, C. (2017) 'The case for temporary flood defences'. May 2020. Available at: <https://www.ice.org.uk/news-and-insight/the-civil-engineer/march-2017/the-case-for-temporary-flood-defences>.

World Resources Institute (online) 'Global Flood Analyser'. Available at: <https://www.wri.org/applications/aqueduct/floods/risk>.

Wu, X., Wang, S., Fu, B., Liu, Y. and Zhu, Y. (2018) 'Land use optimization based on ecosystem service assessment: A case study in the Yanhe watershed', *Land Use Policy*, 72, pp. 303-312.

Xiao, N., Bennett, D.A. and Armstrong, M.P. (2007) 'Interactive evolutionary approaches to multiobjective spatial decision making: A synthetic review', *Computers, Environment and Urban Systems*, 31(3), pp. 232-252.

Zhang, T., Shao, Z., Zhang, Y., Yu, Z. and Jiang, J. (2010) *Advances in Swarm Intelligence*. Berlin, Heidelberg, 2010//. Springer Berlin Heidelberg.

Zhang, W. and Fujimura, S. (2010) 'Improved Vector Evaluated Genetic Algorithm with Archive for Solving Multiobjective PPS Problem'. pp. 1-4.

Zitzler, E., Laumanns, M. and Thiele, L. (2001) *SPEA2: Improving the Strength Pareto Evolutionary Algorithm*. Zurich, Switzerland: Department of Electrical Engineering, Swiss Federal Institute of Technology (ETH) Zurich.